2008-01-28

Dissecting Small RNA Loading Pathway in *Drosophila melanogaster*: A Dissertation

Tingting Du
University of Massachusetts Medical School

DISSECTING SMALL RNA LOADING PATHWAY IN *DROSOPHILA MELANOGASTER*

A Dissertation Presented

By

Tingting Du

Submitted to the Faculty of the

University of Massachusetts Graduate School of Biomedical Sciences, Worcester

in partial fulfillment of the requirements for the degree of

DOCTOR OF PHILOSOPHY

January 28th, 2008

Biochemistry and Molecular Pharmacology

COPYRIGHT INFORMATION

The chapters of the dissertation have appeared in whole or part in publications below:

Tomari, Y.*, Du, T.*, Haley, B.*, Schwarz, D.S., Bennett, R.,Cook, H.A., Koppetsch, B.S., Theurkauf, W.E., and Zamore, P.D. (2004). RISC assembly defects in the *Drosophila* RNAi mutant *armitage*. *Cell* 116, 831-841.

Förstemann, K., Tomari, Y., Du, T., Vagin, V.V., Denli, A.M., Bratu, D.P., Klattenhoff, C., Theurkauf, W.E., and Zamore, P.D. (2005). Normal microRNA maturation and germ-linestem cell maintenance requires Loquacious, a double-stranded RNA-binding domain protein. *PLoS Biol* 3(7): e236

Du, T., Zamore, P.D. (2005). microPrimer: the biogenesis and function of microRNA. *Development* 132(21): 4645-52.

Du, T., Zamore, P.D. (2007). Beginning to understand microRNA function. *Cell Res.* 17(8):661-3.

* These authors contributed equally to this work

DISSECTING SMALL RNA LOADING PATHWAY
IN *DROSOPHILA MELANOGASTER*

A Dissertation Presented
By
Tingting Du

The signature of the Dissertation Defense Committee signifies completion and approval as to style and content of the Dissertation

____

Phillip D. Zamore, Thesis Advisor

____

Kendall Knight, Member of Committee

____

William Theurkauf, Member of Committee

____

Thoru Pederson, Member of Committee

____

Eric Sontheimer, Member of Committee

The signature of the Chair of the Committee signifies that the written dissertation meets the requirements of the Dissertation Committee

____

Zuoshang Xu, Chair of Committee

The signature of the Dean of the Graduate School of Biomedical Sciences signifies that the student has met all graduation requirements of the school

____

Anthony Carruthers, Ph.D., Dean of the Graduate School of Biochemical Sciences
Department of Biochemistry and Molecular Pharmacology

January 28th, 2008

ACKNOWLEDGEMENTS

There are several people I would like to thank for their support, advice and friendship. First, I want to thank my thesis adviser Phil Zamore, for giving me the opportunity to work in such an exciting field and for all his guidance, support and encouragement during my thesis research. He has been a wonderful mentor, teaching me not only how to be a good scientist, but more importantly how to be a good person. I have benefited and will continue to benefit from what I learned from him throughout my scientific career. I also want to thank Phil for gathering an amazing group of people to make our lab such a pleasant place to do science, to share original ideas, and to have fun.

I want to thank all the former and current members of Zamore lab. They are not only my colleagues, but also my best friends. I would like to thank them all for making my Ph.D. study such a memorable experience, for sharing my pleasure when I was happy, and for always being there for me when I got frustrated. I received a lot of help from György when I first joined the lab. He had been very patient with me and had always encouraged me when I faced difficulties. I really appreciate it and wish him the best luck in Dundee. I want to thank Yuki for his help and collaboration during my research. I could not have achieved much without his input into our projects. He is a terrific scientist and has been most modest despite his brilliancy. I also received a lot of scientific input for my research from Dianne, Ben, Alla, Klaus, Vasia and Hervé. I would like to thank Tiffanie, Gwen and Shengmei for their help and Megha, Wee, Vasia, Chengjian (and his wife, my good friend Xiaolan) and Jennifer for their emotional support and the laughs we have shared.

I would like to thank our collaborators Theurkauf lab, especially Birgit, Carla, Heather and Bill, for sharing their reagents and ideas, and for all the help and technical support they provided during my research. I want to thank Traci Hall lab for generously offering us the recombinant proteins, and Carthew lab, Liu lab and Hannon lab for sending us fly stocks and reagents. I want to thank my committee members (Zuoshang Xu, Kendall Knight, William Theurkauf, Celia Schiffer, Thoru Pederson and Eric Sontheimer) for their insightful suggestions and guidance for my research. I also want to thank everybody in the BMP department for always being helpful and friendly to me.

I want to send special appreciation to my family in China, especially my parents and my grandma. I would not have gone so far without their love and support. They have always been supportive for my career choice no matter what. I want to thank them for all the sacrifice they made for me by letting me go abroad for my Ph.D. study and I am truly sorry for not being able to take care of them and even to visit them often as a child or a grandchild should. I am the luckiest person in the world for having them as my family and I will try my best to make them feel the same. Lastly I want to thank Chao-shun for being such a caring, loving and understanding boyfriend and for every wonderful thing he has brought to my life.

TABLE OF CONTENTS

List of Figures

List of Tables

CHAPTER I: Introduction

1. RNA interference

1.1 History of RNAi

Seventeen years ago, Jorgensen and colleagues attempted to produce darker pigmented petunia petals by overexpressing a chimeric petunia chalcone synthase (CHS) gene that encodes a key enzyme in flower coloration (Napoli et al., 1990; van der Krol et al., 1990). To their surprise, a large percentage of the transgenic plants produced totally white flowers and/or patterned flowers with white or pale nonclonal sectors on a wild-type pigmented background, instead of dark purple flowers they expected. The decreased coloration resulted from the reduction in expression of both exogenous and endogenous CHS gene. They dubbed the phenomenon "cosuppression". In the mid 90's, the Baulcombe group further pursued the mechanism underlining cosuppression in plants. Based on the results of a series of experiments, he proposed that RNA is the direct trigger as well as the target of the silencing effect (Voinnet and Baulcombe, 1997). Meanwhile, *C. elegans* researchers Fire and Kemphues et al observed that introducing either sense or antisense RNA into the worm can conform silencing of homologous gene, which contradicts the long-existing presumption that antisense RNA-mediated silencing is achieved by base-paring to their complementary mRNAs (Fire et al., 1991; Guo and Kemphues, 1995).

In 1998, Fire, Mello and their colleagues published their Nobel-winning paper, which not only solved the mystery of earlier paradoxical findings, but more importantly gave rise to a whole new field in biological research (Fire et al., 1998). In their paper, they demonstrated for the first time that the trigger for RNA–induced silencing is indeed double-stranded RNA (dsRNA), which can be introduced by either viral infection as observed in plants or aberrant transcription by bacteria polymerase during the preparation of RNA samples for injection in Kemphues' worm experiment. They named the phenomenon of dsRNA induced gene silencing RNA interference (RNAi). In their 1998 paper, Fire and Mello also described several key features of RNAi in worms. First, the silence is highly efficient; only a few molecules per injected cell are sufficient to silencing a highly expressed endogenous gene, suggesting a catalytic or amplification mechanism involved. Second, the dsRNA-mediated interference is able to cross cellular boundaries in a single organism and can even be transmitted across generations. Third, dsRNA corresponding to introns or promoter sequences does not elicit silencing, indicating silencing at a post-transcriptional level.

Soon after their discovery, RNAi was elucidated and utilized in various organisms including *Drosophila* (Kennerdell and Carthew, 1998; Misquitta and Paterson, 1999), trypanosomes (Ngo et al., 1998), hydra (Lohmann et al., 1999), planaria (Sanchez Alvarado and Newmark, 1999), zebrafish (Wargelius et al., 1999), mouse (Svoboda et al., 2000; Wianny and Zernicka-Goetz, 2000) and was confirmed in plants (Waterhouse et al., 1998). Meanwhile, fly researchers successfully recapitulated dsRNA-induced silencing in cell-free systems from either *Drosophila* syncitial blastoderm embryos (Tuschl et al., 1999; Zamore et al., 2000) or cultured Schneider 2 (S2) cells (Caplen et al., 2000; Clemens et al., 2000). Establishment of these in vitro systems has ever since been contributing to the understanding of the RNAi machinery not only in flies, but also in higher organisms, by revealing the components in the pathway, what roles they play and how they cooperate to work most efficiently.

Challenge arose when it came to mammalian systems. Although introduction of dsRNA could efficiently reduce gene expression in mouse oocytes and early embryos (Svoboda et al., 2000; Wianny and Zernicka-Goetz, 2000), its application in mammalian cell cultures had been problematic (Ui-Tei et al., 2000). This is because that in mammalian cells dsRNA >30bp can also trigger profound physiological reactions that lead to the induction of interferon synthesis, which eventually triggers sequence independent global mRNA degradation in the cell (Stark et al., 1998). In 1999, Hamilton and Baulcombe for the first time reported the accumulation of small (~25 nucleotide) RNAs upon the introduction of dsRNA (Hamilton and Baulcombe, 1999). Because the presence of these RNAs, which correspond to both the sense and antisense strands of the silenced gene, correlates perfectly with the silencing effect, they proposed that 'they are components of the systemic signal and specificity determinants of PTGS' (PTGS in plants equals to RNAi in animals). Subsequently, Zamore et al demonstrated that small RNA of similar size (21-23 nt long) can be processed from the dsRNA silencing trigger in *Drosophila* embryo lysate system

(Zamore et al., 2000). Moreover, cleavage of the target mRNA occurs at 21-23 nt apart in the region of the identity of trigger dsRNA, which strongly suggests that small RNAs are directly guiding the mRNA cleavage. In the mean time, using lysate from fly S2 cells, the Hannon lab also detected the small RNA population derived from dsRNA silencing trigger (Hammond et al., 2000). They showed that these small RNAs are incorporated in a ribonucleotide-protein (RNP) complex where they serve as guides that target specific mRNA based upon sequence recognition. They termed the small RNA-protein complex RISC (RNA-induced silencing complex). These small RNAs were subsequently detected by injection of radiolabeled dsRNA in worms (Parrish et al., 2000) and by injection of dsRNA in single *Drosophila* embryos (Yang et al., 2000). Tuschl and colleagues characterized the properties of these small RNAs in greater detail. They demonstrated that these small RNAs are double-stranded with 2-nt overhanging 3′ end, both bearing a 5′ phosphate and 3′ hydroxyl group, all of which are characteristics of the ribonulease III (RNase III) cleavage product (Elbashir et al., 2001b; Elbashir et al., 2001c). They named these small RNAs small interfering RNAs (siRNAs). The Tuschl lab for the first time successfully used synthetic siRNA to trigger target mRNA cleavage in the lysate system, and determined that the target cleavage site is located near center of the region covered by the small RNA (Elbashir et al., 2001b). It is this finding together with their subsequent application of synthetic siRNA in mammalian cell lines to silence endogenous and heterologous genes that boosted the utilization of RNAi as a research tool especially in mammalian systems and posted the possibility to use RNAi for therapeutical purposes (Elbashir et al., 2001a).

1.2 RNAi in *Drosophila*

In *Drosophila*, ‘foreign’ long dsRNAs, such as those introduced experimentally or produced by viral infection, enter the RNAi pathway when they are processed into ~21 nucleotide, double-stranded siRNAs by the RNase III endonuclease Dicer-2 (Dcr-2)(Bernstein et al., 2001). (Flies encode two dicer proteins (Hoa et al., 2003; Lee et al., 2004b).) These siRNAs are subsequently loaded into an effector complex—RISC—containing Argonaute2 (Ago2) by the RISC-loading complex (RLC) (Hammond et al., 2001). Dcr-2 and its dsRNA-binding protein partner, R2D2, are core components of the RLC (Liu et al., 2003; Tomari et al., 2004a). They form a stable heterodimer that identifies the siRNA guide and passenger strands: R2D2 binds to the more stably paired end of the siRNA duplex, thereby positioning Dcr-2 at the less stable end, designating this RNA strand as the future guide (Tomari et al., 2004b). After binding the siRNA, the Dcr-2/R2D2 heterodimer, perhaps together with other RLC components, recruits Ago2 to the double-stranded siRNA (Pham et al., 2004; Pham and Sontheimer, 2005; Preall et al., 2006). The geometry of the siRNA within the Dcr-2/R2D2 heterodimer is preserved when it is passed to Ago2: the 5′ end of the guide siRNA binds the Ago2 5′ phosphate-binding pocket, and the passenger strand assumes the position of a target mRNA (Tolia and Joshua-Tor, 2007). Ago2 is an RNA-guided, Mg^{2+}-dependent endonuclease (Martinez and Tuschl, 2004; Meister et al., 2004; Rand et al., 2004; Rivas et al., 2005; Schwarz et al., 2004; Song et al., 2004). This nuclease activity acts not only in siRNA-guided mRNA cleavage, but also in the maturation of Ago2 to its active form, RISC. Because in immature RISC (pre-RISC) the passenger strand occupies the position of a target RNA, a critical step in RISC assembly is cleavage of the passenger strand by Ago2, a step that facilitates separation of the two siRNA strands (Kim et al., 2007; Leuschner et al., 2006; Matranga et al., 2005; Miyoshi et al., 2005; Rand et al., 2005). Dissociation of the passenger strand leaves Ago2 loaded with a single-stranded siRNA guide. In *Drosophila*, a single-stranded RNA methyltransferase DmHen1 methylates the 3′ termini of Ago2 loaded siRNA, completing the final step in RISC assembly (Horwich et al., 2007). Such mature RISC can then find its mRNA targets by nucleobase complementarity to the siRNA guide and destroy them by Ago2-catalyzed endonucleolytic cleavage.

1.3 RNAi comes in different flavors

Unlike flies and mammals where the sole source of siRNA is from Dicer processing of dsRNA, plants, fungi and some animals such as *C. elegans* exploit RNA-dependent RNA polymerase (RdRP) activity to generate secondary siRNAs by copying the mRNA that is targeted by primary siRNAs.

Plants

Plants have evolved several RNAi-related pathways producing siRNAs that differ by their origin, their biogenesis and loading, as well as their designated targets (Brodersen and Voinnet, 2006).

The most abundant endogenously-produced siRNAs in plants are 24 nt in length. They originate from loci that contain direct or inverted repeats, and from dispersed repetitive elements, such as tranposons and retroelements (Kasschau et al., 2007; Llave et al., 2002a). These class of siRNAs are produced by Dicer-like 3 (DCL3) (*Arabidopsis* genome encodes 4 dicer and 10 argonaute genes) and get loaded into AGO4 or AGO6-containing RISC (Chan et al., 2004; Xie et al., 2004; Zheng et al., 2007; Zilberman et al., 2003). Their accumulation also requires the activity of RNA-dependent RNA polymerase 2 (RDR2), one of the six RDR paralogs in *Arabidopsis*, two isoforms of RNA polymerase IV, polIVa and polIVb, as well as the methyltransferase HEN1(Boutet et al., 2003; El-Shami et al., 2007; Herr et al., 2005; Kanoh et al., 2005; Li et al., 2005; Onodera et al., 2005; Pontier et al., 2005). Because these siRNAs guide heterochromatin formation by regulating DNA methylation and histone modification at the loci where they derive from, they are also known as *cis*-acting siRNA (casiRNA)(Chan et al., 2004; Tran et al., 2005; Zilberman et al., 2003).

Experimentally introduced inverted-repeat (IR) or simultaneously expressed sense and antisense transcripts can be processed into siRNAs of two distinct sizes, 24 nt and 21 nt (Hamilton et al., 2002; Tang et al., 2003). The 24 nt siRNAs are generated by the similar mechanism that produces casiRNA, whereas the 21 nt siRNA population is made by a different dicer, Dicer-like 4 (DCL4), together with the double-stranded RNA binding protein DRB4 (Dunoyer et al., 2005; Hiraguri et al., 2005; Nakazawa et al., 2007). These 21 nt siRNAs are usually loaded into AGO1-RISC that directs the endonucleolytic cleavage of its homologous mRNA (Beclin et al., 2002).

In plants, a distinct PTGS pathway is evolved to defend the invasion of viruses and foreign genes (Waterhouse and Fusaro, 2006; Waterhouse et al., 2001). In this pathway, an initial pool of small RNAs, the primary siRNAs, derived from one region of the transcript, induce the production of secondary siRNAs corresponding to regions outside that targeted by the primary siRNA. This phenomenon, dubbed ‘transitivity’, adds an amplification step to the siRNA production, thus reinforcing more robust and persistent silencing (Sijen et al., 2001; Vaistij et al., 2002; Voinnet et al., 1998). The transitivity is achieved by RDR6, which can synthesize the complementary stand of the siRNA targeted RNA to produce new dsRNA as dicing substrate (Qu et al., 2005). Two Dicers, DCL4 and DCL2, which produce 21 nt and 22 nt siRNAs respectively, function hierarchically to generate both primary and secondary siRNAs subsequently loaded into AGO1 to direct target mRNA destruction (Bouche et al., 2006; Deleris et al., 2006; Fusaro et al., 2006; Moissiard et al., 2007; Xie et al., 2004).

The RDR6/DCL4 dependent pathway also catalyzes formation of *trans*-acting siRNAs (tasiRNAs), the small RNA class that functions *in trans* to modulate the endogenous gene expression at post-transcriptional level (Fahlgren et al., 2006; Gasciolli et al., 2005; Peragine et al., 2004; Vazquez et al., 2004b). The production of tasiRNA involves the dual action of miRNA (discussed below) and siRNA biogenesis machinery (Allen et al., 2005; Axtell et al., 2006; Yoshikawa et al., 2005). The non-coding, single-stranded primary tasiRNA transcripts, pri-tasiRNAs, or *TAS* transcripts contain a binding site for a miRNA that guides cleavage at a defined point. The cleavage by miRNA not only designates *TAS* transcripts as target for RDR6-mediated transitivity, but more importantly defines the dsRNA terminus, which is crucial for the accuracy of the phased dicing reaction by DCL4, producing mature 21 nt tasiRNAs that function though AGO1 or AGO7 (Adenot et al., 2006; Fahlgren et al., 2006; Hunter et al., 2003; Xu et al., 2006).

Yet another class of siRNA in plants, the natural antisense transcript siRNA (nat-siRNA), is formed from the overlapping region of a pair of natural antisense transcripts (NATs) (Borsani et al., 2005). Although a few examples of nat-siRNA have been described in detail to date (Borsani et al., 2005; Katiyar-Agarwal et al., 2007; Katiyar-Agarwal et al., 2006), analysis of transcript profiles from a microarray database has revealed that more than 1,000 pairs of NATs exit in *Arabidopsis* , suggesting nat-siRNAs may serve as one of the major sources of endogenous siRNAs for gene regulation in response to different environmental conditions or upon pathogen infection (Jen et al., 2005; Wang et al., 2005). The nat-siRNAs vary in their sizes and biogenesis pathway. In one of the examples, the pathway involves the DCL2/RDR6 dependent production of a single 24 nt primary nat-siRNA and the subsequent generation of a phased series of 21 nt secondary nat-siRNAs by DCL1(Borsani et al., 2005). While in other cases though, significantly longer siRNAs (lsiRNAs), which are 30-40 nt in length, are produced from NAT pairs (Katiyar-Agarwal et al., 2007). One such lsiRNA, AtlsiRNA-1, whose expression is induced by bacterium infection, requires DCL1, DCL4, AGO7, HYL1, HEN1, RDR6 and Pol IV for its accumulation and destabilizes its target mRNA through 5′-3′ decay pathway (Katiyar-Agarwal et al., 2007).

C. elegans

Worms also exhibit transitivity in dsRNA induced RNAi by generating two distinct classes of siRNA, the primary siRNA and secondary siRNA (Sijen et al., 2001). The primary siRNA is generated by DCR-1 processing of initial dsRNA trigger, thus possesses the characteristics of a canonical siRNA, a 5′ phosphate and a 3′ hydroxyl group (Pak and Fire, 2007; Sijen et al., 2007). The few primary siRNAs loaded into RDE-1 trigger the production of far more abundant secondary siRNAs by the RdRP, RRF-1(Smardon et al., 2000). These secondary siRNAs are associated with SAGO-1, SAGO-2 or CSR-1 containing RISC and function to down-regulate their targets by an unknown mechanism (Aoki et al., 2007; Yigit et al., 2006).

The secondary siRNA in worms differs from that in plants in several aspects. First, *C elegans* secondary siRNAs are structurally different from primary siRNAs; they carry a di- or triphophate group at their 5′ end characteristic of transcription rather than monophosphate that is hallmark of dicing (Pak and Fire, 2007; Sijen et al., 2007). Secondly, worm secondary siRNAs are primarily antisense to the target message, in contrast to plant secondary siRNAs which arise from both sense and antisense strands

(Sijen et al., 2001; Tijsterman et al., 2002). Finally, whereas in plants the secondary siRNAs derive from both upstream and downstream regions of the trigger sequence, in *C. elegans* the spreading is strongly biased toward the upstream region (Alder et al., 2003; Sijen et al., 2001). These features of worm secondary siRNAs strongly suggest that they are produced directly by transcription, without a dsRNA intermediate or dicing.

Worms also possess other classes of small RNAs, including 21U-RNAs, 26-mer siRNAs and tiny non-coding RNAs (tncRNA). 21U-RNAs originate from a few distinct regions of chromosome IV (Ruby et al., 2006). They all start from uracil and bear 5′ monophosphate but blocked 3′ termini. Strikingly, all the 21U-RNA genomic loci share two upstream sequence motifs, which are well conserved between *C. elegans* and *C. briggsae*. On the contrary, not a single sequence among the > 10,000 21U-RNA is conserved between these two nematodes (Ruby et al., 2006). Together, these data suggest that 21U-RNA represent a distinct class of small RNAs which likely act *in cis* to regulate their own genomic loci. Very little is known about 26-mer siRNA population except that they are longer (26 nt in length) than usual siRNAs or miRNAs, always begin with guanosine, and like 21U RNA, 26-mer siRNAs has a 5′ monophosphate but blocked 3′ termini (Ruby et al., 2006). The previously named tiny non-coding RNAs (tncRNAs) which correspond to the antisense strands of the protein-coding transcripts are likely to be the endogenous secondary siRNAs, because they bear 5′ di- or triphosphate, signature of RdRP-catalyzed transcription (Ambros et al., 2003; Lim et al., 2003; Ruby et al., 2006).

2. microRNA

2.1 microHistory

The first miRNA, *lin-4*, was identified in 1993 in a genetic screen for mutants that disrupt the timing of post-embryonic development in *Caenorhabditis elegans* (Lee et al., 1993). Cloning of the locus revealed that *lin-4* produces a 22-nucleotide non-coding RNA, rather than a protein-coding mRNA (Lee et al., 1993). *lin-4* represses the expression of *lin-14*, which encodes a nuclear protein (Lee et al., 1993; Wightman et al., 1993) whose concentration must be reduced for worms to progress from their first larval stage to the second (Rougvie, 2005). The negative regulation of *lin-14* by *lin-4* requires partial complementarity between *lin-4* and sites in the 3′-untranslated region (UTR) of *lin-14* mRNA (Ha et al., 1996; Olsen and Ambros, 1999). It was not until 2000 that a second miRNA, *let-7*, was discovered, again in worms (Reinhart et al., 2000). *let-7* functions in a manner similar to *lin-4*, repressing the expression of the *lin-41* and *hbl-1* mRNAs by binding to their 3′ UTRs (Lin et al., 2003; Reinhart et al., 2000; Slack et al., 2000; Vella et al., 2004). *let-7* is conserved throughout metazoans (Pasquinelli et al., 2000), and the discovery of *let-7* (Reinhart et al., 2000), together with the subsequent large scale searches for additional miRNAs, established miRNAs as a new and large class of ribo-regulators (Lagos-Quintana et al., 2001; Lau et al., 2001; Lee and Ambros, 2001), and fueled speculation that tiny RNAs are a major feature of the gene regulatory networks of animals. Now over 5300 miRNAs have been identified in plants, animals and viruses, as reported by miRBase (Release 10.1, Dec 2007), a public database that stores experimentally validated miRNAs and their homologues (Griffiths-Jones, 2004; Griffiths-Jones et al., 2006). There are currently 541 human miRNAs deposited in the miRBase, predicted to regulate as many as 1/3 of all human genes (Lewis et al., 2005; Xie et al., 2005). Moreover, recent studies have suggested that number of miRNAs in a vertebrate genome can be as many as 800-1000 (Bentwich et al., 2005; Berezikov et al., 2005). Besides, a number of computational algorisms predicted human miRNA candidate genes to be a striking 3,000-5,000 (Berezikov et al., 2006; Hertel and Stadler, 2006; Sheng et al., 2007), albeit a large portion of which remain to be validated.

2.2 microMaturation

Most miRNAs are transcribed by RNA polymerase II as primary miRNAs (pri-miRNAs), which range from hundreds to thousands of nucleotides in length (Cai et al., 2004; Lee et al., 2004a; Parizotto et al., 2004), although a few are transcribed by RNA polymerase III (Borchert et al., 2006). The majority (>80%) of the known mammalian miRNAs are within the introns of protein-coding genes, rather than in their own unique transcription units (Kim and Kim, 2007; Rodriguez et al., 2004). Intronic miRNAs usually lie in the same orientation as, and are coordinately expressed with, the pre-mRNA in which they reside; that is, they share a single primary transcript (Rodriguez et al., 2004; Baskerville and Bartel, 2005), and miRNA processing appears to occur before splicing catalysis (Kim and Kim, 2007).

Figure I-1

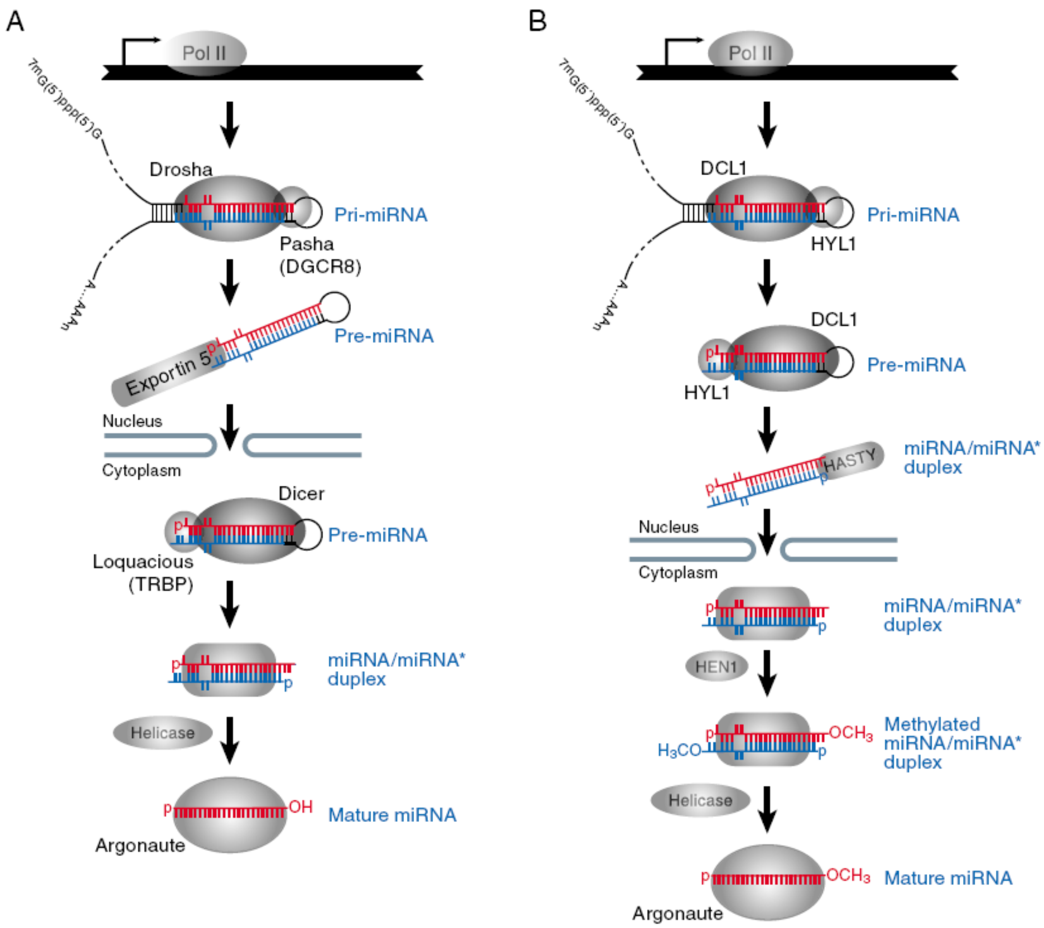
A
Pol II
7mG(5')ppp(5')G
Drosha
Pri-miRNA
Pasha
(DGCR8)
A...AAAn
Pre-miRNA
Exportin 5
Nucleus
Cytoplasm
Dicer
Pre-miRNA
Loquacious
(TRBP)
miRNA/miRNA*
duplex
Helicase
Mature miRNA
OH
Argonaute
B
Pol II
DCL1
Pri-miRNA
HYL1
DCL1
Pre-miRNA
HYL1
HASTY
miRNA/miRNA*
duplex
Nucleus
Cytoplasm
miRNA/miRNA*
duplex
HEN1
H3CO
OCH3
Methylated
miRNA/miRNA*
duplex
Helicase
Mature miRNA
Argonaute

Figure Legend I-1. The miRNA biogenesis pathway. (A) Animal and (B) plant miRNA biogenesis. Mature miRNAs are indicated in red, whereas the miRNA* strands are in blue.

Animal microMaturation

In animals, two processing steps yield mature miRNAs (Figure 1A). Each step is catalyzed by a ribonuclease III (RNase III) endonuclease together with a double-stranded RNA-binding domain (dsRBD) protein partner. First, Drosha, a nuclear RNase III, cleaves the flanks of pri-miRNA to liberate an ~70- nucleotide stem loop, the precursor miRNA (pre-miRNA) (Lee et al., 2002; Lee et al., 2003; Denli et al., 2004; Gregory et al., 2004; Han et al., 2004; Landthaler et al., 2004). A typical animal pri-miRNA comprises (1) an imperfect stem region of ~33 bp in length, that is about one helical turn longer than the slightly more than two helical turns of the stem of the resulting pre-miRNA; (2) a large terminal loop (≥10 nucleotides) in the hairpin; and (3) long 5′ and 3′ single-stranded RNA (ssRNA) extensions at the base of the future pre-miRNA (Lee et al., 2003; Zeng and Cullen, 2005; Zeng et al., 2005). A recent report demonstrated that whereas the flanking ssRNA segments are critical for Drosha processing, the terminal loop is unessential (Han et al., 2006). The cleavage site is largely determined by the distance from the ssRNA-stem loop junction (SD junction) (Han et al., 2006). Accurate and efficient pri-miRNA processing by Drosha requires a dsRBD protein, known as Pasha in *Drosophila*, Pash-1 in *C. elegans* and DGCR8 in mammals (Denli et al., 2004; Gregory et al., 2004; Han et al., 2004a; Landthaler et al., 2004). A detailed biochemical analysis supports a model where DGCR8 functions as a molecular anchor by directly binding the pri-miRNA at the SD junction, and subsequently positioning the processing center of Drosha for precise endonuleolytic cleavage (Han et al., 2006). The resulting pre-miRNA has 5′

phosphate and 3′ hydroxy termini, and two- or three nucleotide 3′ single-stranded overhanging ends, all of which are characteristics of RNase III cleavage of dsRNA. Thus, Drosha cleavage defines either the 5′ or the 3′ end of the mature miRNA. (The mature miRNA resides in the 5′ arm of some pre-miRNA and in the 3′ arm in others.) The pre-miRNA is then exported from nucleus to cytoplasm by Exportin 5/RanGTP, which specifically recognizes the characteristic end structure of pre-miRNAs (Bohnsack et al., 2004; Lund et al., 2004; Yi et al., 2003; Zeng and Cullen, 2004).

In the cytoplasm, a second RNase III, Dicer, together with its dsRBD protein partner, Loquacious (Loqs) in *Drosophila* or the *trans-activator RNA (tar)*-binding protein (TRBP) or PACT in humans, makes a pair of cuts that defines the other end of the mature miRNA, liberating an ~21-nucleotide RNA duplex (Bernstein et al., 2001; Chendrimada et al., 2005; Forstemann et al., 2005; Grishok et al., 2001; Hutvagner et al., 2001; Jiang et al., 2005; Ketting et al., 2001; Lee et al., 2006; Saito et al., 2005). This RNA duplex has essentially the same structure as a double-stranded siRNA, except that the mature miRNA is only partially paired to the miRNA* – the small RNA that resides on the side of the pre-miRNA stem opposite the miRNA – because the stems of pre-miRNAs are imperfectly double stranded. From the miRNA/miRNA* duplex, one strand, the miRNA, preferentially enters the protein complex that represses target gene expression, the RNA-induced silencing complex (RISC), whereas the other strand, the miRNA* strand, is degraded. The choice of strand relies on the local thermodynamic stability of the miRNA/miRNA* duplex – the strand whose 5′ end is less stably paired is loaded into the RISC (Khvorova et al., 2003; Schwarz et al., 2003). This thermodynamic difference arises, in part, because miRNAs tend to begin with uracil, and, in part, because miRNA/miRNA* duplexes contain mismatches and bulges that favor the miRNA strand being loaded into the RISC (Han et al., 2006). Recent deep sequencing efforts in *C. elegans* indicate that miRNA* species is present at about 1% of the frequency of the miRNA, which substantiate the asymmetric loading of miR/miR* duplex (Ruby et al., 2006).

In humans, an additional step in pre-miRNA processing has been reported for the miRNAs that reside in the 5′ arm of the precursor and exhibit extensive complementarity with their pairing miR* strand at the central region (Diederichs and Haber, 2007). After entering the cytoplasm, pre-miRNA binds to a preassembled complex comprising Ago2, Dicer and TRBP, the human RLC (Chendrimada et al., 2005; Gregory et al., 2005; Maniataki and Mourelatos, 2005). In this complex, Ago2, presumably loaded with unprocessed miRNA strand in the 5′ arm, directs an endonuleolytic cleavage of the 3′ arm harboring the miRNA* strand at around 10 nt from the 3′ terminus of the precursor. The resulting nicked hairpin is subsequently processed by Dicer, generating the miRNA/ nicked miRNA* duplex which is unwound by an unknown helicase activity.

Recently, an alternative processing pathway was identified for a distinct sub-group of miRNAs in *Drosophila*, C. *elegans* and mammals (Berezikov et al., 2007; Okamura et al., 2007; Ruby et al., 2007). These miRNAs exploit the pre-mRNA splicing machinery to generate a pre-miRNA directly, bypassing the processing of a pri-miRNA by Drosha. For these miRNAs, the pre-miRNA is at once the precursor of a mature miRNA and a compact, fully functional intron, hence the name, ‘mirtrons’.

Plant microMaturation

miRNA maturation in plants differs from the pathway in animals because plants lack a Drosha homolog (Figure 1B). Instead, the RNase III enzyme DICER-LIKE 1 (DCL1), which is homologous to animal Dicer, is required for miRNA maturation (Kurihara and Watanabe, 2004; Papp et al., 2003; Park et al., 2002; Reinhart et al., 2002; Xie et al., 2004). In plants, DCL1 is localized in the nucleus and can make both the first pair of cuts made by Drosha and the second pair of cuts made by animal Dicer. As for animal Dicer, a dsRNA-binding domain protein partner, HYL1, is required for efficient and accurate processing of the pri-miRNA (Han et al., 2004b; Hiraguri et al., 2005; Kurihara et al., 2006; Papp et al., 2003; Vazquez et al., 2004a). The resulting miRNA/miRNA* duplex is exported from the nucleus by HASTY (HST), the plant ortholog of Exportin 5, and completes its assembly into the RISC in the cytoplasm (Park et al., 2005; Peragine et al., 2004). Unlike animal miRNAs, which end with free 2´, 3´ hydroxyl groups, plant miRNAs have a methyl group on the 2´ position on the ribose of the last nucleotide (Li et al., 2005; Yang et al., 2006). The terminal methyl group is added by the nuclear *S*-adenosyl methionine (SAM)-dependent methyltranferase Hua Enhancer (HEN1), and the modification of the miRNA by HEN1 either protects the miRNA from further modification (e.g. uridylation) or degradation, or may facilitate its assembly into the RISC (Boutet et al., 2003; Li et al., 2005; Yu et al., 2005). In plants, RNA-dependent RNA polymerases may use small RNAs as primers to synthesize double-stranded RNA from aberrant single-stranded transcripts, raising the possibility that the terminal methoxy modification on miRNA serves to prevent miRNA from acting as primers.

2.3 The RISC directs gene silencing

The RISC carries out small RNA-directed gene silencing in both the miRNA and the RNAi pathways in plants and animals (Doench et al., 2003; Hammond et al., 2000; Hammond et al., 2001; Hutvagner and Zamore, 2002; Zeng et al., 2002). When the small RNA guide in the RISC pairs extensively to a target mRNA, the RISC functions as an endonuclease, cleaving the mRNA between the target nucleotides paired to bases 10 and 11 of the miRNA or siRNA. The core component of every RISC is a member of the Argonaute (Ago) protein family, whose members all contain a central PAZ domain (named after the family member proteins Piwi, Argonaute and Zwille) and a carboxy terminal PIWI domain. Structural studies show that the PIWI domain binds to small RNAs at their 5′ end, whereas the PAZ domain binds to the 3′ end of single-stranded RNAs (Lingel et al., 2004; Ma et al., 2005; Parker et al., 2004, 2005; Song et al., 2003; Yan et al., 2003). Moreover, the three-dimensional structure of the PIWI domain closely resembles that of RNase H, the enzyme that cleaves the RNA strand of an RNA-DNA hybrid (Nowotny et al., 2005; Song et al., 2004), and both structural and biochemical studies have confirmed that Argonaute is the target-cleaving endonuclease of the RISC (Baumberger and Baulcombe, 2005; Liu et al., 2004; Parker et al., 2005; Qi et al., 2005; Rand et al., 2004; Rivas et al., 2005; Song et al., 2004). Notably, a subpopulation of Argonaute proteins do not retain all the amino acids that are crucial for RISC catalytic activity, and thus cannot cleave a target RNA even when the small RNA guide is sufficiently complimentary to the target (Liu et al., 2004; Meister et al., 2004; Rivas et al., 2005). The RISC-associated proteins include the putative RNA-binding protein VIG (Vasa intronic gene), the Fragile-X related protein in *Drosophila*, the exonuclease Tudor-SN, the RNA recognition motif (RRM)-containing protein TNRC6B/KIAA1093 in human and several putative helicases and ribosomal proteins (Caudy et al., 2003; Caudy et al., 2002; Chendrimada et al., 2007; Hutvagner and Zamore, 2002; Ishizuka et al., 2002; Meister et al., 2005; Mourelatos et al., 2002; Robb and Rana, 2007). The molecular function of these proteins in RNA silencing is largely unknown.

2.4 microMechanism

miRNAs regulate their target genes via two main mechanisms: target mRNA cleavage and ‘translational repression’. (One example of miRNA induced translation activation has been reported very recently (Vasudevan et al., 2007). Because the biological significance of the phenomenon is yet to be proven, I won’t discuss it here.)

In plants, most miRNAs have perfect or near perfect complementarity to their mRNA targets (Rhoades et al., 2002). Upon binding to their mRNA targets, the miRNA-containing RISCs function as endonucleases, cleaving the mRNA (Llave et al., 2002b; Tang et al., 2003). Single miRNA-binding motifs are found both in the coding regions, such as the miR-166-targeting site in the *PHABULOSA* mRNA, and in the untranslated regions of miRNA-regulated plant mRNAs, such as the miR-156-targeting site in the *SPL4* mRNA, albeit mainly in coding sequences, perhaps because cleavage here most strongly inactivates translation of the mRNA into functional protein (Rhoades et al., 2002). At least eight animal miRNAs, miR-127, miR-136, miR-196, miR-431, miR-433-3p, miR-433-5p, miR-434-3p and miR-434-5, and two viral miRNAs, miR-BART2 and SVmiRNA, also act to cleave their targets (Davis et al., 2005; Mansfield et al., 2004; Pfeffer et al., 2004; Sullivan et al., 2005; Yekta et al., 2004)

In animals, miRNAs typically bind to the 3′ untranslated region (UTR) of their target mRNAs through sequences that are only partially complementary. The 5′ region of the miRNA (roughly nucleotides 2–8) contributes disproportionately to target-RNA binding (Brennecke et al., 2005; Chen and Rajewsky, 2006; Lai, 2004; Lewis et al., 2005; Lewis et al., 2003; Stark et al., 2005; Xie et al., 2005). This ‘seed region’ is the primary determinant of binding specificity, making miRNAs surprisingly promiscuous: many miRNAs regulate hundreds of different mRNAs (Lewis et al., 2005; Xie et al., 2005). A common consequence of such seed-mediated miRNA binding is a decrease in the amount of the protein encoded by the target mRNA. However, the precise molecular mechanism of miRNA mediated translational repression remains controversial. In fact, distinct mechanisms of repression have been proposed by different laboratories for different miRNA-target pairs and even for the same miRNA studied with remarkably similar experiments.

Early studies in *C. elegans* suggest that miRNAs block protein synthesis after the initiation of translation, because the abundance of repressed mRNA in polyribosomes appear to be unaltered by miRNA binding (Olsen and Ambros, 1999). Studies in cultured mammalian cells provided additional support for this model, as a significant fraction of miRNA target mRNA remains associated with polyribosomes, despite a large decrease in protein accumulation from these mRNAs (Petersen et al., 2006). Moreover, the polysomes with which miRNAs associate appear to be translationally active, suggesting that the observed translational inhibition reflects either ribosomes departing the mRNA during protein synthesis or targeted destruction of nascent polypeptide chains as they emerge from the polypeptide exit tunnel (Maroney et al., 2006; Nottrott et al., 2006). Yet, other studies in flies and mammals are at odds with these findings, suggesting that miRNAs do, in fact, block mRNA translation at the initiation step (Humphreys et al., 2005; Pillai et al., 2005). In these experiments, miRNA-directed inhibition requires the 7-methyl guanosine cap, implying a role for miRNA in blocking recognition of the cap by the translation initiation factor eIF4E.

Controversy also dogs the link between miRNA-directed mRNA repression and target mRNA degradation. Some studies report that mRNA levels are unchanged upon miRNA targeting, but others observe destruction of the mRNA upon miRNA binding, perhaps as a consequence of deadenylation and subsequent decapping by standard mRNA decay enzymes (Bagga et al., 2005; Behm-Ansmant et al., 2006; Giraldez et al., 2006; Lim et al., 2005; Rehwinkel et al., 2005; Standart and Jackson, 2007; Wu et al., 2006). Argonaute proteins, miRNAs, and their mRNA targets, all accumulate in cytoplasmic "Processing bodies" (P-bodies) that function to store and to degrade translationally silenced mRNA (Liu et al., 2005; Pillai et al., 2005; Sen and Blau, 2005). Though there are lines of evidence suggesting a direct role for P-bodies in miRNA-mediated silencing, other data suggest that the movement of miRNA-repressed mRNAs to P-bodies is a consequence, not a cause, of miRNA-directed translational repression (Behm-Ansmant et al., 2006; Chu and Rana, 2006; Ding et al., 2005; Jackson and Standart, 2007). For at least a subgroup of miRNAs, miRNA-mediated translational repression is reversible, with the mRNA shuttling between P-bodies and actively translating polysomes, and the P-body serving as a temporary refuge for miRNA-repressed, translationally quiescent mRNAs (Bhattacharyya et al., 2006).

Despite the diversity of modes proposed for miRNA-directed translational inhibition, little was known about the molecular basis of any until recently. Several studies conducted in human and *Drosophila* systems provide long overdue insight into how miRNAs decrease the rate of translational initiation. Kiriakidou and colleagues identify within human Argonaute2 (Ago2) protein a motif similar to eukaryotic initiation factor 4E (eIF4E) which is required for the direct binding of Ago2 to a cap-analog resin as well as miRNA-directed translational repression at the initiation step (Kiriakidou et al., 2007). Thus, the authors propose a straightforward model in which Ago2, bound to the mRNA target by a miRNA, competes with eIF4E for the mRNA cap, reducing the translation of the mRNA target into protein. Chendrimada et al on the other hand reveal a role for a different translation factor, the protein eIF6, in miRNA-directed translational repression (Chendrimada et al., 2007). eIF6 has long been known to bind to free 60S ribosomal subunits, preventing their joining the 40S subunit to generate translationally competent 80S ribosome particles (Ceci et al., 2003). By identifying eIF6 as a RISC- associating protein, the depletion of which impair the miRNA-mediated mRNA silencing, Chendrimada et al support a distinct model that miRNAs block translation by recruiting eIF6 to their mRNA targets; eIF6 would then antagonize the joining of the two ribosomal subunits on the miRNA-regulated mRNA.

Two other groups successfully recapitulate some aspects of miRNA-directed translational repression using cell-free lysate systems. Thermann and colleagues used lysate from *Drosophila* embryos to study the silencing of a reporter mRNA bearing in its 3´ UTR six copies of an authentic miR-2 binding site (Thermann and Hentze, 2007). They observed a reduction in 80S ribosome assembly on the reporter mRNA, suggesting inhibition at the translation initiation step. Interestingly, some larger messenger ribonucleoprotein particles (mRNPs) formed on the reporter mRNA upon miRNA binding, even when polysome formation was blocked. The authors refer to these particles as ‘pseudo-polysomes’, the identity of which awaits to be elucidated in the future. Contemporaneously, Wakiyama and colleagues established a cell-free system with extracts prepared from human HEK293F cells overexpressing miRNA pathway components (Wakiyama et al., 2007). In their system, both the cap and poly(A) tail are required for let-7 directed translational repression. They also observed the let-7 induced deadenylation of the targeted mRNAs. Based on their data, Wakiyama et al propose the role of let-7 to disrupt the cap-poly(A) synergy that is required for efficient translation by deadenylation. However, it is as well possible that deadenylation is the result rather than the cause of translational repression.

Clearly, only the tip of the iceberg has been revealed about the molecular basis of miRNA-directed translational repression. It is very likely that mechanisms of miRNA-directed mRNA regulation differ among organisms, among miRNAs, and even among different developmental stages. Alternatively, the location of miRNA-binding sites within an mRNA or the position of mismatches and bulges within the miRNA-binding sites may influence the mechanism by which productive translation is repressed. Supporting this idea, a recent screen for suppressors of miRNA-mediated regulation in *Drosophila* cells revealed that different miRNA-targeted mRNAs elicit different requirement for decapping activators in order to be silenced (Eulalio et al., 2007). Their results suggest that even in a single cell type, miRNAs mediate post-transcriptional gene silencing by more than one mechanism.

3. piRNA

Piwi-interacting RNA (piRNA) pathway is the most recently discovered small RNA pathway in animals (Aravin et al., 2001). piRNAs are 24-30 nt in length, slightly longer than siRNAs and miRNAs. Indicated by their name, this class of small RNAs associate with Piwi clade of argonaute proteins.

The Argonaute superfamily can be divided into two clades: the Ago clade and the Piwi clade. All plant Argonaute proteins and the single fission yeast family member belong to the Ago clade, whereas ciliates and slime molds only contain members of the Piwi clades. The genomes of multicellular animals on the other hand encode multiple members from both Piwi and Ago clades. Like members of Ago clade that function though their small RNA partner, miRNAs and siRNAs , Piwi clade proteins associate specifically with piRNAs and play roles in control of mobile genetic elements and germline development in animals.

Most *Drosophila* piRNAs match to repetitive elements in the genome, hence also called repeat-associated small RNA (rasiRNA) (Aravin et al., 2003). Large-scale sequencing of small RNAs in fly enabled identification of discrete genomic loci (piRNA clusters) that give rise to most piRNAs (Brennecke et al., 2007). These piRNA clusters range from several to hundreds of kilobases in length and reside exclusive in pericentromeric or telomeric heterochromatin. Similar piRNA loci also exist in mammals and zebrafish (Aravin et al., 2006; Aravin et al., 2007; Girard et al., 2006; Houwing et al., 2007; Lau et al., 2006). In particular, mammalian piRNAs can be divided into two populations, the prepachytene piRNAs and pachytene piRNAs (Aravin et al., 2007). Prepachytene piRNAs accumulate in germ cells before meiosis. A large fraction of them correspond to repetitive elements similar to those in *Drosophila* and zebrafish. In contrast, the pachytene piRNAs, which originate from different loci from prepachytene piRNA and appear around the pachytene stage of meiosis, are relatively depleted of repeats, suggesting piRNA may play different roles at different stages of germline development.

The biogenesis of piRNAs is not yet fully understood. However, piRNAs are likely produced from long single-stranded precursor RNAs instead of dsRNA because of their Dicer-independent and profoundly strand-biased accumulation (Houwing et al., 2007; Vagin et al., 2006). Cloning of piRNAs associated with different Piwi proteins in fly support a model whereby piRNAs are generated by reciprocal cycles of Piwi-catalyzed endonucleolytic cleavage followed by 3′ trimming by an exonulease (Brennecke et al., 2007; Gunawardane et al., 2007).

The so called Ping-Pong amplification loop likely begins with an initial pool of piRNAs produced from antisense strand of transposons and incorporated into Aubergine (Aub) or Piwi (Figure 2). When encountering the transposon mRNA (the sense strand), Aub/Piwi RISC cleaves between the target nucleotides paired to bases 10 and 11 of their associated piRNA. The cleavage event not only inactivates the mRNA, but also creates the 5′ end of the Ago3 associated piRNAs. A yet-to-be-identified 3′-5′ exonuclease subsequently trims the 3′ end, followed by the adding of a 2′-O-methyl group by the Hen1 methyltransferase. The mature piRNA-Ago3 complex then in turn cleaves the antisense strand of transposon, generating the 5′ end of additional Aub/Piwi associated piRNAs from the original place to form a self-amplifying loop. This model is supported by the facts that (1) Piwi and Aub predominantly complex with piRNAs antisense to the transposons, whereas Ago3 incorporate sense piRNAs; (2) in contrast to strong preference of uracil at position 1 for piRNAs associated with Aub and Piwi, Ago3-incorporating piRNAs typically contain an adenosine at nucleotide 10; (3) multiple pairs can be found in which the first 10 nucleotides of piRNAs in Aub and in Ago3 are perfectly complementary to each other (Brennecke et al., 2007; Gunawardane et al., 2007). Signatures of such amplification loop are also observed in zebrafish and mammalian prepachytene piRNAs, indicating the biogenesis pathway is conserved among animals (Aravin et al., 2007; Houwing et al., 2007).

Figure I-2

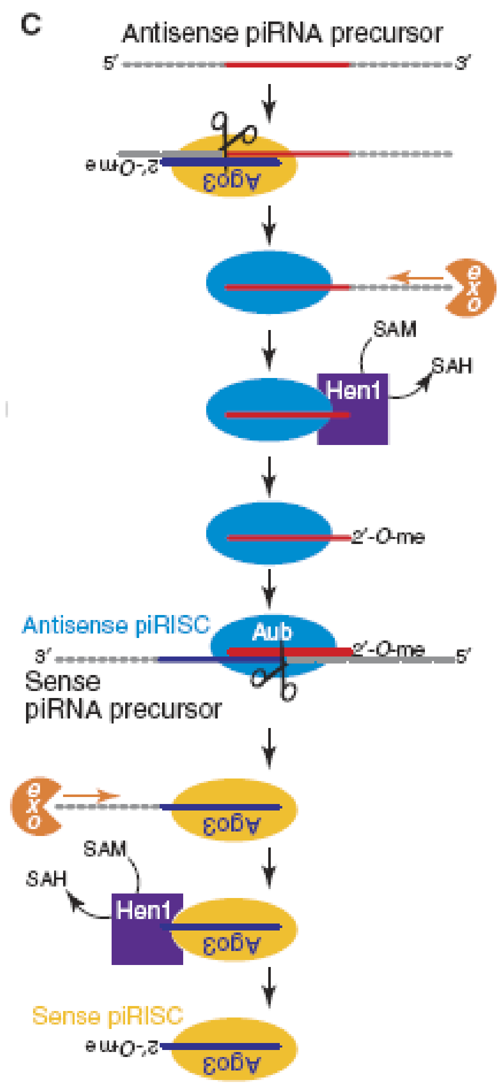
C
Antisense piRNA precursor
5′
3′
2′-O-me
Ago3
exo
SAM
SAH
Hen1
2′-O-me
Antisense piRISC
Aub
3′
5′
Sense
piRNA precursor
Sense piRISC

Figure legend I-2. Speculative model for the production of piRNA in animal germ cells (From Matranga and Zamore 2007, *Current Biology*).

CHAPTER II: RISC Assembly Defects in the *Drosophila* RNAi Mutant *armitage*

Disclaimer: The following chapter is a collaborative effort. Experiments for Figure 1, 2 (A, B and D panel), 6 (C and D panel in collaboration with YT), and supplemental figure 3 (A panel) were done by the author. Experiments for the remaining figures were done by Yukihide Tomari (Figure 3,4, 6 and S1), Benjamin Haley (Figure S2, S3B-D, Table S1), and Birgit S. Koppetsch (Figure 1C).

Summary

The putative RNA helicase, Armitage (Armi), is required to repress *oskar* translation in *Drosophila* oocytes; *armi* mutant females are sterile and *armi* mutations disrupt anteroposterior and dorsoventral patterning. Here, we show that *armi* is required for RNAi. Lysates from *armi* mutant ovaries are defective for RNAi in vitro. Native gel analysis of protein-siRNA complexes in wild-type and *armi* mutant ovary lysates suggests that *armi* mutants support early steps in the RNAi pathway but are defective in the production of active RNA-induced silencing complex (RISC), which mediates target RNA destruction in RNAi. Our results suggest that *armi* is required for RISC maturation.

Introduction

In eukaryotes, long double-stranded RNA (dsRNA) silences genes homologous in sequence, a process termed RNA interference (RNAi) (Fire et al., 1998). RNAi and other examples of RNA silencing have been observed in animals, plants, protozoa, and fungi (Caplen et al., 2001; Cogoni and Macino, 1997; Kennerdell and Carthew, 1998; Lohmann et al., 1999; Ngo et al., 1998; Sanchez Alvarado and Newmark, 1999; Schramke and Allshire, 2003; Volpe et al., 2002; Waterhouse et al., 1998; Wianny and Zernicka-Goetz, 2000). In plants, green algae, and invertebrates, RNAi defends the genome against mobile genetic elements, such as transposons and viruses, whose expression and activity increase in RNAi-defective mutants (Aravin et al., 2001; Dalmay et al., 2000; Galiana-Arnoux et al., 2006; Ketting et al., 1999; Mourrain et al., 2000; Ratcliff et al., 1999; Sijen and Plasterk, 2003; Tabara et al., 1999; van Rij et al., 2006; Wang et al., 2006).

Long dsRNA is converted by Dicer, a multidomain ribonuclease III enzyme, into small interfering RNAs (siRNAs) (Bernstein et al., 2001; Billy et al., 2001; Zamore et al., 2000), which serve as the specificity determinants of the RNAi pathway (Elbashir et al., 2001b; Hamilton and Baulcombe, 1999; Hammond et al., 2000; Zamore et al., 2000). siRNAs direct mRNA cleavage as part of a protein-siRNA complex called the RNA-induced silencing complex (RISC) (Hammond et al., 2000; Hammond et al., 2001). Members of the Argonaute family of proteins are core components of RISC or RISC-like complexes in flies (Hammond et al., 2001), worms (Hutvagner et al., 2004; Tabara et al., 2002), and humans (Caudy et al., 2002; Hutvagner and Zamore, 2002; Martinez et al., 2002; Mourelatos et al., 2002) and are required genetically for RNA silencing in every organism where their function has been studied (Catalanotto et al., 2002; Caudy et al., 2002; Doi et al., 2003; Fagard et al., 2000; Grishok et al., 2000;

Morel et al., 2002; Pal-Bhadra et al., 2002; Tabara et al., 1999; Williams and Rubin, 2002).

Genetic studies also reveal the importance of helicase-domain proteins in the RNAi pathway. Putative DEA(H/D)-box helicases are required for posttranscriptional gene silencing (PTGS) in the green alga *Chlamydomonas reinhardtii* (Wu-Scharf et al., 2000) and RNAi in *C. elegans* (Tabara et al., 2002; Tijsterman et al., 2002). In cultured *Drosophila* S2 cells, the putative helicase Dmp68 is a component of affinity-purified RISC (Ishizuka et al., 2002). Similarly, a putative DEAD-box RNA helicase, Gemin3, is a component of human RISC (Hutvagner and Zamore, 2002). Dicer, too, contains a putative ATP-dependent RNA helicase domain (Bernstein et al., 2001). Except for Dicer, no specific biochemical function in RNAi has been ascribed to any of these helicase proteins.

armitage (*armi*) was identified in a screen for maternal effect mutants that disrupt axis specification in *Drosophila* (Cook et al., 2004). Armitage protein (Armi) is a member of a family of putative ATP-dependent helicases distinct from the DEA(H/D) box proteins (Koonin, 1992). Armi is homologous across its putative helicase domain to SDE3 (Cook et al., 2004), which is required for PTGS in *Arabidopsis* (Dalmay et al., 2001). Because PTGS in plants is mechanistically related to RNAi in animals, Armi may play a role in RNAi in flies. Here, we show that *armi* is required for RNAi. Lysates from *armi* mutant ovaries are defective for RNAi in vitro. Native gel analysis of protein-siRNA complexes in wild-type and *armi* mutant ovary lysates suggests that *armi* mutants support early steps in the RNAi pathway but are defective in the production of the RISC. Our results suggest that *armi* is required for the assembly of siRNA into functional RISC.

Results

Ovary Lysate Recapitulates RNAi In Vitro

Drosophila syncitial blastoderm embryo lysate has been widely used to study the RNAi pathway (Tuschl et al., 1999). However, *armi* flies lay few eggs, making it difficult to collect enough embryos to make lysate. To surmount this problem, we prepared lysates from ovaries manually dissected from wild-type or mutant females. Approximately 10 µl of lysate can be prepared from ~ 50 ovaries.

We used the well-characterized siRNA-directed mRNA cleavage assay (Elbashir et al., 2001b; Elbashir et al., 2001c) to evaluate the capacity of ovary lysate to support RNAi in vitro. Incubation in ovary lysate of a 5′ ^{32}P-cap-radiolabeled firefly luciferase mRNA target with a complementary siRNA duplex yielded the 5′ cleavage product diagnostic of RNAi (Figure 1). siRNAs containing 5′ hydroxyl groups are rapidly phosphorylated in vitro and in vivo, but modifications that block phosphorylation eliminate siRNA activity (Chiu and Rana, 2002; Martinez et al., 2002; Nykanen et al., 2001; Saxena et al., 2003; Schwarz et al., 2002). Replacing the 5′ hydroxyl of the antisense siRNA strand with a 5′ methoxy group completely blocked RNAi in the ovary lysate (Figure 1A). In *Drosophila*, siRNAs bearing a single 2′-deoxy nucleotide at the 5′ end are poor substrates for the kinase that phosphorylates 5′ hydroxy siRNAs (Nykanen et al., 2001). A comparison of initial cleavage rates shows that in ovary lysate, target cleavage was slower for siRNAs with a 2′-deoxy nucleotide at the 5′ end of the antisense strand than for standard siRNAs (Figure 1B). Furthermore, the rate of target cleavage was fastest when the siRNA was phosphorylated before its addition to the reaction (Figure 1B). A similar enhancement from pre-phosphorylation was reported for siRNA injected into *Drosophila* embryos (Boutla et al., 2001). We conclude that lysates from *Drosophila* ovaries faithfully recapitulate RNAi directed by siRNA duplexes.

armi **Ovary Lysates Are Defective in RNAi**

In contrast to wild-type, lysates prepared from *armi*$^{72.1}$ ovaries do not support siRNA-directed target cleavage in vitro: no cleavage product was observed in the *armi*$^{72.1}$ lysate after 2 hr (Figure 2A). This result was observed for more than ten independently prepared lysates. To determine if the RNAi defect was allele specific, we tested ovaries from *armi*^{1}. Phenotypically, this allele is weaker than *armi*$^{72.1}$ in its effects on both male fertility (above) and oogenesis. For *armi*$^{72.1}$ females, 92% of the eggs lacked dorsal appendages, compared to 67% for *armi*^{1} eggs, and some *armi*^{1} eggs had wild-type or partially fused dorsal appendages (Figure 2B). Consistent with its weaker phenotype, the *armi*^{1} allele showed a small amount of RNAi activity in vitro (Figure 2C). The two alleles were analyzed together at least four times using independently prepared lysates. In all assays, total protein concentration was adjusted to be equal. Lysate from the revertant allele, *armi*^{rev}, which has wild-type dorsal

Figure II-1

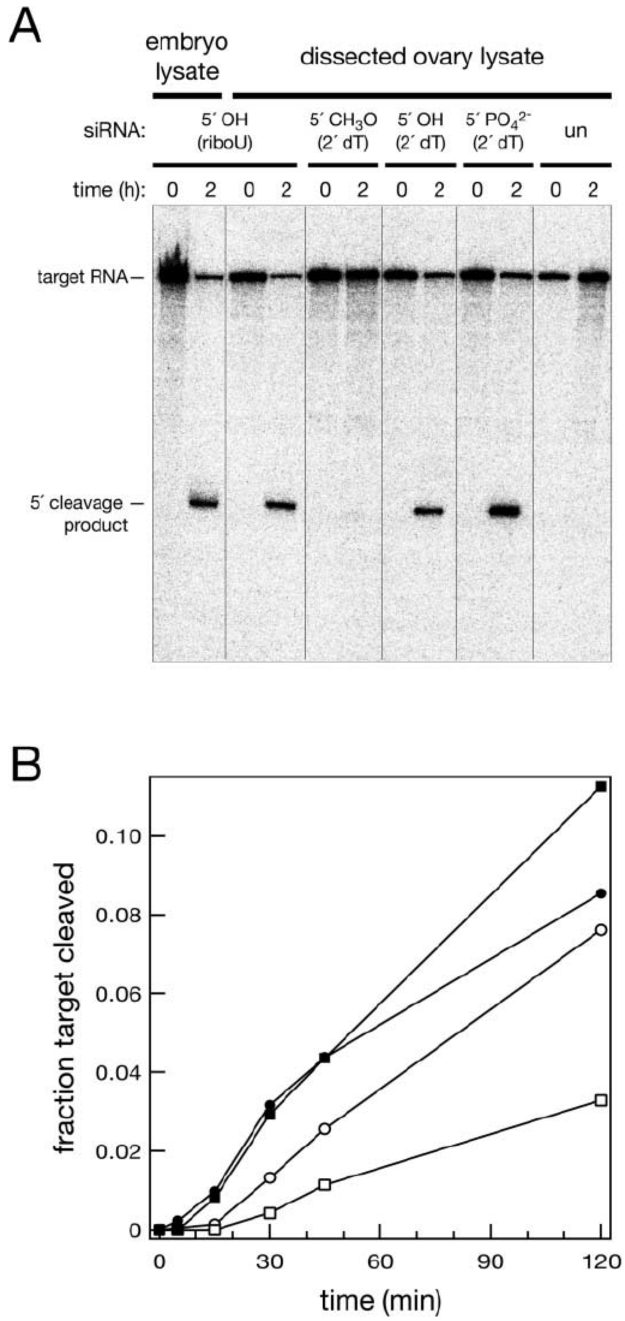
A
embryo lysate
dissected ovary lysate
siRNA:
5′ OH (riboU)
5′ CH3O (2′ dT)
5′ OH (2′ dT)
5′ PO4 2- (2′ dT)
un
time (h): 0 2 0 2 0 2 0 2 0 2 0 2
target RNA
5′ cleavage product
B
fraction target cleaved
0.10
0.08
0.06
0.04
0.02
0
0 30 60 90 120
time (min)

Figure Legend II-1. *Drosophila* Ovary Lysate Can Recapitulate RNAi In Vitro (A) RNAi reactions in embryo and ovary lysates using complementary siRNA duplexes (with 5′ modifications) or an unrelated siRNA (un). (B) mRNA cleavage rate in ovary lysate using 5′ modified siRNA. Filled squares, 5′ PO_4^{2-} (2′ dT); filled circles, 5′ PO_4^{2-} (2′ riboU); open squares, 5′ OH (2′ dT); open circles, 5′ OH (2′ riboU).

appendages, showed robust RNAi, demonstrating that the RNAi defect in the mutants is caused by mutation of *armi*, not an unlinked gene.

armi **Ovary Lysates Are Impaired in RISC Assembly**

The rate of target cleavage was much slower for $armi^{1}$ than for wild-type (Figure 2D). Since the rate of target cleavage in this assay usually reflects the concentration of RISC (Schwarz et al., 2003), we hypothesized that *armi* mutants are defective in RISC assembly. To test this hypothesis, we developed a method to measure RISC that requires less lysate than previously described techniques (Figure 3A). Double-stranded siRNA was incubated with ovary lysate in a standard RNAi reaction. To detect RISC, we added a 5′ ^{32}P-radiolabled, 2′-*O*-methyl oligonucleotide complementary to the antisense strand of the siRNA. Like target RNAs, 2′-*O*-methyl oligonucleotides can bind to RISC containing a complementary siRNA, but unlike RNA targets, they cannot be cleaved and binding is essentially irreversible (Hutvagner et al., 2004). RISC/2′-*O*-methyl oligonucleotide complexes were then resolved by electrophoresis through an agarose gel.

To validate the method, we examined RISC formation in embryo lysate. Four distinct complexes (C1, C2, C3, C4) were formed when siRNA was added to the reaction (Supplemental Figure S1A). Formation of these complexes required ATP and was disrupted by pre-treatment of the lysate with the alkylating agent *N*-ethylmaleimide (NEM), but it was refractory to NEM treatment after RISC assembly; these are all properties of RNAi itself (Nykanen et al., 2001). No complex was

Figure II-2

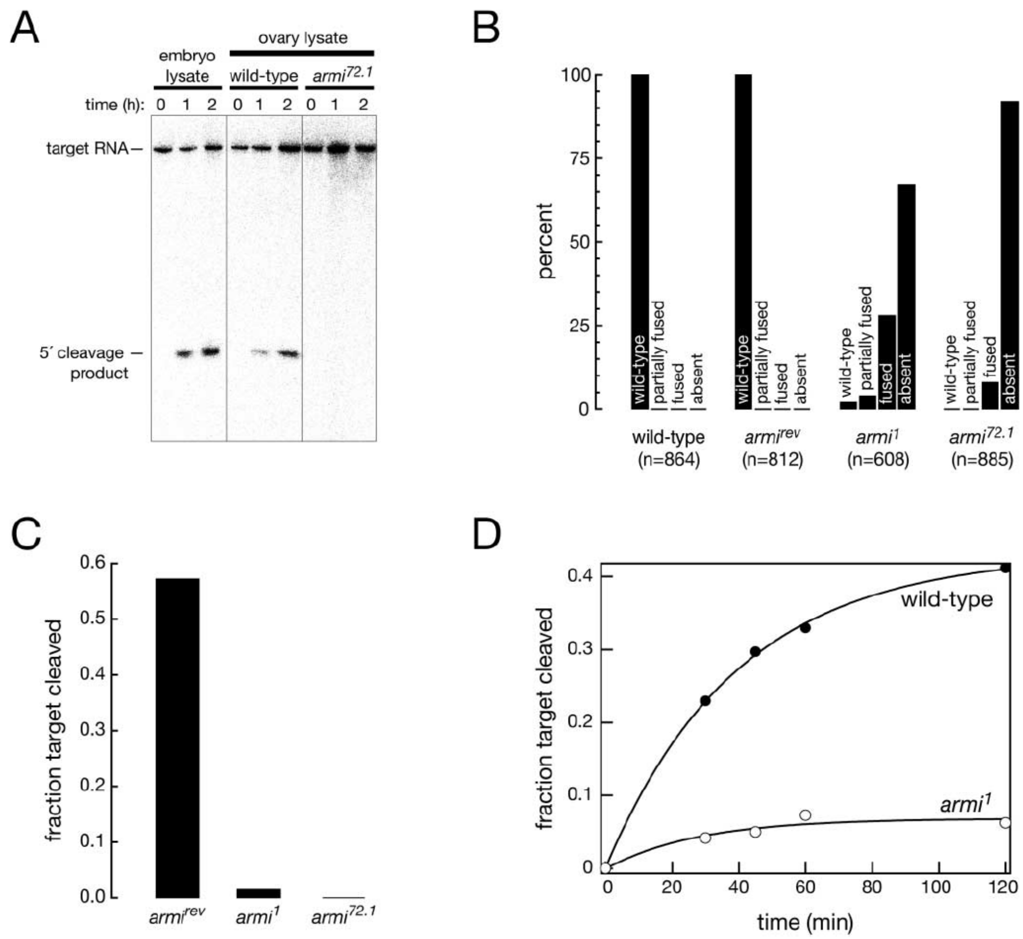
A
embryo lysate
ovary lysate
wild-type
armi72.1
time (h): 0 1 2 0 1 2 0 1 2
target RNA
5′ cleavage product
B
percent
100
75
50
25
0
wild-type
partially fused
fused
absent
wild-type (n=864)
armirev (n=812)
armi1 (n=608)
armi72.1 (n=885)
C
fraction target cleaved
0.6
0.5
0.4
0.3
0.2
0.1
0.0
armirev
armi1
armi72.1
D
fraction target cleaved
0.4
0.3
0.2
0.1
0
wild-type
armi1
0 20 40 60 80 100 120
time (min)

Figure Legend II-2. *armi* Ovary Lysates Are Defective in RNAi (A) RNAi reactions in lysates from 0–2 hr embryos, wild-type or *armi*$^{72.1}$ mutant ovaries. (B) Dorsal appendage phenotype was assessed for alleles of *armi*. (C) The fraction of target mRNA cleaved after 2 hr in an RNAi reaction using ovary lysates from *armi* alleles. (D) mRNA cleavage rate in wild-type and *armi*^{1} ovary lysates programmed with siRNA.

observed with an siRNA unrelated to the 2′-*O*-methyl oligonucleotide (Supplemental Figure S1A, “un”). The amount of complex formed by different siRNA sequences correlated well with their capacity to mediate cleavage (data not shown). The four complexes were also detected in wild-type ovary lysate (Supplemental Figure S1B), suggesting that the same RNAi machinery is used during oogenesis and early embryogenesis. The lower amount of RISC formed in ovary compared to embryo lysates can be explained by the lower overall protein concentration of ovary lysates.

We used the 2′-*O*-methyl oligonucleotide/native gel assay to analyze RISC assembly in *armi* mutant ovary lysates. *armi* mutants were deficient in RISC assembly. Representative data are shown in Figure 3B and quantitative results from four independent assays in Figure 3C. The extent of the deficit correlated with allele strength: less C3/C4 complex formed in lysate from the strong $armi^{72.1}$ allele than from $armi^{1}$ (Figures 3B and 3C). Compared to the phenotypically wild-type $armi^{rev}$, >10-fold less RISC was produced in $armi^{72.1}$.

The defect in RISC assembly in *armi* mutants is similar to that observed in lysates from aub^{HN2} ovaries (Figures 3B and 3C). *aub* mutants do not support RNAi following egg activation and fail to silence the *Ste* locus in testes (Kennerdell et al., 2002; Schmidt et al., 1999), and lysates from aub^{HN2} ovaries do not support RNAi in vitro (data not shown). Since RISC assembly in vitro was not detectable in aub^{HN2} lysates, our data suggest that Aub might be the primary Argonaute protein recruited to exogenous siRNA in *Drosophila* ovaries, or alternatively some component(s) of the

Figure II-3

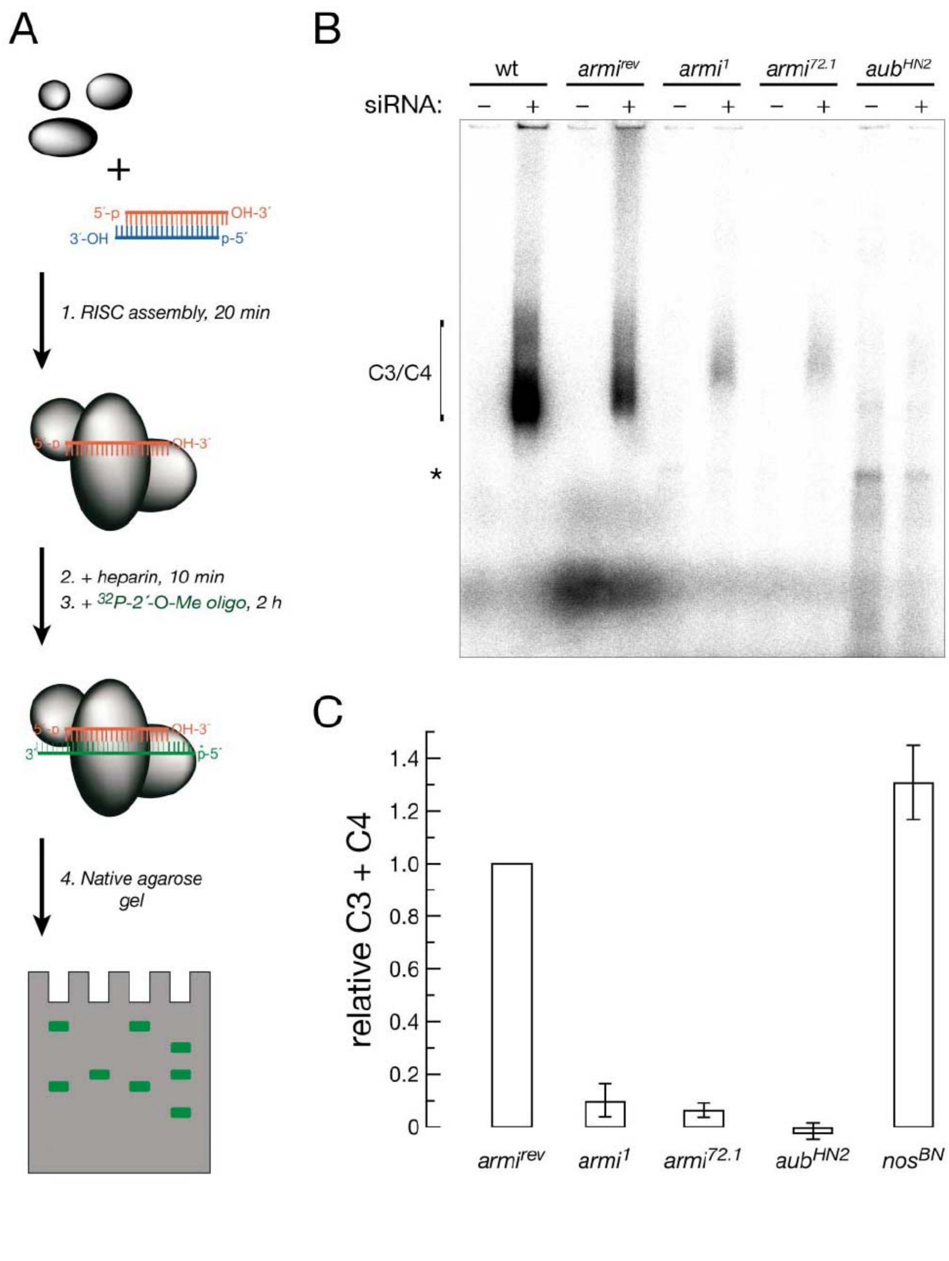
A
1. RISC assembly, 20 min
2. + heparin, 10 min
3. + 32P-2´-O-Me oligo, 2 h
4. Native agarose gel
B
wt
armi^rev
armi^1
armi^72.1
aub^HN2
siRNA:
C3/C4
*
C
relative C3 + C4
armi^rev
armi^1
armi^72.1
aub^HN2
nos^BN

Figure Legend II-3. Armi and Aub Are Required for RISC Assembly (A) RISC assembly assay. (B) A representative RISC assembly assay using wild-type and mutant *Drosophila* ovary lysates. A complex formed irrespective of siRNA addition is marked with an asterisk. (C) Amount of RISC complexes C3/C4 formed in wild-type and mutant ovary lysates. The data are the average of four independent trials; error bars indicate standard deviation. For each trial, the data were normalized to the amount of complex observed in $armi^{rev}$ lysate, and the background observed in the absence of siRNA was subtracted from the amount of complex formed when siRNA was included in the corresponding reaction. 5´-phosphorylated, 2´ dT siRNA was used to maximize RISC assembly. All reactions contained equal amounts of total protein.

RNAi machinery is affected by the *aub* mutation indirectly. In contrast, ovaries from *nanos*^{BN}, a maternal effect mutant not implicated in RNAi, were fully competent for both RISC assembly (Figure 3C) and siRNA-directed target RNA cleavage (data not shown).

Identification of Intermediates in RISC Assembly

These data suggest that both *armi* and *aub* are required genetically for RISC assembly, but they provide no insight into the molecular basis of their RISC assembly defect(s). At what step(s) in RISC assembly are *armi* and *aub* blocked? In order to answer this question, we identified protein-siRNA intermediates in the RISC assembly pathway. Our 2′-*O*-methyl oligonucleotide/native gel method detects only complexes competent to bind target RNA (mature RISC). Therefore, we used a native gel assay designed to detect intermediates in the assembly of RISC. We radiolabeled the siRNA, allowing detection of complexes containing either single-stranded or double-stranded siRNA and used functionally asymmetric siRNAs (Schwarz et al., 2003) to distinguish between complexes containing single- and double-stranded siRNA.

RISC contains only a single siRNA strand (Martinez et al., 2002; Schwarz et al., 2003; Schwarz et al., 2002). Functionally asymmetric siRNAs load only one of the two strands of an siRNA duplex into RISC and degrade the other strand (Schwarz et al., 2003); the relative stability of the 5′ ends of the two strands determines which is loaded into RISC (Aza-Blanc et al., 2003; Khvorova et al., 2003; Schwarz et al., 2003). siRNA 1 (Figure 4A) loads its antisense strand into RISC, whereas siRNA 2 loads the sense strand (Schwarz et al., 2003). The two siRNA duplexes are identical, except that siRNA 2 contains a C-to-U substitution at position 1, which inverts the asymmetry (Schwarz et al., 2003). For both siRNAs, the antisense strand was 3′ ^{32}P-radiolabeled and will always be present in complexes that contain double-stranded siRNA. However, RISC will contain the ^{32}P-radiolabeled antisense strand only for siRNA 1. siRNA 2 will also make RISC, but it will contain the nonradioactive sense strand.

When either siRNA 1 or siRNA 2 was used to assemble RISC in embryo lysate, two complexes (B and A, Figure 4B) were detected in the native gel assay; a third complex was detected only with siRNA 1 (Figure 4B). This third complex therefore contains single-stranded siRNA and corresponds to RISC. Complexes B and A are good candidates for RISC assembly intermediates. Formation of all three complexes was dramatically reduced when the antisense siRNA strand contained a 5′ methoxy group (siRNA 3, Figure 4B), a modification which blocks RNAi (Nykanen et al., 2001). When the antisense strand of the siRNA contained a single 5′-deoxy nucleotide, making it a poor substrate for phosphorylation in the lysate (Nykanen et al., 2001), assembly of all three complexes was reduced (siRNA 4, Figure 4B). Phosphorylating the 5′ deoxy-substituted siRNA before the reaction restored complex assembly (siRNA 5, Figure 4B). Formation of complex A and of RISC required ATP. In contrast, complex B assembled efficiently in the absence of ATP, but only if the siRNA was phosphorylated prior to the reaction (compare −ATP, siRNA 4 versus siRNA 5, Figure 4B).

Complexes B, A, and RISC also formed in ovary lysate (Figure 4C). As for embryo lysate, complexes B and A contained double-stranded siRNA, whereas RISC contained single-stranded (compare siRNA 1 and 2, Figure 4C). No complexes formed in ovary lysate when siRNA 5′ phosphorylation was blocked (siRNA 3, Figure 4C) and complex assembly was reduced when siRNA phosphorylation was slow (siRNA 4, Figure 4C).

To determine the relationship of complexes B, A, and RISC, we monitored the kinetics of complex formation (Figure 4D) and analyzed the data by kinetic modeling (Figure 4E). Of all possible models relating free siRNA, B, A, and RISC, only the simple linear pathway siRNA → B → A → RISC fit well to our data (see Experimental Procedures). The modeled rate constants for the pathway are consistent with the observation that formation of complex B is ATP independent, but RISC is ATP dependent.

Complex A Contains the R2D2/Dicer-2 Heterodimer

Liu and colleagues have previously proposed that a heterodimeric complex, comprising Dicer-2 (Dcr-2) and the dsRNA binding protein R2D2, loads siRNA into RISC (Liu et al., 2003). Complex A contains the Dcr-2/R2D2 heterodimer. R2D2 and Dcr-2 are readily crosslinked to ^{32}P-radiolabeled siRNA with UV light (Liu et al., 2003). We synthesized an siRNA containing a single photocrosslinkable nucleoside

Figure II-4

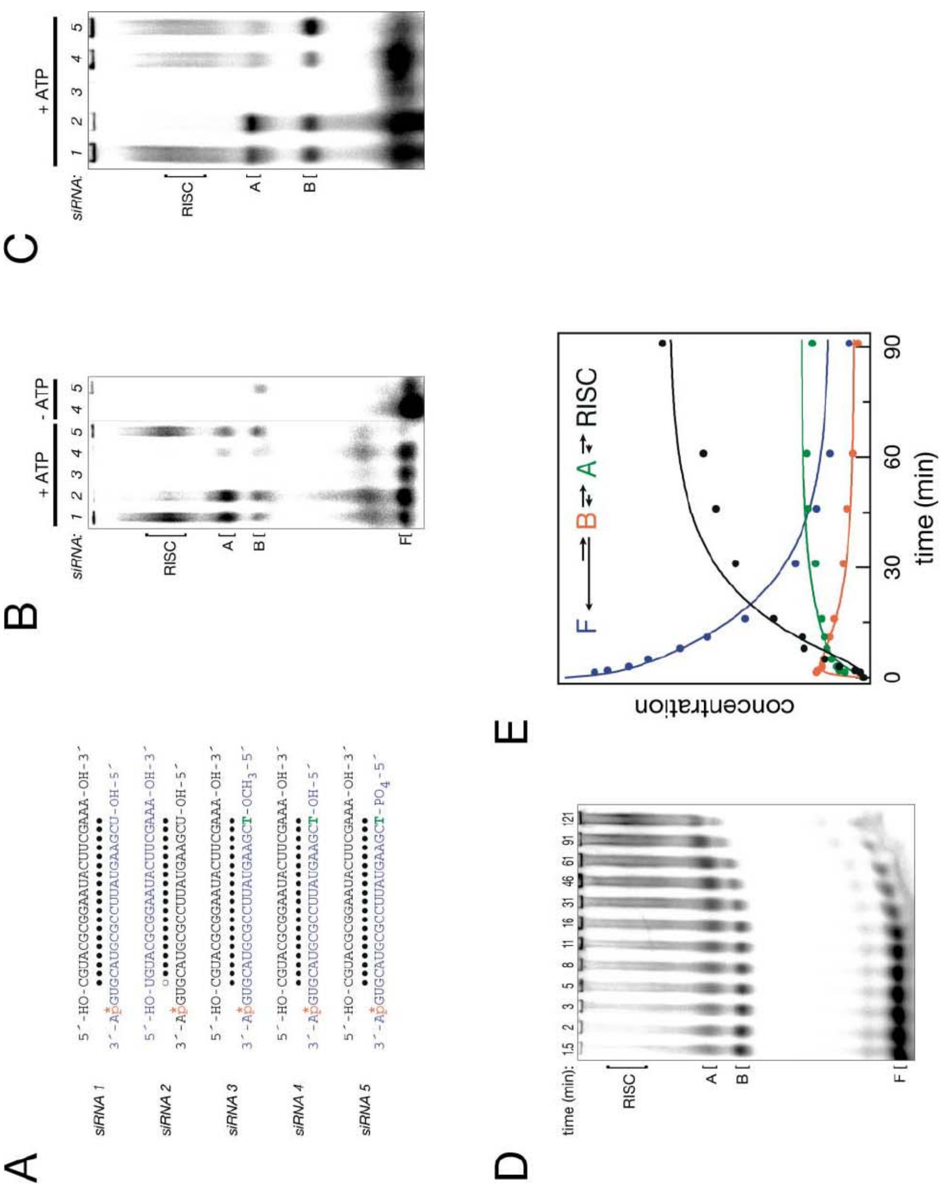
A
siRNA 1
siRNA 2
siRNA 3
siRNA 4
siRNA 5
B
siRNA:
+ ATP
- ATP
RISC
A
B
F
C
siRNA:
+ ATP
RISC
A
B
D
time (min): 1.5 2 3 5 8 11 16 31 46 61 91 121
RISC
A
B
F
E
F → B ⇌ A ⇌ RISC
concentration
time (min)
0
30
60
90

Figure Legend II-4. Identification of Intermediates in RISC Assembly (A) siRNA duplexes used for native gel analysis. The strand that enters the RISC is indicated in blue, deoxynucleotides are in green, and the ^{32}P-radiolabeled phosphates are red, marked with an asterisk. (B) Native gel analysis of the protein-siRNA complexes formed in embryo lysate using the 3′ ^{32}P-radiolabeled siRNAs in (A). F, free siRNA. (C) Native gel analysis of the protein-siRNA complexes formed in wild-type ovary lysate using the 3′ ^{32}P-radiolabeled siRNAs in (A). Free siRNA is not shown on this gel. (D) Timecourse of the assembly of 5′ ^{32}P-radiolabeled siRNA into protein complexes. (E) Kinetic modeling of the data in (D). Blue circles, free siRNA; red, complex B; green, complex A; black, RISC. Solid lines show the corresponding modeled timecourses. The length of the arrows indicates the relative forward and reverse rate constants that best describe the data.

base (5-iodouracil) at position 20 (Supplemental Figure S2A). The ^{32}P-5-iodouracil siRNA was incubated with embryo lysate to assemble complexes, then irradiated with 302 nm light, which initiates protein-RNA crosslinking only at the 5-iodo-substituted nucleoside. Proteins covalently linked to the ^{32}P-radiolabeled siRNA were resolved by SDS-PAGE. Two proteins—~200 kDa and ~40 kDa—efficiently crosslinked to the siRNA (Supplemental Figure S2D). Both crosslinked proteins were coimmunoprecipitated with either α-Dcr-2 or α-R2D2 serum, but not normal rabbit serum (Figure 5A). Neither crosslink was observed in ovary lysates prepared from *r2d2* homozygous mutant females (data not shown), suggesting the binding affinity of Dcr-2 to siRNA is much lower than that of Dcr-2/R2D2 heterodimer. Additional experiments validating the UV crosslinking assay are provided in Supplemental Methods, Supplemental Figure S2, and Supplemental Table S1.

The crosslinking was repeated, and the reaction analyzed by native gel electrophoresis to resolve complexes B, A, and RISC. Each complex was eluted from the gel and analyzed by SDS-PAGE. Figure 5B shows that the R2D2 and Dcr-2 crosslinks were present in complexes A and RISC, but not B. In a parallel experiment, complexes B, A, and RISC were isolated (without crosslinking) and analyzed by Western blotting with either α-Dcr-2 or α-R2D2 antibodies. Again, complexes A and RISC, but not B, contained both Dcr-2 and R2D2 (Figure 5B). Finally, we tested complex assembly in ovary lysates prepared from *r2d2* homozygous mutant females. Only complex B formed in these lysates (Figure 5C). We conclude that complex A contains the previously identified Dcr-2/R2D2 heterodimer (Liu et al., 2003), and that both Dcr-2 and R2D2 remain associated with at least a subpopulation of RISC, consistent with earlier reports that Dcr-2 in flies and both DCR-1 and the nematode homolog of R2D2, RDE-4, coimmunoprecipitate with Argonaute proteins (Hammond et al., 2001; Tabara et al., 2002).

armi **Mutants Are Defective for the Conversion of Complex A to RISC**

RISC does not form in ovary lysates from *armi* or *aub* mutants (Figures 3B and 3C). However, both complexes B and A were readily detected in *armi* and *aub* mutants (Figure 5D). Thus, *armi* and *aub* mutants are impaired in a step in RISC assembly after binding of the siRNA to the Dcr-2/R2D2 heterodimer.

Armi might act after the formation of complex A to unwind siRNA duplexes prior to their assembly into RISC. To test this hypothesis, we tested if single-stranded siRNA circumvented the requirement for *armi*. In vitro and in vivo, single-stranded siRNA triggers RNAi, albeit inefficiently (Martinez et al., 2002; Schwarz et al., 2002). *armi* ovary lysates failed to support RNAi when the reactions were programmed with 5′-phosphorylated, single-stranded siRNA (Supplemental Figure S3A). The defect with single-stranded siRNA correlated with allele strength: some activity was seen in lysates from the weak allele, $armi^{1}$, but none for the strong allele, $armi^{72.1}$. The requirement for a putative ATPase—Armi—in RNAi triggered by single-stranded siRNA suggested to us the presence of an additional ATP-dependent step in the RISC assembly, after siRNA unwinding.

Figure II-5

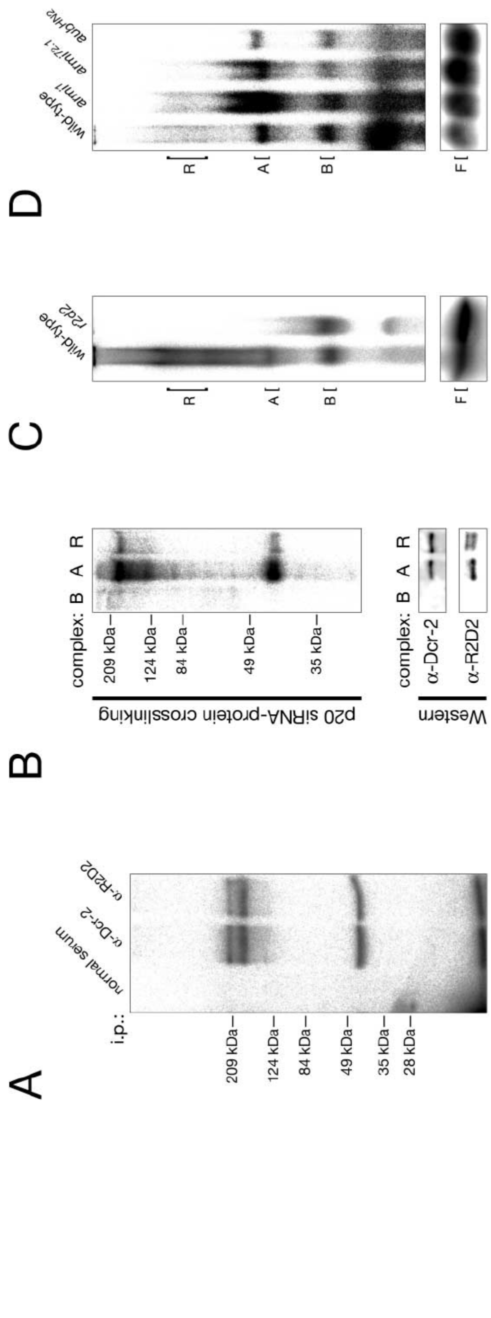
A
i.p.:
normal serum
α-Dcr-2
α-R2D2
209 kDa
124 kDa
84 kDa
49 kDa
35 kDa
28 kDa
B
p20 siRNA-protein crosslinking
complex: B A R
209 kDa
124 kDa
84 kDa
49 kDa
35 kDa
Western
complex: B A R
α-Dcr-2
α-R2D2
C
wild-type
r2d2
R
A
B
F
D
wild-type
armi
armi72.1
aub-HN2
R
A
B
F

Figure Legend II-5. A Dcr-2/R2D2-Containing Complex Is Formed in *armi* and *aub*, but Not *r2d2* Mutant Ovary Lysate (A) Dcr-2 and R2D2 are efficiently crosslinked by 302 nm light to an siRNA containing 5-iodouracil at position 20. The siRNA was incubated with embryo lysate, crosslinked with UV light, immunoprecipitated with the antiserum indicated above each lane, then analyzed by 4%–20% gradient SDS-PAGE. (B) Upper panel: the 5-iodouracil siRNA was incubated with embryo lysate crosslinked, then resolved on a native gel. Complexes B, A, and R (RISC) were excised from the gel and the protein-siRNA crosslinks present in complexes B, A, and R (RISC) analyzed by 10% SDS-PAGE. Lower panel: complexes B, A, and R (RISC) were isolated from a native gel, then analyzed by Western blotting with α-Dcr-2 or α-R2D2 antisera. (C) Native gel analysis of the complexes formed in *r2d2* and (D) $armi^{1}$, $armi^{72.1}$, and aub^{HN2} homozygous mutant ovary lysates. Minor variations in the abundance of B and A did not correlate with *armi* allele strength, suggesting that neither Armi nor Aub are required for their production. In (C) and (D), the portion of the gel corresponding to free siRNA, F, is shown below. Equal amounts of total protein were used in each reaction. The siRNA was 5′ ^{32}P-radiolabeled in (A)–(C) and 3′ ^{32}P-radiolabeled in (D). Less RISC was detected for wild-type lysate in this experiment compared to (C) because the lysate was diluted 3-fold to equalize its protein concentration to that of the *aub* mutant lysate.

To test if loading of single-stranded siRNA into RISC requires ATP, we added 5′-phosphorylated, single-stranded siRNA to embryo lysates depleted of ATP. After incubation for 2 hr, no cleavage product was detected, suggesting that there is at least one ATP-dependent step downstream of siRNA unwinding (Supplemental Figure S3B). The stability of single-stranded siRNA was not reduced by ATP depletion. In fact, single-stranded siRNA was slightly more stable in the absence of ATP (Supplemental Figure S3C). Thus differential stability cannot account for the requirement for ATP in RNAi triggered by single-stranded siRNA. In the RNAi pathway, there are at least three steps after siRNA unwinding: RISC assembly, target recognition, and target cleavage. To assess if either target recognition or cleavage was ATP dependent, we incubated single-stranded siRNA in a standard RNAi reaction with ATP to assemble RISC. Next, NEM was added to inactivate the ATP-regenerating enzyme, creatine kinase, and to block further RISC assembly. NEM was quenched with dithiothreitol (DTT), and hexokinase and glucose added to deplete ATP. Finally, mRNA target was added and the reaction incubated for 2 hr. By using this protocol, high ATP levels were maintained during RISC assembly, but less than 100 nM ATP was present during the encounter of RISC with the target RNA. Target recognition and cleavage did not require ATP when RISC was programmed with either double- or single-stranded siRNA, provided that ATP was supplied during RISC assembly (Supplemental Figure S3D).

Discussions

In *Drosophila*, mutations affecting the RNAi pathway are often lethal or female sterile, making the molecular characterization of these mutants difficult. Our finding that lysates that support RNAi in vitro can be prepared from manually dissected ovaries has allowed us to analyze the molecular function of *armi*, a maternal effect gene required for RNAi. Our methods should find broad application in the molecular characterization of other maternal genes required for the RNAi pathway.

We detected four distinct RISC-like complexes common to embryo and ovary lysates (C1-4 in Supplemental Figure S1 and Figure 3). In ovaries, formation of these complexes is reduced >10-fold in *armi* mutants and is undetectable in *aub* mutants, which were shown previously to be RNAi defective (Kennerdell et al., 2002). These isoforms may play distinct regulatory roles (e.g., translational repression versus cleavage). Alternatively, the smallest, most abundant complexes may contain only the most stably associated protein constituents, whereas the larger, less abundant complexes may correspond to "holo-RISC" that retain more weakly bound proteins. Clearly, a major challenge for the future is to define the protein constituents of each complex, their functional capacity, and their biological role. The development of a native gel assay that resolves distinct RISC complexes represents a step toward that goal. Aub is a member of Argonaute protein family and is required for RNAi in fly oocytes both in vitro and in vivo (Figure 3 and (Kennerdell et al., 2002)). However, it was shown that Ago2 is the core of RISC that mediates RNAi in every tissue analyzed (Hammond et al., 2001; Kim et al., 2007). Thus, it is unlikely that Aub is the core component of siRNA-RISC. Rather the effect of *aub* on RNAi could be indirect by affecting the expression or stability of some RNAi component protein(s). We have also identified two intermediates in RISC assembly. Complex B forms rapidly upon incubation of siRNA in lysate, in the absence of ATP. The siRNA is then transferred to complex A, which contains the previously identified R2D2/Dcr-2 heterodimer. The siRNA is double stranded in both B and A. RISC is formed from complex A by a process that requires both siRNA unwinding and ATP. Both *aub* and *armi* are required genetically for the production of RISC from complex A. The involvement of Armi, a putative RNA helicase protein, in the production of RISC from complex A and our finding that incorporation of single-stranded siRNA into RISC requires ATP suggest that Armi functions to incorporate single-stranded siRNA into RISC (Figure 7). However, our data cannot distinguish between direct and indirect roles for Armi in RISC assembly. After the publication of this manuscript, two groups reported that the human orthologue of Armi, RNA helicase MOV10, is associated with Ago2 containing RISC (Chendrimada et al., 2007; Meister et al., 2005), suggesting the role of Armi in RISC assembly is conserved among animals.

The *Arabidopsis* homolog of Armi, SDE3, together with the RNA-dependent RNA polymerase (RdRP) SDE1/SGS2, is required for PTGS triggered by transgenes that express single-stranded sense mRNA, but not silencing triggered by some RNA viruses (Dalmay et al., 2001). SDE3 has been proposed to facilitate the conversion of dsRNA into siRNA or the conversion of mRNA into complementary RNA by SDE1/SGS2 (Dalmay et al., 2001). Recent studies show that SDE3 is not required for the production of siRNAs derived directly from a long dsRNA hairpin (Himber et al., 2003). Instead, SDE3 seems to play a role in the production of siRNAs generated by an RdRP-dependent amplification mechanism. Our data are not consistent with either of these functions for Armi. First, *Drosophila* genomic, biochemical, and genetic data exclude a role for an RdRP in RNAi (Celotto and Graveley, 2002; Roignant et al., 2003; Schwarz et al., 2002; Tang et al., 2003). Second, Armi is required for RISC assembly in *Drosophila* ovary lysates when RISC is programmed with siRNA, suggesting a role for Armi downstream of the conversion of dsRNA into siRNA, but upstream of target recognition by RISC. The apparently divergent functions of SDE3 and Armi could be reconciled if RISC is required for RdRP-mediated amplification of silencing. Alternatively, SDE3 and Armi may not have homologous functions.

Besides its role in siRNA mediated RNAi pathway, Armi is also essential for the function or production of another class of small RNAs, the piRNAs. piRNAs silence repetitive elements in fly germlines by an unknown mechanism (Klattenhoff and Theurkauf, 2008). In *armi* mutants, the accumulation of piRNA is diminished, causing the desilencing of a series of selfish genetic elements (Tomari et al., 2004a; Vagin et al., 2006). It is possible that Armi plays independent roles in these two pathways. Alternatively, Armi might be the common factor shared by these two classes of small RNAs. If the later is true, our study on the molecular function of Armi in RNAi pathway may shed light on the understanding of piRNA loading in the future.

Experimental Procedures

General Methods

Target RNA cleavage assay was performed as described (Haley et al., 2003). ATP depletion and NEM quenching were as published (Nykanen et al., 2001).

Ovary Lysate Preparation

Wild-type or mutant fly ovaries were dissected with forceps (World Precision Instruments 500232) and collected in 1 × PBS buffer in 0.5 ml microcentrifuge tubes. Ovaries were centrifuged at 11,000 × g for 5 min at 4°C. The PBS was removed from the ovary pellet, then ovaries were homogenized in 1 ml ice-cold lysis buffer (100 mM potassium acetate, 30 mM HEPES-KOH at pH 7.4, 2 mM magnesium acetate) containing 5 mM DTT and 1 mg/ml complete "mini" EDTA-free protease inhibitor tablets (Roche) per gram of ovaries using a plastic "pellet pestle" (Kontes). Lysate was clarified by centrifugation at 14,000 × g for 25 min at 4°C. The supernatant was aliquoted into chilled microcentrifuge tubes, flash frozen in liquid nitrogen, and stored at −80°C. RNAi reactions were assembled using equal amounts of total protein for all genotypes within an experiment.

Synthetic siRNA

The siRNAs were prepared from synthetic 21 nt RNAs (Dharmacon Research). Sense siRNA sequences used were 5′-HO-CGU ACG CGG AAU ACU UCG AAA-3′ (5′ OH [riboU], 5′ CH_3O [2′ dT], 5′ OH [2′ dT]) and 5′-HO-UGA GGU AGU

AGG UUG UAU AGU-3′ (un). Antisense siRNA sequences used were 5′-HO-UCG AAG UAU UCC GCG UAC GUG-3′ (5′ OH [riboU]); 5′-CH_3O-dTCG AAG UAU UCC GCG UAC GUG-3′ (5′ CH_3O [2′ dT]); 5′-HO-dTCG AAG UAU UCC GCG UAC GUG-3′ (5′ OH [2′ dT]); and 5′-HO-UAU ACA ACC UAC UAC CUC AUU-3′ (un). Appropriate pairs of siRNA strands were annealed to form siRNA duplexes as described (Elbashir et al., 2001b) and used at a final concentration of ≤20 nM (Figure 1and Figure 4) or ≤50 nM (Figure 2). siRNA single strands were phosphorylated with polynucleotide kinase according to the manufacturer's protocol (PNK; New England Biolabs) and used at 200 nM (final concentration).

RISC Assembly

RISC assembly was as described (Zamore et al., 2000), except that the reaction contained 40% (v/v) embryo or ovary lysate and 50 nM siRNA duplex. Lysates were adjusted with lysis buffer to contain equal amounts of protein. Following incubation at 25°C for 20 min, 1 mg/ml heparin was added and incubated for 10 min. Heparin served to reduce nonspecific binding of proteins to the 2′-*O*-methyl oligonucleotide and to quench RISC assembly. (Mature RISC is refractory to heparin: 1 mg/ml [final concentration] heparin added at the start of the reaction blocked RNAi in the cleavage assay, but had no effect when added together with target RNA.) Then the 5′ ^{32}P-radiolabled 2′-*O*-methyl oligonucleotide (5′-CAU CAC GUA CGC GGA AUA CUU CGA AAU GUC C-3′) was added at 2 nM final concentration and incubated for 2 hr. After the addition of 3.0% (w/v) Ficoll-400, complexes were resolved by native gel electrophoresis at 4 W for 2 hr at room temperature. Native gels were 1 mm thick, 1.5% (w/v) agarose (GTG grade), 0.5 × TBE with 1.5 mM $MgCl_2$, cast vertically between a standard glass plate and a ground glass plate (National Glass Works, Worcester, Massachusetts). To detect intermediates in RISC assembly, ^{32}P-radiolabeled siRNA was incubated with lysate for 1 hr, unless otherwise noted. No heparin was added to these reactions. After incubation, the samples were adjusted to 3.0% (w/v) Ficoll-400 and resolved by vertical native gel electrophoresis as above. Gels were dried under vacuum onto Hybond-N+ nylon membrane (Amersham).

Kinetic Modeling

Data from native gel analysis of siRNA-containing complexes were initially fit using Berkeley Madonna 8.0.1 software to the global model:

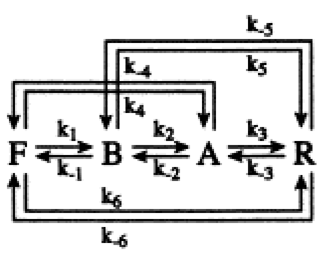

Rates for k_4, k_{-4}, k_5, k_{-5}, k_6, and k_{-6} ranged from 5-fold (k_5) to 10^8-fold (k_{-4}) slower than the slowest forward rate for the linear pathway F → B → A → RISC. The data were therefore modeled neglecting rates k_4, k_{-4}, k_5, k_{-5}, k_6, and k_{-6} to generate Figure 4E.

Crosslinking

5′ ^{32}P-radiolabeled siRNA duplex was used at 4 million counts per minute in a standard RNAi reaction, incubated 45–60 min at 25°C, then transferred to a 96-well round bottom plate on ice. Samples were irradiated for 10–15 min with 302 nm light using an Ultraviolet Products model TM-36 transilluminator inverted directly onto the polystyrene lid of the 96-well plate. Samples were then adjusted to 1 × SDS-SB (62.5 mM Tris-HCl, pH 6.8, 10% glycerol, 2% SDS, 0.02% (w/v) Bromophenol Blue, 100 mM DTT), heated to 95°C for 5 min, and resolved by SDS-polyacrylamide gel electrophoresis.

Immunoprecipitation and Western Blotting

Normal rabbit, α-Dcr-2, and α-R2D2 antisera were first bound to protein A agarose beads for 2 hr at 4°C in lysis buffer. After washing with RIPA buffer (150 mM NaCl, 1% [v/v] NP40, 0.5% [w/v] sodium deoxycholate, 0.1% SDS, 25 mM Tris-HCl, pH 7.6), the beads (25 μl) were incubated with 15 μl of crosslinked lysate for 2 hr at 4°C. After washing in RIPA buffer, the beads were boiled in 1 × SDS-SB and the eluted proteins resolved by SDS-PAGE. For Western blotting, the complexes were excised from the native gel, boiled in 1 × SDS-SB at 95°C for 10 min, and resolved by SDS-PAGE. Western blotting was performed with 1:1000 dilution for α-Dcr-2 antisera and 1:5000 for α-R2D2.

Validation of the Site-Specific Crosslinking Assay

We used protein-RNA photocrosslinking to identify siRNA-associated proteins. siRNA duplexes containing a single UV-crosslinkable nucleoside (5-iodouridine; Supplemental Figure S2A) at position 20 of the antisense strand (Supplemental Figure S2B) was incubated with embryo lysate, the crosslinked proteins fractionated by gel filtration chromatography, and the chromatographic fractions exposed to 302 nm UV light to initiate crosslinking. Two proteins, ~ 200 kDa and ~ 40 kDa, were crosslinked to the siRNA and co-eluted as a single, ~ 350 kDa peak (Supplemental Figures S2E and S2F). Efficient crosslinking to the ~ 200 kDa protein required both UV irradiation, and the 5-iodo-uracil substitution did not occur with a blunt-ended RNA duplex (Supplemental Figures S2C and S2D) or single-stranded siRNA (data not shown) and required the 5′ phosphate of the siRNA (data not shown). The crosslinked protein was not detected when the 5-iodo-uracil was at position 12 of the siRNA (Supplemental Figures S2B and S2D). The apparent molecular weights of the two *Drosophila* Dicer proteins are ~270 kDa (Dicer-1; Dcr-1) and ~200 kDa (Dicer-2; Dcr-2) (Liu et al., 2003). Consistent with the idea that the crosslinked protein was one of the two *Drosophila* Dicer proteins, Dicer activity—monitored by the conversion of long dsRNA into siRNA—copurified with the crosslinked proteins (Supplemental Figures S2E and S2F).

Our crosslinking experiments suggested that one of the two *Drosophila* Dicers bound tightly to siRNA. This conclusion is consistent with earlier studies demonstrating that siRNA duplexes are competitive inhibitors of Dicer activity in

Drosophila embryo lysate (Tang et al., 2003). To determine if one or both of the *Drosophila* Dicer proteins bound tightly to siRNA, we used an siRNA duplex tethered to paramagnetic beads to purify siRNA bound proteins. Because the siRNA duplex was linked to the beads via the 5′ end of the strand that is not loaded into RISC (Supplemental Figure S2A) (Schwarz et al., 2003), RISC does not form on the beads (data not shown). Consequently, the tethered siRNA duplex bound proteins that interact with double-stranded, but not single-stranded, siRNA. Proteins bound to the siRNA were recovered by irradiating the beads with 302 nm light to break a photocleavable linkage tethering the siRNA duplex to the beads (Supplemental Figure S2G). The only high molecular weight protein liberated by photocleavage was a ~ 200 kDa protein (Supplemental Figure S1B). Mass spectrometry of 13 tryptic peptides of this protein revealed that it was Dcr-2 (Supplemental Table S1); no Dcr-1 peptides were detected. These data, together with our immunoprecipitation experiments (Figure 5A), provide strong support for our conclusion that the ~ 200 kDa protein detected by UV crosslinking is Dcr-2.

Photocleavage and Protein Recovery

90 pmoles of siRNA containing a 5′ PC-biotinylated linker (Glen Research) was conjugated to 600 µl M-280 Dyna-beads (Dynal) by incubation at 4°C. The paramagnetic beads were incubated for 60 min at 25°C in a 1 ml standard RNAi reaction. After incubation, beads were captured on a Dynal MPC-E magnetic stage, washed four times in ice-cold lysis buffer containing 0.1% (w/v) NP-40, resuspended

in 200 µl ice-cold lysis buffer, transferred to a 96-well plate (30 µl per well), immersed in ice, and photocleaved by irradiation for 20 min with a 302 nm light source ~ 7.5 cm from the samples. Beads were captured with the magnet and the supernatant dialyzed against 2% (v/v) glacial acetic acid in a 10 kDa cutoff dialysis cup (Pierce) for 12–16 hr. The dialysate was lyophilized, resuspended in 2 × SDS-SB, resolved by electrophoresis through an 8% SDS-polyacrylamide gel, and stained with silver. Bands were excised, digested with trypsin in situ, and the resulting peptides analyzed by electrospray mass spectrometry.

Figure II-S1

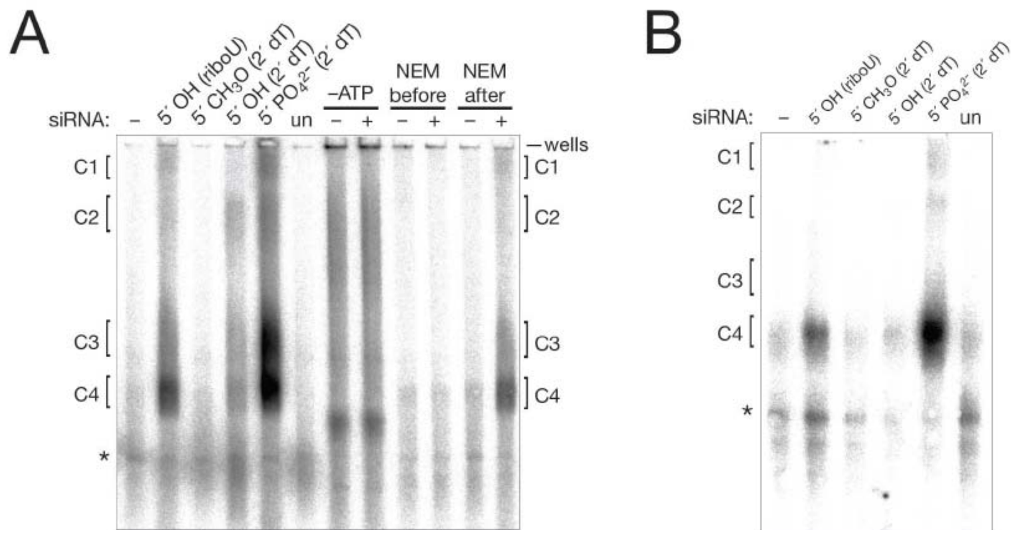

A
siRNA:
–
5′ OH (riboU)
5′ CH3O (2′ dT)
5′ OH (2′ dT)
5′ PO4 2– (2′ dT)
un
–ATP
NEM before
NEM after
– + – + – +
wells
C1
C2
C3
C4
*
B
siRNA:
–
5′ OH (riboU)
5′ CH3O (2′ dT)
5′ OH (2′ dT)
5′ PO4 2– (2′ dT)
un
C1
C2
C3
C4
*

Figure Legend II-S1. Validation of the 2′-*O*-Methyl Oligonucleotide/Native Gel Assay (A) RISC-like complexes formed in embryo lysate only in the presence of siRNA are labeled C1-C4. A complex formed irrespective of siRNA addition is marked with an asterisk. (B) RISC assembly assay using wild-type ovary lysate. In both (A) and (B), assembly of complexes capable of binding the 2′-*O*-methyl oligonucleotide required a 5′ phosphate on the strand of the siRNA complementary to the oligonucleotide.

Figure II-S2

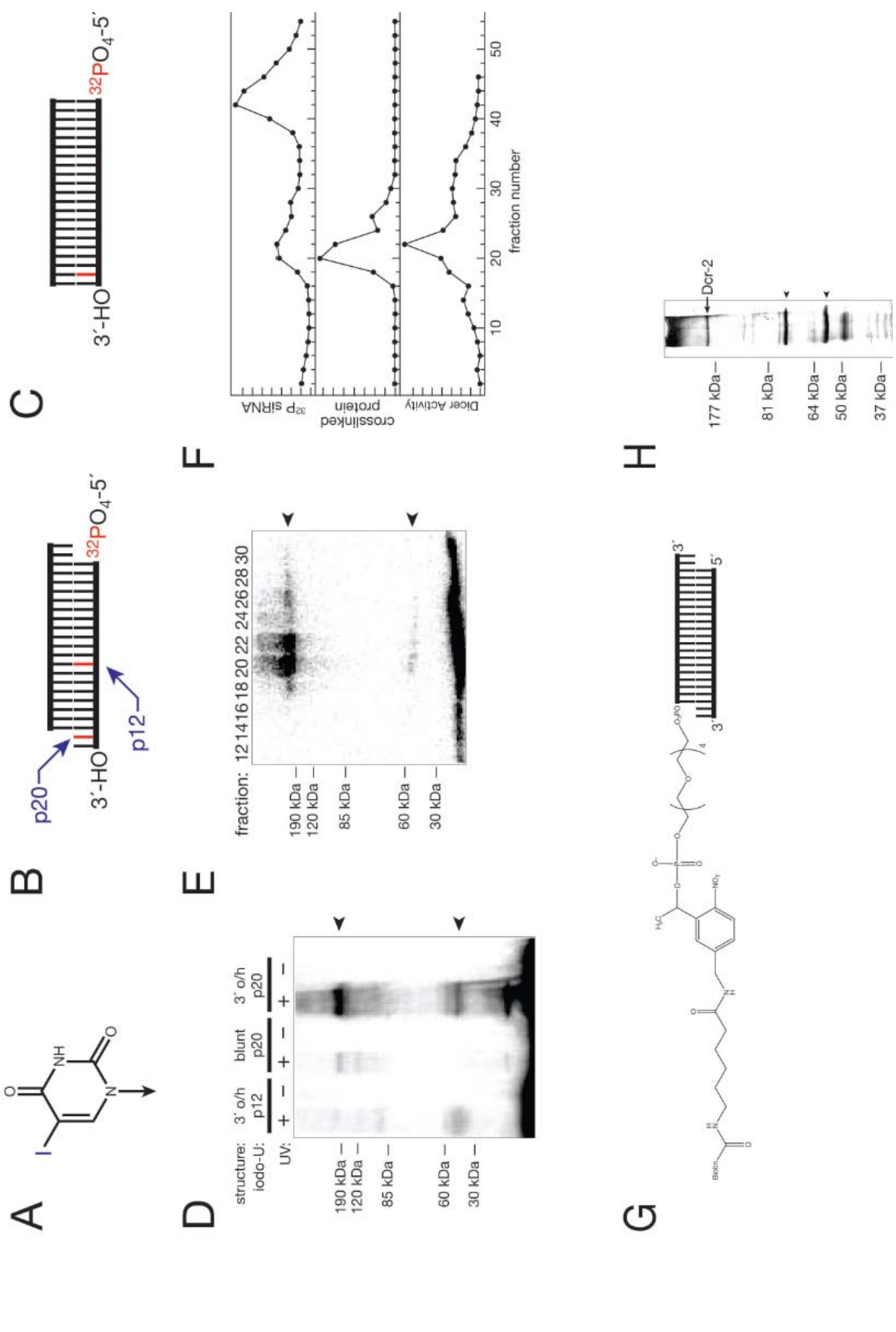
A
B
C
D
E
F
G
H
p20
p12
3´-HO
32PO4-5´
structure:
iodo-U:
UV:
3´ o/h p12
blunt p20
3´ o/h p20
190 kDa
120 kDa
85 kDa
60 kDa
30 kDa
fraction: 12 14 16 18 20 22 24 26 28 30
32P siRNA
crosslinked protein
Dicer Activity
fraction number
Dcr-2
177 kDa
81 kDa
64 kDa
50 kDa
37 kDa

Figure Legend II-S2. Dcr-2 Binds Tightly and Crosslinks to siRNA (A) The photo-crosslinkable nucleoside 5-iodo-uridine. Only the base is shown for simplicity. (B) and (C) Schematic of the siRNAs used for RNA-protein UV crosslinking. (D) A ~ 200 kDa protein UV crosslinks specifically to the p20-substituted siRNA duplex. The 5´-^{32}P-radiolabled RNA duplexes depicted in (B) and (C) were incubated in standard RNAi reaction, crosslinked at 302 nm, and analyzed on an 8% SDS-polyacrylamide gel. (E) A ~ 200 kDa protein co-purifies with the peak of double-stranded siRNA. 5´-^{32}P-radiolabeled siRNA, containing 5-iodo-uracil at position 20, was incubated in a standard RNAi reaction, then the reaction was resolved by gel filtration on a Superdex-200 column. Fractions were collected, exposed to 302 nm light, and analyzed as in (D). Arrowheads mark proteins crosslinked to ^{32}P-siRNA. (F) The ~ 200 kDa protein crosslinked to siRNA copurifies with both Dicer activity and the peak of double-stranded siRNA (cf. Figure 5C in Nykänen et al., 2001). (G) Schematic of the 5´ photo-cleavable (PC) biotinylated siRNA duplex. (H) Proteins, stained with silver, purified using 5´ PC-biotin siRNA paramagnetic beads. The ~ 200 kDa band (Dcr-2) was isolated only when the paramagnetic streptavidin-coated beads contained siRNA. Arrowheads mark proteins nonspecifically recovered from both siRNA-conjugated beads and beads alone.

Figure II-S3

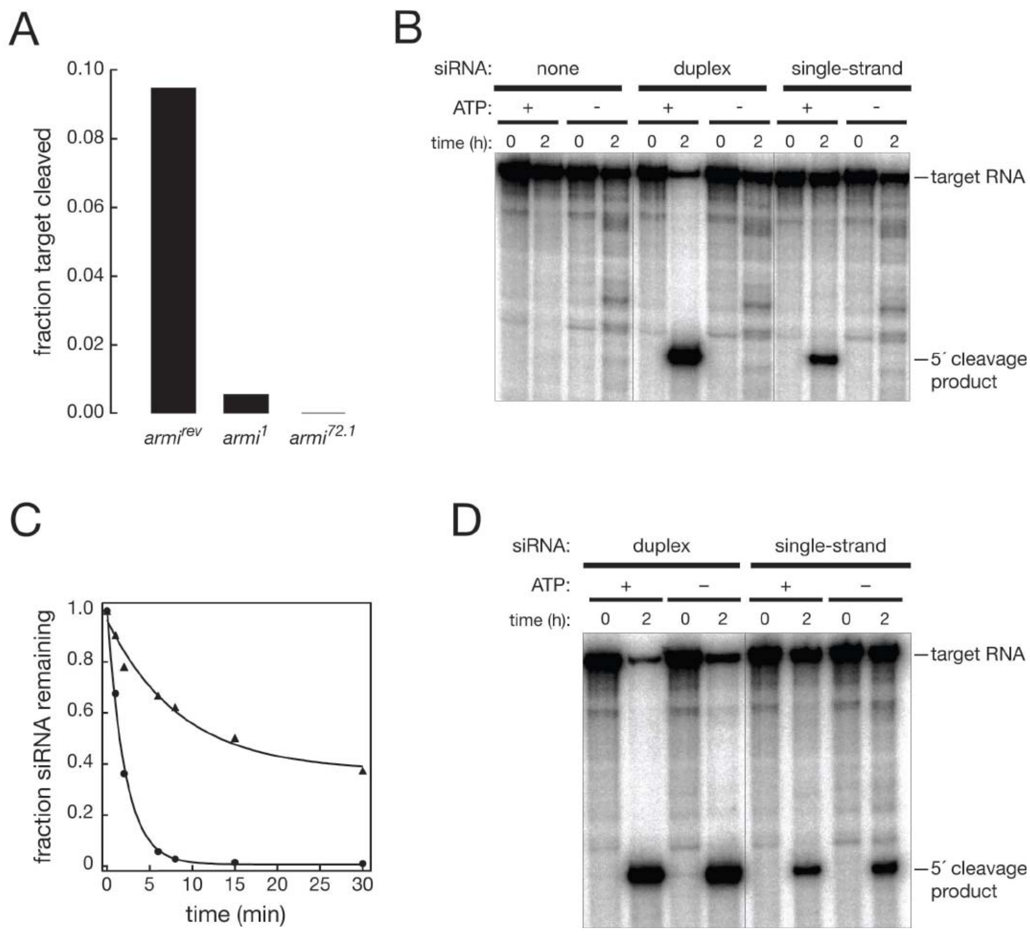
A
0.10
0.08
0.06
0.04
0.02
0.00
fraction target cleaved
armi[rev]
armi[1]
armi[72.1]
B
siRNA: none duplex single-strand
ATP: + - + - + -
time (h): 0 2 0 2 0 2 0 2 0 2 0 2
target RNA
5´ cleavage product
C
1.0
0.8
0.6
0.4
0.2
0
fraction siRNA remaining
0 5 10 15 20 25 30
time (min)
D
siRNA: duplex single-strand
ATP: + − + −
time (h): 0 2 0 2 0 2 0 2
target RNA
5´ cleavage product

Figure Legend II-S3. *armi* Ovary Lysates Are Defective in the ATP-Dependent Incorporation of Single-Stranded siRNA into RISC (A) Target mRNA cleavage for wild-type and mutant ovary lysates using single-stranded siRNA. (B) RNAi in embryo lysate using double- or single-stranded siRNA in the presence or the absence of ATP. (C) The fraction of single-stranded siRNA remaining after incubation in embryo lysate in the presence (circles) or the absence (triangles) of ATP. (D) Target recognition and cleavage directed by single-stranded siRNA does not require ATP. After 30 min preincubation of siRNA in the presence of ATP to permit RISC assembly, ATP was removed (–) or retained (+), and target RNA added to test for RISC-directed target cleavage.

Table II-S1

Supplemental Table 1. Peptide-mass fingerprinting of ~ 200 kDa Protein (Dicer-2)

m/z submitted	MH+ matched	Peptide Sequences	Amino Acid Position in Dicer-2
862.49	862.5151	NYAILLR	753-759
1212.69	1212.6377	TIQQIYQYR	514-522
1225.68	1261.6727	FVLFTADKER	502-511
1261.69	1348.6398	NVLTPQFMVGR	417-427
1348.69	1363.7197	FVNFQESQGHR	1539-1549
1363.69	1519.7393	MYFLLHAEALR	999-1009
1519.81	1635.8131	NNISPDFESVLER	428-440
1635.86	1648.7654	DLTEQLTFVVHNR	944-956
1648.82	1648.7654	NQFHMPTGNIYGNR	1135-1148
1727.87	1727.8029	VGFYVGEQGVDDWTR	85-99
1774	1773.9288	YLLQALTHPSYPTNR	1449-1463

Peptide Fingerprinting of the ~ 200 kDa Protein (Dicer-2) Peptides identified after trypsin digestion of the ~ 200 kDa protein band excised from a silver-stained 8% denaturing protein gel. Peptides were analyzed by electrospray mass spectrometry. Mass error was +/- 0.2000 Da.

CHAPTER III: Identifying The Role of Dcr-1/Loqs in RNAi Pathway

Disclaimer: The following chapter was a collaborative effort. All the experiments were done by the author with the following exceptions: Figure 5C was done by Yukihide Tomari, Figure 8 was done by Benjamin Haley, and Figure S3 was done by Megha Ghildiyal.

Summary

In *Drosophila*, the two best understood RNA silencing pathways are the small interfering RNA (siRNA) mediated RNA interference (RNAi) pathway and the microRNA pathway. These two pathways were originally proposed to be parallel and separate. Increasingly, however, the two pathways appear to be interconnected. Here we show that the Dicer-1/Loquacious (Dcr-1/Loqs) complex, which is required for microRNA processing, plays an additional role in RNAi pathway triggered by long dsRNA. *loqs* mutant flies are partially defective in the silencing of *white* by a dsRNA trigger in vivo. The defect results from the lower level of dsRNA-derived siRNAs accumulated in *loqs* than in wild type flies. We futher investigate the molecular role of Loqs in RNAi pathway. Our data suggest that, in vivo and in vitro, the Dcr-1/Loqs complex binds to siRNA. In vitro, the binding of the Dcr-1/Loqs complex to siRNA is the earliest detectable step in siRNA-triggered Ago2-RISC assembly. Futhermore, the binding of Dcr-1/Loqs to siRNA appears to facilitate dsRNA dicing by Dcr-2/R2D2, supported by the fact that dicing activity is much lower in *loqs* lysate than in wild

type. Together, our data reveal considerable functional and genetic overlap between the miRNA and siRNA pathways, with the two sharing components previously thought to be restricted to just a single pathway.

Introduction

In most eukaryotes, long double-stranded RNA (dsRNA) triggers the destruction of messenger RNAs with complementary sequences, a phenomenon termed RNA interference (RNAi) (Fire et al., 1998; Kennerdell and Carthew, 1998; Ngo et al., 1998; Waterhouse et al., 1998). In *Drosophila*, 'foreign' long dsRNAs, such as those introduced experimentally or produced by viral infection, enter the RNAi pathway when they are processed into ~21 nucleotide, double-stranded small interfering RNAs (siRNAs) by the RNase III endonuclease Dicer-2 (Dcr-2) (Hamilton and Baulcombe, 1999; Zamore et al., 2000; Bernstein et al., 2001; Elbashir et al., 2001). (Flies encode two dicer proteins (Hoa et al., 2003; Lee et al., 2004).) These siRNAs are subsequently loaded into an effector complex—RISC (RNA-induced silencing complex)—containing Argonaute2 (Ago2) by the RISC-loading complex (RLC) (reviewed in Tomari and Zamore, 2005). Dcr-2 and its dsRNA-binding protein partner, R2D2, are core components of the RLC (Liu et al., 2003; Tomari et al., 2004b). They form a stable heterodimer that identifies the siRNA guide and passenger strands: R2D2 binds to the more stably paired end of the siRNA duplex, thereby positioning Dcr-2 at the less stable end, designating this RNA strand as the future guide (Tomari et al., 2004a). The two activities of Dcr-2/R2D2, dsRNA processing and siRNA loading, are uncoupled, based on the observations that the newly diced siRNA is released from Dcr-2 before it can enter RISC assembly pathway, and that the siRNA strand selection is independent of dicing polarity (Preall et al., 2006). After binding the siRNA, the Dcr-2/R2D2 heterodimer, perhaps together with other RLC components, recruits Ago2 to the double-stranded siRNA (Pham et al., 2004; Pham and Sontheimer, 2005; Preall et al., 2006). The geometry of the siRNA within the Dcr-2/R2D2 heterodimer is preserved when it is passed to Ago2: the 5´ end of the guide siRNA binds the Ago2 5´ phosphate-binding pocket, and the passenger strand assumes the position of a target mRNA.

Ago2 is an RNA-guided, Mg^{2+}-dependent endonuclease (Martinez and Tuschl, 2004; Meister et al., 2004; Rand et al., 2004; Schwarz et al., 2004; Song et al., 2004; Rivas et al., 2005). This nuclease activity acts not only in siRNA-guided mRNA cleavage, but also in the maturation of Ago2 to its active form, RISC. Because in immature RISC (pre-RISC) the passenger strand occupies the position of a target RNA, a critical step in RISC assembly is cleavage of the passenger strand by Ago2, a step that facilitates separation of the two siRNA strands (Matranga et al., 2005; Miyoshi et al., 2005; Rand et al., 2005; Kim et al., 2006; Leuschner et al., 2006). Dissociation of the passenger strand leaves Ago2 loaded a single-stranded siRNA guide. Such mature RISC can then find its mRNA targets by nucleobase complementarity to the siRNA guide and destroy them by Ago2-catalyzed endonucleolytic cleavage.

Plants and animals also produce a second class of small regulatory RNAs, microRNAs (miRNAs) (Lee et al., 1993; Pasquinelli et al., 2000; Reinhart et al., 2000; Lagos-Quintana et al., 2001; Lau et al., 2001; Lee and Ambros, 2001; Reinhart et al., 2002; Bartel, 2004; Du and Zamore, 2005). miRNAs are typically transcribed by RNA polymerase II as if they were mRNAs, but are then processed sequentially to generate a ~22 nt small RNA from the initial >1,000 nt transcript, the primary miRNA (pri-miRNA) (Lee et al., 2002). In animals, the RNase III enzyme Drosha acts with a dsRNA-binding domain (dsRBD) protein partner, named Pasha in flies, to excise from the pri-miRNA a ~70 nt stem-loop RNA, the pre-miRNA (Lee et al., 2003; Denli et al., 2004; Gregory et al., 2004; Han et al., 2004; Yeom et al., 2006). Cleavage of the pri-miRNA by Drosha defines either the 5′ end or 3′ end of the mature miRNA, which can reside on either arm of the stem of the pre-miRNA. (A few miRNAs are transcribed directly into pre-miRNAs by RNA polymerase III, at least in human cells (Borchert et al., 2006).)

Pre-miRNAs are converted to miRNAs by Dicer (Grishok et al., 2001; Hutvágner et al., 2001; Ketting et al., 2001). In flies it is Dicer-1 (Dcr-1), together with its dsRBD protein partner, Loquacious, (Loqs), that cleaves pre-miRNA (Lee et al., 2004; Forstemann et al., 2005; Jiang et al., 2005; Saito et al., 2005). Dcr-1 cleavage of a pre-miRNA liberates an siRNA-like duplex in which the miRNA is partially paired to a ~22 nt small RNA derived from the other arm of the pre-miRNA stem. This small RNA is the miRNA* (Bartel, 2004). The miRNA strand preferentially assembles into mature RISC, whereas the miRNA* strand is degraded.

It has been proposed that the RNAi and miRNA pathways are separate and parallel, with each using a unique set of proteins to produce small RNAs, to assemble functional RNA-guided enzyme complexes, and to regulate target mRNAs (Okamura et al., 2004). Such a simple picture likely underestimates the in vivo complexity of these two RNA silencing pathways. First, *dcr-1* mutant, which is defective in miRNA production, is also impaired in siRNA-directed RNAi (Lee et al., 2004). Second, Ago2, the Argonaute protein that mediates RNAi in flies, binds at least one endogenous miRNA (Forstemann et al., 2007). Finally, *ago1* and *ago2* interact genetically in embryonic patterning and morphogenesis, suggesting that they function in a common pathway (Meyer et al., 2006).

Here we show that the Dicer-1/Loquacious (Dcr-1/Loqs) complex, which is required for microRNA processing, also plays an important role in RNAi pathway triggered by long dsRNA. *loqs* mutant flies are partially defective in the silencing of *white* by a dsRNA trigger in vivo, which results from lower level of dsRNA-derived siRNAs accumulated in *loqs* than in wild type flies. We futher investigate the molecular role of Loqs in RNAi pathway. Our data suggest that, in vivo and in vitro, the Dcr-1/Loqs complex binds to siRNA. In vitro, the binding of the Dcr-1/Loqs complex to siRNA is the earliest detectable step in siRNA-triggered Ago2-RISC assembly. Futhermore, the binding of Dcr-1/Loqs to siRNA appears to facilitate dsRNA dicing by Dcr-2/R2D2, supported by the fact that the dicing activity is much lower in *loqs* lysate than in wild-type. Together, our data reveal considerable functional and genetic overlap between the miRNA and siRNA pathways, with the two sharing components previously thought to be restricted to just a single pathway.

Results

Loqs is required in vivo for maximal silencing triggered by a long inverted repeat

In flies and other eukaryotes, long inverted repeat (IR) RNAs trigger silencing of complementary mRNAs because they are almost entirely double-stranded. The *Drosophila white* gene, which encodes a protein required for the production and distribution of red eye pigment, can be silenced by a transgene (*GMR-whiteIR*, henceforth, *white*-IR) that expresses in developing eye tissue a 621 nt dsRNA hairpin corresponding to the third exon of *white* (Kennerdell and Carthew, 2000). The extent of silencing is proportionate to the number of copies of the IR-*white* transgene (Kennerdell and Carthew, 2000; Lee et al., 2004b) (Figure 1A), but is relatively insensitive to the number of copies of *white* present (TD and PDZ, unpublished). RNAi in *Drosophila* requires Dcr-2, which transforms long dsRNA into siRNA, R2D2, which collaborates with Dcr-2 to load siRNA into RISC, and Ago2, the core component of siRNA-RISC. Thus, IR-silencing of *white* mRNA is lost in all three mutants: *dcr-2* (Supplemental Figure S1A)(Lee et al., 2004b) , *r2d2* (Figure 1B) and *ago2* (Supplemental Figure S1A)(Kim et al., 2007). We quantified the extent of *white* silencing by extracting the eye pigment in acidic ethanol and measuring its absorbance at 480 nm (Figures 1E and S2). Loss of R2D2 function in flies expressing one (or two) copies of the *white* IR transgene and two copies of the endogenous *white* locus restored red pigment levels to 74 ± 13 (or 73 ± 15 for two copies of IR-*white*, n=5) percent of wild-type flies lacking the *white*-IR. Similarly strong loss of silencing was also observed for *dcr-2*(*dcr-2*^{L811fsX}: 92 ± 18% for two copies of IR-*white*; n=4) and *ago-2* (*ago-2*^{414} : 89 ± 6% for two copies of IR-*white*, n=4). *loqs*^{f00791} mutant flies were also defective in IR-triggered *white* silencing, but to a much smaller extent (Figure 1C and 1E). The *loqs*^{f00791} mutation restored pigment levels in flies carrying one copy of the *white* IR-expressing transgene to 12 ± 2% of wild-type and to 8 ± 0.6% for flies carrying two copies of the *white*-IR (n = 5; Figures 1C and 1E). *loqs*^{f00791} heterozygotes were statistically indistinguishable from wild-type flies bearing one copy of IR-*white*, whose eye pigment concentration was 4 ± 0.5 (or 2 ± 0.6 for two copies of IR-*white*) percent of wild-type in the absence of the IR-*white* transgene.

Insertion of a mini-*white*-expressing piggyBac transposon causes the *loqs*^{f00791} allele. Thus, *loq*s^{f00791} heterozygotes have two copies of the endogenous *white* locus and one copy of mini-*white*; *loqs*^{f00791} homozygotes have two copies of endogenous *white* and two copies of mini-*white*. The presence of this additional copy of mini-*white* did not account for the darker red color of *white*-silenced *loqs*^{f00791} flies, because *loqs*^{f00791} heterozygotes bearing two copies of *white,* one copy of mini-*white* (in the piggyBac transposon inserted at *loqs*), and one copy of a P-element expressing mini-*white* were effectively silenced by IR-*white* (Figure 1D). In the absence of the IR-*white* transgene, the total amount of *white* expression in these flies was higher than

Figure III-1

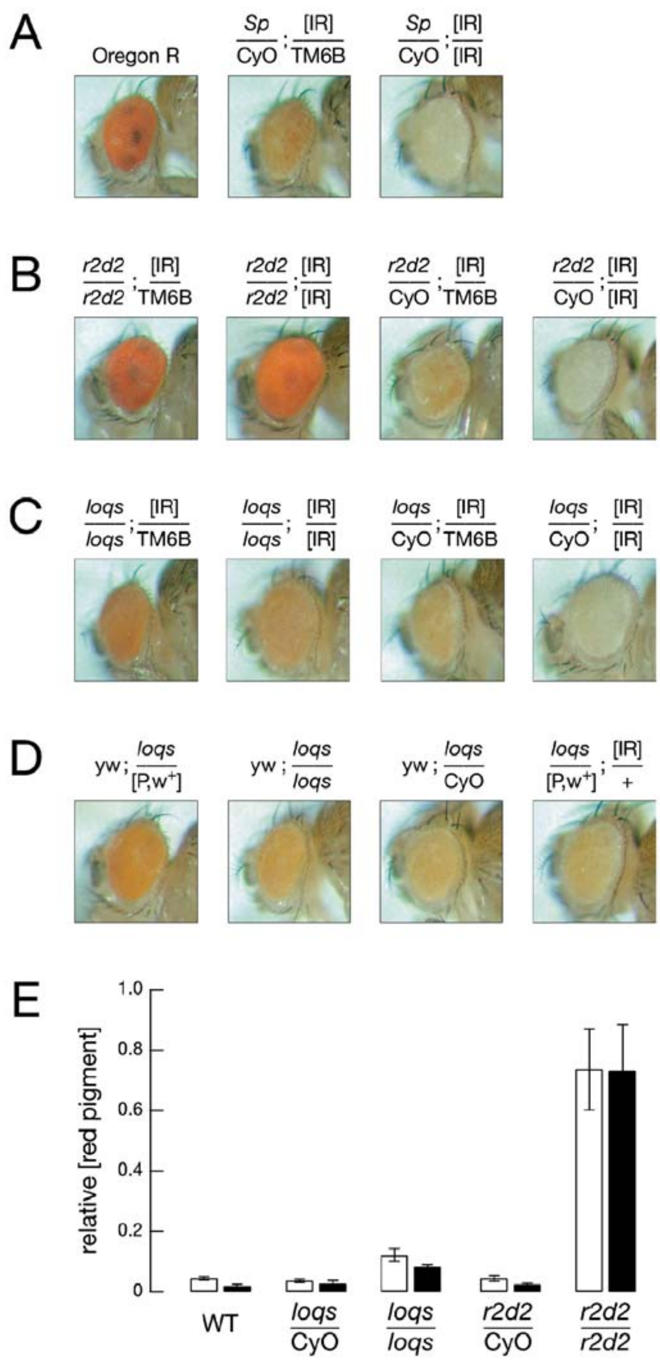
A
Oregon R
Sp / CyO ; [IR] / TM6B
Sp / CyO ; [IR] / [IR]
B
r2d2 / r2d2 ; [IR] / TM6B
r2d2 / r2d2 ; [IR] / [IR]
r2d2 / CyO ; [IR] / TM6B
r2d2 / CyO ; [IR] / [IR]
C
loqs / loqs ; [IR] / TM6B
loqs / loqs ; [IR] / [IR]
loqs / CyO ; [IR] / TM6B
loqs / CyO ; [IR] / [IR]
D
yw ; loqs / [P,w+]
yw ; loqs / loqs
yw ; loqs / CyO
loqs / [P,w+] ; [IR] / +
E
relative [red pigment]
1.0
0.8
0.6
0.4
0.2
0
WT
loqs / CyO
loqs / loqs
r2d2 / CyO
r2d2 / r2d2

Figure Legend III-1. Silencing of *white* by an IR Partially Depends on *loqs.* (A) The red eye color of wild-type flies (left) changes to orange (center) and white (right) in response to one or two copies, respectively, of a *white* IR transgene, which silences the endogenous *white* gene. (B) Homozygous mutant $r2d2^{1}$ flies fail to silence white, even in the presence of two copies of the *white*-IR transgene; heterozygous *r2d2*/CyO flies repress *white* expression. (C) In flies homozygous for $loqs^{f00791}$, silencing of *white* by the *white*-IR is less efficient; two copies of the *white*-IR do not produce completely white eyes, whereas they do in heterozygous $loqs^{f00791}$/CyO. (D) The eye color change in $loqs^{f00791}$ flies is not caused by the increased white^{+} gene dose resulting from the mini-white marker in the piggyBac transposon that causes the $loqs^{f00791}$ mutation. Flies trans-heterozygous for $loqs^{f00791}$ and a mini-white-marked P-element have more red eye pigment than $loqs^{f00791}$ homozygous flies, but show more efficient silencing by the *white*-IR than $loqs^{f00791}$ homozygous animals. (E) The eye pigment of the indicated genotypes was extracted and quantified by green light (480 nm) absorbance, relative to wild-type flies bearing no *white*-IR transgenes. The graph shows the mean and standard deviation of five independent measurements per genotype.

in *loqs*^{f00791} homozygotes (Figure 1D). Thus, reduction of Loqs function accounted for the partial desilencing of *white* in this system. Because *loqs*^{f00791} is a partial loss-of-function allele in the soma, we analyzed the silencing phenotype of *trans*-heterozygous flies bearing one copy of *loqs*^{f00791} and one copy of a new allele created by FLP recombinase-induced mitotic recombination of two, tandem, FRT-bearing piggyBac transposons flanking *loqs* (Supplementary Figure S3). This new allele, *loqs*$^{\Delta 1}$, completely deletes *loqs*, as well as an adjacent gene; *loqs*$^{\Delta 1}$ is homozygous lethal. The loss of *white* silencing was essentially the same in the *loqs*^{f00791} homozygotes and in the *loqs*^{f00791}/*loqs*$^{\Delta 1}$ *trans*-heterozygotes (Figure 1A and B), demonstrating that *loqs*, rather than a second gene fortuitously mutated in the original *loqs*^{f00791} stock, plays a role in robust RNAi in vivo.

It was reported recently that *loqs*^{f00791} mutation does not cosegregate with female sterility, suggesting the existence of a second mutation on the same chromosome which may affect fly development (Park et al., 2007). To exclude the possibility that the defect in RNAi in *loqs* mutants was caused by the second mutation, we tested silencing in flies bearing one copy of the *white*-IR, one mutant *loqs* allele, *loqs*^{f00791}, and one wild-type copy of *loqs* generated by precise excision (*loqs*^{ex}) of the piggyBac transposon causing the original *loqs* mutation. These flies should be homozygous for any second site mutation present on the original *loqs*^{f00791} chromosome, but not for the *loqs* mutation itself. We compared silencing in these genotypes to flies bearing one copy of the *white*-IR, one copy of the *loqs*^{f00791} mutation, and one wild-type copy of *loqs* on a chromosome, CyO, whose origins are distinct from that used to generate the *loqs* piggyBac allele. The *loqs*^{f00791}/*loqs*^{excision} flies were fully competent for *white* silencing (Supplemental Figure S1C). Together, our data suggest that the defect in RNAi is caused by loss of Loqs function, not a second site mutation.

The modest loss of silencing in the *loqs*^{f00791} mutant flies may reflect the incomplete loss of Loqs protein in this allele. However, Carthew and co-workers previously reported that a *dcr-1* null mutation leads to a similar, partial loss of *white* IR-silencing (Lee et al., 2004b). The small eye phenotype of *dcr-1* null mutants unfortunately renders a quantitative comparison to *loqs*^{f00791} impossible. We propose that—as for pre-miRNA processing—Dcr-1 and Loqs act together to enhance silencing by siRNAs.

To test the possibility that *loqs* mutation indirectly affects RNAi by influencing the expression of core RNAi components, we checked the expression level of different proteins in *loqs* mutant heads. We could detect no significant change in the concentrations of Dcr-2, R2D2 or Ago-2 in *loqs* mutant heads compared to wild type (Supplementary Figure S4B). However, it is still possible that *loqs* exerts its indirect effect on RNAi by affecting the expression of other facilitating factors or by altering the complex organization or subcellular localization of RNAi components. In addition to its obligatory role in miRNA biogenesis, Dcr-1 plays a supporting role in RNAi. Unexpectedly, the concentration of Dcr-1 protein was doubled in *loqs* mutants. However, increased Dcr-1 expression is unlikely to explain the impairment in RNAi in *loqs* mutant flies, because flies homozygous for *loqs* and heterozygous for *dcr-1* were more impaired in RNAi than *loqs*^{f00791} homozygotes that were wild-type for *dcr-*

1 (Supplemental Figure S1D). Loss of Loqs did lead to a decrease in Ago1 protein, perhaps because Dcr-1, Loqs, and Ago1 are transiently associated during the assembly of miRNAs into Ago1-RISC; loss of Loqs might destabilize this complex.

Reduced *white* siRNA accumulation in *loqs* mutant eyes

white silencing is directed by the siRNAs produced from the *white*-IR by Dcr-2 (Lee et al., 2004). Previously, we used microarrays containing 22-nt long probes tiled at one nt resolution across the sense and antisense strands of the *white*-IR to detect the siRNAs produced from the silencing trigger transgene. We found that the *white*-IR generated a unique set of siRNAs whose phasing suggests that Dcr-2 cleaves the IR transcript processively, beginning at the 4 nt loop and moving in ~21 nt steps across the dsRNA. This characteristic set of sense and antisense strand siRNAs were detected in wild-type heads, but most if not all were lost in a *dcr-2* mutant (Vagin et al., 2006). The siRNAs derived from the *white*-IR transcript were similarly lost in *r2d2* and *ago2* mutants (Figure 2A). Since the *white* siRNAs were completely lost in *ago2* mutant flies, and that Ago1 protein level was unchanged in *ago2* mutants (Supplemental Figure 4A), loss of RNAi in the absence of Ago2 did not reflect the loading of siRNAs into an inappropriate RISC complex, such as Ago1-RISC, indicating that Ago2 is the sole argonaute for *white*-IR derived siRNAs.

Neither R2D2 nor Ago2 is required for siRNA production *per se*. Rather, in vitro data suggest that R2D2 collaborates with Dcr-2 to load Ago2 (Liu et al., 2003). Thus, the disappearance of *white* siRNAs upon loss of the RISC loading machinery or the

Figure III-2

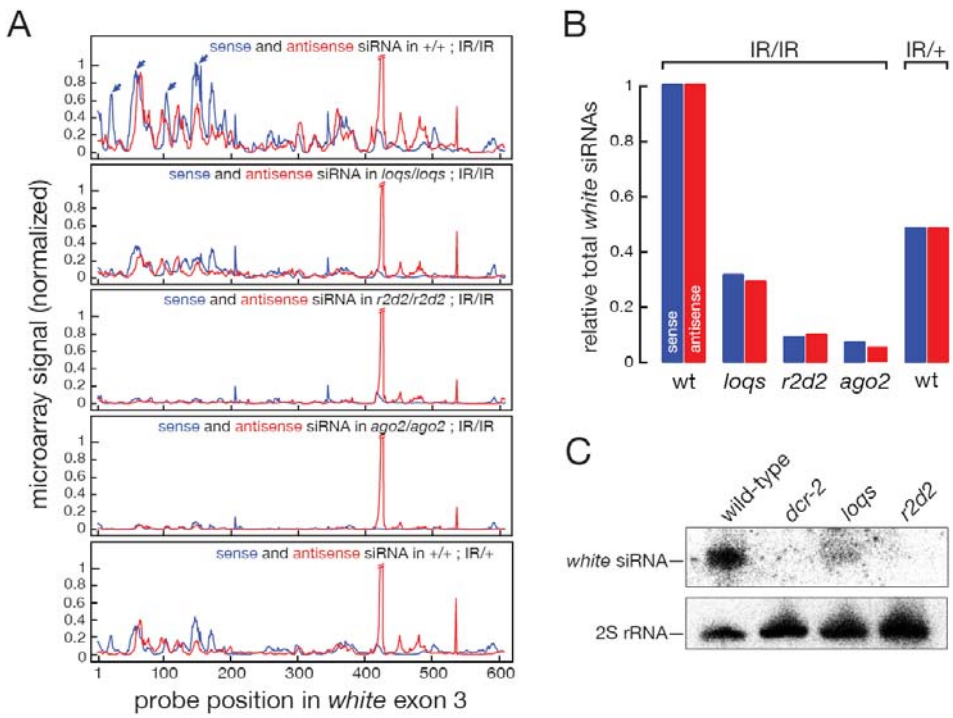
A
sense and antisense siRNA in +/+ ; IR/IR
sense and antisense siRNA in loqs/loqs ; IR/IR
sense and antisense siRNA in r2d2/r2d2 ; IR/IR
sense and antisense siRNA in ago2/ago2 ; IR/IR
sense and antisense siRNA in +/+ ; IR/+
microarray signal (normalized)
probe position in white exon 3
B
IR/IR
IR/+
relative total white siRNAs
sense
antisense
wt
loqs
r2d2
ago2
wt
C
wild-type
dcr-2
loqs
r2d2
white siRNA
2S rRNA

Figure Legend III-2. *white* siRNA accumulation is reduced in *loqs* mutant eyes. (A) Microarray analysis of the siRNAs derived from the *white*-IR trigger in the indicated genotypes. The allele used here are $loqs^{f00791}$, $r2d2^{1}$, and $ago2^{414}$. The arrows indicate the siRNA peaks for which probes were used in (C). (B) The amount of total *white* sense and antisense siRNAs in different mutants relative to that in wild-type flies expressing one (IR/+) or two (IR/IR) copies of the *white*-IR transgene. (C) Northern hybridization confirmed the microarray data in (A).

core RISC component, Ago2, suggests that, in vivo, siRNAs are unstable if they are unable to assemble into RISC. In vitro, siRNAs accumulate in the RLC in the absence of Ago2 (Tomari et al., 2004a; Miyoshi et al., 2005). Alternatively, the loss of siRNAs in *ago2*^{414} might indicate that Dcr-2/R2D2 cannot release siRNA in the absence of Ago2, preventing Dcr-2 from recycling after a single round of dsRNA cleavage and dramatically reducing siRNA production.

Considerably more siRNA was detected in *loqs*^{f00791} homozygotes than in the *dcr-2*, *r2d2* and *ago2* mutants (Figure 2A). Nonetheless, the amount of total siRNA in the *loqs* mutant was about one-third that detected in wild-type flies (Figure 2B). Northern hybridization using a mixture of four probes for *white* sense siRNAs confirmed the microarray analysis (Figure 2C). The concentration of siRNA in fly heads was directly proportional to the number of copies of the silencing trigger, with a single *white*-IR transgene generating about half as much total sense and antisense siRNA as two copies of the transgene (Figure 2B). In contrast, the extent of silencing was not proportional to the amount of siRNA: a single copy of the *white*-IR reduced the amount of red eye pigment to 4% of the wild-type concentration. Given the instability of the siRNAs in the absence of Ago2, these data suggest that the capacity to make Ago2-RISC in the presence of exogenous dsRNA exceeds the amount of Ago2-RISC required to silence *white*, a highly-expressed mRNA.

Although the magnitude of the siRNA signal was reduced in *loqs,* the distribution of siRNAs across the sequence of *white* exon 3 was essentially identical to wild-type (Figure 2A). There are two means how *loqs* mutation might impair siRNA accumulation: by diminishing the siRNA production by Dcr-2; or by affecting efficient siRNA loading into mature RISC; or the combination of both. Thus, we went on to test both possibilities.

loqs ovary lysate is defective in dsRNA dicing

To test whether *loqs* effects dsRNA dicing, we preformed the well-characterized in vitro dsRNA dicing assay in both wild-type and *loqs*^{f00791} ovary lysates (Zamore et al., 2000). Incubating a uniformly ^{32}P-radiolabeled 500 bp GFP dsRNA with either lysate yielded siRNAs of a unified length of 21nt. However, the dicing efficiency was much lower in *loqs* lysate than in wild-type lysate (Figure 3A). The result shown in Figure 3A represents four separate dicing experiments, using two sets of independently prepared lysates. The defect was not caused by the presence of inhibitory molecules in the *loqs* lysate, because addition of *loqs* lysate to wild-type lysate did not inhibit the dicing activity in the wild-type lysate (data not shown). Furthermore, addition of *dcr-2* lysate that did not exhibit any dicing activity could rescue the dicing in *loqs* lysate to virtually wild-type level (Figure 3B). The fact that *loqs* and *dcr-2* lysates can complement each other also indicates that the Dcr-2/R2D2 dicing complex in *loqs* lysate is fully functional.

The dicing defect in *loqs* lysate seems to affect a step downstream of Dcr-2 processing of dsRNA. The purified Dcr-2 or Dcr-2/R2D2 heterodimer could totally rescue *dcr-2* lysate for dsRNA processing (Figure 3C). However, neither of them was able to rescue dicing in *loqs* lysate. An important step in RISC loading is the transfer

Figure III-3

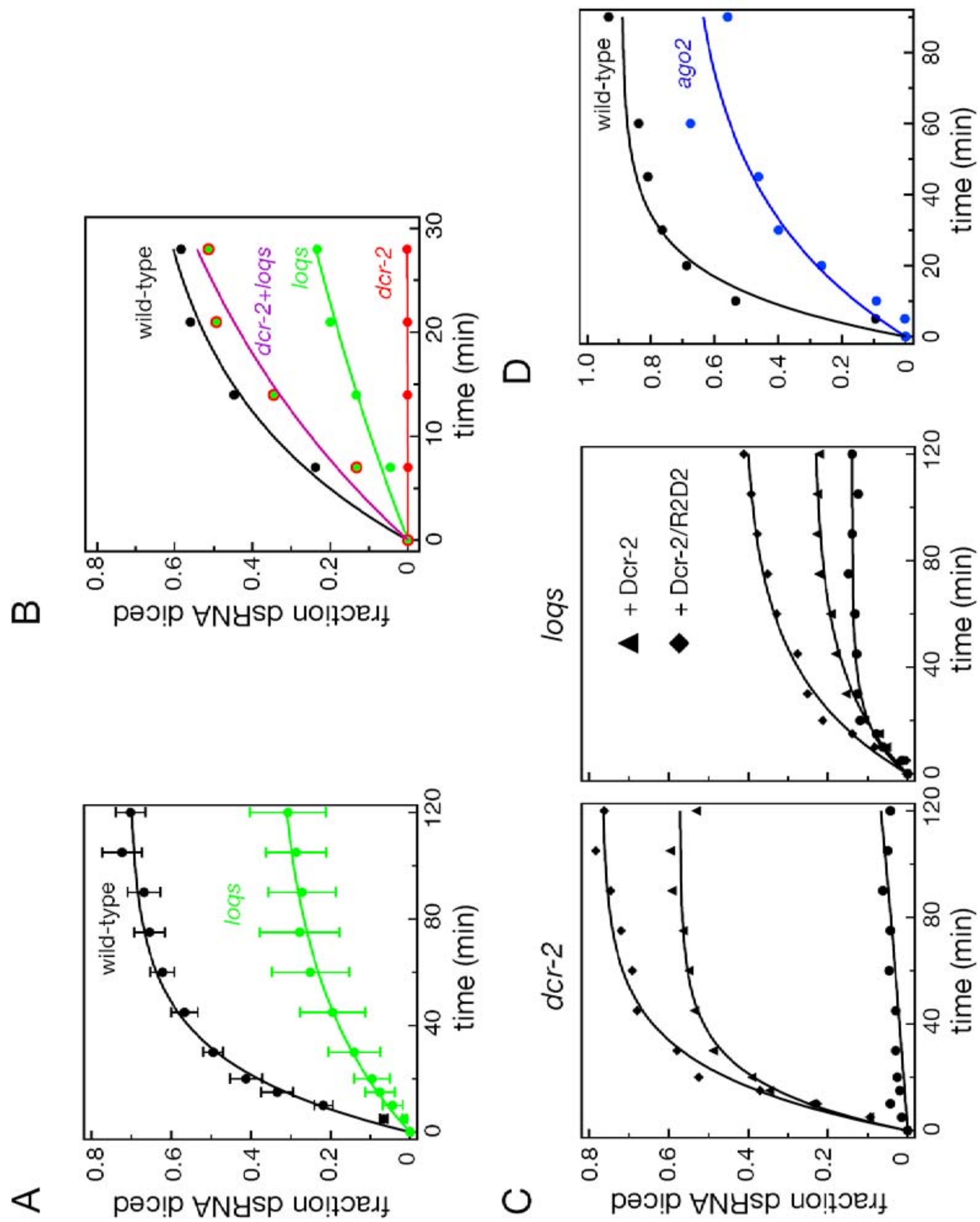
A
B
C
D
fraction dsRNA diced
time (min)
wild-type
loqs
dcr-2+loqs
dcr-2
ago2
+ Dcr-2
+ Dcr-2/R2D2

Figure Legend III-3. *loqs* lysate is defective in dsRNA dicing. (A) The rate of dsRNA processing is slower in *loqs* than in wild-type lysate. The data were averaged from four independent experiments and were fit to a first order exponential equation. (B) Analysis of dicing activity in different ovary lysates. For '*dcr-2*+*loqs*', *dcr-2* and *loqs* lysate were mixed at 1:1 ratio. In all the experiments, the final protein concentration in the reaction was adjusted to equal. (C) Testing rescue of dicing activity by Dcr-2 or Dcr-2/R2D2 recombinant protein. 1 nM final concentration of Dcr-2 or Dcr-2/R2D2 recombinant protein was added to *dcr-2* or *loqs* lysate. '•', no recombinant protein added. (D) *ago2* lysate exhibits dsRNA processing defect.

of double-stranded siRNA from Dcr-2/R2D2 to Ago2 in the RLC (Pham et al., 2004; Pham and Sontheimer, 2005; Tomari et al., 2004b). However, Ago2 *per se* is not required for dsRNA processing. Suprisingly, we observed a similar dsRNA dicing defect in *ago2* ovary lysate (Figure 3D). The apparent dicing defect in a known siRNA loading mutant promped us to test whether Dcr-1/Loqs also functions in siRNA loading.

Loqs associates with *white* siRNAs

If Loqs were a component of the siRNA loading machinery, the protein should associate with *white*-IR siRNA in vivo. We prepared lysate from the heads of flies expressing two copies of the *white*-IR transgene and examined the small RNAs immunoprecipitated with either anti-Loqs polyclonal or anti-Ago1 monoclonal antibodies. Western blotting demonstrated that more than 90% of total Loqs and Ago1 was immunoprecipitated by the corresponding antibody (data not shown). We used Northern hybridization to detect *white* siRNAs in the immunoprecipitates. Although the majority of *white* siRNA remained in the supernatant, we could detect *white* siRNA in the Loqs immunoprecipitate, but not in the Ago1 immunoprecipitate (Figure 4). No siRNA was detected in the absence of the *white*-IR transgene. The low abundance of siRNA bound to Loqs-containing complex could partially due to the fact that at steady state the majority of endogenous siRNAs are present in Ago2 RISC as opposing to intermediate loading complexes, which may also explain our array result where *ago2* mutants exhibited complete loss of siRNA (Figure 2). As expected,

Figure III-4

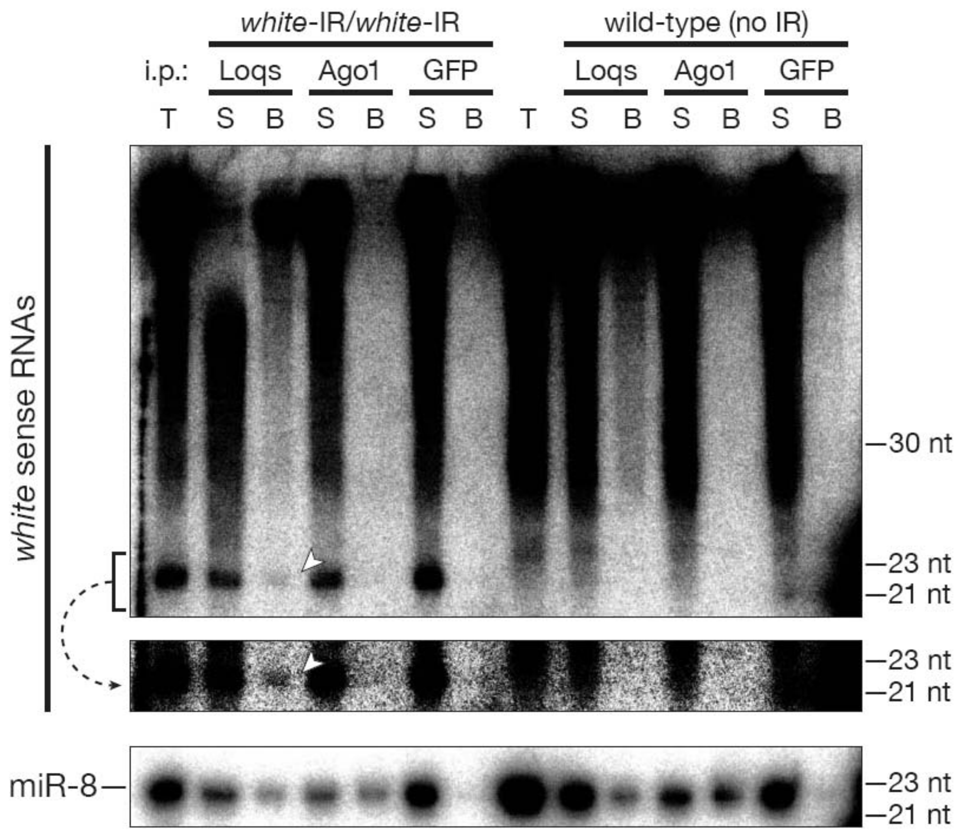
white-IR/white-IR
wild-type (no IR)
i.p.:
Loqs
Ago1
GFP
Loqs
Ago1
GFP
T S B S B S B T S B S B S B
white sense RNAs
—30 nt
—23 nt
—21 nt
—23 nt
—21 nt
miR-8—
—23 nt
—21 nt

Figure Legend III-4. Loqs associates with *white* siRNAs. Northern analysis of *white* siRNA immunoprecipitated from fly head lysates with either anti-Loqs or anti-Ago1 antibodies. The same membrane was reprobed for miR-8. Neither *white* siRNAs nor miR-8 were immunoprecipitated by the control antibody, anti-GFP. Equivalent amounts of total input RNA (T), supernatant (S), and RNA bound (B) to the antibody-beads (i.e., the immunoprecipitate) were loaded on the gel.

the miRNA, miR-8, was readily detected in both the Loqs and Ago1 immunoprecipitates, irrespective of the presence of the *white*-IR. Association of miR-8 with Loqs is consistent with the role of Loqs in the production of mature miRNAs, which are typically loaded into Ago1-RISC.

Dcr-1/Loqs complex with siRNA in vitro

We used native gel analysis to test whether siRNAs formed a stable complex with Loqs during the in vitro assembly of an siRNA into Ago2-RISC. In this assay, 5′ ^{32}P-radiolabeled siRNA was incubated with embryo or ovary lysate, then the protein-siRNA complexes were resolved by electrophoresis through a vertical agarose gel. At least three siRNA-containing complexes could be detected in this gel system: complex B, the RLC and RISC (Tomari et al., 2004a). Kinetic modeling supported a pathway in which the double-stranded siRNA first forms complex B, is then transferred to the RLC, and finally associates with Ago2 to form RISC (Tomari et al., 2004b). While both the RLC and RISC contain Dcr-2 and R2D2, complex B does not. Intriguingly, complex B was completely absent when siRNA was incubated with *loqs*^{f00791} mutant ovary lysate, although both the RLC and RISC were assembled (Figure 5A).

loqs^{f00791} is a strong loss-of-function allele in the female germ line, but only a weak hypomorph in the soma. Thus, the concentration of Loqs, relative to wild-type, is reduced far less in *loqs*^{f00791} heads than in ovaries. Nonetheless, in extracts prepared from *loqs*^{f00791} mutant heads, complex B assembly was less than in wild-type

Figure III-5

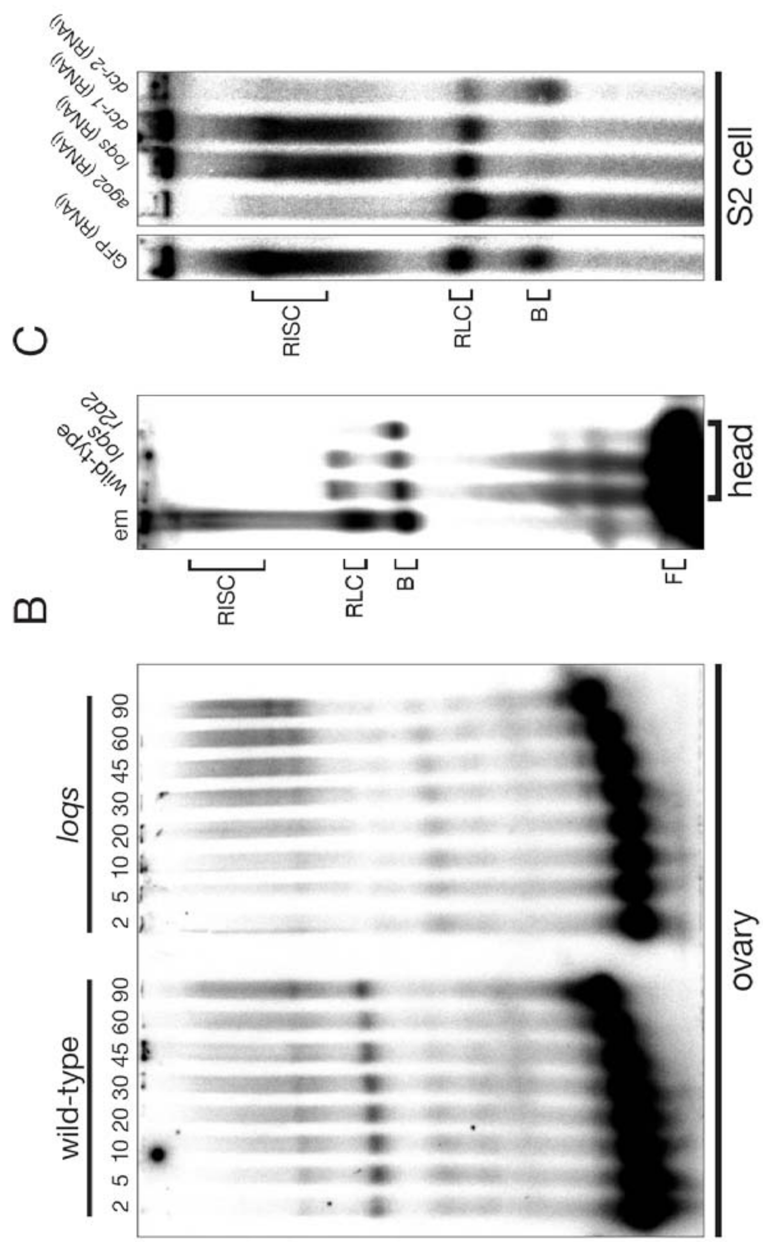
A
time (min):
wild-type
loqs
2 5 10 20 30 45 60 90
2 5 10 20 30 45 60 90
RISC
RLC
B
F
ovary
B
em
wild-type
loqs
r2d2
RISC
RLC
B
F
head
C
GFP (RNAi)
ago2 (RNAi)
loqs (RNAi)
dcr-1 (RNAi)
dcr-2 (RNAi)
RISC
RLC
B
S2 cell

Figure Legend III-5. An early complex in the RISC assembly pathway requires Loqs. Native gel analysis of siRNA-protein complexes assembled on 5′ ^{32}P-radiolabled siRNA in wild-type and mutant (A) ovary lysates or (B) fly head lysates or in (C) lysates prepared from cultured S2 cells treated with dsRNA corresponding to the indicated genes. Embryo lysate, em; free siRNA unassociated with protein, F.

(Figure 5B). The difference was small, but significant: in five separate assembly experiments, using three sets of independently prepared lysates, the amount of complex B formed in the *loqs* mutant lysate was 70 ± 18% of the wild-type level ($P < 0.0058$; Supplemental Figure S5). In these experiments, the amount of RLC formed was also significantly reduced (59 ± 19% of the wild-type level; $P < 0.0014$), supporting our previous model that complex B is a kinetic precursor to the RLC (Tomari et al., 2004b).

Like *loqs*^{f00791} mutants, *dcr-1* mutants are partially defective in silencing triggered by the *white*-IR transgene. Loqs is the partner of Dcr-1. Thus, we tested if loss of Dcr-1 also led to loss of complex B in vitro. Loss of Dcr-1 is lethal, so we prepared lysate from cultured *Drosophila* S2 cells in which RNAi was used to block expression of *ago2*, *loqs*, *dcr-1*, or *dcr-2*. Depletion was confirmed by measuring the protein concentrations of the target genes (data not shown). In control lysate from S2 cells treated with dsRNA targeting GFP (i.e., *gfp(RNAi)*), siRNA assembled complex B, the RLC, and RISC. Both the *dcr-1(RNAi)* and *loqs (RNAi)* S2 cell lysates formed less complex B than the control lysate (Fig. 5C). In contrast, in the *ago2(RNAi)* lysate, normal amounts of complex B and the RLC were assembled, but RISC was reduced, and assembly of RLC and RISC, but not complex B, was impaired in the *dcr-2(RNAi)* lysate.

To test if Loqs is a component of complex B, we used two-dimensional native gel/Western blotting experiments. We incubated the 5′ ^{32}P-radiolabeled siRNA with wild-type embryo lysate, resolved the complexes on a vertical agarose gel, cut the gel

Figure III-6

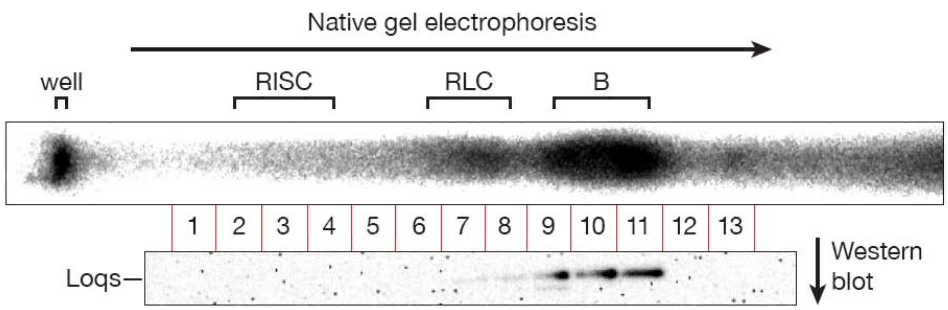
Native gel electrophoresis
well
RISC
RLC
B
1
2
3
4
5
6
7
8
9
10
11
12
13
Loqs
Western blot

Figure Legend III-6. Loqs resides in complex B. A 5′ ^{32}P-radiolabeled siRNA was incubated with embryo lysate, then the resulting protein-siRNA complexes resolved on a native agarose gel. The gel was then divided into 13 slices, and each slice analyzed by Western blotting to detect Loqs protein.

into thirteen slices, and then analyzed each slice by Western blotting using a polycolonal anti-Loqs antibody. The slices containing Loqs coincided with those containing complex B (Figure 6). We conclude that Loqs protein is present in complex B.

Dcr-1/Loqs bind to siRNA in complex B

Both Loqs and Dcr-1 contain dsRBDs. But do they bind to siRNA directly or are they components of a larger complex in which other proteins associate with siRNA? The interaction between Dcr-1 with siRNA was reported previously using short UV mediated site-unspecific crosslinking (Pham et al., 2004). Here, we synthesized an siRNA containing a single photocrosslinkable base (4-thiouracil) at position 20 of the 5′ ^{32}P-radiolabeled guide strand (Figure 7A). The first guide strand nucleotide of the siRNA was unpaired, ensuring that nearly all RISC assembled contained the strand bearing the 4-thiouracil (Schwarz et al., 2003). The siRNA was incubated with embryo lysate to assemble complexes, then irradiated with 302 nm UV light to covalently link the ^{32}P-radiolabeled siRNA through the 4-thio-subsituted nucleotide to nearby proteins. Proteins crosslinked to the siRNA were resolved by SDS-PAGE. We detected several siRNA-crosslinked proteins, including Dcr-2, R2D2 and Ago2 (Figure 7B). We confirmed the identity of the crosslinks by their absence in the corresponding mutant ovary lysates (data not shown). We also detected two crosslinked proteins corresponding to the size of Dcr-1 and Loqs.

To test whether these were Dcr-1 and Loqs, we immunoprecipitated the

Figure III-7

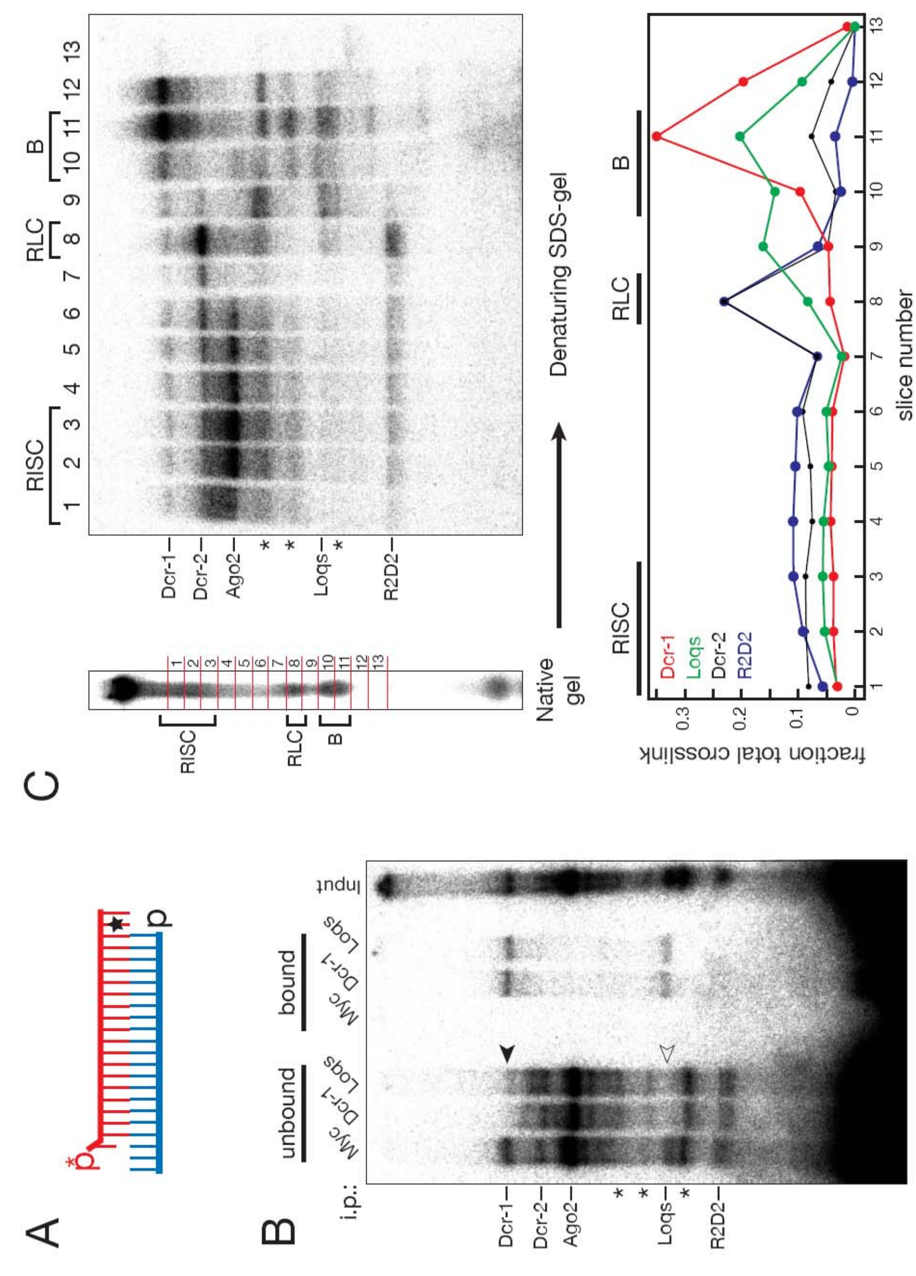
A
B
C
i.p.:
unbound
bound
Myc
Dcr-1
Loqs
Input
Dcr-1
Dcr-2
Ago2
Loqs
R2D2
RISC
RLC
B
Native gel
Denaturing SDS-gel
fraction total crosslink
slice number
Dcr-1
Loqs
Dcr-2
R2D2

Figure Legend III-7. Dcr-1 and Loqs bind to siRNA in complex B. (A) A schematic of the siRNA duplex used in crosslinking experiments. The star indicates the position of the 4-thiouracil on the guide strand. (B) Confirmation of Dcr-1 and Loqs crosslinks. Both siRNA-crosslinked Dcr-1 (solid arrow head) and Loqs (open arrow head) were recovered with the immunoprecipitate and depleted from the supernatant with either anti-Dcr-1 or anti-Loqs antibodies, but not with a control anti-myc antibody. Asterisks indicate siRNA-crosslinked protein whose identities are not known. (C) The 4-thiouracil-substituted siRNA was incubated with embryo lysate, irradiated with 302 nm UV light, then the resulting siRNA-crosslinked proteins resolved on a native agarose gel (left panel). The gel was cut into slices, and each slice was futher analyzed by 4-20% SDS-PAGE. Both the Dcr-1 and Loqs crosslinks were enriched in complex B (right panel). The fraction of each crosslinked protein present in each gel silice is shown in the graph (bottom panel).

crosslinked proteins with either anti-Loqs or anti-Dcr-1 antibody. Western blotting experiments demonstrated that >90% of the bulk Dcr-1 or Loqs protein was immunoprecipitated (data not shown). Both protein crosslinks were recovered in the immunoprecipitate and depleted from the supernatant with either anti-Loqs or anti-Dcr-1 antibody, but not with a control anti-myc tag antibody (Figure 7B). These data suggest that both Dcr-1 and Loqs are in close contact with the siRNA and that siRNA-bound Dcr-1 associates tightly with Loqs (and vice versa).

Does the interaction between Dcr-1, Loqs, and siRNA occur in complex B? We incubated the 5′ ^{32}P-radiolabeled, 4-thiouracil-substitute siRNA in lysate, irradiated to initiate protein-siRNA crosslinking, and then resolved the siRNA-protein complexes by native gel electrophoresis. The native gel was divided into 13 slices and each was analyzed by SDS-PAGE to resolve proteins crosslinked to the radiolabeled siRNA (Figure 7C). As reported previously, the peak of siRNA-crosslinked Ago2 coincided with RISC, whereas the majority of siRNA-crosslinked Dcr-2 and R2D2 comigrated with the RLC. siRNA-crosslinked Dcr-1 and Loqs were both enriched in complex B. Quantitative analysis of the data supports the view that complex B corresponds to Dcr-1, Loqs, and perhaps other proteins bound to siRNA (Figure 7C).

Finally, the siRNA was incubated with lysate, crosslinked, and the reaction resolved by gel filtration chromatography. Every odd numbered chromatographic fraction was further resolved by SDS-PAGE to detect siRNA-crosslinked proteins, and every even numbered fraction analyzed by Western blotting to detect Loqs and Dcr-1 proteins irrespective of their crosslinking status. The peak of both siRNA-

Figure III-8

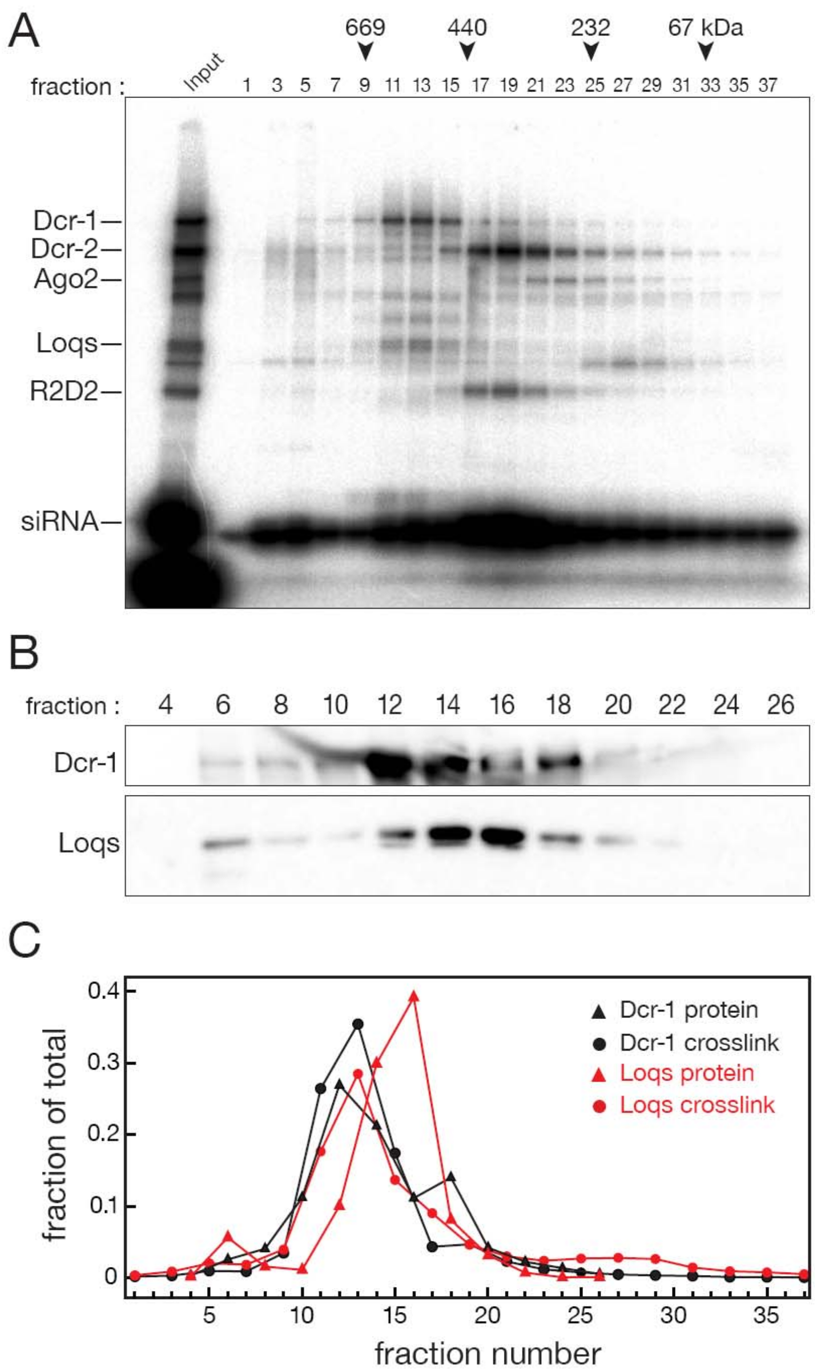
A
669
440
232
67 kDa
fraction :
Input
1 3 5 7 9 11 13 15 17 19 21 23 25 27 29 31 33 35 37
Dcr-1
Dcr-2
Ago2
Loqs
R2D2
siRNA
B
fraction : 4 6 8 10 12 14 16 18 20 22 24 26
Dcr-1
Loqs
C
Dcr-1 protein
Dcr-1 crosslink
Loqs protein
Loqs crosslink
fraction of total
fraction number
0
0.1
0.2
0.3
0.4
5 10 15 20 25 30 35

Figure Legend III-8. siRNA-bound Dcr-1 and Loqs co-fractionate. The 4-thiouracil-substitute siRNA was incubated with embryo lysate, irradiated with 302 nm UV light, and then the reaction resolved by gel filtration chromatography. (A) Each odd numbered chromatographic fraction was resolved by SDS-PAGE; (B) each even numbered fraction was analyzed by Western blotting using anti-Loqs and anti-Dcr-1 antibodies. (C) The fraction of Loqs and Dicer detected by siRNA-crosslinking and Western blotting was measured for each chromatographic fraction.

crosslinked Dcr-1 and siRNA-crosslinked Loqs had an apparent molecular weight of~560,000 (Figure 7A). Remarkably, this size is about the same as the Dcr-1/Loqs complex previously demonstrated to convert pre-miRNA to miRNA/miRNA* duplex (Forstemann et al., 2005), suggesting that the same Dcr-1/Loqs complex participates in both the siRNA and miRNA pathways. The peak of siRNA-crosslinked Loqs and Dcr-1 overlapped fully with the major peak of Dcr-1 protein, but not the major peak of Loqs protein (Figure 7B and 7C). Thus, not all Loqs is associated with Dcr-1, but Dcr-1-associated Loqs can bind siRNA.

Discussions

In *Drosophila*, the two best understood RNA silencing pathways are the siRNA-mediated RNAi pathway and the microRNA pathway. These two pathways were originally proposed to be parallel and separate. Increasingly, however, the two pathways appear to be interconnected, with some proteins shared between them. For example Dcr-1 and Loqs, which function together to process pre-miRNA into mature miRNA, are required in vivo for robust RNAi. Our data suggest that in vivo and in vitro, the Dcr-1/Loqs complex binds to siRNA. In vitro, siRNA bound to Dcr-1/Loqs corresponds to a previously identified RISC assembly intermediate, complex B, which appears to be a kinetic precursor of the RLC. As the name “complex B” was intended to be a placeholder until the components or functions of the complex were known, we propose re-naming it the “DLC” (Dcr-1/Loqs complex).

Although lysate from *loqs* heads or *loqs(RNAi)* S2 cells is quantitatively impaired in RLC assembly, both RLC and RISC still assemble even when complex B is undetectable. The simplest interpretation of these findings is that the DLC enhances the entry of siRNAs into the Ago2-RISC assembly pathway, but is not strictly required for this process. Such a view is also consistent with the reduction in IR-trigger *white* silencing in vivo in *loqs* and *dcr-1* mutants. Despite the modest RNAi defect in vivo and in vitro for *loqs* and *dcr-1* mutants, Carthew and colleagues, using a native acrylamide gel system that does not detect the DLC, found that embryo lysate from *dcr-1* mutants cannot transfer siRNA from the Dcr-2/R2D2 heterodimer (complex "R1") to the RLC (formerly complex "R2")(Lee et al., 2004). On the other hand, Sontheimer and coworkers showed that Dcr-1 could crosslink to siRNA in an R1 like complex (Pham et al., 2004). Consistent with our kinetic model, where the rate constant of siRNA in DLC releasing to free siRNA population is significantly higher than that of other directions, they also proposed that the association of Dcr-1 to siRNA is unstable.

The peaks of both siRNA-crosslinked Dcr-1 and siRNA-crosslinked Loqs co-eluted with the peak of pre-miRNA processing activity, suggesting that the same Dcr-1/Loqs complex that converts pre-miRNA to mature miRNA also functions to assist loading siRNAs into Ago2. However, it remains possible that there are two subpopulations of similar size (for example, Dcr-1 complexed with two isoform of Loqs, Loqs-PA and Loqs-PB, respectively) that are separately dedicated to the two pathways. Alternatively, a transiently associated factor might specify the activity of Dcr-1/Loqs for miRNA biogenesis versus Ago2 loading.

The finding that a Dcr-1/Loqs complex contributes to loading siRNA into Ago2 raises the possibility that Dcr-1/Loqs may also function in miRNA loading, possibly by binding to miRNA/miRNA* duplex. Such a suggestion has been made before, and in cultured S2 cells, both endogenous Dcr-1 and tagged, over-expressed Loqs co-immunoprecipitate with tagged, over-expressed Ago1, the fly Argonaute protein loaded principally with miRNA (Saito et al., 2005). If the Dcr-1/Loqs complex can load both siRNA and miRNA, it seems unlikely that it acts to steer small RNAs towards Ago1- and away from Ago2-RISC. Alternatively, Dcr-1/Loqs may bind preferentially to siRNA, despite the role of the complex in producing miRNA/miRNA* duplexes. Favoring our later hypothesis, a recent report by Liu and colleagues indicated that despite its prominent role in miRNA biogenesis, Loqs is largely dispensable for miRNA loading (Liu et al., 2007).

In addition to their role in siRNA loading, Dcr-1/Loqs also affects dsRNA processing. In *loqs* lysate, the dicing activity is significantly lower than in wild-type. The partial lost cannot be attributed to the loss of dsRNA dicing normally conducted by Dcr-1/Loqs, because no siRNA was detected in *dcr-2* mutant (Vagin et al., 2006) and the lack of dsRNA dicing activity of recombinant Dcr-1/Loqs (Saito et al., 2005). Instead, Dcr-1/Loqs might facilitate dicing via its binding to the freshly made siRNA. Dcr-2/R2D2 can bind to siRNA with high affinity (Liu et al., 2006; Tomari et al., 2007). Efficient processing of long dsRNA will require the fast release of newly made siRNA from Dcr-2/R2D2 to enable the next round of dicing. Under normal condition, Dcr-2/R2D2 might pass diced siRNA to Dcr-1/Loqs, as a result of which renders more efficient dicing. This model is supported by the observation that *ago2* mutant also exhibits in vitro dicing defect, probably caused by the failure of Dcr-2/R2D2 transfering siRNA to Ago2 in the RLC.

Finally, why is the accumulation of siRNA impaired in vivo in *loqs* mutant flies? The apparent explanation would be the in vivo dsRNA processing is defective in *loqs* mutant as reflected in vitro, which would indicate that dicing is the rate limiting step in fly eyes. Alternatively, the phenotype might attribute to the binding activity of Dcr-1/Loqs to siRNA. Probably, the DLC serves as reservoir for newly made siRNAs. In wild-type flies, we envision that siRNAs are first produced by Dcr-2, then stored in the DLC. siRNAs could then be passed to the RLC as unoccupied Dcr-2/R2D2 becomes available. In the absence of Dcr-1 or Loqs, siRNAs are clearly still assembled into RLC and RISC in vivo and in vitro, but in vivo they may be more vulnerable to destruction by ribonucleases without the DLC as a temporary refuge. Of course, both function of DLC could contribute to the loss of siRNA.

Materials and methods

Fly stocks

The following fly stocks were used: Oregon R, P[*w*-IR]/ P[*w*-IR] (on chromosome 2), P[*w*-IR]/ P[*w*-IR] (on chromosome 3), FRT42D *dcr-2*^{L811fsX}/CyO;P[*w*-IR]/TM6B, *r2d2*^{1}/CyO; P[*w*-IR]/TM6B, P[*w*-IR] /CyO;*ago2*^{414}/TM6B, *loqs*^{f00791}/CyO;P[*w*-IR]/TM6B, *cg9293*^{f03884}/CyO, *loqs*^{f00791}/CyO, *loqs*^{excision}/CyO, P[*w*-IR]; *loqs*^{f00791}/CyO; FRT82B *dcr-1*^{Q1147X}/TM6B.

Synthetic siRNA

Duplex siRNAs were prepared by annealing the synthetic RNA (Dharmacon Research) guide strand, 5´-UGA GGU AGU AGG UUG UAU AGU-3´ with the passenger strand, 5´-pUAU ACA ACC UAC UAC CUC CUU-3´. The guide strand was 5´ ^{32}P-radiolabeled with polynucleotide kinase (PNK; New England Biolabs, Beverly, MA, USA) and ^{32}P-γ-ATP, and then gel purified. siRNA duplexes were used at 50 nM final concentration as described (Haley et al., 2003).

Quantifying eye color

Red pigment was measured as described (Pal-Bhadra et al., 2004). For each genotype, heads were manually dissected from 8 males 3–4 days after eclosion. For each individual measurement, two heads were homogenized in 0.1 ml of 0.01 M HCl dissolved in ethanol. The homogenates were incubated at 4°C overnight, warmed to 50°C for 5 min, and then clarified by centrifugation. The optical density of the supernatant was measured at 480 nm and normalized to that recorded for heads from wild-type Oregon R.

Tiling microarrays

Microarray profiling and data analysis of siRNAs derived from the *white*-IR has been described previously (Vagin et al., 2006). Microarray fabrication, hybridization and data acquisition were performed at LC Sciences (Houston, TX, USA). 20 μg total RNA was isolated from wild-type or mutant fly heads using the mirVana kit (Ambion, Austin, TX, USA). Background (defined as the average signal for spots containing the chemical linker but no DNA probe) was subtracted from each intensity value. Intensities greater than ~55 (e^4) or ~148 (e^5) were considered significant (Lu et al., 2005). Control RNAs (ribosomal RNAs, snRNAs, snoRNAs, tRNAs and 'spiked-in' synthetic RNAs) were used for normalization, dividing each 'mutant' reading by the geometric average of all mutant/wt ratios for significantly detected control RNAs. Irreproducible peaks, i.e. those that appeared in only one of a series of replicate experiments, and single-probe peaks, i.e. those peaks where the probe signal was both higher than the average signal and more than five times greater than the signals from its immediate neighbors, were removed from the datasets. For all tiling arrays, color-reversed datasets were averaged. To facilitate comparison among mutants, all data were scaled to the intensity of the peak at position 150 of the sense strand in the wild-type genotype, i.e. the flies carrying two copies of IR on the second or third chromosome. The relative total signal from *white* siRNAs was obtained by summing the readings from all 608 probes, subtracting the artefactual antisense peaking at position 425, then scaling to the total signal from wild-type.

Preparation of Lysate from Heads

Wild-type or mutant flies were flash frozen in liquid nitrogen. Heads were separated from bodies by vigorous shaking in nested, pre-chilled sieves (U.S.A. standard sieve, Humboldt MFG Co., Chicago, IL, USA), allowing the heads to pass through the top sieve (No. 25) and collecting them on the bottom sieve (No. 40). Heads were transferred to 0.5 ml microcentrifuge tubes, pre-chilled in liquid-nitrogen, and then homogenized using a plastic “pellet pestle” (Kontes, Vineland, NJ, USA) in 1 ml ice-cold lysis buffer (100 mM potassium acetate, 30 mM HEPES-KOH at pH 7.4, 2 mM magnesium acetate) containing 5 mM DTT and 1 mg/ml complete “mini” EDTA-free protease inhibitor tablets (Roche) per gram of heads. Lysate was clarified by centrifugation at 14,000 × g for 30 min at 4°C. The supernatant was aliquoted into pre-chilled microcentrifuge tubes, flash frozen in liquid nitrogen, and stored at -80°C. For each experiment, siRNA-protein complexes were assembled using equal amounts of total protein for all genotypes.

Northern hybridization

RNA was isolated from fly heads using the mirVana kit (Ambion). Total RNA was quantified by absorbance at 260 nm and 3 μg of total RNA was resolved by electrophoresis through a 15% denaturing polyacrylamide/urea gel (National Diagnostics, Atlanta, GA, USA). 5′ ^{32}P-radiolabeled RNA oligonucleotides were included as size markers. After electrophoresis, the gel was transferred to Hybond N+ (Amersham-Pharmacia, Little Chalfont, UK) in 0.5x TBE by semi-dry transfer (Bio-Rad, Hercules, CA, USA) at 20 V for 2 h. RNA was crosslinked to the membrane by

UV irradiation (200 µjoules/cm; Stratalinker, Stratagene, La Jolla, CA, USA) and pre-hybridized in Church buffer (Church and Gilbert, 1984) for 1 h at 37°C. Four DNA probes (50 pmol each; IDT, Coralville, IA, USA) were individually 5′ ^{32}P-radiolabeled with polynucleotide kinase (New England Biolabs) and 330 µCi γ-^{32}P-ATP (7,000 µCi/mmol; New England Nuclear, Boston, MA, USA) each, purified on a Sephadex G-25 spin column (Roche, Basel, Switzerland), then mixed. To detect 2S rRNA, 1/50th of the ^{32}P-radiolabeled 2S rRNA probe was diluted with unlabeled probe. The ^{32}P-radiolabeled probes were hybridized in Church buffer at 37°C overnight. After hybridization, membranes were washed twice with 2x SSC/0.1% (w/v) sodium dodecyl sulfate (SDS) and once with 1x SSC/0.1% (w/v) SDS for 30 min. Membranes were analyzed by phosphorimagery (Fuji, Tokyo, Japan).

To re-hybridize membranes, probes were removed by boiling in 0.1% (w/v) SDS for 5 min. The membrane was then re-exposed to confirm probe removal. Probe sequences were 5′-TAC AAC CCT CAA CCA TAT GTA GTC CAA GCA-3′(2S rRNA), 5′-GAC ATC TTT ACC TGA CAG TAT TA-3′(miR-8), 5′-CCA TCA CGG CCA AAA GTT CGC C-3′ (*white* siRNA 1), 5′-GCA TTC AGC AGG GTC GTC TTT C-3′ (*white* siRNA 2), 5′-CCC GGA TGG CGA TAC TTG GAT G-3′ (*white* siRNA 3), and 5′-CCT GCA TCT CCT TGG CGT CCA C-3′ (*white* siRNA 4).

Native gel analysis of siRNA-protein complexes

50 nM 5′ ^{32}P-radiolabeled siRNA duplex was incubated with lysate in a standard RNAi reaction (Haley et al., 2003). Following incubation at 25°C for 30 min,

complexes were resolved by native agarose gel electrophoresis (Tomari et al., 2004b). Gels were dried under vacuum onto Hybond-N+ nylon membrane (Amersham-Pharmacia) and then exposed to a phosphorimager screen.

S2 cell RNAi

Constructs to make dsRNA directed against GFP, *dcr-1, dcr-2* and *loqs* were as described (Forstemann et al., 2005). Templates for the transcription of dsRNA directed against *ago2* were generated by T/A cloning PCR products generated using the oligonucleotides 5′-CGC ACC ATT GTG CAT CCT AAC GAG-3′ and 5′-GGG GAC AAT CGT TCG CTT TGC GTA-3′. The T/A vector contains dual T7 polymerase promoters; transcription templates were generated by PCR amplification of the *ago2* sequence inserted in the T/A vector using a PCR primer corresponding to the T7 polymerase promoter, 5′-CGT AAT ACG ACT CAC TAT AGG-3′.

Crosslinking

50 nM 5′-^{32}P radiolabeled siRNA duplex was incubated in 0–2 hr embryo lysate in a standard RNAi reaction at 25°C for 10 min, then transferred to a 96-well round bottom plate on ice. Samples were irradiated for 15 min with 302 nm light using an Ultraviolet Products model TM-36 transilluminator inverted directly on the polystyrene lid of the 96-well plate. Next, samples were either resolved by native agarose gel electrophoresis or adjusted to 1x SDS-sample buffer (62.5 mM Tris-HCl, pH 6.8, 10% glycerol, 2% SDS, 0.02% (w/v) Bromophenol Blue, 100 mM DTT),

heated to 95°C for 5 min, and resolved by 4–20% gradient SDS-polyacrylamide gel electrophoresis (Criterion pre-cast gels, Bio-Rad).

Immunoprecipitation and Western Blotting

For siRNA immunoprecipitation (Figure 3), anti-Loqs rabbit polyclonal (Forstemann et al., 2005) or anti-Ago1 mouse monoclonal antibodies (Okamura et al., 2004) were incubated in lysis buffer with protein A/G agarose (Calbiochem, San Diego, California, USA) for 2 h. After washing with lysis buffer containing 5 mM DTT, the beads were incubated with 60 µl of head lysate overnight at 4°C. The beads were washed three times with lysis buffer containing 5 mM DTT and 0.5% (v/v) NP-40. For immunoprecipitation of siRNA-crosslinked proteins, anti-myc monoclonal (clone 9E10, Sigma, St. Louis, Missouri, USA), anti-Dcr-1 rabbit polyclonal (Forstemann et al., 2005) and anti-Loqs rabbit polyclonal antibodies were used.

For Western blotting, the proteins were separated on 8% polyacrylamide/SDS gels and transferred to PVDF-membrane (Immobilon-P, Millipore, Billerica, MA, USA) by semi-dry transfer (Bio-Rad) in 25 mM Tris, pH 6.8, 250 mM glycine, 10% (v/v) methanol as anode buffer and 20 mM CAPS, pH 11.0, as cathode buffer at 20 V for 2 hr. All incubations and washes were in Tris-buffered saline (25mM Tris (pH 7.4), 137.5 mM NaCl, 2.5 mM KCl) containing 0.05% (v/v) Tween-20 and 5% fat-free milk powder (Big Y, Worcester, MA).

Gel-filtration chromatography

50 nM 5′ ^{32}P-radiolabeled siRNA duplex was incubated with 0–2 hr embryo lysate in a 200 μL RNAi reaction at 25°C for 1 h (Haley et al., 2003), then chromatographed on a Superdex-200 HR100/300GL column (Amersham-Pharmacia) using a BioCad Sprint (PerSeptive Biosystems, Framingham, Massachusetts, USA) (Nykanen et al., 2001). Protein from every other fraction was precipitated with 10% (v/v) trichloroacetic acid and 0.001% (w/v) deoxycholate, and then the precipitates resolved by electrophoresis through a 4–20% gradient SDS-polyacrylamide gel or analyzed by Western blotting.

Figure III-S1

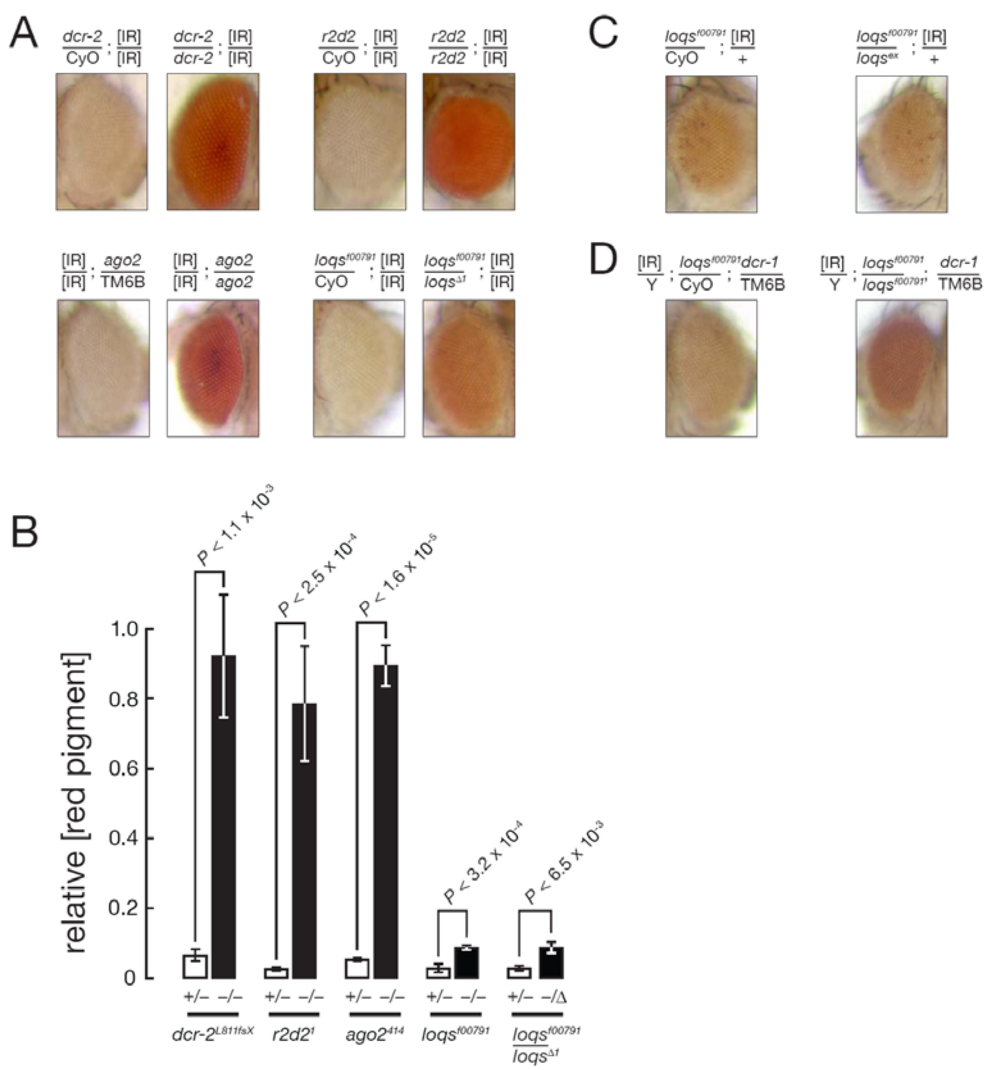

Figure Legend III-S1. Loqs facilitates RNAi in vivo. (A) The eye color of heterozygotes was compared to that of homozygotes for the mutant alleles *dcr-2*^{L811fsX}, *r2d2*^{1}, and *ago2*^{414} for age-matched males bearing two copies of the *white*-inverted repeat transgene ([IR]). For *loqs*, flies heterozygous for *loqs*^{f00791} were compared to *loqs*^{f00791}/*loqs*$^{\Delta 1}$ trans-heterozygotes. (B) The eye pigment of heterozygotes (+/–) and homozygotes (–/–) for the indicated genotypes, each bearing two copies of *white*-IR transgene, was extracted and its absorbance measured at 480 nm. The graph shows the mean ± standard deviation, relative to wild-type flies lacking the *white*-IR transgene, for at least four independent measurements. Statistical significance was estimated using a two-sample Student's *t*-test assuming equal variance. (C) Flies with one mutant *loqs* allele and one *loqs* excision (*loqs*^{ex}) are fully competent for IR-triggered RNAi in vivo. (D) Male flies bearing the *white*-IR transgene on the X chromosome, homozygous for *loqs* and heterozygous for *dcr-1* produce dark orange eyes, indicating that a reduction in Dcr-1 protein does not rescue the partial loss of silencing observed in *loqs* mutants.

Figure III-S2

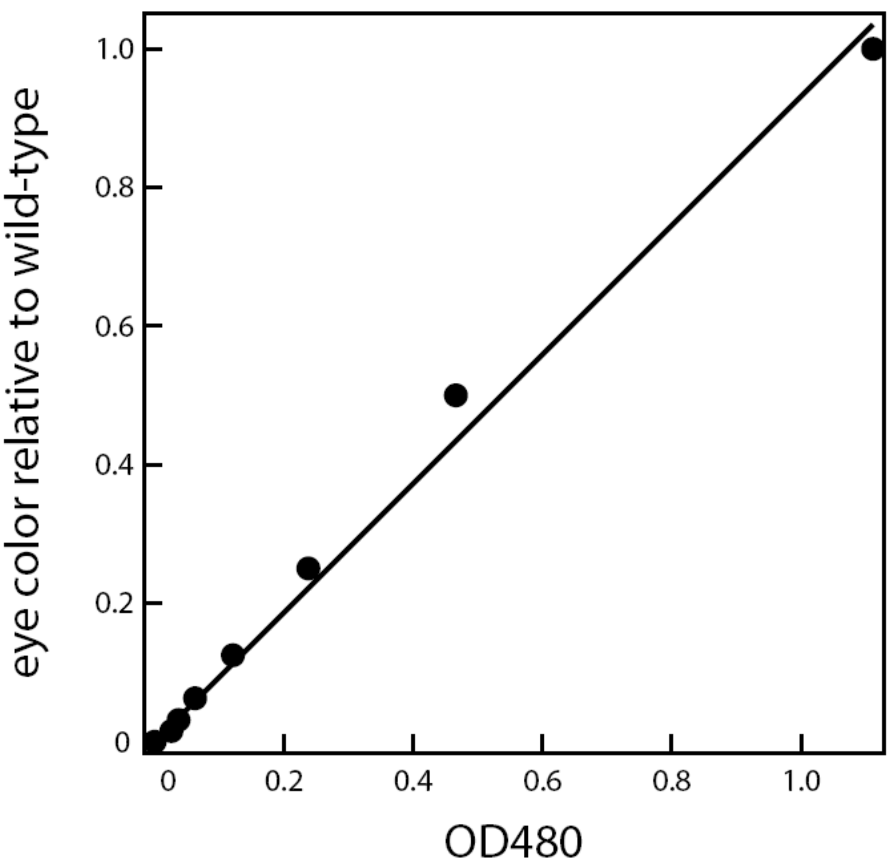

Figure Legend III-S2. A Concentration Series Generated by Dilution of the Eye Pigment Extract from Oregon R Flies. The concentration of each sample, relative to the undiluted sample, was plotted versus its absorbance at 480 nm. The data were fit to a line using Igor Pro 5.01.

Figure III-S3

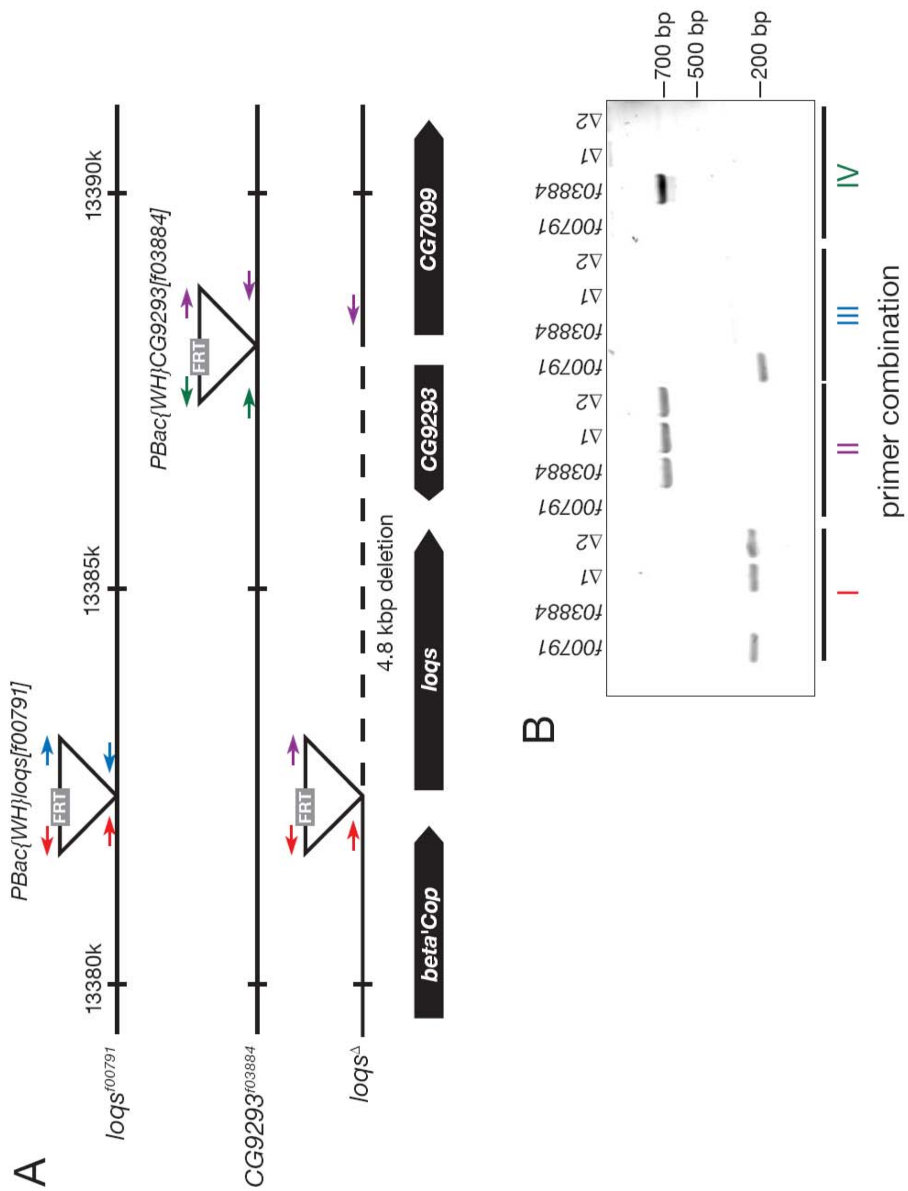

Figure Legend III-S3. Construction of a *loqs* deletion allele. (A) Strategy for making and identifying a 4.8 kbp deletion that removes the *loqs* gene. The deletion was constructed by FLP recombinase-mediated recombination between the FRT site in *PBac{WH}loqs[f00791]* and the FRT site in *PBac{WH}CG9293[f03884]*. (B) PCR analysis using the four colorcoded primer pairs, indicated as arrows in (A), demonstrated that two independent deletion alleles, *loqs*$^{\Delta 1}$ and *loqs*$^{\Delta 2}$, were recovered.

Figure III-S4

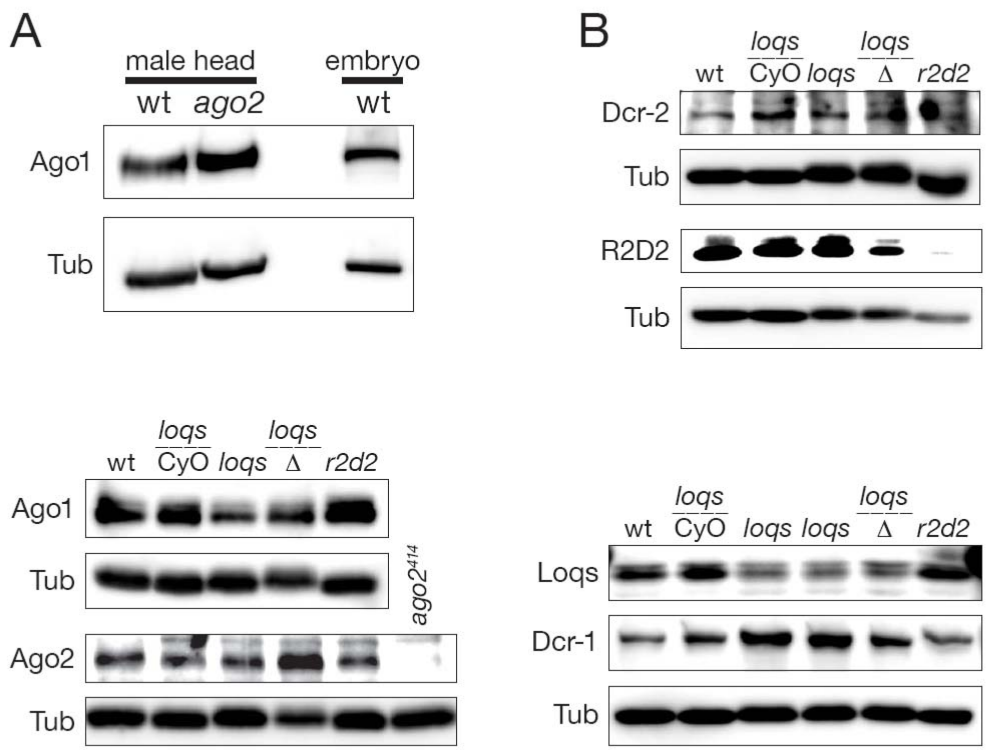

Figure Legend III-S4. Western blotting analysis for Dcr-2, Ago1, Ago2, Loqs, and Dcr-1 proteins in lysates prepared from mutant heads. Tubulin (Tub) served as a loading control. (A) The concentration of Ago1 protein in heads was undiminished by the absence of Ago2. (B) The concentration of Dcr-2, Ago2 and R2D2 proteins was unaltered in *loqs* mutant heads, whereas the concentration of Ago1 decreased and Dcr-1 increased when *loqs* was mutant.

Figure III-S5

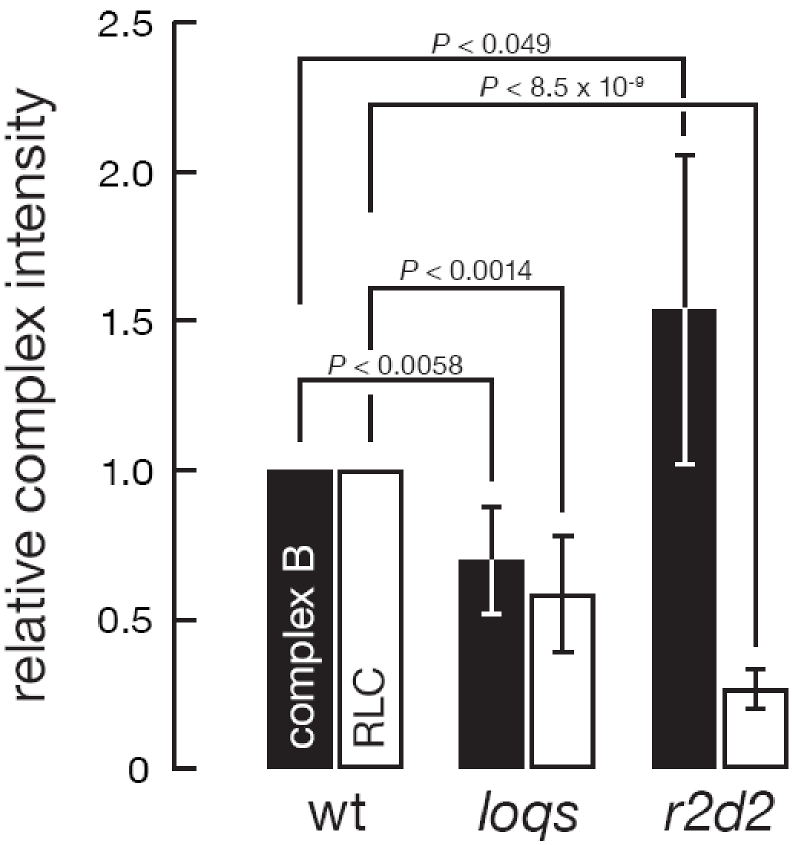

Figure Legend III-S5. Quantification for complexes assembled with 5′ ^{32}P-radiolabeled siRNA in wild-type and mutant head lysates. The amount of complex assembled in mutant lysates was normalized to that assembled in wild-type. The data are the average ± standard deviation for five separate assembly experiments, using three independently prepared lysates.

GENERAL DISCUSSION AND FUTURE PROSPECTS

In the preceding chapters, I have discussed my doctoral research on studying the siRNA loading pathway in *Drosophila* using both biochemical and genetic approaches. We established a gel shift system to identify the intermediate complexes formed during siRNA loading. We detected at least three complexes, named complex B, RISC loading complex (RLC) and RISC. Using kinetic modeling, we determined that the siRNA enters complex B and RLC early during assembly when it remains double-stranded, and then matures in RISC to generate Argonaute bearing only the single-stranded guide. We further characterized the three complexes. We showed that complex B comprises Dcr-1 and Loqs, while both RLC and RISC contain Dcr-2 and R2D2. Our study suggests that the Dcr-2/R2D2 heterodimer plays a central role in RISC assembly. We observed that Dcr-1/Loqs, which function together to process pre-miRNA into mature miRNA, were also involved in siRNA loading. This was surprising, because it has been proposed that the RNAi pathway and miRNA pathway are separate and parallel, with each using a unique set of proteins to produce small RNAs, to assemble functional RNA-guided enzyme complexes, and to regulate target mRNAs. We further examined the molecular function of Dcr-1/Loqs in RNAi pathway. Our data suggest that, in vivo and in vitro, the Dcr-1/Loqs complex binds to siRNA. In vitro, the binding of the Dcr-1/Loqs complex to siRNA is the earliest detectable step in siRNA-triggered Ago2-RISC assembly. Futhermore, the binding of Dcr-1/Loqs to siRNA appears to facilitate dsRNA dicing by Dcr-2/R2D2, because the dicing activity is much lower in *loqs* lysate than in wild type.

Long inverted repeat (IR) triggered *white* silencing in fly eyes is an example of endogenous RNAi. Consistent with our finding that Dcr-1/Loqs function to load siRNA, less *white* siRNA accumulates in *loqs* mutant eyes compared to wild type. As a result, *loqs* mutants are partially defective in IR trigged *white* silencing. Our data suggest considerable functional and genetic overlap between the miRNA and siRNA pathways, with the two sharing key components previously thought to be confined to just one of the two pathways.

Based on our study on siRNA loading pathway, we also elucidated the molecular function of Armitage (Armi) protein in RNAi. We showed that *armi* is required for RNAi. Lysates from *armi* mutant ovaries are defective for RNAi in vitro. Native gel analysis of protein-siRNA complexes suggests that *armi* mutants support early steps in the RNAi pathway, i.e., the formation of complex B and RLC, but are defective in the production of the RISC.

A better understanding of small RNA loading pathway

The molecular roles of three core components, Ago2, Dcr-2 and R2D2, in *Drosophila* RNAi have been extensively studied. Dcr-2/R2D2 heterodimer plays a central role in the siRNA loading pathway in *Drosophila*. First, Dcr-2/R2D2 acts as a gatekeeper for the assembly of Ago2-containing RISC by promoting the incorporation of siRNA duplexes and disfavoring the miRNA/miRNA* duplexes as loading substrates for Ago2 (Tomari et al., 2007). Secondly, the asymmetric binding of Dcr-2/R2D2 to siRNA determines the strand that will get loaded into Ago2 and matures as guide (Tomari et al., 2004b). Thirdly, in the RISC loading complex (RLC), Dcr-2/R2D2 directly transfers the siRNA duplex to Ago2 when the passenger strand gets cleaved and released from the guide (Matranga et al., 2005). All of the above functions of Dcr-2/R2D2 are accomplished in the RLC, which comprises other proteins besides Dcr-2/R2D2 (Pham et al., 2004). We showed that the complex where Dcr-2/R2D2 interacts with siRNA has an apparent molecular weight of ~400 KDa, which is bigger than Dcr-2, R2D2 and siRNA combined (Figure III-8A), also suggesting the existence of other factors. A major challenge for the future will be to identify the other protein components of RLC as well as other loading complexes and to determine their role in siRNA loading.

An siRNA containing a single photocrosslinkable base (4-thiouracil) at position 20 of the guide strand is readily crosslinked to several proteins in embryo or ovary lysates (Figure III-7). In fact, the identities of a number of the crosslinked proteins remain to be revealed. Moreover, at least a subset of these were enriched in complex B, RLC or RISC on native gel or gel-filtration chromataography fractions (Figure III-6 and III-7). Thus, they would serve good candidates for complex B, RLC or RISC components.

What is the molecular role of Dcr-1/Loqs in RNAi pathway?

We and other group showed that in vivo *dcr-1* and *loqs* are required for the maximal silencing of *white* by an inverted-repeat (IR) in eyes (Forstemann et al., 2005; Lee et al., 2004b), and both in vitro and in vivo Dcr-1/Loqs can bind to siRNA in complex B (Figure III-4 and III-7). We also showed that *loqs* mutant lysate is partially defective in long dsRNA dicing. However, we were not able to 'chase' complex B into RISC via RLC (data not shown), raising the question whether complex B is an in-pathway complex. Thus, we will need to conduct further research in order to establish the link between the in vivo RNAi defect of the mutants and our in vitro observations using fly lysates.

It is essential to learn whether the dicing defect we observed in *loqs* lysates is caused directly by the absence of Loqs, or it is rather a secondary defect as a result of the disruption of dicing complex function in the developmentally abnormal *loqs* ovaries. We can test it in different ways. First, I will try to rescue *loqs* lysates with recombinant Loqs or Dcr-1/Loqs proteins. Two Loqs isoforms exist in flies, Loqs-PA and Loqs-PB. It was shown that Loqs-PB, but not Loqs-PA, is required for pre-miRNA processing and maintaining germline stem cells (Park et al., 2007). Thus, by testing two isoforms for their ability of rescue dicing separately, we will come to know whether Loqs-PB and PA play distinct roles in miRNA biogenesis and siRNA loading pathways. If neither of the isoforms, which are fully functional otherwise, can rescue the *loqs* lysates, it will indicate that other factor(s) that is required for dicing is missing in the lysate. Another way to test the direct versus indirect role of Dcr-1/Loqs in dicing is to deplete Dcr-1 and/or Loqs from wild-type lysate and to test the depleted lysate for dicing. If the depleted lysate exhibits similar dicing defect to *loqs* lysates, it will suggest that Dcr-1/Loqs *per se* is required for efficient dicing. Otherwise, the defect is likely to be indirect. A caveat in this experiment will be that some proteins which stably bind to Dcr-1/Loqs may also get depleted from the lysates. However, we will be able to identify them by analyzing the protein constituents of immunoprecipitate. If the dicing defect in *loqs* lysates cannot be rescued by Dcr-1/Loqs recombinant protein, it will suggest that the defect is indirect. Moreover, based on the fact that the Dcr-2/R2D2 complex in *loqs* lysates is fully functional (Figure III-3), the result will indicate the existence of another protein (or other proteins) required for dicing whose function is disrupted in *loqs* lysate. It will be interesting to identify the factor, since no such protein has been reported. I will fractionate wild-type lysates by gel-filtration chromatography, and add back each fraction to *loqs* lysates. Assumably, the fraction(s) containing the unknown dicing factor should be able to rescue the *loqs* lysates. I can then try to identify it by analyzing the protein components in the rescueing fraction(s).

If Dcr-1/Loqs itself is required for dsRNA dicing, what is the molecular mechanism? Dcr-1/Loqs can bind to siRNA directly, whereas Ago2 is the core component of RISC. Intriguingly, both *loqs* and *ago2* lysates are defective in dsRNA dicing. One possible explanation is that the dicing defect is caused by the slower product release in the mutant lysates. In another word, under normal condition Dcr-1/Loqs facilitate siRNA release from Dcr-2/R2D2 immediately after long dsRNA dicing, while Ago2 facilitates siRNA release from Dcr-2/R2D2 by taking over the siRNA in RLC. In fact, product inhibition by siRNA has been reported for plant Dicer (Tang et al., 2003). If this possibility holds ture, we would expect that the addition of a factor which can expedite siRNA release will be able to resue the dicing defect in both *loqs* and *ago2* lysates. P19 protein might serve this goal.

The P19 protein is encoded by the *Tombusvirus* as a counterdefense against the plant RNAi pathway that degrades RNA viruses (Voinnet et al., 1999). P19 functions by specifically binding to siRNAs with high affinity (Silhavy et al., 2002; Vargason et al., 2003; Ye et al., 2003) and it has proven a powerful molecular tool for dissecting small RNA pathways in animal systems (Calabrese and Sharp, 2006; Dunoyer et al., 2004; Lecellier et al., 2005). If addition of recombinant P19 protein can largely rescue the dicing defect in *loqs* and *ago2* lysate in a dosage dependent manner, it will suggest that slower siRNA release is the major cause of the dicing defect. Otherwise, the dicing is deficient for a different reason.

One discrepancy between the in vivo *white* silencing system and the in vitro dsRNA-triggered RNAi system lies in the silencing trigger, with one being a cell expressed long inverted repeat (IR) versus the other being an in vitro transcribed long dsRNA. Although IR-triggered silencing exhibits all the features of RNAi (Lee et al., 2004b) (Figure III-1 and III-2), it is not clear yet whether this type of silencing requires additional factors than typical RNAi, possible due to the small terminal loop. Is Dcr-1/Loqs required for cutting out the loop? We can test this possibility in vitro by testing whether in vitro transcribed *white* IR can be efficiently diced in the Dcr-1 depleted lysates. We can also examine the efficiency of GFP knock-down by transfected GFP dsRNA in *loqs* or *dcr-1* knock-down S2 cells. If Dcr-1 depletion does not diminish IR dicing, as well as *loqs* and *dcr-1* knock-down cells still exhibit

RNAi defect despite the silencing trigger is dsRNA, it will indicate that the requirement of Dcr-1/Loqs for RNAi is not due to the existence of loop structure of the silencing trigger. Otherwise, it will prove the involvement of miRNA processing machinery in the IR-triggered silencing.

REFERENCES

Adenot, X., Elmayan, T., Lauressergues, D., Boutet, S., Bouche, N., Gasciolli, V., and Vaucheret, H. (2006). DRB4-dependent TAS3 trans-acting siRNAs control leaf morphology through AGO7. Curr Biol *16*, 927-932.

Alder, M.N., Dames, S., Gaudet, J., and Mango, S.E. (2003). Gene silencing in Caenorhabditis elegans by transitive RNA interference. RNA *9*, 25-32.

Allen, E., Xie, Z., Gustafson, A.M., and Carrington, J.C. (2005). microRNA-directed phasing during trans-acting siRNA biogenesis in plants. Cell *121*, 207-221.

Ambros, V., Lee, R.C., Lavanway, A., Williams, P.T., and Jewell, D. (2003). microRNAs and other tiny endogenous RNAs in C. elegans. Curr Biol *13*, 807-818.

Aoki, K., Moriguchi, H., Yoshioka, T., Okawa, K., and Tabara, H. (2007). In vitro analyses of the production and activity of secondary small interfering RNAs in C. elegans. EMBO J *26*, 5007-5019.

Aravin, A., Gaidatzis, D., Pfeffer, S., Lagos-Quintana, M., Landgraf, P., Iovino, N., Morris, P., Brownstein, M.J., Kuramochi-Miyagawa, S., Nakano, T., *et al.* (2006). A novel class of small RNAs bind to MILI protein in mouse testes. Nature *442*, 203-207.

Aravin, A.A., Lagos-Quintana, M., Yalcin, A., Zavolan, M., Marks, D., Snyder, B., Gaasterland, T., Meyer, J., and Tuschl, T. (2003). The small RNA profile during Drosophila melanogaster development. Dev Cell *5*, 337-350.

Aravin, A.A., Naumova, N.M., Tulin, A.V., Vagin, V.V., Rozovsky, Y.M., and Gvozdev, V.A. (2001). Double-stranded RNA-mediated silencing of genomic tandem repeats and transposable elements in the D. melanogaster germline. Curr Biol *11*, 1017-1027.

Aravin, A.A., Sachidanandam, R., Girard, A., Fejes-Toth, K., and Hannon, G.J. (2007). Developmentally regulated piRNA clusters implicate MILI in transposon control. Science *316*, 744-747.

Axtell, M.J., Jan, C., Rajagopalan, R., and Bartel, D.P. (2006). A two-hit trigger for siRNA biogenesis in plants. Cell *127*, 565-577.

Aza-Blanc, P., Cooper, C.L., Wagner, K., Batalov, S., Deveraux, Q.L., and Cooke, M.P. (2003). Identification of modulators of TRAIL-induced apoptosis via RNAi-based phenotypic screening. Mol Cell *12*, 627-637.

Bagga, S., Bracht, J., Hunter, S., Massirer, K., Holtz, J., Eachus, R., and Pasquinelli, A.E. (2005). Regulation by let-7 and lin-4 miRNAs results in target mRNA degradation. Cell *122*, 553-563.

Baumberger, N., and Baulcombe, D.C. (2005). Arabidopsis ARGONAUTE1 is an RNA Slicer that selectively recruits microRNAs and short interfering RNAs. Proc Natl Acad Sci U S A *102*, 11928-11933.

Beclin, C., Boutet, S., Waterhouse, P., and Vaucheret, H. (2002). A branched pathway for transgene-induced RNA silencing in plants. Curr Biol *12*, 684-688.

Behm-Ansmant, I., Rehwinkel, J., Doerks, T., Stark, A., Bork, P., and Izaurralde, E. (2006). mRNA degradation by miRNAs and GW182 requires both CCR4:NOT deadenylase and DCP1:DCP2 decapping complexes. Genes Dev *20*, 1885-1898.

Bentwich, I., Avniel, A., Karov, Y., Aharonov, R., Gilad, S., Barad, O., Barzilai, A., Einat, P., Einav, U., Meiri, E*., et al.* (2005). Identification of hundreds of conserved and nonconserved human microRNAs. Nat Genet *37*, 766-770.

Berezikov, E., Chung, W.J., Willis, J., Cuppen, E., and Lai, E.C. (2007). Mammalian mirtron genes. Mol Cell *28*, 328-336.

Berezikov, E., Cuppen, E., and Plasterk, R.H. (2006). Approaches to microRNA discovery. Nat Genet *38 Suppl*, S2-7.

Berezikov, E., Guryev, V., van de Belt, J., Wienholds, E., Plasterk, R.H., and Cuppen, E. (2005). Phylogenetic shadowing and computational identification of human microRNA genes. Cell *120*, 21-24.

Bernstein, E., Caudy, A.A., Hammond, S.M., and Hannon, G.J. (2001). Role for a bidentate ribonuclease in the initiation step of RNA interference. Nature *409*, 363-366.

Bhattacharyya, S.N., Habermacher, R., Martine, U., Closs, E.I., and Filipowicz, W. (2006). Relief of microRNA-mediated translational repression in human cells subjected to stress. Cell *125*, 1111-1124.

Billy, E., Brondani, V., Zhang, H., Muller, U., and Filipowicz, W. (2001). Specific interference with gene expression induced by long, double-stranded RNA in mouse embryonal teratocarcinoma cell lines. Proc Natl Acad Sci U S A *98*, 14428-14433.

Bohnsack, M.T., Czaplinski, K., and Gorlich, D. (2004). Exportin 5 is a RanGTP-dependent dsRNA-binding protein that mediates nuclear export of pre-miRNAs. RNA *10*, 185-191.

Borchert, G.M., Lanier, W., and Davidson, B.L. (2006). RNA polymerase III transcribes human microRNAs. Nat Struct Mol Biol *13*, 1097-1101.

Borsani, O., Zhu, J., Verslues, P.E., Sunkar, R., and Zhu, J.K. (2005). Endogenous siRNAs derived from a pair of natural cis-antisense transcripts regulate salt tolerance in Arabidopsis. Cell *123*, 1279-1291.

Bouche, N., Lauressergues, D., Gasciolli, V., and Vaucheret, H. (2006). An antagonistic function for Arabidopsis DCL2 in development and a new function for DCL4 in generating viral siRNAs. EMBO J *25*, 3347-3356.

Boutet, S., Vazquez, F., Liu, J., Beclin, C., Fagard, M., Gratias, A., Morel, J.B., Crete, P., Chen, X., and Vaucheret, H. (2003). Arabidopsis HEN1: a genetic link between endogenous miRNA controlling development and siRNA controlling transgene silencing and virus resistance. Curr Biol *13*, 843-848.

Boutla, A., Delidakis, C., Livadaras, I., Tsagris, M., and Tabler, M. (2001). Short 5'-phosphorylated double-stranded RNAs induce RNA interference in Drosophila. Curr Biol *11*, 1776-1780.

Brennecke, J., Aravin, A.A., Stark, A., Dus, M., Kellis, M., Sachidanandam, R., and Hannon, G.J. (2007). Discrete small RNA-generating loci as master regulators of transposon activity in Drosophila. Cell *128*, 1089-1103.

Brennecke, J., Stark, A., Russell, R.B., and Cohen, S.M. (2005). Principles of microRNA-target recognition. PLoS Biol *3*, e85.

Brodersen, P., and Voinnet, O. (2006). The diversity of RNA silencing pathways in plants. Trends Genet *22*, 268-280.

Cai, X., Hagedorn, C.H., and Cullen, B.R. (2004). Human microRNAs are processed from capped, polyadenylated transcripts that can also function as mRNAs. RNA *10*, 1957-1966.

Calabrese, J.M., and Sharp, P.A. (2006). Characterization of the short RNAs bound by the P19 suppressor of RNA silencing in mouse embryonic stem cells. RNA *12*, 2092-2102.

Caplen, N.J., Fleenor, J., Fire, A., and Morgan, R.A. (2000). dsRNA-mediated gene silencing in cultured Drosophila cells: a tissue culture model for the analysis of RNA interference. Gene *252*, 95-105.

Caplen, N.J., Parrish, S., Imani, F., Fire, A., and Morgan, R.A. (2001). Specific inhibition of gene expression by small double-stranded RNAs in invertebrate and vertebrate systems. Proc Natl Acad Sci U S A *98*, 9742-9747.

Catalanotto, C., Azzalin, G., Macino, G., and Cogoni, C. (2002). Involvement of small RNAs and role of the qde genes in the gene silencing pathway in Neurospora. Genes Dev *16*, 790-795.

Caudy, A.A., Ketting, R.F., Hammond, S.M., Denli, A.M., Bathoorn, A.M., Tops, B.B., Silva, J.M., Myers, M.M., Hannon, G.J., and Plasterk, R.H. (2003). A micrococcal nuclease homologue in RNAi effector complexes. Nature *425*, 411-414.

Caudy, A.A., Myers, M., Hannon, G.J., and Hammond, S.M. (2002). Fragile X-related protein and VIG associate with the RNA interference machinery. Genes Dev *16*, 2491-2496.

Ceci, M., Gaviraghi, C., Gorrini, C., Sala, L.A., Offenhauser, N., Marchisio, P.C., and Biffo, S. (2003). Release of eIF6 (p27BBP) from the 60S subunit allows 80S ribosome assembly. Nature *426*, 579-584.

Celotto, A.M., and Graveley, B.R. (2002). Exon-specific RNAi: a tool for dissecting the functional relevance of alternative splicing. RNA *8*, 718-724.

Chan, S.W., Zilberman, D., Xie, Z., Johansen, L.K., Carrington, J.C., and Jacobsen, S.E. (2004). RNA silencing genes control de novo DNA methylation. Science *303*, 1336.

Chen, K., and Rajewsky, N. (2006). Natural selection on human microRNA binding sites inferred from SNP data. Nat Genet *38*, 1452-1456.

Chendrimada, T.P., Finn, K.J., Ji, X., Baillat, D., Gregory, R.I., Liebhaber, S.A., Pasquinelli, A.E., and Shiekhattar, R. (2007). microRNA silencing through RISC recruitment of eIF6. Nature *447*, 823-828.

Chendrimada, T.P., Gregory, R.I., Kumaraswamy, E., Norman, J., Cooch, N., Nishikura, K., and Shiekhattar, R. (2005). TRBP recruits the Dicer complex to Ago2 for microRNA processing and gene silencing. Nature *436*, 740-744.

Chiu, Y.L., and Rana, T.M. (2002). RNAi in human cells: basic structural and functional features of small interfering RNA. Molecular cell *10*, 549-561.

Chu, C.Y., and Rana, T.M. (2006). Translation repression in human cells by microRNA-induced gene silencing requires RCK/p54. PLoS Biol *4*, e210.

Church, G.M., and Gilbert, W. (1984). Genomic sequencing. Proc Natl Acad Sci U S A *81*, 1991-1995.

Clemens, J.C., Worby, C.A., Simonson-Leff, N., Muda, M., Maehama, T., Hemmings, B.A., and Dixon, J.E. (2000). Use of double-stranded RNA interference in Drosophila cell lines to dissect signal transduction pathways. Proc Natl Acad Sci U S A *97*, 6499-6503.

Cogoni, C., and Macino, G. (1997). Isolation of quelling-defective (qde) mutants impaired in posttranscriptional transgene-induced gene silencing in Neurospora crassa. Proc Natl Acad Sci U S A *94*, 10233-10238.

Cook, H.A., Koppetsch, B.S., Wu, J., and Theurkauf, W.E. (2004). The Drosophila SDE3 homolog armitage is required for oskar mRNA silencing and embryonic axis specification. Cell *116*, 817-829.

Dalmay, T., Hamilton, A., Rudd, S., Angell, S., and Baulcombe, D.C. (2000). An RNA-dependent RNA polymerase gene in Arabidopsis is required for posttranscriptional gene silencing mediated by a transgene but not by a virus. Cell *101*, 543-553.

Dalmay, T., Horsefield, R., Braunstein, T.H., and Baulcombe, D.C. (2001). SDE3 encodes an RNA helicase required for post-transcriptional gene silencing in Arabidopsis. EMBO J *20*, 2069-2078.

Davis, E., Caiment, F., Tordoir, X., Cavaille, J., Ferguson-Smith, A., Cockett, N., Georges, M., and Charlier, C. (2005). RNAi-mediated allelic trans-interaction at the imprinted Rtl1/Peg11 locus. Curr Biol *15*, 743-749.

Deleris, A., Gallego-Bartolome, J., Bao, J., Kasschau, K.D., Carrington, J.C., and Voinnet, O. (2006). Hierarchical action and inhibition of plant Dicer-like proteins in antiviral defense. Science *313*, 68-71.

Denli, A.M., Tops, B.B., Plasterk, R.H., Ketting, R.F., and Hannon, G.J. (2004). Processing of primary microRNAs by the Microprocessor complex. Nature *432*, 231-235.

Diederichs, S., and Haber, D.A. (2007). Dual role for Argonautes in microRNA processing and posttranscriptional regulation of microRNA expression. Cell *131*, 1097-1108.

Ding, L., Spencer, A., Morita, K., and Han, M. (2005). The developmental timing regulator AIN-1 interacts with miRISCs and may target the argonaute protein ALG-1 to cytoplasmic P bodies in C. elegans. Mol Cell *19*, 437-447.

Doench, J.G., Petersen, C.P., and Sharp, P.A. (2003). siRNAs can function as miRNAs. Genes Dev *17*, 438-442.

Doi, N., Zenno, S., Ueda, R., Ohki-Hamazaki, H., Ui-Tei, K., and Saigo, K. (2003). Short-interfering-RNA-mediated gene silencing in mammalian cells requires Dicer and eIF2C translation initiation factors. Curr Biol *13*, 41-46.

Dunoyer, P., Himber, C., and Voinnet, O. (2005). DICER-LIKE 4 is required for RNA interference and produces the 21-nucleotide small interfering RNA component of the plant cell-to-cell silencing signal. Nature Genet *37*, 1356-1360.

Dunoyer, P., Lecellier, C.H., Parizotto, E.A., Himber, C., and Voinnet, O. (2004). Probing the microRNA and small interfering RNA pathways with virus-encoded suppressors of RNA silencing. Plant Cell *16*, 1235-1250.

El-Shami, M., Pontier, D., Lahmy, S., Braun, L., Picart, C., Vega, D., Hakimi, M.A., Jacobsen, S.E., Cooke, R., and Lagrange, T. (2007). Reiterated WG/GW motifs form functionally and evolutionarily conserved ARGONAUTE-binding platforms in RNAi-related components. Genes Dev *21*, 2539-2544.

Elbashir, S.M., Harborth, J., Lendeckel, W., Yalcin, A., Weber, K., and Tuschl, T. (2001a). Duplexes of 21-nucleotide RNAs mediate RNA interference in cultured mammalian cells. Nature *411*, 494-498.

Elbashir, S.M., Lendeckel, W., and Tuschl, T. (2001b). RNA interference is mediated by 21- and 22-nucleotide RNAs. Genes Dev *15*, 188-200.

Elbashir, S.M., Martinez, J., Patkaniowska, A., Lendeckel, W., and Tuschl, T. (2001c). Functional anatomy of siRNAs for mediating efficient RNAi in Drosophila melanogaster embryo lysate. EMBO J *20*, 6877-6888.

Eulalio, A., Rehwinkel, J., Stricker, M., Huntzinger, E., Yang, S.F., Doerks, T., Dorner, S., Bork, P., Boutros, M., and Izaurralde, E. (2007). Target-specific requirements for enhancers of decapping in miRNA-mediated gene silencing. Genes Dev. *21*, 2558-2570.

Fagard, M., Boutet, S., Morel, J.B., Bellini, C., and Vaucheret, H. (2000). AGO1, QDE-2, and RDE-1 are related proteins required for post-transcriptional gene silencing in plants, quelling in fungi, and RNA interference in animals. Proc Natl Acad Sci U S A *97*, 11650-11654.

Fahlgren, N., Montgomery, T.A., Howell, M.D., Allen, E., Dvorak, S.K., Alexander, A.L., and Carrington, J.C. (2006). Regulation of AUXIN RESPONSE FACTOR3 by TAS3 ta-siRNA affects developmental timing and patterning in Arabidopsis. Curr Biol *16*, 939-944.

Fire, A., Albertson, D., Harrison, S.W., and Moerman, D.G. (1991). Production of antisense RNA leads to effective and specific inhibition of gene expression in C. elegans muscle. Development *113*, 503-514.

Fire, A., Xu, S., Montgomery, M.K., Kostas, S.A., Driver, S.E., and Mello, C.C. (1998). Potent and specific genetic interference by double-stranded RNA in Caenorhabditis elegans. Nature *391*, 806-811.

Forstemann, K., Horwich, M.D., Wee, L., Tomari, Y., and Zamore, P.D. (2007). Drosophila microRNAs are sorted into functionally distinct argonaute complexes after production by dicer-1. Cell *130*, 287-297.

Forstemann, K., Tomari, Y., Du, T., Vagin, V.V., Denli, A.M., Bratu, D.P., Klattenhoff, C., Theurkauf, W.E., and Zamore, P.D. (2005). Normal microRNA maturation and germ-line stem cell maintenance requires Loquacious, a double-stranded RNA-binding domain protein. PLoS Biol *3*, e236.

Fusaro, A.F., Matthew, L., Smith, N.A., Curtin, S.J., Dedic-Hagan, J., Ellacott, G.A., Watson, J.M., Wang, M.B., Brosnan, C., Carroll, B.J., *et al.* (2006). RNA interference-inducing hairpin RNAs in plants act through the viral defence pathway. EMBO rep *7*, 1168-1175.

Galiana-Arnoux, D., Dostert, C., Schneemann, A., Hoffmann, J.A., and Imler, J.L. (2006). Essential function in vivo for Dicer-2 in host defense against RNA viruses in drosophila. Nature Immunol *7*, 590-597.

Gasciolli, V., Mallory, A.C., Bartel, D.P., and Vaucheret, H. (2005). Partially redundant functions of Arabidopsis DICER-like enzymes and a role for DCL4 in producing trans-acting siRNAs. Curr Biol *15*, 1494-1500.

Giraldez, A.J., Mishima, Y., Rihel, J., Grocock, R.J., Van Dongen, S., Inoue, K., Enright, A.J., and Schier, A.F. (2006). Zebrafish miR-430 promotes deadenylation and clearance of maternal mRNAs. Science *312*, 75-79.

Girard, A., Sachidanandam, R., Hannon, G.J., and Carmell, M.A. (2006). A germline-specific class of small RNAs binds mammalian Piwi proteins. Nature *442*, 199-202.

Gregory, R.I., Chendrimada, T.P., Cooch, N., and Shiekhattar, R. (2005). Human RISC couples microRNA biogenesis and posttranscriptional gene silencing. Cell *123*, 631-640.

Gregory, R.I., Yan, K.P., Amuthan, G., Chendrimada, T., Doratotaj, B., Cooch, N., and Shiekhattar, R. (2004). The Microprocessor complex mediates the genesis of microRNAs. Nature *432*, 235-240.

Griffiths-Jones, S. (2004). The microRNA Registry. Nucleic Acids Res *32*, D109-111.

Griffiths-Jones, S., Grocock, R.J., van Dongen, S., Bateman, A., and Enright, A.J. (2006). miRBase: microRNA sequences, targets and gene nomenclature. Nucleic Acids Res *34*, D140-144.

Grishok, A., Pasquinelli, A.E., Conte, D., Li, N., Parrish, S., Ha, I., Baillie, D.L., Fire, A., Ruvkun, G., and Mello, C.C. (2001). Genes and mechanisms related to RNA interference regulate expression of the small temporal RNAs that control C. elegans developmental timing. Cell *106*, 23-34.

Grishok, A., Tabara, H., and Mello, C.C. (2000). Genetic requirements for inheritance of RNAi in C. elegans. Science *287*, 2494-2497.

Gunawardane, L.S., Saito, K., Nishida, K.M., Miyoshi, K., Kawamura, Y., Nagami, T., Siomi, H., and Siomi, M.C. (2007). A slicer-mediated mechanism for repeat-associated siRNA 5' end formation in Drosophila. Science *315*, 1587-1590.

Guo, S., and Kemphues, K.J. (1995). par-1, a gene required for establishing polarity in C. elegans embryos, encodes a putative Ser/Thr kinase that is asymmetrically distributed. Cell *81*, 611-620.

Ha, I., Wightman, B., and Ruvkun, G. (1996). A bulged lin-4/lin-14 RNA duplex is sufficient for Caenorhabditis elegans lin-14 temporal gradient formation. Genes Dev *10*, 3041-3050.

Haley, B., Tang, G., and Zamore, P.D. (2003). In vitro analysis of RNA interference in Drosophila melanogaster. Methods (Duluth) *30*, 330-336.

Hamilton, A., Voinnet, O., Chappell, L., and Baulcombe, D. (2002). Two classes of short interfering RNA in RNA silencing. EMBO J *21*, 4671-4679.

Hamilton, A.J., and Baulcombe, D.C. (1999). A species of small antisense RNA in posttranscriptional gene silencing in plants. Science *286*, 950-952.

Hammond, S.M., Bernstein, E., Beach, D., and Hannon, G.J. (2000). An RNA-directed nuclease mediates post-transcriptional gene silencing in Drosophila cells. Nature *404*, 293-296.

Hammond, S.M., Boettcher, S., Caudy, A.A., Kobayashi, R., and Hannon, G.J. (2001). Argonaute2, a link between genetic and biochemical analyses of RNAi. Science *293*, 1146-1150.

Han, J., Lee, Y., Yeom, K.H., Kim, Y.K., Jin, H., and Kim, V.N. (2004a). The Drosha-DGCR8 complex in primary microRNA processing. Genes Dev *18*, 3016-3027.

Han, J., Lee, Y., Yeom, K.H., Nam, J.W., Heo, I., Rhee, J.K., Sohn, S.Y., Cho, Y., Zhang, B.T., and Kim, V.N. (2006). Molecular basis for the recognition of primary microRNAs by the Drosha-DGCR8 complex. Cell *125*, 887-901.

Han, M.H., Goud, S., Song, L., and Fedoroff, N. (2004b). The Arabidopsis double-stranded RNA-binding protein HYL1 plays a role in microRNA-mediated gene regulation. Proc Natl Acad Sci U S A *101*, 1093-1098.

Herr, A.J., Jensen, M.B., Dalmay, T., and Baulcombe, D.C. (2005). RNA polymerase IV directs silencing of endogenous DNA. Science *308*, 118-120.

Hertel, J., and Stadler, P.F. (2006). Hairpins in a haystack: recognizing microRNA precursors in comparative genomics data. Bioinformatics *22*, e197-202.

Himber, C., Dunoyer, P., Moissiard, G., Ritzenthaler, C., and Voinnet, O. (2003). Transitivity-dependent and -independent cell-to-cell movement of RNA silencing. EMBO J *22*, 4523-4533.

Hiraguri, A., Itoh, R., Kondo, N., Nomura, Y., Aizawa, D., Murai, Y., Koiwa, H., Seki, M., Shinozaki, K., and Fukuhara, T. (2005). Specific interactions between Dicer-like proteins and HYL1/DRB-family dsRNA-binding proteins in Arabidopsis thaliana. Plant Mol Biol *57*, 173-188.

Hoa, N.T., Keene, K.M., Olson, K.E., and Zheng, L. (2003). Characterization of RNA interference in an Anopheles gambiae cell line. Insect Biochem Mol Biol *33*, 949-957.

Horwich, M.D., Li, C., Matranga, C., Vagin, V., Farley, G., Wang, P., and Zamore, P.D. (2007). The Drosophila RNA Methyltransferase, DmHen1, Modifies Germline piRNAs and Single-Stranded siRNAs in RISC. Curr Biol. *17*, 1265-1272

Houwing, S., Kamminga, L.M., Berezikov, E., Cronembold, D., Girard, A., van den Elst, H., Filippov, D.V., Blaser, H., Raz, E., Moens, C.B., *et al.* (2007). A role for

Piwi and piRNAs in germ cell maintenance and transposon silencing in Zebrafish. Cell *129*, 69-82.

Humphreys, D.T., Westman, B.J., Martin, D.I., and Preiss, T. (2005). microRNAs control translation initiation by inhibiting eukaryotic initiation factor 4E/cap and poly(A) tail function. Proc Natl Acad Sci U S A *102*, 16961-16966.

Hunter, C., Sun, H., and Poethig, R.S. (2003). The Arabidopsis heterochronic gene ZIPPY is an ARGONAUTE family member. Curr Biol *13*, 1734-1739.

Hutvagner, G., McLachlan, J., Pasquinelli, A.E., Balint, E., Tuschl, T., and Zamore, P.D. (2001). A cellular function for the RNA-interference enzyme Dicer in the maturation of the let-7 small temporal RNA. Science *293*, 834-838.

Hutvagner, G., Simard, M.J., Mello, C.C., and Zamore, P.D. (2004). Sequence-specific inhibition of small RNA function. PLoS Biol *2*, E98.

Hutvagner, G., and Zamore, P.D. (2002). A microRNA in a multiple-turnover RNAi enzyme complex. Science *297*, 2056-2060.

Ishizuka, A., Siomi, M.C., and Siomi, H. (2002). A Drosophila fragile X protein interacts with components of RNAi and ribosomal proteins. Genes Dev *16*, 2497-2508.

Jackson, R.J., and Standart, N. (2007). How do microRNAs regulate gene expression? Sci STKE *2007*, re1.

Jen, C.H., Michalopoulos, I., Westhead, D.R., and Meyer, P. (2005). Natural antisense transcripts with coding capacity in Arabidopsis may have a regulatory role that is not linked to double-stranded RNA degradation. Genome Biol *6*, R51.

Jiang, F., Ye, X., Liu, X., Fincher, L., McKearin, D., and Liu, Q. (2005). Dicer-1 and R3D1-L catalyze microRNA maturation in Drosophila. Genes Dev *19*, 1674-1679.

Kanoh, J., Sadaie, M., Urano, T., and Ishikawa, F. (2005). Telomere binding protein Taz1 establishes Swi6 heterochromatin independently of RNAi at telomeres. Curr Biol *15*, 1808-1819.

Kasschau, K.D., Fahlgren, N., Chapman, E.J., Sullivan, C.M., Cumbie, J.S., Givan, S.A., and Carrington, J.C. (2007). Genome-wide profiling and analysis of Arabidopsis siRNAs. PLoS Biol *5*, e57.

Katiyar-Agarwal, S., Gao, S., Vivian-Smith, A., and Jin, H. (2007). A novel class of bacteria-induced small RNAs in Arabidopsis. Genes Dev *21*, 3123-3134.

Katiyar-Agarwal, S., Morgan, R., Dahlbeck, D., Borsani, O., Villegas, A., Jr., Zhu, J.K., Staskawicz, B.J., and Jin, H. (2006). A pathogen-inducible endogenous siRNA in plant immunity. Proc Natl Acad Sci U S A *103*, 18002-18007.

Kennerdell, J.R., and Carthew, R.W. (1998). Use of dsRNA-mediated genetic interference to demonstrate that frizzled and frizzled 2 act in the wingless pathway. Cell *95*, 1017-1026.

Kennerdell, J.R., and Carthew, R.W. (2000). Heritable gene silencing in Drosophila using double-stranded RNA. Nat Biotechnol *18*, 896-898.

Kennerdell, J.R., Yamaguchi, S., and Carthew, R.W. (2002). RNAi is activated during Drosophila oocyte maturation in a manner dependent on aubergine and spindle-E. Genes Dev *16*, 1884-1889.

Ketting, R.F., Fischer, S.E., Bernstein, E., Sijen, T., Hannon, G.J., and Plasterk, R.H. (2001). Dicer functions in RNA interference and in synthesis of small RNA involved in developmental timing in C. elegans. Genes Dev *15*, 2654-2659.

Ketting, R.F., Haverkamp, T.H., van Luenen, H.G., and Plasterk, R.H. (1999). Mut-7 of C. elegans, required for transposon silencing and RNA interference, is a homolog of Werner syndrome helicase and RNaseD. Cell *99*, 133-141.

Khvorova, A., Reynolds, A., and Jayasena, S.D. (2003). Functional siRNAs and miRNAs exhibit strand bias. Cell *115*, 209-216.

Kim, K., Lee, Y.S., and Carthew, R.W. (2007). Conversion of pre-RISC to holo-RISC by Ago2 during assembly of RNAi complexes. RNA *13*, 22-29.

Kim, Y.K., and Kim, V.N. (2007). Processing of intronic microRNAs. EMBO J *26*, 775-783.

Kiriakidou, M., Tan, G.S., Lamprinaki, S., De Planell-Saguer, M., Nelson, P.T., and Mourelatos, Z. (2007). An mRNA $^{m(7)}$G cap binding-like motif within human Ago2 represses translation. Cell *129*, 1141-1151.

Klattenhoff, C., and Theurkauf, W. (2008). Biogenesis and germline functions of piRNAs. Development *135*, 3-9.

Koonin, E.V. (1992). A new group of putative RNA helicases. Trends in Biochemical Sciences *17*, 495-497.

Kurihara, Y., Takashi, Y., and Watanabe, Y. (2006). The interaction between DCL1 and HYL1 is important for efficient and precise processing of pri-miRNA in plant microRNA biogenesis. RNA *12*, 206-212.

Kurihara, Y., and Watanabe, Y. (2004). Arabidopsis micro-RNA biogenesis through Dicer-like 1 protein functions. Proc Natl Acad Sci U S A *101*, 12753-12758.

Lagos-Quintana, M., Rauhut, R., Lendeckel, W., and Tuschl, T. (2001). Identification of novel genes coding for small expressed RNAs. Science *294*, 853-858.

Lai, E.C. (2004). Predicting and validating microRNA targets. Genome Biol *5*, 115.

Landthaler, M., Yalcin, A., and Tuschl, T. (2004). The human DiGeorge syndrome critical region gene 8 and Its D. melanogaster homolog are required for miRNA biogenesis. Curr Biol *14*, 2162-2167.

Lau, N.C., Lim, L.P., Weinstein, E.G., and Bartel, D.P. (2001). An abundant class of tiny RNAs with probable regulatory roles in Caenorhabditis elegans. Science *294*, 858-862.

Lau, N.C., Seto, A.G., Kim, J., Kuramochi-Miyagawa, S., Nakano, T., Bartel, D.P., and Kingston, R.E. (2006). Characterization of the piRNA complex from rat testes. Science *313*, 363-367.

Lecellier, C.H., Dunoyer, P., Arar, K., Lehmann-Che, J., Eyquem, S., Himber, C., Saib, A., and Voinnet, O. (2005). A cellular microRNA mediates antiviral defense in human cells. Science *308*, 557-560.

Lee, R.C., and Ambros, V. (2001). An extensive class of small RNAs in Caenorhabditis elegans. Science *294*, 862-864.

Lee, R.C., Feinbaum, R.L., and Ambros, V. (1993). The C. elegans heterochronic gene lin-4 encodes small RNAs with antisense complementarity to lin-14. Cell *75*, 843-854.

Lee, Y., Ahn, C., Han, J., Choi, H., Kim, J., Yim, J., Lee, J., Provost, P., Radmark, O., Kim, S*., et al.* (2003). The nuclear RNase III Drosha initiates microRNA processing. Nature *425*, 415-419.

Lee, Y., Hur, I., Park, S.Y., Kim, Y.K., Suh, M.R., and Kim, V.N. (2006). The role of PACT in the RNA silencing pathway. EMBO J *25*, 522-532.

Lee, Y., Kim, M., Han, J., Yeom, K.H., Lee, S., Baek, S.H., and Kim, V.N. (2004a). microRNA genes are transcribed by RNA polymerase II. EMBO J *23*, 4051-4060.

Lee, Y.S., Nakahara, K., Pham, J.W., Kim, K., He, Z., Sontheimer, E.J., and Carthew, R.W. (2004b). Distinct roles for Drosophila Dicer-1 and Dicer-2 in the siRNA/miRNA silencing pathways. Cell *117*, 69-81.

Leuschner, P.J., Ameres, S.L., Kueng, S., and Martinez, J. (2006). Cleavage of the siRNA passenger strand during RISC assembly in human cells. EMBO R *7*, 314-320.

Lewis, B.P., Burge, C.B., and Bartel, D.P. (2005). Conserved seed pairing, often flanked by adenosines, indicates that thousands of human genes are microRNA targets. Cell *120*, 15-20.

Lewis, B.P., Shih, I.H., Jones-Rhoades, M.W., Bartel, D.P., and Burge, C.B. (2003). Prediction of mammalian microRNA targets. Cell *115*, 787-798.

Li, J., Yang, Z., Yu, B., Liu, J., and Chen, X. (2005). Methylation protects miRNAs and siRNAs from a 3'-end uridylation activity in Arabidopsis. Curr Biol *15*, 1501-1507.

Lim, L.P., Lau, N.C., Garrett-Engele, P., Grimson, A., Schelter, J.M., Castle, J., Bartel, D.P., Linsley, P.S., and Johnson, J.M. (2005). Microarray analysis shows that some microRNAs downregulate large numbers of target mRNAs. Nature *433*, 769-773.

Lim, L.P., Lau, N.C., Weinstein, E.G., Abdelhakim, A., Yekta, S., Rhoades, M.W., Burge, C.B., and Bartel, D.P. (2003). The microRNAs of Caenorhabditis elegans. Genes Dev *17*, 991-1008.

Lin, S.Y., Johnson, S.M., Abraham, M., Vella, M.C., Pasquinelli, A., Gamberi, C., Gottlieb, E., and Slack, F.J. (2003). The C elegans hunchback homolog, hbl-1, controls temporal patterning and is a probable microRNA target. Dev Cell *4*, 639-650.

Lingel, A., Simon, B., Izaurralde, E., and Sattler, M. (2004). Nucleic acid 3'-end recognition by the Argonaute2 PAZ domain. Nat Struct Mol Biol *11*, 576-577.

Liu, J., Carmell, M.A., Rivas, F.V., Marsden, C.G., Thomson, J.M., Song, J.J., Hammond, S.M., Joshua-Tor, L., and Hannon, G.J. (2004). Argonaute2 is the catalytic engine of mammalian RNAi. Science *305*, 1437-1441.

Liu, J., Valencia-Sanchez, M.A., Hannon, G.J., and Parker, R. (2005). MicroRNA-dependent localization of targeted mRNAs to mammalian P-bodies. Nat Cell Biol *7*, 719-723.

Liu, Q., Rand, T.A., Kalidas, S., Du, F., Kim, H.E., Smith, D.P., and Wang, X. (2003). R2D2, a bridge between the initiation and effector steps of the Drosophila RNAi pathway. Science *301*, 1921-1925.

Liu, X., Jiang, F., Kalidas, S., Smith, D., and Liu, Q. (2006). Dicer-2 and R2D2 coordinately bind siRNA to promote assembly of the siRISC complexes. RNA *12*, 1514-1520.

Liu, X., Park, J.K., Jiang, F., Liu, Y., McKearin, D., and Liu, Q. (2007). Dicer-1, but not Loquacious, is critical for assembly of miRNA-induced silencing complexes. RNA *13*, 2324-2329.

Llave, C., Kasschau, K.D., Rector, M.A., and Carrington, J.C. (2002a). Endogenous and silencing-associated small RNAs in plants. Plant Cell *14*, 1605-1619.

Llave, C., Xie, Z., Kasschau, K.D., and Carrington, J.C. (2002b). Cleavage of Scarecrow-like mRNA targets directed by a class of Arabidopsis miRNA. Science *297*, 2053-2056.

Lohmann, J.U., Endl, I., and Bosch, T.C. (1999). Silencing of developmental genes in Hydra. Dev Biol *214*, 211-214.

Lund, E., Guttinger, S., Calado, A., Dahlberg, J.E., and Kutay, U. (2004). Nuclear export of microRNA precursors. Science *303*, 95-98.

Ma, J.B., Yuan, Y.R., Meister, G., Pei, Y., Tuschl, T., and Patel, D.J. (2005). Structural basis for 5'-end-specific recognition of guide RNA by the A. fulgidus Piwi protein. Nature *434*, 666-670.

Maniataki, E., and Mourelatos, Z. (2005). A human, ATP-independent, RISC assembly machine fueled by pre-miRNA. Genes Dev *19*, 2979-2990.

Mansfield, J.H., Harfe, B.D., Nissen, R., Obenauer, J., Srineel, J., Chaudhuri, A., Farzan-Kashani, R., Zuker, M., Pasquinelli, A.E., Ruvkun, G., *et al.* (2004). MicroRNA-responsive 'sensor' transgenes uncover Hox-like and other developmentally regulated patterns of vertebrate microRNA expression. Nat Genet *36*, 1079-1083.

Maroney, P.A., Yu, Y., Fisher, J., and Nilsen, T.W. (2006). Evidence that microRNAs are associated with translating messenger RNAs in human cells. Nat Struct Mol Biol *13*, 1102-1107.

Martinez, J., Patkaniowska, A., Urlaub, H., Luhrmann, R., and Tuschl, T. (2002). Single-stranded antisense siRNAs guide target RNA cleavage in RNAi. Cell *110*, 563-574.

Martinez, J., and Tuschl, T. (2004). RISC is a 5' phosphomonoester-producing RNA endonuclease. Genes Dev *18*, 975-980.

Matranga, C., Tomari, Y., Shin, C., Bartel, D.P., and Zamore, P.D. (2005). Passenger-strand cleavage facilitates assembly of siRNA into Ago2-containing RNAi enzyme complexes. Cell *123*, 607-620.

Meister, G., Landthaler, M., Patkaniowska, A., Dorsett, Y., Teng, G., and Tuschl, T. (2004). Human Argonaute2 mediates RNA cleavage targeted by miRNAs and siRNAs. Mol Cell *15*, 185-197.

Meister, G., Landthaler, M., Peters, L., Chen, P.Y., Urlaub, H., Luhrmann, R., and Tuschl, T. (2005). Identification of novel argonaute-associated proteins. Curr Biol *15*, 2149-2155.

Miyoshi, K., Tsukumo, H., Nagami, T., Siomi, H., and Siomi, M.C. (2005). Slicer function of Drosophila Argonautes and its involvement in RISC formation. Genes Dev *19*, 2837-2848.

Moissiard, G., Parizotto, E.A., Himber, C., and Voinnet, O. (2007). Transitivity in Arabidopsis can be primed, requires the redundant action of the antiviral Dicer-like 4 and Dicer-like 2, and is compromised by viral-encoded suppressor proteins. RNA *13*, 1268-1278.

Morel, J.B., Godon, C., Mourrain, P., Beclin, C., Boutet, S., Feuerbach, F., Proux, F., and Vaucheret, H. (2002). Fertile hypomorphic ARGONAUTE (ago1) mutants impaired in post-transcriptional gene silencing and virus resistance. Plant Cell *14*, 629-639.

Mourelatos, Z., Dostie, J., Paushkin, S., Sharma, A., Charroux, B., Abel, L., Rappsilber, J., Mann, M., and Dreyfuss, G. (2002). miRNPs: a novel class of ribonucleoproteins containing numerous microRNAs. Genes Dev *16*, 720-728.

Mourrain, P., Beclin, C., Elmayan, T., Feuerbach, F., Godon, C., Morel, J.B., Jouette, D., Lacombe, A.M., Nikic, S., Picault, N., *et al.* (2000). Arabidopsis SGS2 and SGS3 genes are required for posttranscriptional gene silencing and natural virus resistance. Cell *101*, 533-542.

Nakazawa, Y., Hiraguri, A., Moriyama, H., and Fukuhara, T. (2007). The dsRNA-binding protein DRB4 interacts with the Dicer-like protein DCL4 in vivo and functions in the trans-acting siRNA pathway. Plant Mol Biol *63*, 777-785.

Ngo, H., Tschudi, C., Gull, K., and Ullu, E. (1998). Double-stranded RNA induces mRNA degradation in Trypanosoma brucei. Proc Natl Acad Sci U S A *95*, 14687-14692.

Nottrott, S., Simard, M.J., and Richter, J.D. (2006). Human let-7a miRNA blocks protein production on actively translating polyribosomes. Nat Struct Mol Biol *13*, 1108-1114.

Nowotny, M., Gaidamakov, S.A., Crouch, R.J., and Yang, W. (2005). Crystal structures of RNase H bound to an RNA/DNA hybrid: substrate specificity and metal-dependent catalysis. Cell *121*, 1005-1016.

Nykanen, A., Haley, B., and Zamore, P.D. (2001). ATP requirements and small interfering RNA structure in the RNA interference pathway. Cell *107*, 309-321.

Okamura, K., Hagen, J.W., Duan, H., Tyler, D.M., and Lai, E.C. (2007). The mirtron pathway generates microRNA-class regulatory RNAs in Drosophila. Cell *130*, 89-100.

Olsen, P.H., and Ambros, V. (1999). The lin-4 regulatory RNA controls developmental timing in Caenorhabditis elegans by blocking LIN-14 protein synthesis after the initiation of translation. Dev Biol *216*, 671-680.

Onodera, Y., Haag, J.R., Ream, T., Nunes, P.C., Pontes, O., and Pikaard, C.S. (2005). Plant nuclear RNA polymerase IV mediates siRNA and DNA methylation-dependent heterochromatin formation. Cell *120*, 613-622.

Pak, J., and Fire, A. (2007). Distinct populations of primary and secondary effectors during RNAi in C. elegans. Science *315*, 241-244.

Pal-Bhadra, M., Bhadra, U., and Birchler, J.A. (2002). RNAi related mechanisms affect both transcriptional and posttranscriptional transgene silencing in Drosophila. Mol Cell *9*, 315-327.

Papp, I., Mette, M.F., Aufsatz, W., Daxinger, L., Schauer, S.E., Ray, A., van der Winden, J., Matzke, M., and Matzke, A.J. (2003). Evidence for nuclear processing of plant micro RNA and short interfering RNA precursors. Plant Physiol *132*, 1382-1390.

Parizotto, E.A., Dunoyer, P., Rahm, N., Himber, C., and Voinnet, O. (2004). In vivo investigation of the transcription, processing, endonucleolytic activity, and functional relevance of the spatial distribution of a plant miRNA. Genes Dev *18*, 2237-2242.

Park, J.K., Liu, X., Strauss, T.J., McKearin, D.M., and Liu, Q. (2007). The miRNA pathway intrinsically controls self-renewal of Drosophila germline stem cells. Curr Biol *17*, 533-538.

Park, M.Y., Wu, G., Gonzalez-Sulser, A., Vaucheret, H., and Poethig, R.S. (2005). Nuclear processing and export of microRNAs in Arabidopsis. Proc Natl Acad Sci U S A *102*, 3691-3696.

Park, W., Li, J., Song, R., Messing, J., and Chen, X. (2002). CARPEL FACTORY, a Dicer homolog, and HEN1, a novel protein, act in microRNA metabolism in Arabidopsis thaliana. Curr Biol *12*, 1484-1495.

Parker, J.S., Roe, S.M., and Barford, D. (2004). Crystal structure of a PIWI protein suggests mechanisms for siRNA recognition and slicer activity. EMBO J *23*, 4727-4737.

Parker, J.S., Roe, S.M., and Barford, D. (2005). Structural insights into mRNA recognition from a PIWI domain-siRNA guide complex. Nature *434*, 663-666.

Parrish, S., Fleenor, J., Xu, S., Mello, C., and Fire, A. (2000). Functional anatomy of a dsRNA trigger: differential requirement for the two trigger strands in RNA interference. Mol Cell *6*, 1077-1087.

Pasquinelli, A.E., Reinhart, B.J., Slack, F., Martindale, M.Q., Kuroda, M.I., Maller, B., Hayward, D.C., Ball, E.E., Degnan, B., Muller, P*., et al.* (2000). Conservation of the sequence and temporal expression of let-7 heterochronic regulatory RNA. Nature *408*, 86-89.

Peragine, A., Yoshikawa, M., Wu, G., Albrecht, H.L., and Poethig, R.S. (2004). SGS3 and SGS2/SDE1/RDR6 are required for juvenile development and the production of trans-acting siRNAs in Arabidopsis. Genes Dev *18*, 2368-2379.

Petersen, C.P., Bordeleau, M.E., Pelletier, J., and Sharp, P.A. (2006). Short RNAs repress translation after initiation in mammalian cells. Mol Cell *21*, 533-542.

Pfeffer, S., Zavolan, M., Grasser, F.A., Chien, M., Russo, J.J., Ju, J., John, B., Enright, A.J., Marks, D., Sander, C*., et al.* (2004). Identification of virus-encoded microRNAs. Science *304*, 734-736.

Pham, J.W., Pellino, J.L., Lee, Y.S., Carthew, R.W., and Sontheimer, E.J. (2004). A Dicer-2-dependent 80s complex cleaves targeted mRNAs during RNAi in Drosophila. Cell *117*, 83-94.

Pham, J.W., and Sontheimer, E.J. (2005). Molecular requirements for RNA-induced silencing complex assembly in the Drosophila RNA interference pathway. J Biol Chem *280*, 39278-39283.

Pillai, R.S., Bhattacharyya, S.N., Artus, C.G., Zoller, T., Cougot, N., Basyuk, E., Bertrand, E., and Filipowicz, W. (2005). Inhibition of translational initiation by let-7 microRNA in human cells. Science *309*, 1573-1576.

Pontier, D., Yahubyan, G., Vega, D., Bulski, A., Saez-Vasquez, J., Hakimi, M.A., Lerbs-Mache, S., Colot, V., and Lagrange, T. (2005). Reinforcement of silencing at transposons and highly repeated sequences requires the concerted action of two distinct RNA polymerases IV in Arabidopsis. Genes Dev *19*, 2030-2040.

Preall, J.B., He, Z., Gorra, J.M., and Sontheimer, E.J. (2006). Short interfering RNA strand selection is independent of dsRNA processing polarity during RNAi in Drosophila. Curr Biol *16*, 530-535.

Qi, Y., Denli, A.M., and Hannon, G.J. (2005). Biochemical specialization within Arabidopsis RNA silencing pathways. Mol Cell *19*, 421-428.

Qu, F., Ye, X., Hou, G., Sato, S., Clemente, T.E., and Morris, T.J. (2005). RDR6 has a broad-spectrum but temperature-dependent antiviral defense role in Nicotiana benthamiana. J Virol *79*, 15209-15217.

Rand, T.A., Ginalski, K., Grishin, N.V., and Wang, X. (2004). Biochemical identification of Argonaute 2 as the sole protein required for RNA-induced silencing complex activity. Proc Natl Acad Sci U S A *101*, 14385-14389.

Rand, T.A., Petersen, S., Du, F., and Wang, X. (2005). Argonaute2 cleaves the anti-guide strand of siRNA during RISC activation. Cell *123*, 621-629.

Ratcliff, F.G., MacFarlane, S.A., and Baulcombe, D.C. (1999). Gene silencing without DNA. rna-mediated cross-protection between viruses. Plant Cell *11*, 1207-1216.

Rehwinkel, J., Behm-Ansmant, I., Gatfield, D., and Izaurralde, E. (2005). A crucial role for GW182 and the DCP1:DCP2 decapping complex in miRNA-mediated gene silencing. RNA *11*, 1640-1647.

Reinhart, B.J., Slack, F.J., Basson, M., Pasquinelli, A.E., Bettinger, J.C., Rougvie, A.E., Horvitz, H.R., and Ruvkun, G. (2000). The 21-nucleotide let-7 RNA regulates developmental timing in Caenorhabditis elegans. Nature *403*, 901-906.

Reinhart, B.J., Weinstein, E.G., Rhoades, M.W., Bartel, B., and Bartel, D.P. (2002). microRNAs in plants. Genes Dev *16*, 1616-1626.

Rhoades, M.W., Reinhart, B.J., Lim, L.P., Burge, C.B., Bartel, B., and Bartel, D.P. (2002). Prediction of plant microRNA targets. Cell *110*, 513-520.

Rivas, F.V., Tolia, N.H., Song, J.J., Aragon, J.P., Liu, J., Hannon, G.J., and Joshua-Tor, L. (2005). Purified Argonaute2 and an siRNA form recombinant human RISC. Nat Struct Mol Biol *12*, 340-349.

Robb, G.B., and Rana, T.M. (2007). RNA helicase A interacts with RISC in human cells and functions in RISC loading. Mol Cell *26*, 523-537.

Rodriguez, A., Griffiths-Jones, S., Ashurst, J.L., and Bradley, A. (2004). Identification of mammalian microRNA host genes and transcription units. Genome Res *14*, 1902-1910.

Roignant, J.Y., Carre, C., Mugat, B., Szymczak, D., Lepesant, J.A., and Antoniewski, C. (2003). Absence of transitive and systemic pathways allows cell-specific and isoform-specific RNAi in Drosophila. RNA *9*, 299-308.

Rougvie, A.E. (2005). Intrinsic and extrinsic regulators of developmental timing: from miRNAs to nutritional cues. Development *132*, 3787-3798.

Ruby, J.G., Jan, C., Player, C., Axtell, M.J., Lee, W., Nusbaum, C., Ge, H., and Bartel, D.P. (2006). Large-scale sequencing reveals 21U-RNAs and additional microRNAs and endogenous siRNAs in C. elegans. Cell *127*, 1193-1207.

Ruby, J.G., Jan, C.H., and Bartel, D.P. (2007). Intronic microRNA precursors that bypass Drosha processing. Nature *448*, 83-86.

Saito, K., Ishizuka, A., Siomi, H., and Siomi, M.C. (2005). Processing of pre-microRNAs by the Dicer-1-Loquacious complex in Drosophila cells. PLoS Biol *3*, e235.

Sanchez Alvarado, A., and Newmark, P.A. (1999). Double-stranded RNA specifically disrupts gene expression during planarian regeneration. Proc Natl Acad Sci U S A *96*, 5049-5054.

Saxena, S., Jonsson, Z.O., and Dutta, A. (2003). Small RNAs with imperfect match to endogenous mRNA repress translation. Implications for off-target activity of small inhibitory RNA in mammalian cells. J Biol Chem *278*, 44312-44319.

Schmidt, A., Palumbo, G., Bozzetti, M.P., Tritto, P., Pimpinelli, S., and Schafer, U. (1999). Genetic and molecular characterization of sting, a gene involved in crystal formation and meiotic drive in the male germ line of Drosophila melanogaster. Genetics *151*, 749-760.

Schramke, V., and Allshire, R. (2003). Hairpin RNAs and retrotransposon LTRs effect RNAi and chromatin-based gene silencing. Science *301*, 1069-1074.

Schwarz, D.S., Hutvagner, G., Du, T., Xu, Z., Aronin, N., and Zamore, P.D. (2003). Asymmetry in the assembly of the RNAi enzyme complex. Cell *115*, 199-208.

Schwarz, D.S., Hutvagner, G., Haley, B., and Zamore, P.D. (2002). Evidence that siRNAs function as guides, not primers, in the Drosophila and human RNAi pathways. Molecular Cell *10*, 537-548.

Schwarz, D.S., Tomari, Y., and Zamore, P.D. (2004). The RNA-induced silencing complex is a Mg2+-dependent endonuclease. Curr Biol *14*, 787-791.

Sheng, Y., Engstrom, P.G., and Lenhard, B. (2007). Mammalian microRNA prediction through a support vector machine model of sequence and structure. PLoS ONE *2*, e946.

Sijen, T., Fleenor, J., Simmer, F., Thijssen, K.L., Parrish, S., Timmons, L., Plasterk, R.H., and Fire, A. (2001). On the role of RNA amplification in dsRNA-triggered gene silencing. Cell *107*, 465-476.

Sijen, T., and Plasterk, R.H. (2003). Transposon silencing in the Caenorhabditis elegans germ line by natural RNAi. Nature *426*, 310-314.

Sijen, T., Steiner, F.A., Thijssen, K.L., and Plasterk, R.H. (2007). Secondary siRNAs result from unprimed RNA synthesis and form a distinct class. Science *315*, 244-247.

Silhavy, D., Molnar, A., Lucioli, A., Szittya, G., Hornyik, C., Tavazza, M., and Burgyan, J. (2002). A viral protein suppresses RNA silencing and binds silencing-generated, 21- to 25-nucleotide double-stranded RNAs. EMBO J *21*, 3070-3080.

Slack, F.J., Basson, M., Liu, Z., Ambros, V., Horvitz, H.R., and Ruvkun, G. (2000). The lin-41 RBCC gene acts in the C. elegans heterochronic pathway between the let-7 regulatory RNA and the LIN-29 transcription factor. Mol Cell *5*, 659-669.

Smardon, A., Spoerke, J.M., Stacey, S.C., Klein, M.E., Mackin, N., and Maine, E.M. (2000). EGO-1 is related to RNA-directed RNA polymerase and functions in germ-line development and RNA interference in C. elegans. Curr Biol *10*, 169-178.

Song, J.J., Liu, J., Tolia, N.H., Schneiderman, J., Smith, S.K., Martienssen, R.A., Hannon, G.J., and Joshua-Tor, L. (2003). The crystal structure of the Argonaute2 PAZ domain reveals an RNA binding motif in RNAi effector complexes. Nat Struct Biol *10*, 1026-1032.

Song, J.J., Smith, S.K., Hannon, G.J., and Joshua-Tor, L. (2004). Crystal structure of Argonaute and its implications for RISC slicer activity. Science *305*, 1434-1437.

Standart, N., and Jackson, R.J. (2007). microRNAs repress translation of ^{m7}Gppp-capped target mRNAs in vitro by inhibiting initiation and promoting deadenylation. Genes Dev *21*, 1975-1982.

Stark, A., Brennecke, J., Bushati, N., Russell, R.B., and Cohen, S.M. (2005). Animal MicroRNAs confer robustness to gene expression and have a significant impact on 3'UTR evolution. Cell *123*, 1133-1146.

Stark, G.R., Kerr, I.M., Williams, B.R., Silverman, R.H., and Schreiber, R.D. (1998). How cells respond to interferons. Ann Rev of Biochem *67*, 227-264.

Sullivan, C.S., Grundhoff, A.T., Tevethia, S., Pipas, J.M., and Ganem, D. (2005). SV40-encoded microRNAs regulate viral gene expression and reduce susceptibility to cytotoxic T cells. Nature *435*, 682-686.

Svoboda, P., Stein, P., Hayashi, H., and Schultz, R.M. (2000). Selective reduction of dormant maternal mRNAs in mouse oocytes by RNA interference. Development *127*, 4147-4156.

Tabara, H., Sarkissian, M., Kelly, W.G., Fleenor, J., Grishok, A., Timmons, L., Fire, A., and Mello, C.C. (1999). The rde-1 gene, RNA interference, and transposon silencing in C. elegans. Cell *99*, 123-132.

Tabara, H., Yigit, E., Siomi, H., and Mello, C.C. (2002). The dsRNA binding protein RDE-4 interacts with RDE-1, DCR-1, and a DExH-box helicase to direct RNAi in C. elegans. Cell *109*, 861-871.

Tang, G., Reinhart, B.J., Bartel, D.P., and Zamore, P.D. (2003). A biochemical framework for RNA silencing in plants. Genes Dev *17*, 49-63.

Thermann, R., and Hentze, M.W. (2007). Drosophila miR2 induces pseudo-polysomes and inhibits translation initiation. Nature *447*, 875-878.

Tijsterman, M., Ketting, R.F., Okihara, K.L., Sijen, T., and Plasterk, R.H. (2002). RNA helicase MUT-14-dependent gene silencing triggered in C. elegans by short antisense RNAs. Science *295*, 694-697.

Tolia, N.H., and Joshua-Tor, L. (2007). Slicer and the argonautes. Nat Chem Biol *3*, 36-43.

Tomari, Y., Du, T., Haley, B., Schwarz, D.S., Bennett, R., Cook, H.A., Koppetsch, B.S., Theurkauf, W.E., and Zamore, P.D. (2004a). RISC assembly defects in the Drosophila RNAi mutant armitage. Cell *116*, 831-841.

Tomari, Y., Du, T., and Zamore, P.D. (2007). Sorting of Drosophila small silencing RNAs. Cell *130*, 299-308.

Tomari, Y., Matranga, C., Haley, B., Martinez, N., and Zamore, P.D. (2004b). A protein sensor for siRNA asymmetry. Science *306*, 1377-1380.

Tran, R.K., Henikoff, J.G., Zilberman, D., Ditt, R.F., Jacobsen, S.E., and Henikoff, S. (2005). DNA methylation profiling identifies CG methylation clusters in Arabidopsis genes. Curr Biol *15*, 154-159.

Tuschl, T., Zamore, P.D., Lehmann, R., Bartel, D.P., and Sharp, P.A. (1999). Targeted mRNA degradation by double-stranded RNA in vitro. Genes Dev *13*, 3191-3197.

Ui-Tei, K., Zenno, S., Miyata, Y., and Saigo, K. (2000). Sensitive assay of RNA interference in Drosophila and Chinese hamster cultured cells using firefly luciferase gene as target. FEBS Lett *479*, 79-82.

Vagin, V.V., Sigova, A., Li, C., Seitz, H., Gvozdev, V., and Zamore, P.D. (2006). A distinct small RNA pathway silences selfish genetic elements in the germline. Science *313*, 320-324.

Vaistij, F.E., Jones, L., and Baulcombe, D.C. (2002). Spreading of RNA targeting and DNA methylation in RNA silencing requires transcription of the target gene and a putative RNA-dependent RNA polymerase. Plant Cell *14*, 857-867.

van Rij, R.P., Saleh, M.C., Berry, B., Foo, C., Houk, A., Antoniewski, C., and Andino, R. (2006). The RNA silencing endonuclease Argonaute 2 mediates specific antiviral immunity in Drosophila melanogaster. Genes Dev *20*, 2985-2995.

Vargason, J.M., Szittya, G., Burgyan, J., and Tanaka Hall, T.M. (2003). Size selective recognition of siRNA by an RNA silencing suppressor. Cell *115*, 799-811.

Vasudevan, S., Tong, Y., and Steitz, J.A. (2007). Switching from repression to activation: microRNAs can up-regulate translation. Science *318*, 1931-1934.

Vazquez, F., Gasciolli, V., Crete, P., and Vaucheret, H. (2004a). The nuclear dsRNA binding protein HYL1 is required for microRNA accumulation and plant development, but not posttranscriptional transgene silencing. Curr Biol *14*, 346-351.

Vazquez, F., Vaucheret, H., Rajagopalan, R., Lepers, C., Gasciolli, V., Mallory, A.C., Hilbert, J.L., Bartel, D.P., and Crete, P. (2004b). Endogenous trans-acting siRNAs regulate the accumulation of Arabidopsis mRNAs. Mol Cell *16*, 69-79.

Vella, M.C., Choi, E.Y., Lin, S.Y., Reinert, K., and Slack, F.J. (2004). The C. elegans microRNA let-7 binds to imperfect let-7 complementary sites from the lin-41 3'UTR. Genes Dev *18*, 132-137.

Voinnet, O., and Baulcombe, D.C. (1997). Systemic signalling in gene silencing. Nature *389*, 553.

Voinnet, O., Pinto, Y.M., and Baulcombe, D.C. (1999). Suppression of gene silencing: a general strategy used by diverse DNA and RNA viruses of plants. Proc Natl Acad Sci U S A *96*, 14147-14152.

Voinnet, O., Vain, P., Angell, S., and Baulcombe, D.C. (1998). Systemic spread of sequence-specific transgene RNA degradation in plants is initiated by localized introduction of ectopic promoterless DNA. Cell *95*, 177-187.

Volpe, T.A., Kidner, C., Hall, I.M., Teng, G., Grewal, S.I., and Martienssen, R.A. (2002). Regulation of heterochromatic silencing and histone H3 lysine-9 methylation by RNAi. Science *297*, 1833-1837.

Wakiyama, M., Takimoto, K., Ohara, O., and Yokoyama, S. (2007). let-7 microRNA-mediated mRNA deadenylation and translational repression in a mammalian cell-free system. Genes Dev *21*, 1857-1862.

Wang, X.H., Aliyari, R., Li, W.X., Li, H.W., Kim, K., Carthew, R., Atkinson, P., and Ding, S.W. (2006). RNA interference directs innate immunity against viruses in adult Drosophila. Science *312*, 452-454.

Wang, X.J., Gaasterland, T., and Chua, N.H. (2005). Genome-wide prediction and identification of cis-natural antisense transcripts in Arabidopsis thaliana. Genome Biol *6*, R30.

Wargelius, A., Ellingsen, S., and Fjose, A. (1999). Double-stranded RNA induces specific developmental defects in zebrafish embryos. Biochem Biophys Res Commun *263*, 156-161.

Waterhouse, P.M., and Fusaro, A.F. (2006). Plant science. Viruses face a double defense by plant small RNAs. Science *313*, 54-55.

Waterhouse, P.M., Graham, M.W., and Wang, M.B. (1998). Virus resistance and gene silencing in plants can be induced by simultaneous expression of sense and antisense RNA. Proc Natl Acad Sci U S A *95*, 13959-13964.

Waterhouse, P.M., Wang, M.B., and Lough, T. (2001). Gene silencing as an adaptive defence against viruses. Nature *411*, 834-842.

Wianny, F., and Zernicka-Goetz, M. (2000). Specific interference with gene function by double-stranded RNA in early mouse development. Nat Cell Biol *2*, 70-75.

Wightman, B., Ha, I., and Ruvkun, G. (1993). Posttranscriptional regulation of the heterochronic gene lin-14 by lin-4 mediates temporal pattern formation in C. elegans. Cell *75*, 855-862.

Williams, R.W., and Rubin, G.M. (2002). ARGONAUTE1 is required for efficient RNA interference in Drosophila embryos. Proc Natl Acad Sci U S A *99*, 6889-6894.

Wu-Scharf, D., Jeong, B., Zhang, C., and Cerutti, H. (2000). Transgene and transposon silencing in Chlamydomonas reinhardtii by a DEAH-box RNA helicase. Science *290*, 1159-1162.

Wu, L., Fan, J., and Belasco, J.G. (2006). microRNAs direct rapid deadenylation of mRNA. Proc Natl Acad Sci U S A *103*, 4034-4039.

Xie, X., Lu, J., Kulbokas, E.J., Golub, T.R., Mootha, V., Lindblad-Toh, K., Lander, E.S., and Kellis, M. (2005). Systematic discovery of regulatory motifs in human promoters and 3' UTRs by comparison of several mammals. Nature *434*, 338-345.

Xie, Z., Johansen, L.K., Gustafson, A.M., Kasschau, K.D., Lellis, A.D., Zilberman, D., Jacobsen, S.E., and Carrington, J.C. (2004). Genetic and functional diversification of small RNA pathways in plants. PLoS Biol *2*, E104.

Xu, L., Yang, L., Pi, L., Liu, Q., Ling, Q., Wang, H., Poethig, R.S., and Huang, H. (2006). Genetic interaction between the AS1-AS2 and RDR6-SGS3-AGO7 pathways for leaf morphogenesis. Plant Cell Physiol *47*, 853-863.

Yan, K.S., Yan, S., Farooq, A., Han, A., Zeng, L., and Zhou, M.M. (2003). Structure and conserved RNA binding of the PAZ domain. Nature *426*, 468-474.

Yang, D., Lu, H., and Erickson, J.W. (2000). Evidence that processed small dsRNAs may mediate sequence-specific mRNA degradation during RNAi in Drosophila embryos. Curr Biol *10*, 1191-1200.

Yang, Z., Ebright, Y.W., Yu, B., and Chen, X. (2006). HEN1 recognizes 21-24 nt small RNA duplexes and deposits a methyl group onto the 2' OH of the 3' terminal nucleotide. Nucleic Acids Res *34*, 667-675.

Ye, K., Malinina, L., and Patel, D.J. (2003). Recognition of small interfering RNA by a viral suppressor of RNA silencing. Nature *426*, 874-878.

Yekta, S., Shih, I.H., and Bartel, D.P. (2004). microRNA-directed cleavage of HOXB8 mRNA. Science *304*, 594-596.

Yi, R., Qin, Y., Macara, I.G., and Cullen, B.R. (2003). Exportin-5 mediates the nuclear export of pre-microRNAs and short hairpin RNAs. Genes Dev *17*, 3011-3016.

Yigit, E., Batista, P.J., Bei, Y., Pang, K.M., Chen, C.C., Tolia, N.H., Joshua-Tor, L., Mitani, S., Simard, M.J., and Mello, C.C. (2006). Analysis of the C. elegans Argonaute family reveals that distinct Argonautes act sequentially during RNAi. Cell *127*, 747-757.

Yoshikawa, M., Peragine, A., Park, M.Y., and Poethig, R.S. (2005). A pathway for the biogenesis of trans-acting siRNAs in Arabidopsis. Genes Dev *19*, 2164-2175.

Yu, B., Yang, Z., Li, J., Minakhina, S., Yang, M., Padgett, R.W., Steward, R., and Chen, X. (2005). Methylation as a crucial step in plant microRNA biogenesis. Science *307*, 932-935.

Zamore, P.D., Tuschl, T., Sharp, P.A., and Bartel, D.P. (2000). RNAi: double-stranded RNA directs the ATP-dependent cleavage of mRNA at 21 to 23 nucleotide intervals. Cell *101*, 25-33.

Zeng, Y., and Cullen, B.R. (2004). Structural requirements for pre-microRNA binding and nuclear export by Exportin 5. Nucleic Acids Res *32*, 4776-4785.

Zeng, Y., and Cullen, B.R. (2005). Efficient processing of primary microRNA hairpins by Drosha requires flanking nonstructured RNA sequences. J Biol Chem *280*, 27595-27603.

Wagner, E.J., and Cullen, B.R. (2002). Both natural and designed microRNAs can inhibit the expression of cognate mRNAs when expressed in human cells. Mol Cell *9*, 1327-1333.

Zeng, Y., Sen, G.L., and Blau, H.M. (2005). Argonaute 2/RISC resides in sites of mammalian mRNA decay known as cytoplasmic bodies. Nat Cell Biol *7*, 633-636.

Zeng, Y., Yi, R., and Cullen, B.R. (2005). Recognition and cleavage of primary microRNA precursors by the nuclear processing enzyme Drosha. EMBO J *24*, 138-148.

Zheng, X., Zhu, J., Kapoor, A., and Zhu, J.K. (2007). Role of Arabidopsis AGO6 in siRNA accumulation, DNA methylation and transcriptional gene silencing. EMBO J *26*, 1691-1701.

Zilberman, D., Cao, X., and Jacobsen, S.E. (2003). ARGONAUTE4 control of locus-specific siRNA accumulation and DNA and histone methylation. Science *299*, 716-719.

Cell, Vol. 115, 199–208, October 17, 2003, Copyright ©2003 by Cell Press

Asymmetry in the Assembly of the RNAi Enzyme Complex

Dianne S. Schwarz,[1,3] György Hutvágner,[1,3] Tingting Du,[1] Zuoshang Xu,[1] Neil Aronin,[2] and Phillip D. Zamore[1,*]
[1]Department of Biochemistry and Molecular Pharmacology and
[2]Department of Medicine
University of Massachusetts Medical School
Lazare Research Building
364 Plantation Street
Worcester, Massachusetts 01605

Summary

A key step in RNA interference (RNAi) is assembly of the RISC, the protein-siRNA complex that mediates target RNA cleavage. Here, we show that the two strands of an siRNA duplex are not equally eligible for assembly into RISC. Rather, both the absolute and relative stabilities of the base pairs at the 5′ ends of the two siRNA strands determine the degree to which each strand participates in the RNAi pathway. siRNA duplexes can be functionally asymmetric, with only one of the two strands able to trigger RNAi. Asymmetry is the hallmark of a related class of small, single-stranded, noncoding RNAs, microRNAs (miRNAs). We suggest that single-stranded miRNAs are initially generated as siRNA-like duplexes whose structures predestine one strand to enter the RISC and the other strand to be destroyed. Thus, the common step of RISC assembly is an unexpected source of asymmetry for both siRNA function and miRNA biogenesis.

Introduction

Two types of ~21 nt RNAs trigger posttranscriptional gene silencing in animals: small interfering RNAs (siRNAs) and microRNAs (miRNAs). Both siRNAs and miRNAs are produced by the cleavage of double-stranded RNA (dsRNA) precursors by Dicer, a member of the RNase III family of dsRNA-specific endonucleases (Bernstein et al., 2001; Billy et al., 2001; Grishok et al., 2001; Hutvágner et al., 2001; Ketting et al., 2001; Knight and Bass, 2001; Paddison et al., 2002; Park et al., 2002; Provost et al., 2002; Reinhart et al., 2002; Zhang et al., 2002; Doi et al., 2003; Myers et al., 2003). siRNAs result when transposons, viruses, or endogenous genes express long dsRNA or when dsRNA is introduced experimentally into plant or animal cells to trigger gene silencing, a process known as RNA interference (RNAi) (Fire et al., 1998; Hamilton and Baulcombe, 1999; Zamore et al., 2000; Elbashir et al., 2001a; Hammond et al., 2001; Sijen et al., 2001; Catalanotto et al., 2002). In contrast, miRNAs are the products of endogenous, noncoding genes whose precursor RNA transcripts can form small stem loops from which mature miRNAs are cleaved by Dicer (Lagos-Quintana et al., 2001, 2002, 2003; Lau et al., 2001; Lee and Ambros, 2001; Mourelatos et al., 2002; Reinhart et al., 2002; Ambros et al., 2003; Brennecke et al., 2003; Lim et al., 2003a, 2003b). miRNAs are encoded in genes distinct from the mRNAs whose expression they control.

siRNAs were first identified as the specificity determinants of the RNAi pathway, where they act as guides to direct endonucleolytic cleavage of their target RNAs (Hamilton and Baulcombe, 1999; Hammond et al., 2000; Zamore et al., 2000; Elbashir et al., 2001a). Prototypical siRNA duplexes are 21 nt double-stranded RNAs that contain 19 base pairs, with 2 nt, 3′ overhanging ends (Elbashir et al., 2001a; Nykänen et al., 2001; Tang et al., 2003). Active siRNAs, like miRNAs, contain 5′ phosphates and 3′ hydroxyls (Zamore et al., 2000; Boutla et al., 2001; Hutvágner et al., 2001; Nykänen et al., 2001; Chiu and Rana, 2002; Mallory et al., 2002). Recent evidence suggests that siRNAs and miRNAs are functionally interchangeable, with the choice of mRNA cleavage or translational repression determined solely by the degree of complementarity between the small RNA and its target (Hutvágner and Zamore, 2002; Doench et al., 2003; Zeng and Cullen, 2003). siRNAs and miRNAs are found in similar, if not identical, complexes, suggesting that a single, bifunctional complex—the RNA-induced silencing complex (RISC)—mediates both cleavage and translational control (Caudy et al., 2002; Hutvágner and Zamore, 2002; Martinez et al., 2002; Mourelatos et al., 2002).

Each RISC contains only one of the two strands of the siRNA duplex (Martinez et al., 2002). Both siRNA strands can be competent to direct RNAi (Elbashir et al., 2001a, 2001b; Nykänen et al., 2001). That is, the anti-sense strand of an siRNA can direct cleavage of a corresponding sense RNA target, whereas the sense siRNA strand directs cleavage of an anti-sense target. Here, we show that small changes in siRNA sequence have profound and predictable effects on the extent to which the individual strands of an siRNA duplex enter the RNAi pathway, a phenomenon we term siRNA functional asymmetry. We designed siRNAs that are fully asymmetric, with only one of the two siRNA strands forming RISC in vitro. Such highly asymmetric siRNA duplexes resemble intermediates previously proposed for the miRNA biogenesis pathway (Hutvágner and Zamore, 2002; Reinhart et al., 2002; Lim et al., 2003b). Our data suggest that RISC assembly is governed by an enzyme that selects which strand of an siRNA is loaded into RISC. This strand is always the one whose 5′ end is less tightly paired to its complement. We propose that for each siRNA duplex that is unwound, only one strand enters the RISC complex, whereas the other strand is degraded. For miRNAs, it is the miRNA strand of a short-lived, siRNA duplex-like intermediate that assembles into a RISC complex, causing miRNAs to accumulate in vivo as single-stranded RNAs. Designing siRNAs to be more like these double-stranded miRNA intermediates produces highly functional siRNAs, even when targeting mRNA sequences apparently refractory to cleavage by siRNAs selected by conventional siRNA design rules.

*Correspondence: phillip.zamore@umassmed.edu
[3]These authors contributed equally to this work.

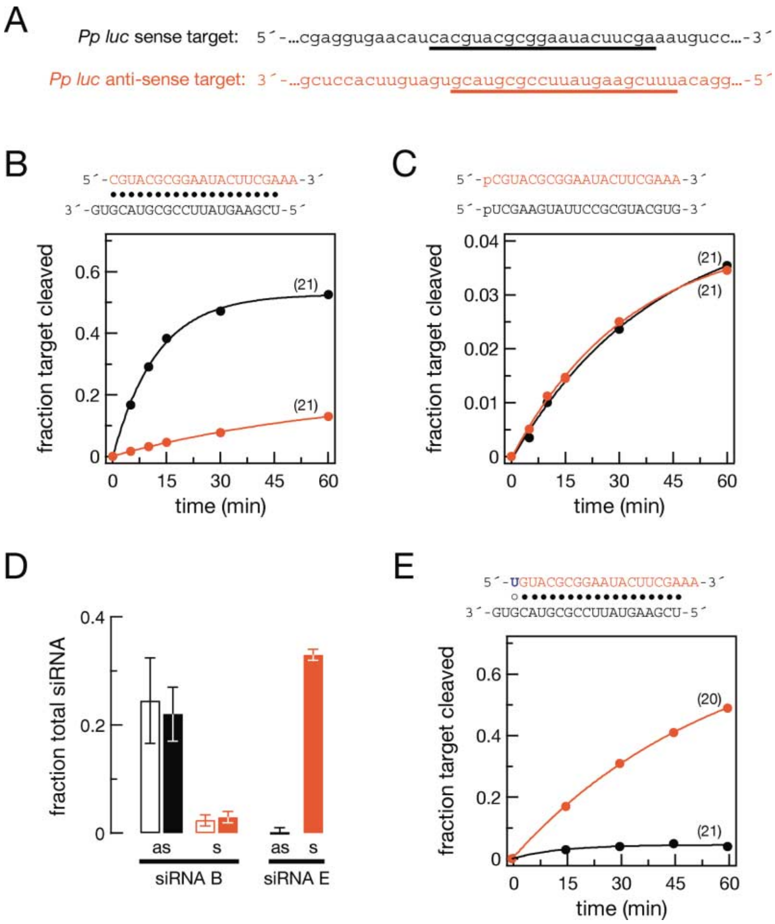

Figure 1. The Two Strands of an siRNA Duplex Do Not Equally Populate the RISC

(A) Firefly luciferase sense and anti-sense target RNA sequences.

(B) In vitro RNAi reactions programmed with the siRNA duplex indicated above the graph.

(C) In vitro RNAi reactions as in (B) but programmed with either the anti-sense or sense single-stranded, 5′ phosphorylated siRNAs indicated above the graph.

(D) Fraction of anti-sense (black) and sense (red) siRNA strands assembled into RISC (open columns) or present as single strands (filled columns) after incubation with *Drosophila* embryo lysate for the siRNA duplexes shown in (B) and (E). The average of four trials ± standard deviation is shown.

(E) In vitro RNAi reactions programmed with the siRNA duplex indicated above the graph and the target RNAs in (A). Throughout the figures, the number of Watson-Crick base pairs formed between the siRNA guide strand and the target RNA is indicated in parentheses, and siRNA bases that mismatch with the target RNA are noted in blue.

Results and Discussion

Functionally Asymmetric siRNA Duplexes

To assess if the two strands of an siRNA duplex are equally competent to direct RNAi, we measured the in vitro rates of sense and anti-sense target cleavage for an siRNA duplex directed against firefly luciferase mRNA (Figure 1A). For this siRNA, the anti-sense siRNA strand directed more-efficient RNAi against its sense target RNA than the sense siRNA strand did toward the anti-sense target (Figure 1B). (Throughout this paper, anti-sense siRNA strands and their sense target RNAs are presented in black and sense siRNAs and their anti-sense targets in red.) Control experiments showed that using siRNA duplexes with 5′ phosphates did not alter this result (data not shown), indicating that different rates of 5′ phosphorylation for the two strands cannot explain the asymmetry.

Single-stranded siRNA can direct RNAi but is >10-fold less effective than siRNA duplexes, reflecting the reduced stability of single-stranded RNA in vitro and in vivo (Schwarz et al., 2002). Surprisingly, the two strands of the luciferase siRNA duplex, used individually as 5′ phosphorylated single-strands, had identical rates of target cleavage (Figure 1C). Thus, the difference in the cleavage rates of the sense and anti-sense strands cannot reflect a difference in the inherent susceptibility of the two targets to RNAi. Instead, the finding that the two siRNA strands are equally effective as single strands but show dramatically different activities when paired to each other suggests that the asymmetry in their function is established at a step in the RNAi pathway before the encounter of the programmed RISC with its RNA target.

Differential RISC Assembly and siRNA Functional Asymmetry

siRNA unwinding correlates with siRNA function (Nykänen et al., 2001; Martinez et al., 2002), likely because siRNA duplex unwinding is required to assemble a RISC competent to base pair with its target RNA. We measured the accumulation of single-stranded siRNA from the luciferase siRNA duplex after 1 hr incubation in an in vitro RNAi reaction in the absence of target RNA. In this reaction, ~22% of the anti-sense strand of the luciferase siRNA was converted to single-strand (Figure 1D, siRNA B, solid black bar). Remarkably, we did not detect a corresponding amount of single-stranded sense siRNA (Figure 1D, siRNA B, solid red bar). Since the production of single-stranded anti-sense siRNA must be accompanied by an equal amount of single-stranded sense siRNA, the missing sense strand must have been destroyed after unwinding.

We also used a novel RISC-capture assay to measure the fraction of each siRNA strand that was assembled into RISC (G.H., M. Simard, C. Mello, and P.D.Z., unpublished data). Double-stranded siRNA was incubated in an RNAi reaction for 1 hr, then we added a complementary 2′-*O*-methyl oligonucleotide tethered to a magnetic bead via a biotin-streptavidin linkage. 2′-*O*-methyl oligonucleotides are not cleaved by the RNAi machinery but can bind stably to complementary siRNA within the RISC, so the amount of radioactivity stably associated with the beads is a direct measure of the amount of RISC formed. The assay was performed with siRNA duplexes in which either the sense or the anti-sense strand was 5′-^{32}P-radiolabeled. All RISC activity directed by the siRNA strand complementary to the tethered oligonucleotide was captured on the beads; no RISC was captured by an unrelated 2′-*O*-methyl oligonucleotide (data not shown). The RISC-capture assay recapitulated our unwinding measurements: ten-fold more anti-sense siRNA-containing RISC was detected than sense-strand RISC (Figure 1D, siRNA B, open bars). The simplest explanation is that the two strands of the siRNA duplex are differentially loaded into the RISC and that single-stranded siRNA not assembled into RISC is degraded.

siRNA Structure and RISC Assembly

The finding that the two siRNA strands can have different capacities to form RISC when paired suggests that some feature unique to the duplex determines functional asymmetry. For the siRNA in Figure 1B, the 5′ end of the anti-sense siRNA strand begins with U and is thus paired to the sense siRNA strand by an U:A base pair (two hydrogen bonds). In contrast, the 5′ nucleotide of the sense siRNA strand is linked to the anti-sense strand by a C:G base pair (three hydrogen bonds). A simple hypothesis is that the siRNA strand whose 5′ end is more weakly bound to the complementary strand more readily incorporates into RISC.

As an initial test of this idea, we changed the first nucleotide of the siRNA sense strand from C to U, replacing a C:G pair with a less stable U:G wobble. The sequence of the anti-sense siRNA was not altered (Figure 1E). This single nucleotide substitution increased the rate of cleavage directed by the sense strand and virtually eliminated RNAi directed by the anti-sense strand (Figure 1E). That is, the single C-to-U substitution inverted the functional asymmetry of the siRNA. Assembly of the two strands of the siRNA into RISC was also reversed: nearly 30% of the sense siRNA strand was converted to single strand after 1 hr incubation, but no single-stranded anti-sense strand was detected (Figure 1D, siRNA E).

We calculated the stability of the initial four base pairs of the siRNA strands in Figure 1 using the nearest-neighbor method and the mfold algorithm (Mathews et al., 1999; Zuker, 2003). The 5′ end of the sense siRNA strand in Figure 1E, but not that in Figure 1B, is predicted to exist as an equilibrium of two conformers of nearly equal energy. In one conformer, the 5′ nucleotide of the sense strand is bound to the anti-sense strand by a U:G wobble pair, whereas in the other conformer the 5′ end of this siRNA strand is unpaired (Supplemental Figures S1A–S1C online at http://www.cell.com/cgi/content/full/115/2/199/DC1). The analysis suggests that RISC assembly favors the siRNA strand whose 5′ end has a greater propensity to fray.

To test our hypothesis, we examined the strand-specific rates of cleavage of sense and anti-sense human *Cu, Zn-superoxide dismutase* (*sod1*) RNA targets (Figure 2A) triggered by the siRNA duplexes shown in Figure 2. In Figure 2B, the 5′ ends of both siRNA strands of the duplex are in G:C base pairs, and the two strands are similar in their rates of target cleavage. In Figure 2C, the C at position 19 of the sense strand was changed to A, causing the anti-sense strand to begin with an unpaired nucleotide. This change, which was made to the sense-strand of the siRNA, caused the rate of target cleavage guided by the anti-sense siRNA strand to be dramatically enhanced and the sense strand rate to be suppressed (Figure 2C). Because the enhancement of sense target cleavage was caused by a mutation in the sense siRNA strand, which does not participate in the recognition of this target, the effect of the mutation must be on a step in the RNAi pathway that is spatially or temporally coupled to siRNA unwinding. However, the suppression of anti-sense target cleavage might have resulted from the single-nucleotide mismatch between the sense strand and its target RNA generated by the C-to-U substitution.

To exclude this possibility, we used a different strategy to unpair the 5′ end of the anti-sense strand. In Figure 2D, the sense strand is identical to that in Figure 2B, but the first nucleotide of the anti-sense strand was changed from G to U, creating a U-C mismatch at its 5′ end in place of the G-A of Figure 2C. This siRNA duplex still showed pronounced asymmetry, with the anti-sense strand guiding target cleavage to the nearly complete exclusion of the sense strand (Figure 2D). Thus, the suppression of the cleavage rate of the sense strand in Figure 2C was not a consequence of the position 19 mismatch with the anti-sense target. This finding is consistent with previous studies that suggest that mismatches with the target RNA are well tolerated if they occur near the 3′ end of the siRNA guide strand (Amarzguioui et al., 2003). When we paired the sense strand of Figure 2C with the anti-sense strand of Figure 2D to create the duplex in Figure 2E, the resulting siRNA directed anti-sense target cleavage significantly better than the siRNA in Figure 2C, although the two siRNAs contain the same sense strand (Figure 2E).

Figures 2F–2H show a similar analysis in which the 5′ end of the sense strand or position 19 of the anti-sense strand of the siRNA in Figure 2B was altered to produce siRNA duplexes in which the 5′ end of the sense strand was either fully unpaired (Figures 2F and 2G) or in an A:U base pair (Figure 2H). Again, unpairing the 5′ end of an siRNA strand—the sense strand in this case—caused that strand to function to the exclusion of the other strand. When the sense strand 5′ end was present in an A:U base pair and the anti-sense strand 5′ end was in a G:C pair, the sense strand dominated the reaction (Figure 2H), but the anti-sense strand retained activity similar to that seen for the original siRNA (Figure 2B). We conclude that the relative ease with which the 5′ ends of the two siRNAs can be liberated from the duplex determines the degree of asymmetry. Additional data supporting this idea is shown in Supplemental Figure S1. Figure S1F shows an siRNA that cleaved the two *sod1* target RNAs (Figure S1D) with modest functional asymmetry that reflects the collective base pairing

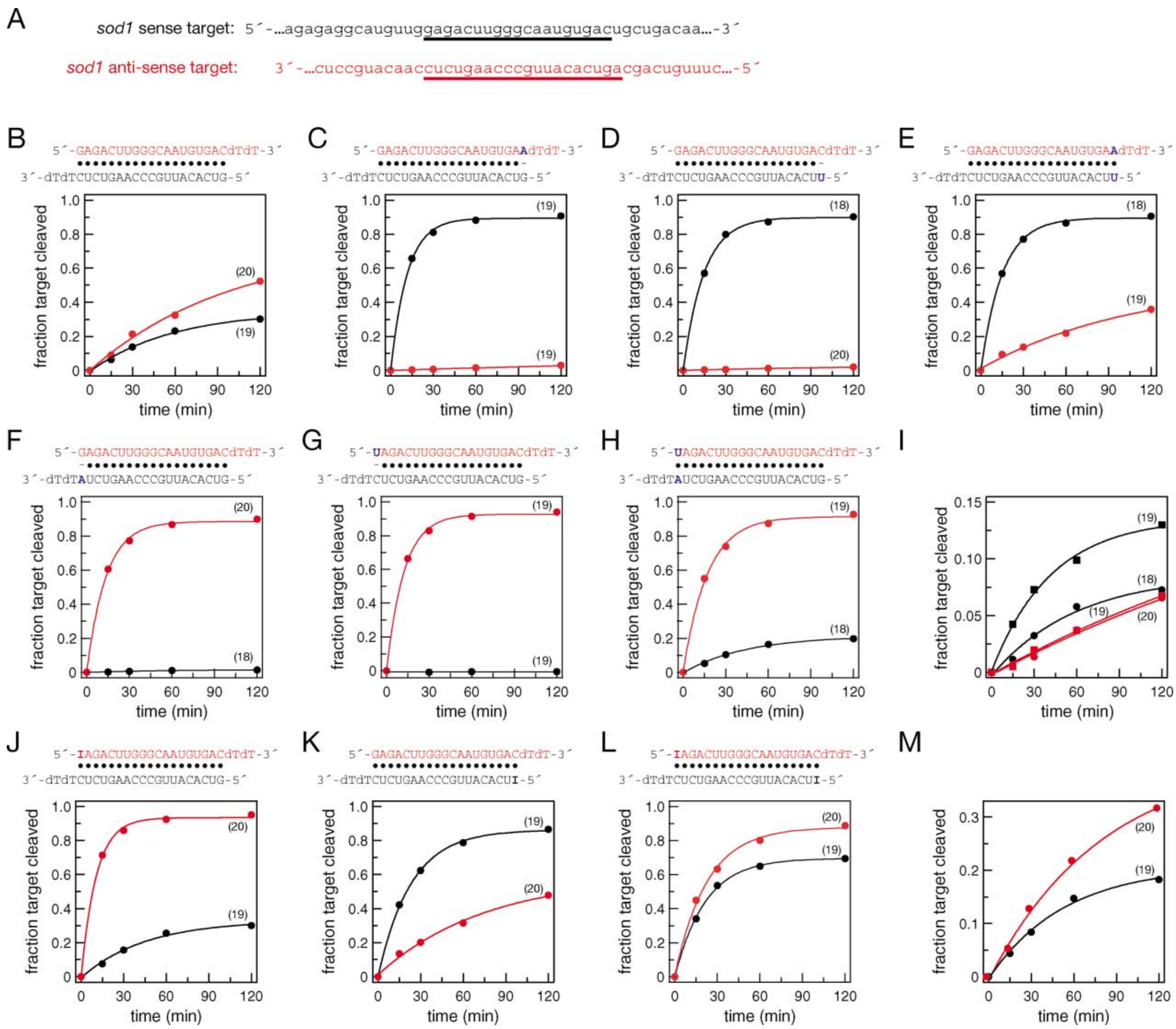

Figure 2. 5′ Terminal, Single-Nucleotide Mismatches Make siRNA Duplexes Functionally Asymmetric

(A) The sequences at the cleavage site of the 560 nt *sod1* RNA sense or 578 nt *sod1* anti-sense target RNAs. The siRNAs in this figure and in Figure 3 cleave the sense target to yield a 320 nt 5′ product and the anti-sense target to yield a 261 nt 5′ product.

(B–H) In vitro RNAi reactions programmed with the siRNA indicated above each graph using the target RNAs diagrammed in (A).

(I) In vitro RNAi reactions programmed with anti-sense or sense single-stranded, 5′ phosphorylated siRNAs (the single nucleotide mismatch with target RNA is underlined): black squares, 5′-pGUCACAUUGCCCAAGUCUCdTdT-3′; black circles, 5′-pUUCACAUUGCCCAAGUCUCdTdT-3′; red squares, 5′-pGAGACUUGGGCAAUGUGAAdTdT-3′; red circles, 5′-pGAGACUUGGGCAAUGUGACdTdT-3′.

(J–M) A single hydrogen bond difference can cause the two strands of an siRNA duplex to assemble differentially into RISC. (J–L) In vitro RNAi reactions programmed with the siRNA indicated above each graph using the target RNAs in (A). (M) In vitro RNAi reactions as in (J)–(L) but programmed with anti-sense or sense single-stranded, 5′ phosphorylated siRNAs: black circles, 5′-IUCACAUUGCCCAAGUCUCdTdT-3′; red circles, 5′-IAGACUUGGGCAAUGUGACdTdT-3′.

strength of the first four nucleotides of each siRNA strand (Figure S1E; see below). Asymmetry was dramatically increased when a G:U wobble was introduced at the 5′ end of the anti-sense strand of the siRNA (Figure S1G), but no asymmetry was seen when the individual single-strands strands were used to trigger RNAi (Figure S1H), demonstrating that differential RISC assembly, not target accessibility, explains the functional asymmetry of the siRNA duplex.

A Single Hydrogen Bond Can Determine Which siRNA Strand Directs RNAi

How small a difference in siRNA base pairing can the RISC-assembly machinery sense? To explore this question, we altered the siRNA in Figure 2B by introducing inosine (I) in place of the initial guanosines of the siRNA strands. These siRNAs cleave the same sites on the two target RNAs as the siRNA in Figure 2B but contain I:C pairs instead of G:C. An I:C pair is similar in energy to an A:U (Turner et al., 1987). When the sense strand began with I, it directed target cleavage more efficiently than the anti-sense strand (Figure 2J). An inosine at the 5′ end of the anti-sense strand had the opposite effect (Figure 2K). Thus, a difference of a single hydrogen bond has a measurable effect on the symmetry of RISC assembly. When both siRNA strands began with I, the relative efficacy of the two siRNA strands (Figure 2L) was restored to that measured for the individual single strands (Figure 2M). Thus, the small difference in rates in Figure 2L reflects a difference in the intrinsic capacity of the two strands to guide cleavage, not a difference in their assembly into RISC. We note that the absolute rates are faster for the siRNA in Figure 2L than that in Figure 2B, suggesting that production of RISC from an individual strand is governed not only by the relative propensity of the two 5′ ends to fray, but also by their absolute propensities to fray.

We hypothesize that siRNA end fraying provides an entry site for an ATP-dependent RNA helicase that unwinds siRNA duplexes (Figure 4A). The involvement of a helicase in RISC assembly is supported by previous observations. (1) Both siRNA unwinding and production of functional RISC require ATP in vitro (Nykänen et al., 2001), and (2) several proteins with sequence homology to ATP-dependent RNA helicases have been implicated in RNA silencing (Wu-Scharf et al., 2000; Dalmay et al., 2001; Hutvágner and Zamore, 2002; Ishizuka et al., 2002; Kennerdell et al., 2002; Tabara et al., 2002; Tijsterman et al., 2002). However, other mechanisms are possible, including strand selection by an ATP-dependent nuclease or the concerted action on the siRNA of an ATPase and single-stranded RNA binding proteins and/or nucleases.

Four to six bases of single-stranded nucleic acid are bound by the well-studied helicases PcrA (Velankar et al., 1999) and NS3 (Kim et al., 1998). Therefore, we tested the effect of single-nucleotide mismatches in this region of the siRNA using a series of siRNAs containing a mismatch at the second, third, or fourth position of each siRNA strand. We also analyzed siRNAs bearing G:U wobble pairs at the second, third, or both second and third positions (Figure 3). These siRNAs were again based on the siRNA in Figure 2B and targeted the *sod1* sense and anti-sense RNAs in Figure 2A. The results of this series demonstrate that mismatches, but not G:U wobbles, at positions 2–4 of an siRNA strand alter the relative loading of the two siRNA strands into RISC. Mismatches at position five have very modest effects on the relative loading of the siRNA strands into RISC (data not shown). In contrast, the effects of internal mismatches at positions 6–15 cannot be explained by their influencing the symmetry of RISC assembly (data not shown). In sum, these data are consistent with the action of a nonprocessive helicase that can bind about four nucleotides of RNA.

Implications of siRNA Asymmetry for miRNA Biogenesis

miRNAs are derived from the double-stranded stem of hairpin precursor RNAs by cleavage catalyzed by the double-stranded RNA-specific endonuclease Dicer (Lee et al., 1993; Pasquinelli et al., 2000; Reinhart et al., 2000; Grishok et al., 2001; Hutvágner et al., 2001; Ketting et al., 2001; Lagos-Quintana et al., 2001, 2002; Lau et al., 2001; Lee and Ambros, 2001; Reinhart et al., 2002). Pre-miRNA processing by Dicer may generate a product with the essential structure of an siRNA duplex, as first suggested by Bartel and colleagues (Reinhart et al., 2002; Lim et al., 2003b). Using a small RNA cloning strategy to identify mature miRNAs in *C. elegans*, they recovered small RNAs corresponding to the non-miRNA side of the precursor's stem (Lim et al., 2003b). Although these miRNA* sequences were recovered at about 100 times lower frequency than the miRNAs themselves, they could always be paired with the corresponding miRNA to give miRNA duplexes with 2 nt overhanging 3′ ends (Lim et al., 2003b). Their data suggest that miRNAs are born as duplexes but accumulate as single-strands because some subsequent process stabilizes the miRNA, destabilizes the miRNA*, or both.

We propose that incorporation of miRNA into RISC is this process. Our results with siRNA suggest that preferential assembly of a miRNA into the RISC would be accompanied by destruction of its * strand (Figure 4A). To favor miRNA accumulation, miRNA duplexes would present the miRNA in a structure that loads the miRNA strand, but not the miRNA*, into RISC.

Is this idea plausible? We deduced the miRNA duplex that might be generated by processing of pre-*let-7* ("conceptual dicing," Figure 4B). Pre-miRNA stems are only partially double stranded; the typical animal pre-miRNA contains mismatches, internal loops, and G:U base pairs predicted to distort an RNA helix. As a consequence, miRNA duplexes should also contain terminal and internal mismatches and G:U base pairs. For pre-*let-7*, the 5′ end of *let-7* is unpaired in the predicted miRNA duplex, whereas the 5′ end of the * strand is paired. The results presented in Figures 1 and 2 predict that this structure should cause the *let-7* strand to enter the RISC and the *let-7** strand to be degraded. Emboldened by this thought experiment, we extended the analysis to other *Drosophila* miRNA genes (Lagos-Quintana et al., 2001). For each, we inferred from its precursor structure the double strand predicted to be produced by Dicer. These conceptually diced miRNA duplexes are shown in Figure 4C. For 20 of the 27 duplexes analyzed (including pre-*let-7*), the difference in the base pairing of the first five nucleotides of the miRNA versus the miRNA* strand accurately predicted the miRNA, and not the miRNA*, to accumulate in vivo. The analysis succeeded irrespective of which side of the pre-miRNA stem encoded the mature miRNA. In this analysis, we relied on our observations that single mismatches in the first four nucleotides of an siRNA strand, an initial G:U wobble pair, but not internal G:U wobbles, directed the asymmetric incorporation of an siRNA strand into RISC (Figures 1, 2, 3, and S1). However, our experiments with siRNA predict that both the miRNA and the miRNA* strand should accumulate for miR-2a-2, miR-4, miR-5, one of the three miR-6 paralogs, miR-8, miR-10, and miR-13a. Recently, Tuschl and colleagues reported an exhaustive effort to clone and sequence miRNAs from *Drosophila* (Aravin et al., 2003). They found that miR-2a-2*, miR-4*, miR-8*, miR-10*, and miR-13a* are all expressed in vivo. We have confirmed by Northern hybridization that both miR-10 and miR-10* are expressed in adult *Drosophila* males and females and in syncitial blastoderm embryos (Supplemental Figure S2). Thus, of the seven miRNAs we predict to accumulate as both miRNA and miRNA* species, five have now been confirmed experimentally. No miRNA* species were cloned by Tuschl and colleagues for any of the miRNAs we predicted to accumulate asymmetrically (Aravin et al., 2003). These data strengthen our proposal that pre-miRNAs specify on which side of the stem the miRNA resides by generating miRNA duplexes from which only one of the two strands is assembled into RISC. When these double-stranded miRNA intermediates do not

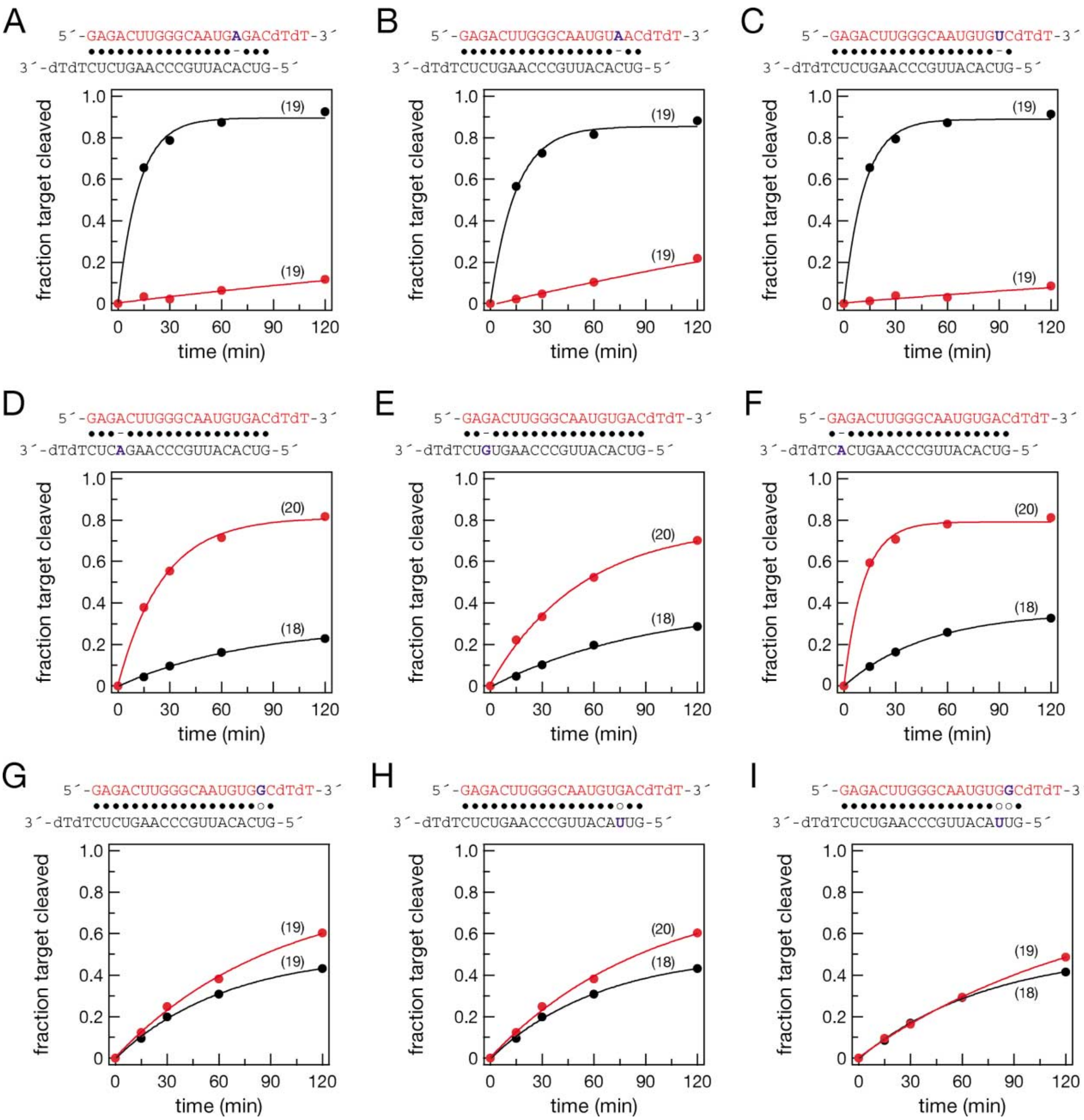

Figure 3. The First Four Base Pairs of the siRNA Duplex Determine Strand-Specific Activity

Internal, single-nucleotide mismatches (A–F) near the 5′ ends of an siRNA strand generate functional asymmetry but internal G:U wobble pairs (G–I) do not. Target RNAs were as in Figure 2A.

contain structural features enforcing asymmetric RISC assembly, both strands accumulate in vivo. It is tempting to speculate that pre-miRNAs such as pre-miR-10, which generates roughly equal amounts of small RNA products from both sides of the precursor stem, regulate target RNAs with partial complementary to either small RNA product.

Implications for RNA Silencing

Our observations have important implications for the design of functional siRNAs for mammalian RNAi. We have shown that siRNA structure can profoundly influence the entry of the anti-sense siRNA strand into the RNAi pathway. A review of the published literature suggests that the structure of the siRNA duplex, rather than that of the target site, explains most reports of ineffective siRNAs duplexes. Such inactive duplexes may be coaxed back to life simply by modifying the *sense* strand of the siRNA. An example of this is shown in Supplemental Figure S1 for an ineffective siRNA directed against the *huntingtin* (*htt*) mRNA (Figure S2K). Changing the G:C (Figure S2K) to an A:U pair (Figure S2L) or a G-A mismatch (Figure S2M) dramatically improved its target cleavage rate in vitro and its efficacy in vivo (E. Milkani, N.A., and P.D.Z., unpublished data). Because RNAi is a natural cellular pathway, siRNAs should be designed to

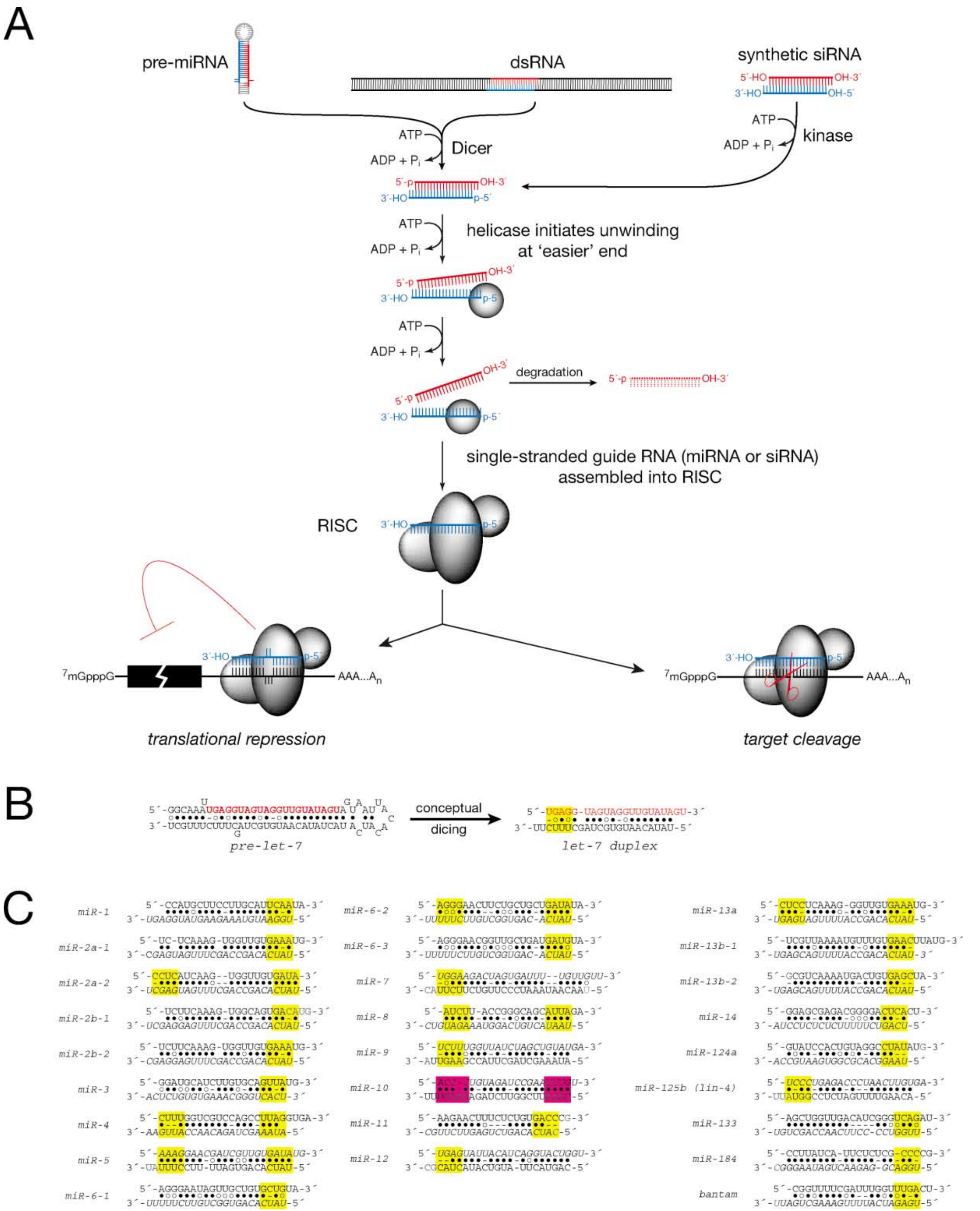

Figure 4. Asymmetric RISC Assembly Can Explain siRNA and miRNA Strand Choice

(A) A model for RISC assembly. Dicing of both pre-miRNAs and dsRNA is proposed to generate a duplex intermediate that is a substrate for an ATP-dependent RNA helicase that directs only one of the two strands into RISC; the other strand is degraded.

(B and C) Asymmetric RISC assembly from double-stranded intermediates explains why miRNAs accumulate in vivo as single strands. (B) pre-*let-7* might be processed by Dicer into a miRNA duplex in which the 5′ end of *let-7*, but not that of *let-7**, is unpaired. (C) The miRNA duplexes predicted to result from Dicer cleavage of *Drosophila* miRNA precursors. The end bearing features predicted to promote asymmetric siRNA strand incorporation into RISC is highlighted in yellow, and the mature miRNA sequence is in italics. Analysis of the predicted miR-10/miR-10* duplex, for which both ends are highlighted in purple, provides little information as to why miR-10 would predominate in vivo. miRNA sequences are from Lagos-Quintana et al. (2001) and Brennecke et al. (2003), with minor sequence corrections from Aravin et al. (2003); miRNA* sequences for miR-2a-2, miR-4, miR-8, miR-10, and miR-13a are as reported by Aravin et al. (2003).

reflect the biological requirements for entry of the anti-sense strand into RISC. In cultured HeLa cells, siRNAs designed according to the mechanism-based rules presented in this paper show maximum suppression of target mRNA expression at concentrations ~100-fold lower than those typically used in mammalian RNAi studies (Schwarz et al., 2002, and our unpublished data). Rana and colleagues previously noted the disproportionate influence of the 5′ nucleotides of the anti-sense strand on siRNA function (Chiu and Rana, 2003). Consistent with our in vitro data, Khvorova and colleagues have found that a low base-pairing stability at the 5′ end of the anti-sense strand, but not the sense strand, characterizes functional siRNAs in cultured cells (Khvorova et al., 2003 [this issue of *Cell*]).

siRNAs designed to function asymmetrically may also be used to enhance RNAi specificity. Expression profiling studies show that the sense strand of an siRNA can direct off-target gene silencing (Jackson et al., 2003). A potential remedy for such sequence-specific but undesirable effects is to redesign the siRNA so that only the anti-sense strand enters the RNAi pathway.

Our observations also suggest a need to revise the current design rules for the construction of short hairpin RNA (shRNA) vectors, which produce siRNAs transcriptionally in cultured cells or in vivo (Brummelkamp et al., 2002; McManus et al., 2002; Paddison et al., 2002; Paul et al., 2002; Sui et al., 2002; Yu et al., 2002). We suggest that shRNAs be designed to place the 5′ end of the anti-sense siRNA strand in a mismatch or G:U base pair. Moreover, a recent report suggests that some shRNAs may induce the interferon response (Bridge et al., 2003). Mismatches and G:U pairs could be designed into these shRNAs simultaneously to promote entry of the correct siRNA strand into the RNAi pathway and to diminish the capacity of the shRNA stem to trigger nonsequence-specific responses to double-stranded RNA. Redesigning shRNAs to more fully reflect the natural mechanism of miRNA incorporation into RISC should make them more effective, allowing lower levels of shRNA to silence target mRNAs in vivo.

Experimental Procedures

General Methods

In vitro RNAi reactions and analysis was carried out as previously described (Tuschl et al., 1999; Zamore et al., 2000; Haley et al., 2003). Target RNAs were used at ~5 nM concentration so that reactions were mainly under single-turnover conditions. Target cleavage under these conditions was proportionate to siRNA concentration. siRNA unwinding assays were as published (Nykänen et al., 2001).

siRNA Preparation

Synthetic RNA (Dharmacon) was deprotected according to the manufacturer's protocol. siRNA strands were annealed (Elbashir et al., 2001a) and used at a final concentration of ≤50 (Figures 1B, 2, 3, and Supplemental Figures S1F–S1H) or ≤100 nM (Figures 1D, 1E, and Supplemental Figures S1K–S1M). siRNA single strands were phosphorylated with polynucleotide kinase (PNK; New England Biolabs) and 1 mM ATP and used at 500 nM final concentration.

Target RNA Preparation

Target RNAs were transcribed with recombinant histidine-tagged T7 RNA polymerase from PCR products as described (Nykänen et al., 2001; Hutvágner and Zamore, 2002) except for sense *sod1* mRNA, which was transcribed from a plasmid template (Crow et al., 1997) linearized with BamHI. PCR templates for *htt* sense and anti-sense and *sod1* anti-sense target RNAs were generated by amplifying 0.1 ng/μl (final concentration) plasmid template encoding *htt* or *sod1* cDNA using the following primer pairs: *htt* sense target, 5′-GCGTAATACGACTCACTATAGGAACAGTATGTCTCAGACATC-3′ and 5′-UUCGAAGUAUUCCGCGUACGU-3′; *htt* anti-sense target, 5′-GCGTAATACGACTCACTATAGGACAAGCCTAATTAGTGATGC-3′ and 5′-GAACAGTATGTCTCAGACATC-3′; *sod1* anti-sense target, 5′-GCGTAATACGACTCACTATAGGGCTTTGTTAGCAGCCGGAT-3′ and 5′-GGGAGACCACAACGGTTTCCC-3′.

Immobilized 2′-*O*-methyl Oligonucleotide Capture of RISC

The 5′ end of the siRNA strand to be measured was ^{32}P-radiolabeled with PNK. 10 pmol biotinylated 2′-*O*-Methyl RNA was immobilized on Dynabeads M280 (Dynal) by incubation in 10 μl lysis buffer containing 2 mM DTT for 1 hr on ice with the equivalent of 50 μl of the suspension of beads provided by the manufacturer. The beads were then washed to remove unbound oligonucleotide. 50 nM siRNA was preincubated in a standard 50 μl in vitro RNAi reaction for 15 min at 25°C. Then, all of the immobilized 2′-*O*-Methyl oligonucleotide was added to the reaction and the incubation continued for 1 hr at 25°C. After incubation, the beads were rapidly washed three times with lysis buffer containing 0.1% (w/v) NP-40 and 2 mM DTT followed by a wash with the same buffer without NP-40. Input and bound radioactivity were determined by scintillation counting (Beckman). The 5′-biotin moiety was linked via a six-carbon spacer arm. 2′-*O*-methyl oligonucleotides (IDT) were: 5′-biotin-ACAUUUCGAAGUAU UCCGCGUACGUGAUGUU-3′ (to capture the siRNA sense strand) and 5′-biotin-CAUCACGUACGCGGAAUACUUCGAAAUGUCC-3′ (to capture the anti-sense strand).

Acknowledgments

We thank Martin Simard for noting the unpaired end of *let-7* in pre-*let-7*; Steve Blacklow and Barbara Golden for suggesting we use inosine to test siRNA asymmetry; Natasha Caplen, Tom Tuschl, and Anastasia Khvorova for sharing data before publication; Eftim Milkani for help preparing Figure 4; Juanita McLachlan for preparing lysates and maintaining our fly colony; and David Bartel, Craig Mello, Tariq Rana, and members of the Zamore lab for encouragement, helpful discussions, and comments on the manuscript. Most importantly, we thank Doug Turner for patiently teaching us to calculate theoretical free energies. G.H. is a Charles A. King Trust fellow of the Medical Foundation. P.D.Z. is a Pew Scholar in the Biomedical Sciences and a W.M. Keck Foundation Young Scholar in Medical Research. This work was supported in part by grants from the National Institutes of Health to P.D.Z. (GM62862-01 and GM65236-01), to N.A. (R01 NS38194), and to Z.X. and P.D.Z. (R21 NS44952-01), and by a grant from the Hereditary Disease Foundation to N.A. and P.D.Z.

Received: June 18, 2003
Revised: August 22, 2003
Accepted: September 12, 2003
Published: October 16, 2003

References

Amarzguioui, M., Holen, T., Babaie, E., and Prydz, H. (2003). Tolerance for mutations and chemical modifications in a siRNA. Nucleic Acids Res. *31*, 589–595.

Ambros, V., Bartel, B., Bartel, D.P., Burge, C.B., Carrington, J.C., Chen, X., Dreyfuss, G., Eddy, S.R., Griffiths-Jones, S., Marshall, M., et al. (2003). A uniform system for microRNA annotation. RNA *9*, 277–279.

Aravin, A.A., Lagos-Quintana, M., Yalcin, A., Zavolan, M., Marks, D., Snyder, B., Gaasterland, T., Meyer, J., and Tuschl, T. (2003). The small RNA profile during Drosophila melanogaster development. Dev. Cell *5*, 337–350.

Bernstein, E., Caudy, A.A., Hammond, S.M., and Hannon, G.J. (2001). Role for a bidentate ribonuclease in the initiation step of RNA interference. Nature *409*, 363–366.

Billy, E., Brondani, V., Zhang, H., Muller, U., and Filipowicz, W. (2001). Specific interference with gene expression induced by long, double-stranded RNA in mouse embryonal teratocarcinoma cell lines. Proc. Natl. Acad. Sci. USA *98*, 14428–14433.

Boutla, A., Delidakis, C., Livadaras, I., Tsagris, M., and Tabler, M. (2001). Short 5′-phosphorylated double-stranded RNAs induce RNA interference in *Drosophila*. Curr. Biol. *11*, 1776–1780.

Brennecke, J., Hipfner, D.R., Stark, A., Russell, R.B., and Cohen, S.M. (2003). bantam encodes a developmentally regulated microRNA that controls cell proliferation and regulates the proapoptotic gene hid in *Drosophila*. Cell *113*, 25–36.

Bridge, A.J., Pebernard, S., Ducraux, A., Nicoulaz, A.L., and Iggo, R. (2003). Induction of an interferon response by RNAi vectors in mammalian cells. Nat. Genet. *34*, 263–264.

Brummelkamp, T.R., Bernards, R., and Agami, R. (2002). A system for stable expression of short interfering RNAs in mammalian cells. Science *296*, 550–553.

Catalanotto, C., Azzalin, G., Macino, G., and Cogoni, C. (2002). Involvement of small RNAs and role of the qde genes in the gene silencing pathway in Neurospora. Genes Dev. *16*, 790–795.

Caudy, A.A., Myers, M., Hannon, G.J., and Hammond, S.M. (2002). Fragile X-related protein and VIG associate with the RNA interference machinery. Genes Dev. *16*, 2491–2496.

Chiu, Y., and Rana, T.M. (2003). siRNA function in RNAi: a chemical modification analysis. RNA *9*, 1034–1048.

Chiu, Y.-L., and Rana, T.M. (2002). RNAi in human cells: basic structural and functional features of small interfering RNA. Mol. Cell *10*, 549–561.

Crow, J.P., Sampson, J.B., Zhuang, Y., Thompson, J.A., and Beckman, J.S. (1997). Decreased zinc affinity of amyotrophic lateral sclerosis-associated superoxide dismutase mutants leads to enhanced catalysis of tyrosine nitration by peroxynitrite. J. Neurochem. *69*, 1936–1944.

Dalmay, T., Horsefield, R., Braunstein, T.H., and Baulcombe, D.C. (2001). SDE3 encodes an RNA helicase required for post-transcriptional gene silencing in Arabidopsis. EMBO J. *20*, 2069–2078.

Doench, J.G., Petersen, C.P., and Sharp, P.A. (2003). siRNAs can function as miRNAs. Genes Dev. *17*, 438–442.

Doi, N., Zenno, S., Ueda, R., Ohki-Hamazaki, H., Ui-Tei, K., and Saigo, K. (2003). Short-interfering-RNA-mediated gene silencing in mammalian cells requires Dicer and eIF2C translation initiation factors. Curr. Biol. *13*, 41–46.

Elbashir, S.M., Lendeckel, W., and Tuschl, T. (2001a). RNA interference is mediated by 21- and 22-nucleotide RNAs. Genes Dev. *15*, 188–200.

Elbashir, S.M., Martinez, J., Patkaniowska, A., Lendeckel, W., and Tuschl, T. (2001b). Functional anatomy of siRNAs for mediating efficient RNAi in Drosophila melanogaster embryo lysate. EMBO J. *20*, 6877–6888.

Fire, A., Xu, S., Montgomery, M.K., Kostas, S.A., Driver, S.E., and Mello, C.C. (1998). Potent and specific genetic interference by double-stranded RNA in Caenorhabditis elegans. Nature *391*, 806–811.

Grishok, A., Pasquinelli, A.E., Conte, D., Li, N., Parrish, S., Ha, I., Baillie, D.L., Fire, A., Ruvkun, G., and Mello, C.C. (2001). Genes and mechanisms related to RNA interference regulate expression of the small temporal RNAs that control *C. elegans* developmental timing. Cell *106*, 23–34.

Haley, B., Tang, G., and Zamore, P.D. (2003). In vitro analysis of RNA interference in Drosophila melanogaster. Methods *30*, 330–336.

Hamilton, A.J., and Baulcombe, D.C. (1999). A species of small antisense RNA in posttranscriptional gene silencing in plants. Science *286*, 950–952.

Hammond, S.M., Bernstein, E., Beach, D., and Hannon, G.J. (2000). An RNA-directed nuclease mediates post-transcriptional gene silencing in Drosophila cells. Nature *404*, 293–296.

Hammond, S.M., Caudy, A.A., and Hannon, G.J. (2001). Post-transcriptional gene silencing by double-stranded RNA. Nat. Rev. Genet. *2*, 110–119.

Hutvágner, G., and Zamore, P.D. (2002). A MicroRNA in a Multiple-Turnover RNAi Enzyme Complex. Science *297*, 2056–2060.

Hutvágner, G., McLachlan, J., Pasquinelli, A.E., Balint, É., Tuschl, T., and Zamore, P.D. (2001). A cellular function for the RNA-interference enzyme Dicer in the maturation of the let-7 small temporal RNA. Science *293*, 834–838.

Ishizuka, A., Siomi, M.C., and Siomi, H. (2002). A Drosophila fragile X protein interacts with components of RNAi and ribosomal proteins. Genes Dev. *16*, 2497–2508.

Jackson, A.L., Bartz, S.R., Schelter, J., Kobayashi, S.V., Burchard, J., Mao, M., Li, B., Cavet, G., and Linsley, P.S. (2003). Expression profiling reveals off-target gene regulation by RNAi. Nat. Biotechnol. *21*, 635–637.

Kennerdell, J.R., Yamaguchi, S., and Carthew, R.W. (2002). RNAi is activated during Drosophila oocyte maturation in a manner dependent on aubergine and spindle-E. Genes Dev. *16*, 1884–1889.

Ketting, R.F., Fischer, S.E., Bernstein, E., Sijen, T., Hannon, G.J., and Plasterk, R.H. (2001). Dicer functions in RNA interference and in synthesis of small RNA involved in developmental timing in C. elegans. Genes Dev. *15*, 2654–2659.

Khvorova, A., Reynolds, A., and Jayasena, S.D. (2003). Functional siRNAs and miRNAs exhibit strand bias. Cell *115*, this issue, 209–216.

Kim, J.L., Morgenstern, K.A., Griffith, J.P., Dwyer, M.D., Thomson, J.A., Murcko, M.A., Lin, C., and Caron, P.R. (1998). Hepatitis C virus NS3 RNA helicase domain with a bound oligonucleotide: the crystal structure provides insights into the mode of unwinding. Structure *6*, 89–100.

Knight, S.W., and Bass, B.L. (2001). A role for the RNase III enzyme DCR-1 in RNA interference and germ line development in Caenorhabditis elegans. Science *293*, 2269–2271.

Lagos-Quintana, M., Rauhut, R., Lendeckel, W., and Tuschl, T. (2001). Identification of novel genes coding for small expressed RNAs. Science *294*, 853–858.

Lagos-Quintana, M., Rauhut, R., Yalcin, A., Meyer, J., Lendeckel, W., and Tuschl, T. (2002). Identification of tissue-specific microRNAs from mouse. Curr. Biol. *12*, 735–739.

Lagos-Quintana, M., Rauhut, R., Meyer, J., Borkhardt, A., and Tuschl, T. (2003). New microRNAs from mouse and human. RNA *9*, 175–179.

Lau, N.C., Lim, L.P., Weinstein, E.G., and Bartel, D.P. (2001). An sbundant class of tiny RNAs with probable regulatory roles in *Caenorhabditis elegans*. Science *294*, 858–862.

Lee, R.C., and Ambros, V. (2001). An extensive class of small RNAs in Caenorhabditis elegans. Science *294*, 862–864.

Lee, R.C., Feinbaum, R.L., and Ambros, V. (1993). The C. elegans heterochronic gene lin-4 encodes small RNAs with antisense complementarity to lin-14. Cell *75*, 843–854.

Lim, L.P., Glasner, M.E., Yekta, S., Burge, C.B., and Bartel, D.P. (2003a). Vertebrate microRNA genes. Science *299*, 1540.

Lim, L.P., Lau, N.C., Weinstein, E.G., Abdelhakim, A., Yekta, S., Rhoades, M.W., Burge, C.B., and Bartel, D.P. (2003b). The microRNAs of Caenorhabditis elegans. Genes Dev. *17*, 991–1008.

Mallory, A.C., Reinhart, B.J., Bartel, D., Vance, V.B., and Bowman, L.H. (2002). A viral suppressor of RNA silencing differentially regulates the accumulation of short interfering RNAs and micro-RNAs in tobacco. Proc. Natl. Acad. Sci. USA *99*, 15228–15233.

Martinez, J., Patkaniowska, A., Urlaub, H., Lührmann, R., and Tuschl, T. (2002). Single-stranded antisense siRNAs guide target RNA cleavage in RNAi. Cell *110*, 563–574.

Mathews, D.H., Sabina, J., Zuker, M., and Turner, D.H. (1999). Expanded sequence dependence of thermodynamic parameters improves prediction of RNA secondary structure. J. Mol. Biol. *288*, 911–940.

McManus, M.T., Petersen, C.P., Haines, B.B., Chen, J., and Sharp, P.A. (2002). Gene silencing using micro-RNA designed hairpins. RNA *8*, 842–850.

Mourelatos, Z., Dostie, J., Paushkin, S., Sharma, A.K., Charroux, B., Abel, L., Rappsilber, J., Mann, M., and Dreyfuss, G. (2002). miRNPs: a novel class of ribonucleoproteins containing numerous microRNAs. Genes Dev. *16*, 720–728.

Myers, J.W., Jones, J.T., Meyer, T., and Ferrell, J.E. (2003). Recombinant Dicer efficiently converts large dsRNAs into siRNAs suitable for gene silencing. Nat. Biotechnol. *21*, 324–328.

Nykänen, A., Haley, B., and Zamore, P.D. (2001). ATP requirements and small interfering RNA structure in the RNA interference pathway. Cell *107*, 309–321.

Paddison, P.J., Caudy, A.A., Bernstein, E., Hannon, G.J., and Conklin, D.S. (2002). Short hairpin RNAs (shRNAs) induce sequence-specific silencing in mammalian cells. Genes Dev. *16*, 948–958.

Park, W., Li, J., Song, R., Messing, J., and Chen, X. (2002). CARPEL FACTORY, a Dicer homolog, and HEN1, a novel protein, act in microRNA metabolism in *Arabidopsis thaliana*. Curr. Biol. *12*, 1484–1495.

Pasquinelli, A.E., Reinhart, B.J., Slack, F., Martindale, M.Q., Kuroda, M.I., Maller, B., Hayward, D.C., Ball, E.E., Degnan, B., Muller, P., et al. (2000). Conservation of the sequence and temporal expression of let-7 heterochronic regulatory RNA. Nature *408*, 86–89.

Paul, C.P., Good, P.D., Winer, I., and Engelke, D.R. (2002). Effective expression of small interfering RNA in human cells. Nat. Biotechnol. *20*, 505–508.

Provost, P., Dishart, D., Doucet, J., Frendewey, D., Samuelsson, B., and Radmark, O. (2002). Ribonuclease activity and RNA binding of recombinant human Dicer. EMBO J. *21*, 5864–5874.

Reinhart, B.J., Slack, F.J., Basson, M., Pasquinelli, A.E., Bettinger, J.C., Rougvie, A.E., Horvitz, H.R., and Ruvkun, G. (2000). The 21-nucleotide let-7 RNA regulates developmental timing in Caenorhabditis elegans. Nature *403*, 901–906.

Reinhart, B.J., Weinstein, E.G., Rhoades, M.W., Bartel, B., and Bartel, D.P. (2002). MicroRNAs in plants. Genes Dev. *16*, 1616–1626.

Schwarz, D.S., Hutvágner, G., Haley, B., and Zamore, P.D. (2002). Evidence that siRNAs function as guides, not primers, in the *Drosophila* and human RNAi pathways. Mol. Cell *10*, 537–548.

Sijen, T., Fleenor, J., Simmer, F., Thijssen, K.L., Parrish, S., Timmons, L., Plasterk, R.H., and Fire, A. (2001). On the role of RNA amplification in dsRNA-triggered gene silencing. Cell *107*, 465–476.

Sui, G., Soohoo, C., Affar el, B., Gay, F., Shi, Y., and Forrester, W.C. (2002). A DNA vector-based RNAi technology to suppress gene expression in mammalian cells. Proc. Natl. Acad. Sci. USA *99*, 5515–5520.

Tabara, H., Yigit, E., Siomi, H., and Mello, C.C. (2002). The dsRNA binding protein RDE-4 interacts with RDE-1, DCR-1, and a DexH-box helicase to direct RNAi in *C. elegans*. Cell *109*, 861–871.

Tang, G., Reinhart, B.J., Bartel, D.P., and Zamore, P.D. (2003). A biochemical framework for RNA silencing in plants. Genes Dev. *17*, 49–63.

Tijsterman, M., Ketting, R.F., Okihara, K.L., Sijen, T., and Plasterk, R.H. (2002). RNA helicase MUT-14-dependent gene silencing triggered in C. elegans by short antisense RNAs. Science *295*, 694–697.

Turner, D.H., Sugimoto, N., Kierzek, R., and Dreiker, S.D. (1987). Free energy increments for hydrogen bonds in nucleic acid base pairs. J. Am. Chem. Soc. *109*, 3783–3785.

Tuschl, T., Zamore, P.D., Lehmann, R., Bartel, D.P., and Sharp, P.A. (1999). Targeted mRNA degradation by double-stranded RNA in vitro. Genes Dev. *13*, 3191–3197.

Velankar, S.S., Soultanas, P., Dillingham, M.S., Subramanya, H.S., and Wigley, D.B. (1999). Crystal structures of complexes of PcrA DNA helicase with a DNA substrate indicate an inchworm mechanism. Cell *97*, 75–84.

Wu-Scharf, D., Jeong, B., Zhang, C., and Cerutti, H. (2000). Transgene and transposon silencing in Chlamydomonas reinhardtii by a DEAH-box RNA helicase. Science *290*, 1159–1163.

Yu, J.Y., DeRuiter, S.L., and Turner, D.L. (2002). RNA interference by expression of short-interfering RNAs and hairpin RNAs in mammalian cells. Proc. Natl. Acad. Sci. USA *99*, 6047–6052.

Zamore, P.D., Tuschl, T., Sharp, P.A., and Bartel, D.P. (2000). RNAi: double-stranded RNA directs the ATP-dependent cleavage of mRNA at 21 to 23 nucleotide intervals. Cell *101*, 25–33.

Zeng, Y., Yi, R., and Cullen, B.R. (2003). MicroRNAs and small interfering RNAs can inhibit mRNA expression by similar mechanisms. Proc. Natl. Acad. Sci. USA *100*, 9779–9784.

Zhang, H., Kolb, F.A., Brondani, V., Billy, E., and Filipowicz, W. (2002). Human Dicer preferentially cleaves dsRNAs at their termini without a requirement for ATP. EMBO J. *21*, 5875–5885.

Zuker, M. (2003). Mfold web server for nucleic acid folding and hybridization prediction. Nucleic Acids Res. *31*, 1–10.

Cell, Vol. 116, 831–841, March 19, 2004, Copyright ©2004 by Cell Press

RISC Assembly Defects in the *Drosophila* RNAi Mutant *armitage*

Yukihide Tomari,[1,3] Tingting Du,[1,3] Benjamin Haley,[1,3] Dianne S. Schwarz,[1] Ryan Bennett,[1] Heather A. Cook,[2] Birgit S. Koppetsch,[2] William E. Theurkauf,[2,*] and Phillip D. Zamore[1,*]
[1]Department of Biochemistry and Molecular Pharmacology
University of Massachusetts Medical School
Worcester, Massachusetts 01605
[2]Program in Molecular Medicine
University of Massachusetts Medical School
Worcester, Massachusetts 01605

Summary

The putative RNA helicase, Armitage (Armi), is required to repress *oskar* translation in *Drosophila* oocytes; *armi* mutant females are sterile and *armi* mutations disrupt anteroposterior and dorsoventral patterning. Here, we show that *armi* is required for RNAi. *armi* mutant male germ cells fail to silence *Stellate*, a gene regulated endogenously by RNAi, and lysates from *armi* mutant ovaries are defective for RNAi in vitro. Native gel analysis of protein-siRNA complexes in wild-type and *armi* mutant ovary lysates suggests that *armi* mutants support early steps in the RNAi pathway but are defective in the production of active RNA-induced silencing complex (RISC), which mediates target RNA destruction in RNAi. Our results suggest that *armi* is required for RISC maturation.

Introduction

In eukaryotes, long double-stranded RNA (dsRNA) silences genes homologous in sequence, a process termed RNA interference (RNAi; Fire et al., 1998). RNAi and other examples of RNA silencing have been observed in animals, plants, protozoa, and fungi (Cogoni and Macino, 1997; Kennerdell and Carthew, 1998; Ngo et al., 1998; Waterhouse et al., 1998; Lohmann et al., 1999; Sánchez-Alvarado and Newmark, 1999; Wianny and Zernicka-Goetz, 2000; Caplen et al., 2001; Elbashir et al., 2001a; Volpe et al., 2002; Schramke and Allshire, 2003). In plants, green algae, and invertebrates, RNAi defends the genome against mobile genetic elements, such as transposons and viruses, whose expression and activity increase in RNAi-defective mutants (Ketting et al., 1999; Ratcliff et al., 1999; Tabara et al., 1999; Dalmay et al., 2000; Mourrain et al., 2000; Wu-Scharf et al., 2000; Aravin et al., 2001; Sijen and Plasterk, 2003). The RNAi pathway also regulates endogenous gene expression for at least one *Drosophila* gene, *Stellate* (*Ste*), which is targeted for destruction by dsRNA transcribed from the *Suppressor-of-Stellate* (*Su(Ste)*) locus (Aravin et al., 2001).

*Correspondence: phillip.zamore@umassmed.edu (P.D.Z.) or william.theurkauf@umassmed.edu (W.E.T.)
[3]These authors contributed equally to this work.

Long dsRNA is converted by Dicer, a multidomain ribonuclease III enzyme, into small interfering RNAs (siRNAs) (Zamore et al., 2000; Bernstein et al., 2001; Billy et al., 2001), which serve as the specificity determinants of the RNAi pathway (Hamilton and Baulcombe, 1999; Hammond et al., 2000; Zamore et al., 2000; Elbashir et al., 2001b). siRNAs direct mRNA cleavage as part of a protein-siRNA complex called the RNA-induced silencing complex (RISC; Hammond et al., 2000, 2001). Members of the Argonaute family of proteins are core components of RISC or RISC-like complexes in flies (Hammond et al., 2001), worms (Tabara et al., 2002; Hutvágner et al., 2004), and humans (Caudy et al., 2002; Hutvágner and Zamore, 2002; Martinez et al., 2002; Mourelatos et al., 2002) and are required genetically for RNA silencing in every organism where their function has been studied (Tabara et al., 1999; Fagard et al., 2000; Grishok et al., 2000; Catalanotto et al., 2002; Caudy et al., 2002; Morel et al., 2002; Pal-Bhadra et al., 2002; Williams and Rubin, 2002; Doi et al., 2003).

Genetic studies also reveal the importance of helicase-domain proteins in the RNAi pathway. Putative DEA(H/D)-box helicases are required for posttranscriptional gene silencing (PTGS) in the green alga *Chlamydomonas reinhardtii* (Wu-Scharf et al., 2000) and RNAi in *C. elegans* (Tabara et al., 2002; Tijsterman et al., 2002). In *Drosophila*, mutations in *spindle-E* (*spn-E*), a gene encoding a putative DEAD-box helicase, abrogate endogenous RNAi-based repression of the *Ste* locus and trigger expression of retrotransposon mRNA in the germline (Aravin et al., 2001; Stapleton et al., 2001). In cultured *Drosophila* S2 cells, the putative helicase Dmp68 is a component of affinity-purified RISC (Ishizuka et al., 2002). Similarly, a putative DEAD-box RNA helicase, Gemin3, is a component of human RISC (Hutvágner and Zamore, 2002). Dicer, too, contains a putative ATP-dependent RNA helicase domain (Bernstein et al., 2001). Except for Dicer, no specific biochemical function in RNAi has been ascribed to any of these helicase proteins.

armitage (*armi*) was identified in a screen for maternal effect mutants that disrupt axis specification in *Drosophila* (Cook et al., 2004 [this issue of *Cell*]). Armitage protein (Armi) is a member of a family of putative ATP-dependent helicases distinct from the DEA(H/D) box proteins (Koonin, 1992). Armi is homologous across its putative helicase domain to SDE3 (Cook et al., 2004), which is required for PTGS in *Arabidopsis* (Dalmay et al., 2001). Because PTGS in plants is mechanistically related to RNAi in animals, Armi may play a role in RNAi in flies. Here, we show that *armi* is required for RNAi. *armi* mutant male germ cells fail to silence *Stellate*, a gene regulated endogenously by RNAi (Schmidt et al., 1999; Aravin et al., 2001; Stapleton et al., 2001), and lysates from *armi* mutant ovaries are defective for RNAi in vitro. Native gel analysis of protein-siRNA complexes in wild-type and *armi* mutant ovary lysates suggests that *armi* mutants support early steps in the RNAi pathway but are defective in the production of the RISC. Our

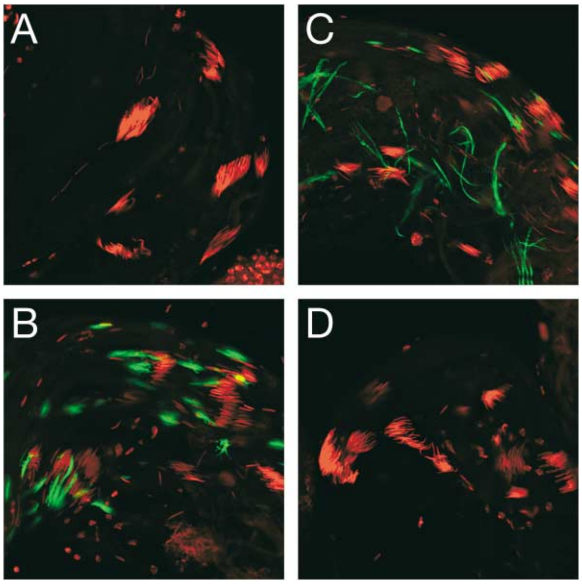

Figure 1. Armi Is Required for *Ste* Silencing in Fly Testes

The testes from wild-type (A), *armi*^{1} (B), *armi*$^{72.1}$ (C), and *armi*$^{rev39.2}$ flies (D) were stained for DNA (red) and Ste protein (green).

results suggest that *armi* is required for the assembly of siRNA into functional RISC.

Results

Armi Is Required for *Ste* Silencing

Silencing of the X-linked *Ste* gene by the highly homologous Y-linked *Su(Ste)* locus is an example of endogenous RNAi (Aravin et al., 2001; Gvozdev et al., 2003). In *Drosophila* testes, symmetrical transcription of *Su(Ste)* produces dsRNA, which is processed into siRNAs (Gvozdev et al., 2003). *Su(Ste)* siRNAs direct the degradation of *Ste* mRNA (Aravin et al., 2001). Inappropriate expression of Ste protein in testes is diagnostic of disruption of the RNAi pathway. Both the Argonaute protein, *aub*, and the putative DEAD-box helicase, *spn-E,* are required for RNAi in *Drosophila* oocytes (Kennerdell et al., 2002). Both mutants fail to silence *Ste*, as evidenced by the accumulation of Ste protein crystals in the testes of *aub* and *spn-E* mutants (Schmidt et al., 1999; Stapleton et al., 2001). No Ste protein is detected in wild-type testes (Figure 1A). Strikingly, Ste protein accumulates in testes of two different *armi* alleles, *armi*^{1} and *armi*$^{72.1}$ (Figures 1B and 1C). Neither allele is expected to be a true null because *armi*^{1} is caused by a P element insertion 5′ to the open reading frame, whereas *armi*$^{72.1}$, which was created by an imprecise excision of the *armi*^{1} P element, corresponds to a deletion of sequences in the 5′ untranslated region (C. Klattenhoff and W.E.T., unpublished observations). Ste silencing is re-established in males homozygous for the revertant chromosome, *armi*$^{rev\ 39.2}$ (henceforth, *armi*^{rev}; Cook et al., 2004), which was generated by excision of the *armi*^{1} P element (Figure 1D). These data suggest a role for Armi in *Drosophila* RNAi.

Immunofluorescent detection of Ste protein in testes implicates both *armi* alleles in endogenous RNAi, but provides only a qualitative measure of allele strength. Since Ste protein in males reduces their fertility (Belloni et al., 2002), the percent of embryos that hatch when mutant males are mated to wild-type (Oregon R) females provides a more quantitative measure of *Ste* dysregulation. We measured hatch rates for the offspring of wild-type, *armi*^{1}, *armi*$^{72.1}$, and *spn-E*^{1} homozygous males mated to Oregon R females. For *spn-E*^{1} males, 82% of the progeny hatched (n = 652). Seventy-five percent of the progeny of *armi*^{1} males hatched (n = 571), but only 45% for *armi*$^{72.1}$ (n = 710). In contrast, 97% of the offspring of wild-type males hatched (n = 688). Thus, *armi*$^{72.1}$ is a stronger allele than *armi*^{1}, at least with respect to the requirement for *armi* in testes.

Ovary Lysate Recapitulates RNAi In Vitro

Drosophila syncitial blastoderm embryo lysate has been used widely to study the RNAi pathway (Tuschl et al., 1999). However, *armi* flies lay few eggs, making it difficult to collect enough embryos to make lysate. To surmount this problem, we prepared lysates from ovaries manually dissected from wild-type or mutant females. Approximately 10 μl of lysate can be prepared from ~50 ovaries.

We used the well-characterized siRNA-directed mRNA cleavage assay (Elbashir et al., 2001b, 2001c) to evaluate the capacity of ovary lysate to support RNAi in vitro. Incubation in ovary lysate of a 5′ ^{32}P-cap-radiolabeled firefly luciferase mRNA target with a complementary siRNA duplex yielded the 5′ cleavage product diagnostic of RNAi (Figure 2A). siRNAs containing 5′ hydroxyl groups are rapidly phosphorylated in vitro and in vivo, but modifications that block phosphorylation eliminate siRNA activity (Nykänen et al., 2001; Chiu and Rana, 2002; Martinez et al., 2002; Schwarz et al., 2002; Saxena et al., 2003). Replacing the 5′ hydroxyl of the antisense siRNA strand with a 5′ methoxy group completely blocked RNAi in the ovary lysate (Figure 2A). In *Drosophila*, siRNAs bearing a single 2′-deoxy nucleotide at the 5′ end are poor substrates for the kinase that phosphorylates 5′ hydroxy siRNAs (Nykänen et al., 2001). A comparison of initial cleavage rates shows that in ovary lysate, target cleavage was slower for siRNAs with a 2′-deoxy nucleotide at the 5′ end of the antisense strand than for standard siRNAs (Figure 2B). Furthermore, the rate of target cleavage was fastest when the siRNA was phosphorylated before its addition to the reaction (Figure 2B). A similar enhancement from pre-phosphorylation was reported for siRNA injected into *Drosophila* embryos (Boutla et al., 2001). We conclude that lysates from *Drosophila* ovaries faithfully recapitulate RNAi directed by siRNA duplexes.

armi Ovary Lysates Are Defective in RNAi

In contrast to wild-type, lysates prepared from *armi*$^{72.1}$ ovaries do not support siRNA-directed target cleavage in vitro: no cleavage product was observed in the *armi*$^{72.1}$ lysate after 2 hr (Figure 3A). This result was observed for more than ten independently prepared lysates. To determine if the RNAi defect was allele specific, we tested ovaries from *armi*^{1}. Phenotypically, this allele is weaker than *armi*$^{72.1}$ in its effects on both male fertility (above) and oogenesis. For *armi*$^{72.1}$ females, 92% of the eggs lacked dorsal appendages, compared to 67% for *armi*^{1} eggs, and some *armi*^{1} eggs had wild-type or par-

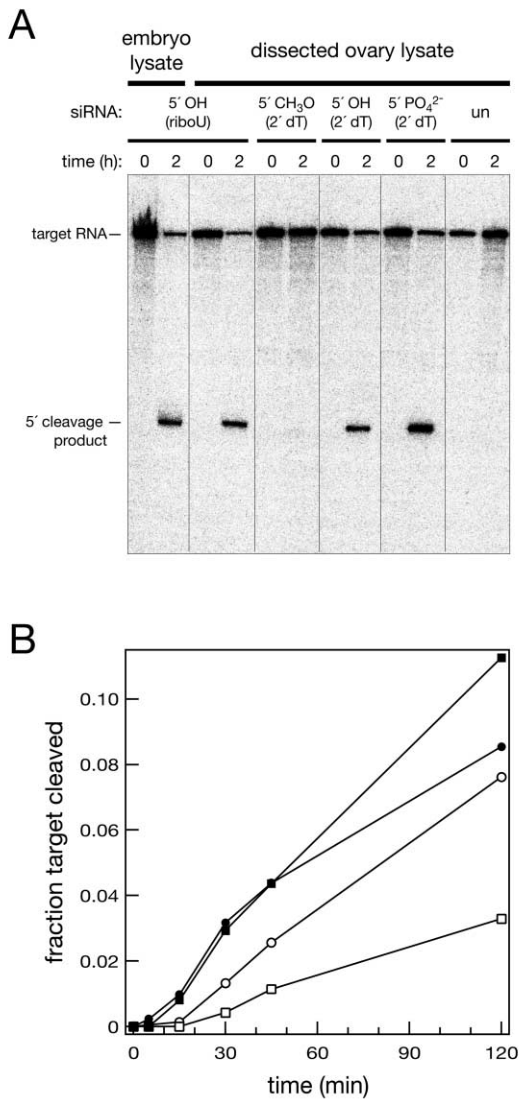

Figure 2. *Drosophila* Ovary Lysate Can Recapitulate RNAi In Vitro

(A) RNAi reactions in embryo and ovary lysates using complementary siRNA duplexes (with 5′ modifications) or an unrelated siRNA (un).

(B) mRNA cleavage rate in ovary lysate using 5′ modified siRNA. Filled squares, 5′ PO_4^{2-} (2′ dT); filled circles, 5′ PO_4^{2-} (2′ riboU); open squares, 5′ OH (2′ dT); open circles, 5′ OH (2′ riboU).

tially fused dorsal appendages (Figure 3B). Consistent with its weaker phenotype, the *armi*[1] allele showed a small amount of RNAi activity in vitro (Figure 3C). The two alleles were analyzed together at least four times using independently prepared lysates. In all assays, total protein concentration was adjusted to be equal. Lysate from the revertant allele, *armi*[rev], which has wild-type dorsal appendages, showed robust RNAi, demonstrating that the RNAi defect in the mutants is caused by mutation of *armi*, not an unlinked gene.

armi Ovary Lysates Are Impaired in RISC Assembly

The rate of target cleavage was much slower for *armi*[1] than for wild-type (Figure 3D). Since the rate of target cleavage in this assay usually reflects the concentration of RISC (Schwarz et al., 2003), we hypothesized that *armi* mutants are defective in RISC assembly. To test this hypothesis, we developed a method to measure RISC that requires less lysate than previously described techniques (Figure 4A). Double-stranded siRNA was incubated with ovary lysate in a standard RNAi reaction. To detect RISC, we added a 5′ ^{32}P-radiolabled, 2′-*O*-methyl oligonucleotide complementary to the antisense strand of the siRNA. Like target RNAs, 2′-*O*-methyl oligonucleotides can bind to RISC containing a complementary siRNA, but unlike RNA targets, they cannot be cleaved and binding is essentially irreversible (Hutvágner et al., 2004). RISC/2′-*O*-methyl oligonucleotide complexes were then resolved by electrophoresis through an agarose gel.

To validate the method, we examined RISC formation in embryo lysate. Four distinct complexes (C1, C2, C3, C4) were formed when siRNA was added to the reaction (Supplemental Figure S1A at http://www.cell.com/cgi/content/full/116/6/831/DC1). Formation of these complexes required ATP and was disrupted by pre-treatment of the lysate with the alkylating agent *N*-ethylmaleimide (NEM), but it was refractory to NEM treatment after RISC assembly; these are all properties of RNAi itself (Nykänen et al., 2001). No complex was observed with an siRNA unrelated to the 2′-*O*-methyl oligonucleotide (Supplemental Figure S1A on the *Cell* website, "un"). The amount of complex formed by different siRNA sequences correlated well with their capacity to mediate cleavage (data not shown). The four complexes were also detected in wild-type ovary lysate (Supplemental Figure S1B online), suggesting that the same RNAi machinery is used during oogenesis and early embryogenesis. The lower amount of RISC formed in ovary compared to embryo lysates can be explained by the lower overall protein concentration of ovary lysates.

We used the 2′-*O*-methyl oligonucleotide/native gel assay to analyze RISC assembly in *armi* mutant ovary lysates. *armi* mutants were deficient in RISC assembly. Representative data are shown in Figure 4B and quantitative results from four independent assays in Figure 4C. The extent of the deficit correlated with allele strength: less C3/C4 complex formed in lysate from the strong *armi*[72.1] allele than from *armi*[1] (Figures 4B and 4C). Compared to the phenotypically wild-type *armi*[rev], $>$10-fold less RISC was produced in *armi*[72.1].

The defect in RISC assembly in *armi* mutants is similar to that observed in lysates from *aub*[HN2] ovaries (Figures 4B and 4C). *aub* mutants do not support RNAi following egg activation and fail to silence the *Ste* locus in testes (Schmidt et al., 1999; Kennerdell et al., 2002), and lysates from *aub*[HN2] ovaries do not support RNAi in vitro (data not shown). Aub is one of five *Drosophila* Argonaute proteins, core constituents of RISC. It is therefore not surprising that Aub is required for RISC assembly. Since RISC assembly in vitro was not detectable in *aub*[HN2] lysates, our data suggest that Aub is the primary Argonaute protein recruited to exogenous siRNA in *Drosophila* ovaries. In contrast, ovaries from *nanos*[BN], a maternal effect mutant not implicated in RNAi, were fully competent for both RISC assembly (Figure 4C) and siRNA-directed target RNA cleavage (data not shown).

Identification of Intermediates in RISC Assembly

These data suggest that both *armi* and *aub* are required genetically for RISC assembly, but they provide no in-

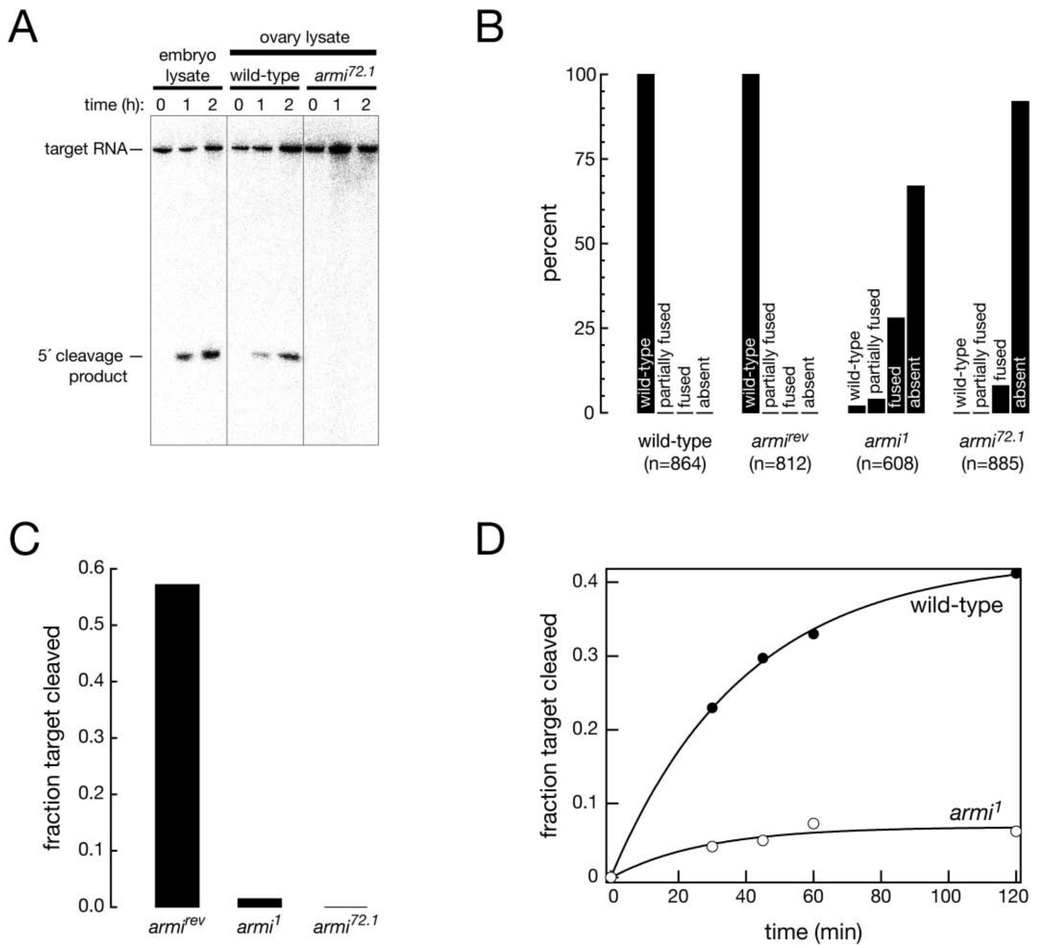

Figure 3. *armi* Ovary Lysates Are Defective in RNAi

(A) RNAi reactions in lysates from 0–2 hr embryos, wild-type or *armi*$^{72.1}$ mutant ovaries.

(B) Dorsal appendage phenotype was assessed for alleles of *armi*.

(C) The fraction of target mRNA cleaved after 2 hr in an RNAi reaction using ovary lysates from *armi* alleles.

(D) mRNA cleavage rate in wild-type and *armi*^{1} ovary lysates programmed with siRNA.

sight into the molecular basis of their RISC assembly defect(s). At what step(s) in RISC assembly are *armi* and *aub* blocked? In order to answer this question, we identified protein-siRNA intermediates in the RISC assembly pathway. Our 2′-*O*-methyl oligonucleotide/native gel method detects only complexes competent to bind target RNA (mature RISC). Therefore, we used a native gel assay designed to detect intermediates in the assembly of RISC. We radiolabeled the siRNA, allowing detection of complexes containing either single-stranded or double-stranded siRNA and used functionally asymmetric siRNAs (Schwarz et al., 2003) to distinguish between complexes containing single- and double-stranded siRNA.

RISC contains only a single siRNA strand (Martinez et al., 2002; Schwarz et al., 2002, 2003). Functionally asymmetric siRNAs load only one of the two strands of an siRNA duplex into RISC and degrade the other strand (Schwarz et al., 2003); the relative stability of the 5′ ends of the two strands determines which is loaded into RISC (Aza-Blanc et al., 2003; Khvorova et al., 2003; Schwarz et al., 2003). siRNA 1 (Figure 5A) loads its antisense strand into RISC, whereas siRNA 2 loads the sense strand (Schwarz et al., 2003). The two siRNA duplexes are identical, except that siRNA 2 contains a C-to-U substitution at position 1, which inverts the asymmetry (Schwarz et al., 2003). For both siRNAs, the antisense strand was 3′ ^{32}P-radiolabeled and will always be present in complexes that contain double-stranded siRNA. However, RISC will contain the ^{32}P-radiolabeled antisense strand only for siRNA 1. siRNA 2 will also make RISC, but it will contain the nonradioactive sense strand.

When either siRNA 1 or siRNA 2 was used to assemble RISC in embryo lysate, two complexes (B and A, Figure 5B) were detected in the native gel assay; a third complex was detected only with siRNA 1 (Figure 5B). This third complex therefore contains single-stranded siRNA and corresponds to RISC. Complexes B and A are good candidates for RISC assembly intermediates. Formation of all three complexes was dramatically reduced when the antisense siRNA strand contained a 5′ methoxy group (siRNA 3, Figure 5B), a modification which blocks RNAi (Nykänen et al., 2001). When the antisense strand of the siRNA contained a single 5′-deoxy nucleotide,

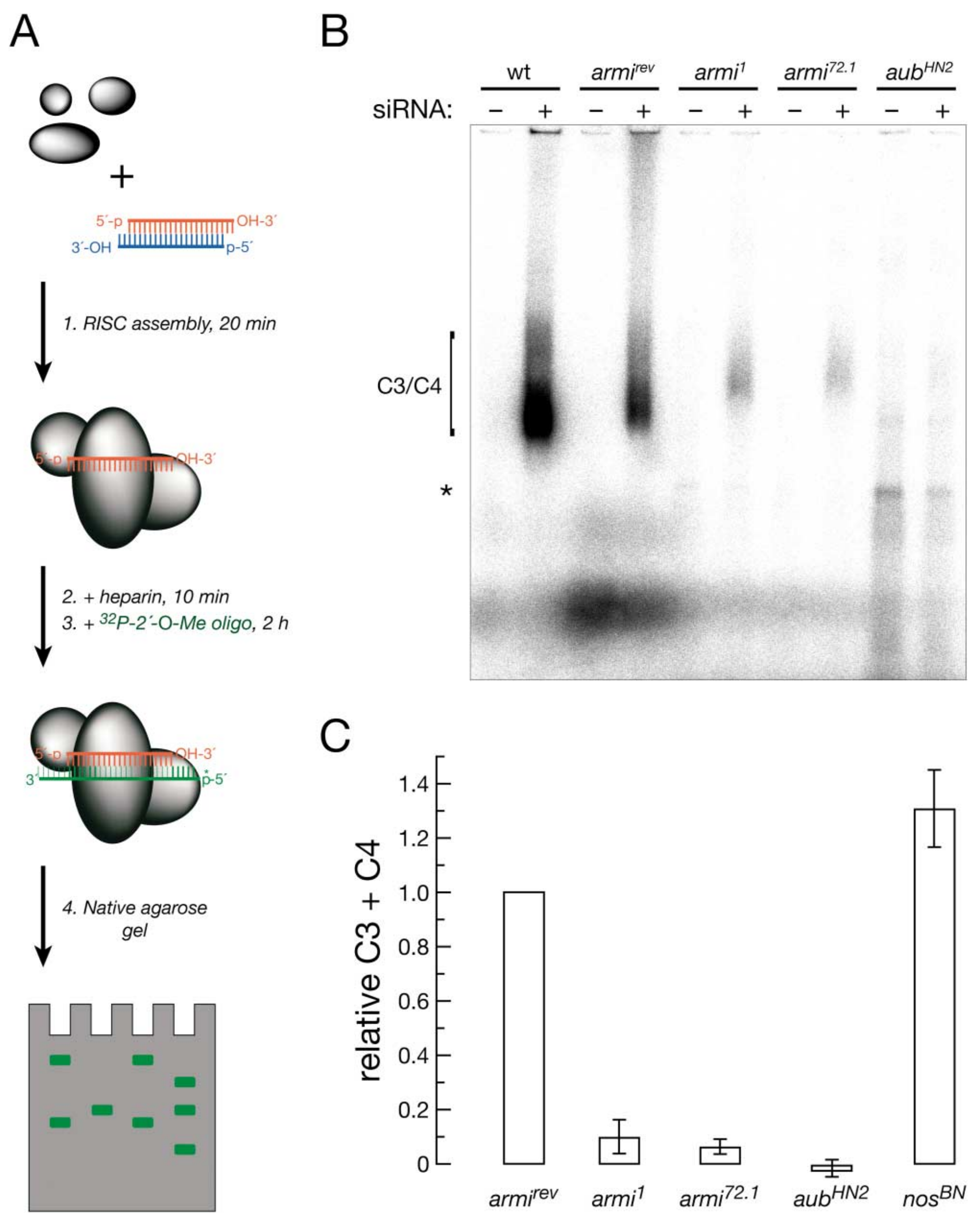

Figure 4. Armi and Aub Are Required for RISC Assembly

(A) RISC assembly assay.

(B) A representative RISC assembly assay using wild-type and mutant *Drosophila* ovary lysates. A complex formed irrespective of siRNA addition is marked with an asterisk.

(C) Amount of RISC complexes C3/C4 formed in wild-type and mutant ovary lysates. The data are the average of four independent trials; error bars indicate standard deviation. For each trial, the data were normalized to the amount of complex observed in *armi^rev* lysate, and the background observed in the absence of siRNA was subtracted from the amount of complex formed when siRNA was included in the corresponding reaction. 5′-phosphorylated, 2′ dT siRNA was used to maximize RISC assembly. All reactions contained equal amounts of total protein.

making it a poor substrate for phosphorylation in the lysate (Nykänen et al., 2001), assembly of all three complexes was reduced (siRNA 4, Figure 5B). Phosphorylating the 5′ deoxy-substituted siRNA before the reaction restored complex assembly (siRNA 5, Figure 5B). Formation of complex A and of RISC required ATP. In contrast, complex B assembled efficiently in the absence of ATP, but only if the siRNA was phosphorylated prior to the reaction (compare −ATP, siRNA 4 versus siRNA 5, Figure 5B).

Complexes B, A, and RISC also formed in ovary lysate (Figure 5C). As for embryo lysate, complexes B and A contained double-stranded siRNA, whereas RISC contained single-stranded (compare siRNA 1 and 2, Figure 5C). No complexes formed in ovary lysate when siRNA 5′ phosphorylation was blocked (siRNA 3, Figure 5C) and complex assembly was reduced when siRNA phosphorylation was slow (siRNA 4, Figure 5C).

To determine the relationship of complexes B, A, and RISC, we monitored the kinetics of complex formation

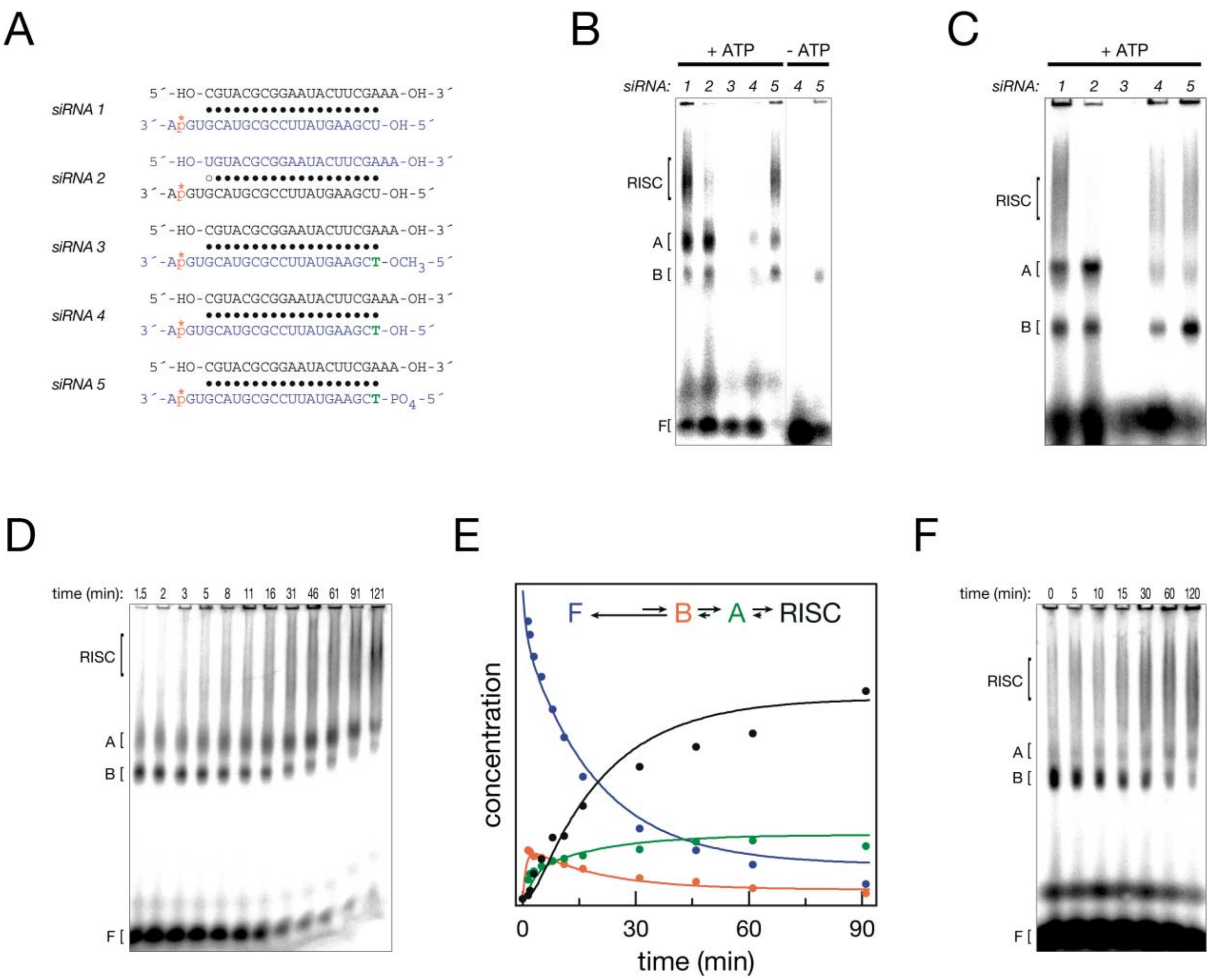

Figure 5. Identification of Intermediates in RISC Assembly

(A) siRNA duplexes used for native gel analysis. The strand that enters the RISC is indicated in blue, deoxynucleotides are in green, and the ^{32}P-radiolabeled phosphates are red, marked with an asterisk.

(B) Native gel analysis of the protein-siRNA complexes formed in embryo lysate using the 3′ ^{32}P-radiolabeled siRNAs in (A). F, free siRNA.

(C) Native gel analysis of the protein-siRNA complexes formed in wild-type ovary lysate using the 3′ ^{32}P-radiolabeled siRNAs in (A). Free siRNA is not shown on this gel.

(D) Timecourse of the assembly of 5′ ^{32}P-radiolabeled siRNA into protein complexes.

(E) Kinetic modeling of the data in (D). Blue circles, free siRNA; red, complex B; green, complex A; black, RISC. Solid lines show the corresponding modeled timecourses. The length of the arrows indicates the relative forward and reverse rate constants that best describe the data.

(F) Complex B can be "chased" into RISC. 5′ ^{32}P-radiolabeled siRNA was preincubated with embryo lysate for 5 min to assemble complex B, then a 20-fold excess of unlabeled siRNA was added (time = 0) and the disappearance of complex B and the production of complexes A and RISC monitored by native gel electrophoresis.

(Figure 5D) and analyzed the data by kinetic modeling (Figure 5E). Of all possible models relating free siRNA, B, A, and RISC, only the simple linear pathway siRNA → B → A → RISC fit well to our data (see Experimental Procedures). The modeled rate constants for the pathway are consistent with the observation that formation of complex B is ATP independent, but RISC is ATP dependent.

We also performed a "chase" experiment to confirm our prediction that complex B is a precursor to RISC (via A). Complex B was assembled by incubating ^{32}P-radiolabeled siRNA in embryo lysate for 5 min, then a 20-fold excess of unlabeled siRNA added to prevent further incorporation of ^{32}P-siRNA into complex. Then we continued the incubation and monitored the formation of complexes. Complex B disappeared with time, A increased with time then peaked at ~60 min, and RISC accumulated throughout the experiment (Figure 5F). The amount of radiolabeled free siRNA was essentially unchanged throughout the experiment, demonstrating that the unlabeled siRNA effectively blocked incorporation of ^{32}P-free siRNA into complex. Thus, B was chased into RISC, likely via A. Together, our kinetic modeling and chase experiment provide support for a RISC assembly pathway in which the siRNA passes through two successive, double-stranded siRNA-containing complexes, B and A, in order to be transformed into the single-stranded siRNA-containing RISC.

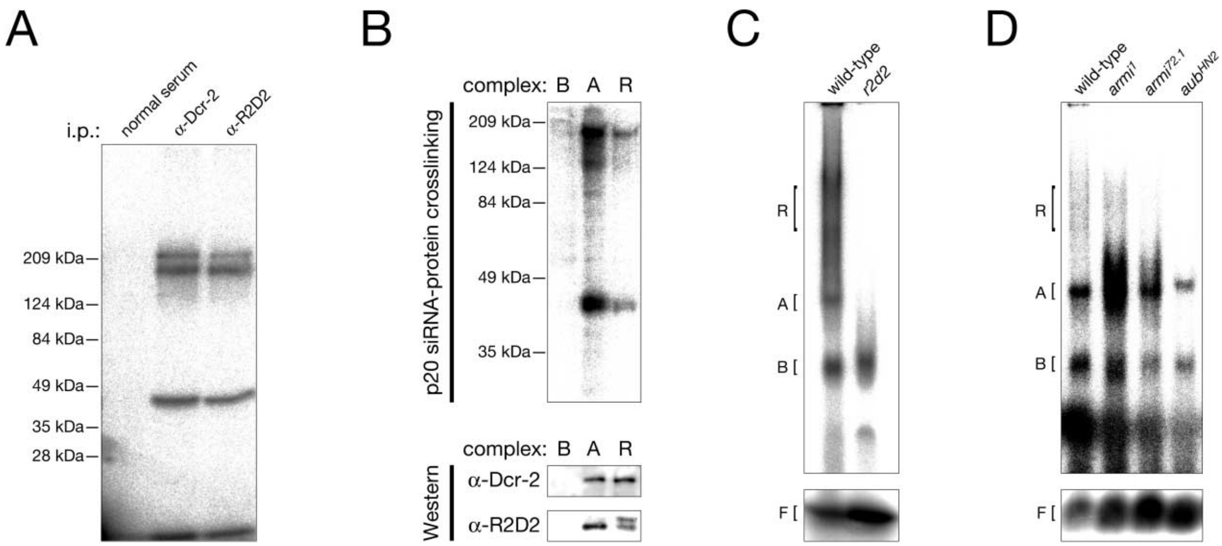

Figure 6. A Dcr-2/R2D2-Containing Complex Is Formed in *armi* and *aub*, but Not *r2d2* Mutant Ovary Lysate

(A) Dcr-2 and R2D2 are efficiently crosslinked by 302 nm light to an siRNA containing 5-iodouracil at position 20. The siRNA was incubated with embryo lysate, crosslinked with UV light, immunoprecipitated with the antiserum indicated above each lane, then analyzed by 4%–20% gradient SDS-PAGE.

(B) Upper panel: the 5-iodouracil siRNA was incubated with embryo lysate crosslinked, then resolved on a native gel. Complexes B, A, and R (RISC) were excised from the gel and the protein-siRNA crosslinks present in complexes B, A, and R (RISC) analyzed by 10% SDS-PAGE. Lower panel: complexes B, A, and R (RISC) were isolated from a native gel, then analyzed by Western blotting with α-Dcr-2 or α-R2D2 antisera.

(C) Native gel analysis of the complexes formed in *r2d2* and (D) *armi*^{1}, *armi*$^{72.1}$, and *aub*^{HN2} homozygous mutant ovary lysates. Minor variations in the abundance of B and A did not correlate with *armi* allele strength, suggesting that neither Armi nor Aub are required for their production. In (C) and (D), the portion of the gel corresponding to free siRNA, F, is shown below. Equal amounts of total protein were used in each reaction. The siRNA was 5′ ^{32}P-radiolabeled in (A)–(C) and 3′ ^{32}P-radiolabeled in (D). Less RISC was detected for wild-type lysate in this experiment compared to (C) because the lysate was diluted 3-fold to equalize its protein concentration to that of the *aub* mutant lysate.

Complex A Contains the R2D2/Dicer-2 Heterodimer

Liu and colleagues have previously proposed that a heterodimeric complex, comprising Dicer-2 (Dcr-2) and the dsRNA binding protein R2D2, loads siRNA into RISC (Liu et al., 2003). Complex A contains the Dcr-2/R2D2 heterodimer. R2D2 and Dcr-2 are readily crosslinked to ^{32}P-radiolabeled siRNA with UV light (Liu et al., 2003). We synthesized an siRNA containing a single photocrosslinkable nucleoside base (5-iodouracil) at position 20 (Supplemental Figure S2A online). The ^{32}P-5-iodouracil siRNA was incubated with embryo lysate to assemble complexes, then irradiated with 302 nm light, which initiates protein-RNA crosslinking only at the 5-iodo-substituted nucleoside. Proteins covalently linked to the ^{32}P-radiolabeled siRNA were resolved by SDS-PAGE. Two proteins—~200 kDa and ~40 kDa—efficiently crosslinked to the siRNA (Supplemental Figure S2D online). Both crosslinked proteins were coimmunoprecipitated with either α-Dcr-2 or α-R2D2 serum, but not normal rabbit serum (Figure 6A). Neither crosslink was observed in ovary lysates prepared from *r2d2* homozygous mutant females (data not shown), a result expected because Dcr-2 is unstable in the absence of R2D2 (Liu et al., 2003). Additional experiments validating the UV crosslinking assay are provided in Supplemental Methods, Supplemental Figure S2, and Supplemental Table S1.

The crosslinking was repeated, and the reaction analyzed by native gel electrophoresis to resolve complexes B, A, and RISC. Each complex was eluted from the gel and analyzed by SDS-PAGE. Figure 6B shows that the R2D2 and Dcr-2 crosslinks were present in complexes A and RISC, but not B. In a parallel experiment, complexes B, A, and RISC were isolated (without crosslinking) and analyzed by Western blotting with either α-Dcr-2 or α-R2D2 antibodies. Again, complexes A and RISC, but not B, contained both Dcr-2 and R2D2 (Figure 6B). Finally, we tested complex assembly in ovary lysates prepared from *r2d2* homozygous mutant females. Only complex B formed in these lysates (Figure 6C). We conclude that complex A contains the previously identified Dcr-2/R2D2 heterodimer (Liu et al., 2003), and that both Dcr-2 and R2D2 remain associated with at least a subpopulation of RISC, consistent with earlier reports that Dcr-2 in flies and both DCR-1 and the nematode homolog of R2D2, RDE-4, coimmunoprecipitate with Argonaute proteins (Hammond et al., 2001; Tabara et al., 2002).

***armi* Mutants Are Defective for the Conversion of Complex A to RISC**

RISC does not form in ovary lysates from *armi* or *aub* mutants (Figures 4B and 4C). However, both complexes B and A were readily detected in *armi* and *aub* mutants (Figure 6D). Thus, *armi* and *aub* mutants are impaired in a step in RISC assembly after binding of the siRNA to the Dcr-2/R2D2 heterodimer.

Armi might act after the formation of complex A to unwind siRNA duplexes prior to their assembly into RISC. To test this hypothesis, we tested if single-stranded siRNA circumvented the requirement for *armi*. In vitro and in vivo, single-stranded siRNA triggers RNAi, albeit inefficiently (Martinez et al., 2002; Schwarz et al., 2002). *armi* ovary lysates failed to support RNAi when the reactions were programmed with 5′-phosphorylated, single-stranded siRNA (Supplemental Figure S3A online). The defect with single-stranded siRNA correlated with allele strength: some activity was seen in lysates from the weak allele, $armi^{1}$, but none for the strong allele, $armi^{72.1}$. The requirement for a putative ATPase—Armi—in RNAi triggered by single-stranded siRNA suggested to us the presence of an additional ATP-dependent step in the RISC assembly, after siRNA unwinding.

To test if loading of single-stranded siRNA into RISC requires ATP, we added 5′-phosphorylated, single-stranded siRNA to embryo lysates depleted of ATP. After incubation for 2 hr, no cleavage product was detected, suggesting that there is at least one ATP-dependent step downstream of siRNA unwinding (Supplemental Figure S3B). The stability of single-stranded siRNA was not reduced by ATP depletion. In fact, single-stranded siRNA was slightly more stable in the absence of ATP (Supplemental Figure S3C online). Thus differential stability cannot account for the requirement for ATP in RNAi triggered by single-stranded siRNA. In the RNAi pathway, there are at least three steps after siRNA unwinding: RISC assembly, target recognition, and target cleavage. To assess if either target recognition or cleavage was ATP dependent, we incubated single-stranded siRNA in a standard RNAi reaction with ATP to assemble RISC. Next, NEM was added to inactivate the ATP-regenerating enzyme, creatine kinase, and to block further RISC assembly. NEM was quenched with dithiothreitol (DTT), and hexokinase and glucose added to deplete ATP. Finally, mRNA target was added and the reaction incubated for 2 hr. Using this protocol, high ATP levels were maintained during RISC assembly, but less than 100 nM ATP was present during the encounter of RISC with the target RNA. Target recognition and cleavage did not require ATP when RISC was programmed with either double- or single-stranded siRNA, provided that ATP was supplied during RISC assembly (Supplemental Figure S3D).

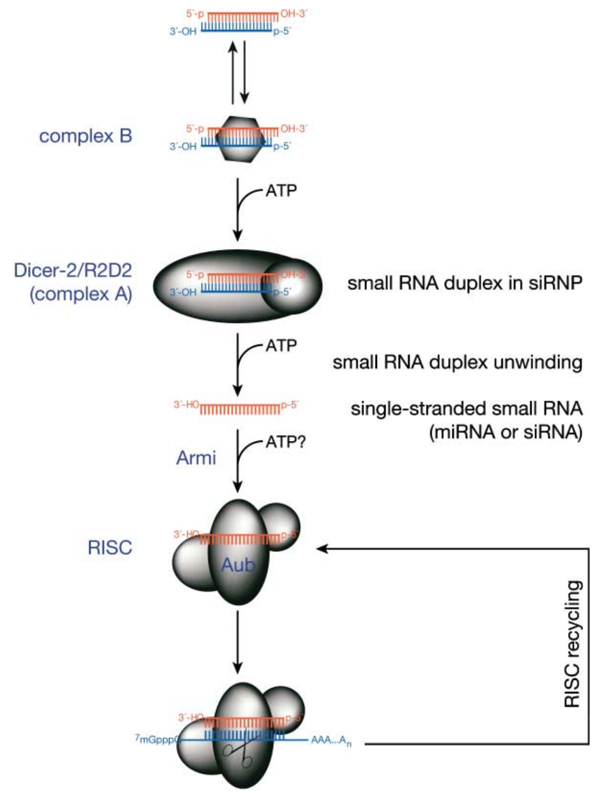

Figure 7. A Model for RNA Silencing in *Drosophila*

Armi is envisioned to facilitate the ATP-dependent incorporation of siRNA into RISC, whereas Aub is drawn as a RISC component.

Discussion

In *Drosophila*, mutations affecting the RNAi pathway are often lethal or female sterile, making the molecular characterization of these mutants difficult. Our finding that lysates that support RNAi in vitro can be prepared from manually dissected ovaries has allowed us to analyze the molecular function of *armi*, a maternal effect gene required for RNAi. Our methods should find broad application in the molecular characterization of other maternal genes required for the RNAi pathway.

We detected four distinct RISC-like complexes common to embryo and ovary lysates (C1-4 in Supplemental Figure S1 and Figure 4). In ovaries, formation of these complexes is reduced >10-fold in *armi* mutants and is undetectable in *aub* mutants, which were shown previously to be RNAi defective (Kennerdell et al., 2002). The requirement for Aub, an Argonaute protein, suggests that the complexes correspond to distinct RISC isoforms built on a common core of Aub and siRNA. These isoforms may play distinct regulatory roles (e.g., translational repression versus cleavage). Alternatively, the smallest, most abundant complexes may contain only the most stably associated protein constituents, whereas the larger, less abundant complexes may correspond to "holo-RISC" that retain more weakly bound proteins. Clearly, a major challenge for the future is to define the protein constituents of each complex, their functional capacity, and their biological role. The development of a native gel assay that resolves distinct RISC complexes represents a step toward that goal.

We have also identified two intermediates in RISC assembly. Complex B forms rapidly upon incubation of siRNA in lysate, in the absence of ATP. The siRNA is then transferred to complex A, which contains the previously identified R2D2/Dcr-2 heterodimer. The siRNA is double stranded in both B and A. RISC is formed from complex A by a process that requires both siRNA unwinding and ATP. Both *aub* and *armi* are required genetically for the production of RISC from complex A. The involvement of Armi, a putative RNA helicase protein, in the production of RISC from complex A and our finding that incorporation of single-stranded siRNA into RISC requires ATP suggest that Armi functions to incorporate single-stranded siRNA into RISC (Figure 7). However, our data cannot distinguish between direct and indirect roles for Armi in RISC assembly.

The *Arabidopsis* homolog of Armi, SDE3, together with the RNA-dependent RNA polymerase (RdRP) SDE1/SGS2, is required for PTGS triggered by transgenes that express single-stranded sense mRNA, but not silencing triggered by some RNA viruses (Dalmay et al., 2001). SDE3 has been proposed to facilitate the conversion of dsRNA into siRNA or the conversion of mRNA into complementary RNA by SDE1/SGS2 (Dalmay et al., 2001; Jorgensen, 2003). Recent studies show that SDE3 is not required for the production of siRNAs derived directly from a long dsRNA hairpin (Himber et al., 2003). Instead, SDE3 seems to play a role in the production of siRNAs generated by an RdRP-dependent amplification mechanism. Our data are not consistent with either of these functions for Armi. First, *Drosophila* genomic, biochemical, and genetic data exclude a role for an RdRP in RNAi (Celotto and Graveley, 2002; Schwarz et al., 2002; Roignant et al., 2003; Tang et al., 2003). Second, Armi is required for RISC assembly in *Drosophila* ovary lysates when RISC is programmed with siRNA, suggesting a role for Armi downstream of the conversion of dsRNA into siRNA, but upstream of target recognition by RISC. The apparently divergent functions of SDE3 and Armi could be reconciled if RISC is required for RdRP-mediated amplification of silencing. Alternatively, SDE3 and Armi may not have homologous functions.

armi mRNA is abundant in oocytes and syncitial blastoderm embryos, but a low level can be detected throughout development, including in somatic tissues (Cook et al., 2004). While the requirement for *armi* in spermatogenesis and oogenesis makes Armi a good candidate for a component of the RNAi machinery in germ cells and early embryos, somatic functions for Armi are also possible. In this respect, *armi* is reminiscent of the maternally expressed Argonaute protein, *piwi*, which is also required during oogenesis. Although *piwi* mutants display no obvious somatic phenotype (Cox et al., 1998), Piwi is required in the soma both for posttranscriptional transgene silencing and for some types of transcriptional silencing (Pal-Bhadra et al., 2002). Whether Armi is likewise required for somatic transgene silencing remains to be tested.

Experimental Procedures

General Methods
Target RNA cleavage assay was performed as described (Haley et al., 2003). ATP depletion and NEM quenching were as published (Nykänen et al., 2001).

Stellate Immunofluorescence
Testes were dissected in testes fixation buffer (1 mM EDTA, 183 mM KCl, 47 mM NaCl, 10 mM Tris, pH 6.8) and fixed with formaldehyde as described (Theurkauf, 1994). Ste protein was labeled with anti-Ste IgG at 1:100. Images were analyzed by confocal microscopy using a Leica TCS-SP inverted laser scanning microscope. DNA was stained with TOTO-3 (Molecular Probes).

Ovary Lysate Preparation
Wild-type or mutant fly ovaries were dissected with forceps (World Precision Instruments 500232) and collected in 1 × PBS buffer in 0.5 ml microcentrifuge tubes. Ovaries were centrifuged at 11,000 × g for 5 min at 4°C. The PBS was removed from the ovary pellet, then ovaries were homogenized in 1 ml ice-cold lysis buffer (100 mM potassium acetate, 30 mM HEPES-KOH at pH 7.4, 2 mM magnesium acetate) containing 5 mM DTT and 1 mg/ml complete "mini" EDTA-free protease inhibitor tablets (Roche) per gram of ovaries using a plastic "pellet pestle" (Kontes). Lysate was clarified by centrifugation at 14,000 × g for 25 min at 4°C. The supernatant was aliquoted into chilled microcentrifuge tubes, flash frozen in liquid nitrogen, and stored at −80°C. RNAi reactions were assembled using equal amounts of total protein for all genotypes within an experiment.

Synthetic siRNA
The siRNAs were prepared from synthetic 21 nt RNAs (Dharmacon Research). Sense siRNA sequences used were 5′-HO-CGU ACG CGG AAU ACU UCG AAA-3′ (5′ OH [riboU], 5′ CH_3O [2′ dT], 5′ OH [2′ dT]) and 5′-HO-UGA GGU AGU AGG UUG UAU AGU-3′ (un). Antisense siRNA sequences used were 5′-HO-UCG AAG UAU UCC GCG UAC GUG-3′ (5′ OH [riboU]); 5′-CH_3O-dTCG AAG UAU UCC GCG UAC GUG-3′ (5′ CH_3O [2′ dT]); 5′-HO-dTCG AAG UAU UCC GCG UAC GUG-3′ (5′ OH [2′ dT]); and 5′-HO-UAU ACA ACC UAC UAC CUC AUU-3′ (un). Appropriate pairs of siRNA strands were annealed to form siRNA duplexes as described (Elbashir et al., 2001b) and used at a final concentration of ≤20 nM (Figures 2, 5H, and 5I) or ≤50 nM (Figure 3). siRNA single strands were phosphorylated with polynucleotide kinase according to the manufacturer's protocol (PNK; New England Biolabs) and used at 200 nM (final concentration).

RISC Assembly
RISC assembly was as described (Zamore et al., 2000), except that the reaction contained 40% (v/v) embryo or ovary lysate and 50 nM siRNA duplex. Lysates were adjusted with lysis buffer to contain equal amounts of protein. Following incubation at 25°C for 20 min, 1 mg/ml heparin was added and incubated for 10 min. Heparin served to reduce nonspecific binding of proteins to the 2′-*O*-methyl oligonucleotide and to quench RISC assembly. (Mature RISC is refractory to heparin: 1 mg/ml [final concentration] heparin added at the start of the reaction blocked RNAi in the cleavage assay, but had no effect when added together with target RNA.) Then the 5′ ^{32}P-radiolabled 2′-*O*-methyl oligonucleotide (5′-CAU CAC GUA CGC GGA AUA CUU CGA AAU GUC C-3′) was added at 2 nM final concentration and incubated for 2 hr. After the addition of 3.0% (w/v) Ficoll-400, complexes were resolved by native gel electrophoresis at 4 W for 2 hr at room temperature. Native gels were 1 mm thick, 1.5% (w/v) agarose (GTG grade), 0.5 × TBE with 1.5 mM $MgCl_2$, cast vertically between a standard glass plate and a ground glass plate (National Glass Works, Worcester, Massachusetts). To detect intermediates in RISC assembly, ^{32}P-radiolabeled siRNA was incubated with lysate for 1 hr, unless otherwise noted. No heparin was added to these reactions. After incubation, the samples were adjusted to 3.0% (w/v) Ficoll-400 and resolved by vertical native gel electrophoresis as above. Gels were dried under vacuum onto Hybond-N+ nylon membrane (Amersham).

Kinetic Modeling
Data from native gel analysis of siRNA-containing complexes were initially fit using Berkeley Madonna 8.0.1 software to the global model:

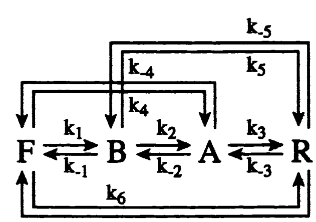

Rates for k_4, k_{-4}, k_5, k_{-5}, k_6, and k_{-6} ranged from 5-fold (k_5) to 10^8-fold (k_{-4}) slower than the slowest forward rate for the linear pathway F → B → A → RISC. The data were therefore modeled neglecting rates k_4, k_{-4}, k_5, k_{-5}, k_6, and k_{-6} to generate Figure 5E.

Crosslinking
5′ ^{32}P-radiolabeled siRNA duplex was used at 4 million counts per minute in a standard RNAi reaction, incubated 45–60 min at 25°C, then transferred to a 96-well round bottom plate on ice. Samples were irradiated for 10–15 min with 302 nm light using an Ultraviolet Products model TM-36 transilluminator inverted directly onto the polystyrene lid of the 96-well plate. Samples were then adjusted to 1 × SDS-SB (62.5 mM Tris-HCl, pH 6.8, 10% glycerol, 2% SDS,

0.02% (w/v) Bromophenol Blue, 100 mM DTT), heated to 95°C for 5 min, and resolved by SDS-polyacrylamide gel electrophoresis.

Immunoprecipitation and Western Blotting

Normal rabbit, α-Dcr-2, and α-R2D2 antisera were first bound to protein A agarose beads for 2 hr at 4°C in lysis buffer. After washing with RIPA buffer (150 mM NaCl, 1% [v/v] NP40, 0.5% [w/v] sodium deoxycholate, 0.1% SDS, 25 mM Tris-HCl, pH 7.6), the beads (25 μl) were incubated with 15 μl of crosslinked lysate for 2 hr at 4°C. After washing in RIPA buffer, the beads were boiled in 1 × SDS-SB and the eluted proteins resolved by SDS-PAGE. For Western blotting, the complexes were excised from the native gel, boiled in 1 × SDS-SB at 95°C for 10 min, and resolved by SDS-PAGE. Western blotting was performed with 1:1000 dilution for α-Dcr-2 antisera and 1:5000 for α-R2D2.

Acknowledgments

We thank John Leszyk for mass spectrometry; Juanita McLachlan for maintaining our fly colony; and members of the Zamore lab for encouragement and helpful discussions. α-Dcr-2 and α-R2D2 antibodies were the kind gifts of Qinghua Liu and Xiaodong Wang; α-Ste antibody was the kind gift of Maria Pia Bozzetti; normal rabbit serum was the kind gift of Alonzo Ross. r2d2 mutant flies were kindly provided by Dean P. Smith. H.A.C. was supported by a postdoctoral training from the NIH and a Research Scholar Grant from the American Cancer Society. P.D.Z. is a Pew Scholar in the Biomedical Sciences and a W.M. Keck Foundation Young Scholar in Medical Research. This work was supported in part by grants from the National Institutes of Health to P.D.Z. (GM62862-01 and GM65236-01) and a grant from the Human Frontiers Science Program to W.E.T. (RG0356/1997-M).

Received: October 3, 2003
Revised: December 31, 2003
Accepted: February 9, 2004
Published: March 18, 2004

References

Aravin, A.A., Naumova, N.M., Tulin, A.V., Vagin, V.V., Rozovsky, Y.M., and Gvozdev, V.A. (2001). Double-stranded RNA-mediated silencing of genomic tandem repeats and transposable elements in the *D. melanogaster* germline. Curr. Biol. *11*, 1017–1027.

Aza-Blanc, P., Cooper, C.L., Wagner, K., Batalov, S., Deveraux, Q.L., and Cooke, M.P. (2003). Identification of modulators of TRAIL-induced apoptosis via RNAi-based phenotypic screening. Mol. Cell *12*, 627–637.

Belloni, M., Tritto, P., Bozzetti, M.P., Palumbo, G., and Robbins, L.G. (2002). Does Stellate cause meiotic drive in Drosophila melanogaster? Genetics *161*, 1551–1559.

Bernstein, E., Caudy, A.A., Hammond, S.M., and Hannon, G.J. (2001). Role for a bidentate ribonuclease in the initiation step of RNA interference. Nature *409*, 363–366.

Billy, E., Brondani, V., Zhang, H., Muller, U., and Filipowicz, W. (2001). Specific interference with gene expression induced by long, double-stranded RNA in mouse embryonal teratocarcinoma cell lines. Proc. Natl. Acad. Sci. USA *98*, 14428–14433.

Boutla, A., Delidakis, C., Livadaras, I., Tsagris, M., and Tabler, M. (2001). Short 5′-phosphorylated double-stranded RNAs induce RNA interference in Drosophila. Curr. Biol. *11*, 1776–1780.

Caplen, N.J., Parrish, S., Imani, F., Fire, A., and Morgan, R.A. (2001). Specific inhibition of gene expression by small double-stranded RNAs in invertebrate and vertebrate systems. Proc. Natl. Acad. Sci. USA *98*, 9742–9747.

Catalanotto, C., Azzalin, G., Macino, G., and Cogoni, C. (2002). Involvement of small RNAs and role of the qde genes in the gene silencing pathway in Neurospora. Genes Dev. *16*, 790–795.

Caudy, A.A., Myers, M., Hannon, G.J., and Hammond, S.M. (2002). Fragile X-related protein and VIG associate with the RNA interference machinery. Genes Dev. *16*, 2491–2496.

Celotto, A.M., and Graveley, B.R. (2002). Exon-specific RNAi: A tool for dissecting the functional relevance of alternative splicing. RNA *8*, 8–24.

Chiu, Y.-L., and Rana, T.M. (2002). RNAi in human cells: Basic structural and functional features of small interfering RNA. Mol. Cell *10*, 549–561.

Cogoni, C., and Macino, G. (1997). Isolation of quelling-defective (qde) mutants impaired in posttranscriptional transgene-induced gene silencing in Neurospora crassa. Proc. Natl. Acad. Sci. USA *94*, 10233–10238.

Cox, D.N., Chao, A., Baker, J., Chang, L., Qiao, D., and Lin, H. (1998). A novel class of evolutionarily conserved genes defined by piwi are essential for stem cell self-renewal. Genes Dev. *12*, 3715–3727.

Dalmay, T., Hamilton, A., Rudd, S., Angell, S., and Baulcombe, D.C. (2000). An RNA-dependent RNA polymerase gene in Arabidopsis is required for posttranscriptional gene silencing mediated by a transgene but not by a virus. Cell *101*, 543–553.

Dalmay, T., Horsefield, R., Braunstein, T.H., and Baulcombe, D.C. (2001). SDE3 encodes an RNA helicase required for post-transcriptional gene silencing in Arabidopsis. EMBO J. *20*, 2069–2078.

Doi, N., Zenno, S., Ueda, R., Ohki-Hamazaki, H., Ui-Tei, K., and Saigo, K. (2003). Short-interfering-RNA-mediated gene silencing in mammalian cells requires Dicer and eIF2C translation initiation factors. Curr. Biol. *13*, 41–46.

Elbashir, S.M., Harborth, J., Lendeckel, W., Yalcin, A., Weber, K., and Tuschl, T. (2001a). Duplexes of 21-nucleotide RNAs mediate RNA interference in cultured mammalian cells. Nature *411*, 494–498.

Elbashir, S.M., Lendeckel, W., and Tuschl, T. (2001b). RNA interference is mediated by 21- and 22-nucleotide RNAs. Genes Dev. *15*, 188–200.

Elbashir, S.M., Martinez, J., Patkaniowska, A., Lendeckel, W., and Tuschl, T. (2001c). Functional anatomy of siRNAs for mediating efficient RNAi in Drosophila melanogaster embryo lysate. EMBO J. *20*, 6877–6888.

Fagard, M., Boutet, S., Morel, J.-B., Bellini, C., and Vaucheret, H. (2000). AGO1, QDE-2, and RDE-1 are related proteins required for post-transcriptional gene silencing in plants, quelling in fungi, and RNA interference in animals. Proc. Natl. Acad. Sci. USA *97*, 11650–11654.

Fire, A., Xu, S., Montgomery, M.K., Kostas, S.A., Driver, S.E., and Mello, C.C. (1998). Potent and specific genetic interference by double-stranded RNA in Caenorhabditis elegans. Nature *391*, 806–811.

Grishok, A., Tabara, H., and Mello, C. (2000). Genetic requirements for inheritance of RNAi in *C. elegans*. Science *287*, 2494–2497.

Gvozdev, V.A., Aravin, A.A., Abramov, Y.A., Klenov, M.S., Kogan, G.L., Lavrov, S.A., Naumova, N.M., Olenkina, O.M., Tulin, A.V., and Vagin, V.V. (2003). Stellate repeats: targets of silencing and modules causing cis-inactivation and trans-activation. Genetica *117*, 239–245.

Haley, B., Tang, G., and Zamore, P.D. (2003). In vitro analysis of RNA interference in Drosophila melanogaster. Methods *30*, 330–336.

Hamilton, A.J., and Baulcombe, D.C. (1999). A species of small antisense RNA in posttranscriptional gene silencing in plants. Science *286*, 950–952.

Hammond, S.M., Bernstein, E., Beach, D., and Hannon, G.J. (2000). An RNA-directed nuclease mediates post-transcriptional gene silencing in Drosophila cells. Nature *404*, 293–296.

Hammond, S.M., Boettcher, S., Caudy, A.A., Kobayashi, R., and Hannon, G.J. (2001). Argonaute2, a link between genetic and biochemical analyses of RNAi. Science *293*, 1146–1150.

Himber, C., Dunoyer, P., Moissiard, G., Ritzenthaler, C., and Voinnet, O. (2003). Transitivity-dependent and -independent cell-to-cell movement of RNA silencing. EMBO J. *22*, 4523–4533.

Hutvágner, G., and Zamore, P.D. (2002). A microRNA in a multiple-turnover RNAi enzyme complex. Science *297*, 2056–2060.

Hutvágner, G., Simard, M.J., Mello, C.C., and Zamore, P.D. (2004). Sequence-specific inhibition of small RNA function. PLoS Biol. *2*, e98. DOI:10.1371/journal.pbio.0020098.

Ishizuka, A., Siomi, M.C., and Siomi, H. (2002). A Drosophila fragile

X protein interacts with components of RNAi and ribosomal proteins. Genes Dev. *16*, 2497–2508.

Jorgensen, R.A. (2003). Sense cosuppression in plants: Past, present, and future. In RNAi: A Guide To Gene Silencing, G.J. Hannon, ed. (Cold Spring Harbor, NY: Cold Spring Harbor Laboratory Press), pp. 5–22.

Kennerdell, J.R., and Carthew, R.W. (1998). Use of dsRNA-mediated genetic interference to demonstrate that *frizzled* and *frizzled 2* act in the wingless pathway. Cell *95*, 1017–1026.

Kennerdell, J.R., Yamaguchi, S., and Carthew, R.W. (2002). RNAi is activated during Drosophila oocyte maturation in a manner dependent on aubergine and spindle-E. Genes Dev. *16*, 1884–1889.

Ketting, R.F., Haverkamp, T.H., van Luenen, H.G., and Plasterk, R.H. (1999). Mut-7 of C. elegans, required for transposon silencing and RNA interference, is a homolog of Werner syndrome helicase and RNaseD. Cell *99*, 133–141.

Khvorova, A., Reynolds, A., and Jayasena, S.D. (2003). Functional siRNAs and miRNAs exhibit strand bias. Cell *115*, 209–216.

Koonin, E.V. (1992). A new group of putative RNA helicases. Trends Biochem. Sci. *17*, 495–497.

Liu, Q., Rand, T.A., Kalidas, S., Du, F., Kim, H.E., Smith, D.P., and Wang, X. (2003). R2D2, a bridge between the initiation and effector steps of the Drosophila RNAi pathway. Science *301*, 1921–1925.

Lohmann, J.U., Endl, I., and Bosch, T.C. (1999). Silencing of developmental genes in hydra. Dev. Biol. *214*, 211–214.

Martinez, J., Patkaniowska, A., Urlaub, H., Lührmann, R., and Tuschl, T. (2002). Single stranded antisense siRNA guide target RNA cleavage in RNAi. Cell *110*, 563–574.

Morel, J.B., Godon, C., Mourrain, P., Beclin, C., Boutet, S., Feuerbach, F., Proux, F., and Vaucheret, H. (2002). Fertile hypomorphic ARGONAUTE (ago1) mutants impaired in post-transcriptional gene silencing and virus resistance. Plant Cell *14*, 629–639.

Mourelatos, Z., Dostie, J., Paushkin, S., Sharma, A.K., Charroux, B., Abel, L., Rappsilber, J., Mann, M., and Dreyfuss, G. (2002). miRNPs: a novel class of Ribonucleoproteins containing numerous microRNAs. Genes Dev. *16*, 720–728.

Mourrain, P., Beclin, C., Elmayan, T., Feuerbach, F., Godon, C., Morel, J.B., Jouette, D., Lacombe, A.M., Nikic, S., Picault, N., et al. (2000). Arabidopsis SGS2 and SGS3 genes are required for posttranscriptional gene silencing and natural virus resistance. Cell *101*, 533–542.

Ngo, H., Tschudi, C., Gull, K., and Ullu, E. (1998). Double-stranded RNA induces mRNA degradation in *Trypanosoma brucei*. Proc. Natl. Acad. Sci. USA *95*, 14687–14692.

Nykänen, A., Haley, B., and Zamore, P.D. (2001). ATP requirements and small interfering RNA structure in the RNA interference pathway. Cell *107*, 309–321.

Pal-Bhadra, M., Bhadra, U., and Birchler, J.A. (2002). RNAi related mechanisms affect both transcriptional and posttranscriptional transgene silencing in *Drosophila*. Mol. Cell *9*, 315–327.

Ratcliff, F.G., MacFarlane, S.A., and Baulcombe, D.C. (1999). Gene silencing without DNA. RNA-mediated cross-protection between viruses. Plant Cell *11*, 1207–1216.

Roignant, J.Y., Carre, C., Mugat, B., Szymczak, D., Lepesant, J.A., and Antoniewski, C. (2003). Absence of transitive and systemic pathways allows cell-specific and isoform-specific RNAi in Drosophila. RNA *9*, 299–308.

Sánchez-Alvarado, A., and Newmark, P.A. (1999). Double-stranded RNA specifically disrupts gene expression during planarian regeneration. Proc. Natl. Acad. Sci. USA *96*, 5049–5054.

Saxena, S., Jonsson, Z.O., and Dutta, A. (2003). Small RNAs with imperfect match to endogenous mRNA repress translation: implications for off-target activity of siRNA in mammalian cells. J. Biol. Chem. *278*, 44312–44319. Published online September 2, 2003. 10.1074/jbc.M307089200.

Schmidt, A., Palumbo, G., Bozzetti, M.P., Tritto, P., Pimpinelli, S., and Schafer, U. (1999). Genetic and molecular characterization of sting, a gene involved in crystal formation and meiotic drive in the male germ line of Drosophila melanogaster. Genetics *151*, 749–760.

Schramke, V., and Allshire, R. (2003). Hairpin RNAs and retrotransposon LTRs effect RNAi and chromatin-based gene silencing. Science *301*, 1069–1074.

Schwarz, D.S., Hutvágner, G., Haley, B., and Zamore, P.D. (2002). Evidence that siRNAs function as guides, not primers, in the *Drosophila* and human RNAi pathways. Mol. Cell *10*, 537–548.

Schwarz, D.S., Hutvágner, G., Du, T., Xu, Z., Aronin, N., and Zamore, P.D. (2003). Asymmetry in the assembly of the RNAi enzyme complex. Cell *115*, 199–208.

Sijen, T., and Plasterk, R.H. (2003). Transposon silencing in the Caenorhabditis elegans germ line by natural RNAi. Nature *426*, 310–314.

Stapleton, W., Das, S., and McKee, B.D. (2001). A role of the Drosophila homeless gene in repression of Stellate in male meiosis. Chromosoma *110*, 228–240.

Tabara, H., Sarkissian, M., Kelly, W.G., Fleenor, J., Grishok, A., Timmons, L., Fire, A., and Mello, C.C. (1999). The rde-1 gene, RNA interference, and transposon silencing in *C. elegans*. Cell *99*, 123–132.

Tabara, H., Yigit, E., Siomi, H., and Mello, C.C. (2002). The dsRNA binding protein RDE-4 interacts with RDE-1, DCR-1, and a DexH-box helicase to direct RNAi in *C. elegans*. Cell *109*, 861–871.

Tang, G., Reinhart, B.J., Bartel, D.P., and Zamore, P.D. (2003). A biochemical framework for RNA silencing in plants. Genes Dev. *17*, 49–63.

Theurkauf, W.E. (1994). Immunofluorescence analysis of the cytoskeleton during oogenesis and early embryogenesis. Methods Cell Biol. *44*, 489–505.

Tijsterman, M., Ketting, R.F., Okihara, K.L., Sijen, T., and Plasterk, R.H. (2002). RNA helicase MUT-14-dependent gene silencing triggered in C. elegans by short antisense RNAs. Science *295*, 694–697.

Tuschl, T., Zamore, P.D., Lehmann, R., Bartel, D.P., and Sharp, P.A. (1999). Targeted mRNA degradation by double-stranded RNA in vitro. Genes Dev. *13*, 3191–3197.

Volpe, T.A., Kidner, C., Hall, I.M., Teng, G., Grewal, S.I.S., and Martienssen, R.A. (2002). Regulation of heterchromatic silencing and histone H3 lysine-9 methylation by RNAi. Science *297*, 1833–1837.

Waterhouse, P.M., Graham, M.W., and Wang, M.B. (1998). Virus resistance and gene silencing in plants can be induced by simultaneous expression of sense and antisense RNA. Proc. Natl. Acad. Sci. USA *95*, 13959–13964.

Wianny, F., and Zernicka-Goetz, M. (2000). Specific interference with gene function by double-stranded RNA in early mouse development. Nat. Cell Biol. *2*, 70–75.

Williams, R.W., and Rubin, G.M. (2002). ARGONAUTE1 is required for efficient RNA interference in Drosophila embryos. Proc. Natl. Acad. Sci. USA *99*, 6889–6894.

Wu-Scharf, D., Jeong, B., Zhang, C., and Cerutti, H. (2000). Transgene and transposon silencing in chlamydomonas reinhardtii by a DEAH-Box RNA helicase. Science *290*, 1159–1163.

Zamore, P.D., Tuschl, T., Sharp, P.A., and Bartel, D.P. (2000). RNAi: double-stranded RNA directs the ATP-dependent cleavage of mRNA at 21 to 23 nucleotide intervals. Cell *101*, 25–33.

Normal microRNA Maturation and Germ-Line Stem Cell Maintenance Requires Loquacious, a Double-Stranded RNA-Binding Domain Protein

Klaus Förstemann[1], Yukihide Tomari[1], Tingting Du[1], Vasily V. Vagin[2], Ahmet M. Denli[3], Diana P. Bratu[4], Carla Klattenhoff[4], William E. Theurkauf[4], Phillip D. Zamore[1*]

1 Department of Biochemistry and Molecular Pharmacology, University of Massachusetts Medical School, Worcester, Massachusetts, United States of America, **2** Institute of Molecular Genetics of RAS, Moscow, Russia, **3** Watson School of Biological Sciences, Cold Spring Harbor Laboratory, Cold Spring Harbor, New York, United States of America, **4** Program in Molecular Medicine, University of Massachusetts Medical School, Worcester, Massachusetts, United States of America,

microRNAs (miRNAs) are single-stranded, 21- to 23-nucleotide cellular RNAs that control the expression of cognate target genes. Primary miRNA (pri-miRNA) transcripts are transformed to mature miRNA by the successive actions of two RNase III endonucleases. Drosha converts pri-miRNA transcripts to precursor miRNA (pre-miRNA); Dicer, in turn, converts pre-miRNA to mature miRNA. Here, we show that normal processing of *Drosophila* pre-miRNAs by Dicer-1 requires the double-stranded RNA-binding domain (dsRBD) protein Loquacious (Loqs), a homolog of human TRBP, a protein first identified as binding the HIV *trans*-activator RNA (TAR). Efficient miRNA-directed silencing of a reporter transgene, complete repression of *white* by a dsRNA trigger, and silencing of the endogenous *Stellate* locus by *Suppressor of Stellate,* all require Loqs. In *loqs*^{f00791} mutant ovaries, germ-line stem cells are not appropriately maintained. Loqs associates with Dcr-1, the *Drosophila* RNase III enzyme that processes pre-miRNA into mature miRNA. Thus, every known *Drosophila* RNase-III endonuclease is paired with a dsRBD protein that facilitates its function in small RNA biogenesis.

Citation: Förstemann K, Tomari Y, Du T, Vagin VV, Denli AM, et al. (2005) Normal microRNA Maturation and Germ-Line Stem Cell Maintenance Requires Loquacious, a Double-Stranded RNA-Binding Domain Protein. PLoS Biol 3(7): e236.

Introduction

MicroRNAs (miRNAs) are 21- to 23-nucleotide single-stranded RNAs that are encoded in the chromosomal DNA and repress cognate mRNA targets [1,2]. They are transcribed as long, hairpin-containing precursors [3] by RNA polymerase II [4–8] and processed in the nucleus by the multidomain RNase III endonuclease Drosha [9]. Drosha is assisted by its double-stranded RNA-binding domain (dsRBD) protein partner, known as Pasha in *Drosophila melanogaster* [10] and DGCR8 in humans [11–13]. Exportin-5 (Ranbp21 in *Drosophila*) binds the resulting precursor miRNA (pre-miRNA)—likely recognizing the approximately two-nucleotide 3′ overhanging ends characteristic of these approximately 70-nucleotide hairpin structures—and transports them to the cytoplasm via the Ran-GDP–Ran-GTP transport system [14–16]. In the cytoplasm, a second RNase III endonuclease, Dicer, converts pre-miRNA into mature miRNA [17–20].

In *Drosophila,* two Dicer paralogs define parallel pathways for small RNA biogenesis. Dicer-1 (Dcr-1) liberates miRNA from pre-miRNA, whereas Dicer-2 (Dcr-2) excises small interfering RNA (siRNA) from long double-stranded RNA (dsRNA) [21–23]. Like Drosha, *Drosophila* Dcr-2 requires a dsRBD partner protein, R2D2, for its function in siRNA biogenesis. Unlike Drosha, Dcr-2 suffices to process its substrate. However, without R2D2, Dcr-2 cannot load the siRNAs it produces into the RNA-induced silencing complex (RISC), the RNA interference (RNAi) effector complex [21,24,25]. Although born as small RNA duplexes, both siRNA and miRNA function in RISC as single-stranded RNA guides for members of the Argonaute family of proteins [26–28]. Among the five *Drosophila* Argonaute proteins, two—Ago1 and Ago2—are required for small RNA-directed cleavage of target RNAs [29]. In fact, the Piwi domain of Argonaute proteins is a structural homolog of the endoribonuclease RNase H, an enzyme that cleaves the RNA strand of DNA–RNA hybrids [30–33]. Both human and *Drosophila* Ago2 and *Drosophila* Ago1 provide the Mg^{2+}-dependent catalytic subunit of RISC [29,31,34,35,36].

The *Drosophila* genome encodes three RNase III endonucleases, all of which act in miRNA or siRNA biogenesis. Whereas both Drosha and Dcr-2 associate with dsRBD proteins that facilitate their functions, no dsRBD protein partner has been assigned to Dcr-1. We asked if Dcr-1 might also partner with a dsRBD protein. Here, we identify the dsRBD protein Loquacious (Loqs), a paralog of R2D2, as the

Received March 14, 2005; Accepted April 30, 2005; Published May 24, 2005
DOI: 10.1371/journal.pbio.0030236

Abbreviations: dsRBD, double-stranded RNA binding domain; dsRNA, double-stranded RNA; GFP, green fluorescent protein; IR, inverted repeat; miRNA, microRNA; PA, protein isoform A; PB, protein isoform B; PC, protein isoform C; pre-miRNA, precursor miRNA; pri-miRNA, primary miRNA; RA, RNA splice variant A; RB, RNA splice variant B; RC, RNA splice variant C; RISC, RNA-induced silencing complex; RNAi, RNA interference; S2, Schneider-2; siRNA, small interfering RNA; TAR, trans-activator RNA; YFP, yellow fluorescent protein

Academic Editor: James C. Carrington, Oregon State University, United States of America

*To whom correspondence should be addressed. E-mail: phillip.zamore@umassmed.edu

partner of Dcr-1. Mutation of *loqs* in flies and depletion of *loqs* in Schneider-2 (S2) cells by dsRNA-triggered RNAi disrupt normal pre-miRNA processing. In vivo, *loqs* is required for robust miRNA-directed silencing and complete target gene repression directed by a transgene expressing dsRNA. Moreover, loss of Loqs function in the ovary disrupts germ-line stem cell maintenance, rendering *loqs* mutant females sterile.

Results

To identify a dsRBD protein partner for Dcr-1, we searched the conserved domain database [37] for all *Drosophila* proteins that contain dsRBDs. The protein encoded by the gene CG6866 has two dsRBDs, which are most closely related to dsRBD 1 and 2 of R2D2, suggesting that the two genes are paralogs (Figure 1A). CG6866 and R2D2 are 37% similar and 25% identical in the region of the two dsRBDs. A third dsRBD at the C-terminus of CG6866 was detected using the PFam collection of protein sequence motifs. This truncated domain deviates from the canonical dsRBD sequence. Because loss of CG6866 function de-silences both endogenous silencing and reporter expression in vivo (below), we named the gene

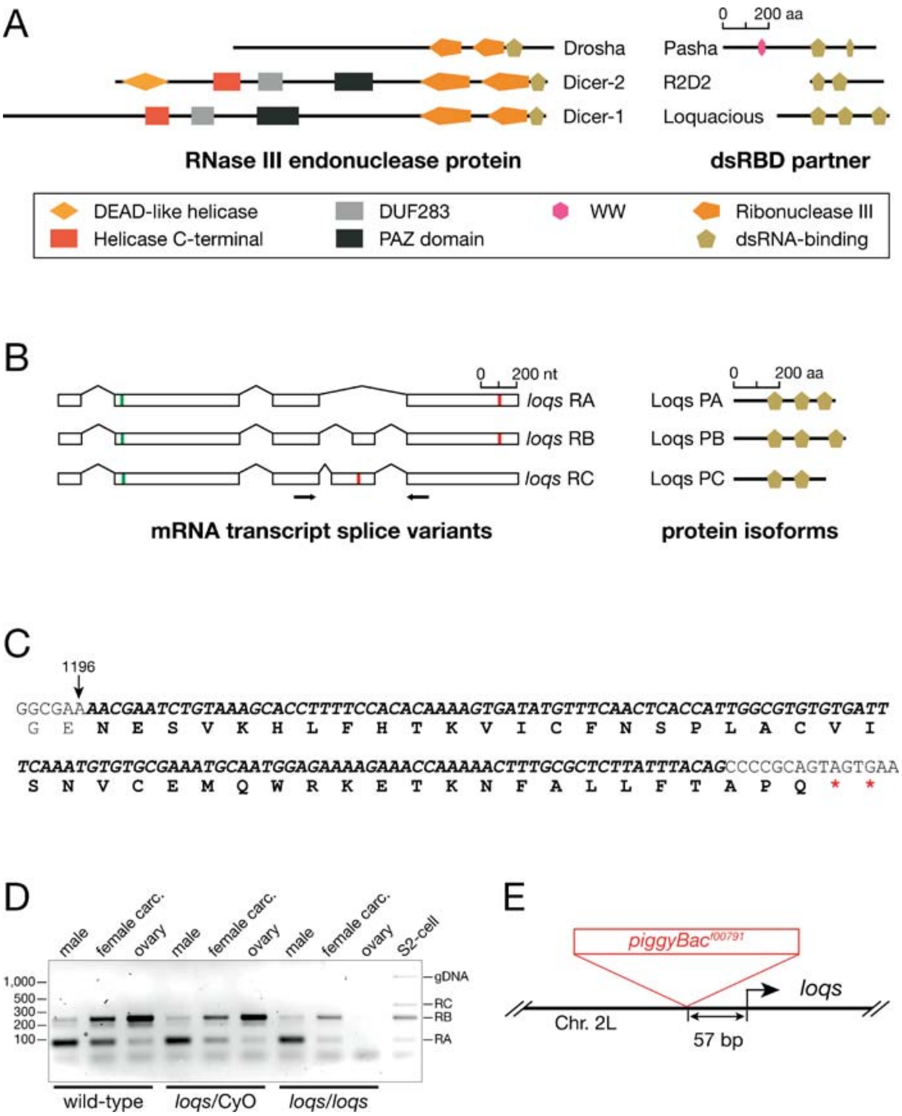

Figure 1. Loqs, a dsRBD Partner Protein for *Drosophila* Dcr-1

(A) Each of the three *D. melanogaster* RNase III endonucleases pairs with a different dsRBD protein, which assists in its function in RNA silencing.

(B) Differential splicing creates three *loqs* mRNA variants, *loqs* RA, RB, and RC. *loqs* RA and RB are reported in FlyBase. The RC splice variant is reported here. Arrows mark the position of the PCR primers used in (D); green lines, start codons; red lines, stop codons. The resulting protein isoforms are diagrammed to the right.

(C) Use of an alternative splice acceptor site extends the 5′ end of exon 4. The mRNA sequence surrounding the new exon–exon junction is shown, with the *loqs* RC-specific sequence in bold; the arrow marks the position of the last nucleotide of exon 3 relative to the putative transcription start site. When translated into protein, the exon 4 extension inserts 43 new amino acids (indicated below the mRNA sequence) and shifts the Loqs PC reading frame, truncating the protein.

(D) RT-PCR analysis of *loqs* mRNA species in males, female carcasses remaining after ovary dissection, dissected ovaries, and S2 cells. Males express more *loqs* RA than *loqs* RB, female somatic tissue expresses both *loqs* RA and *loqs* RB, while ovaries express predominantly *loqs* RB. *loqs* RC was observed only in S2 cells, together with *loqs* RA and *loqs* RB.

(E) The piggyBac transposon insertion f00791 lies 57 bp upstream of the reported transcription start site for *loqs*.

DOI: 10.1371/journal.pbio.0030236.g001

loquacious (loqs). *loqs* is located on the left arm of Chromosome 2 at polytene band 34B9. *loqs* produces at least three different mRNA isoforms through alternative splicing (Figure 1B). The shortest transcript, *loqs* RNA splice variant A (RA), encodes a 419-amino-acid protein, Loqs protein isoform A (PA), with a predicted molecular mass of 45 kDa. The transcript *loqs* RNA splice variant B (RB) contains one additional exon and encodes a protein of 465 amino acids, Loqs protein isoform B (PB), with a predicted molecular mass of 50 kDa. These two mRNA species were identified as cDNAs in the *Drosophila* genome sequencing project and annotated in FlyBase [38] among the *Drosophila* proteins that contain dsRBDs. Using non-quantitative RT-PCR, we detected a third splice variant, *loqs* RNA splice variant C (RC), in which an alternative splice acceptor site for exon 4 is used (Figure 1B, C, and D). Use of the alternative splice site creates a 5′-extended fourth exon and changes the reading frame, resulting in a truncated protein, Loqs protein isoform C (PC), 383 amino acids long (Figure 1C). Loqs PC has a predicted molecular mass of 41 kDa and lacks the entire third dsRBD of Loqs PA and PB (Figure 1B). *loqs* RA is the predominant mRNA species in dissected testes, whereas *loqs* RB is the most abundant species in ovaries. Both isoforms are expressed in the carcasses of males and females after removal of the gonads (Figure 1D and data not shown). Using two independent antibodies raised against an N-terminal Loqs peptide, but not using pre-immune sera, we detected a candidate protein for Loqs PC in S2 cells (see below), suggesting that the three *loqs* transcripts give rise to distinct Loqs protein isoforms.

Thibault and co-workers reported a mutant allele of CG6866, $loqs^{f00791}$, recovered in a large-scale piggyBac transposon mutagenesis screen of *Drosophila* [39]. The f00791 piggyBac inserted 57 nucleotides upstream of the *loqs* transcription start site (Figure 1E); although annotated as lethal, homozygous mutant $loqs^{f00791}$ flies are viable but completely female sterile. Precise excision of the f00791 piggyBac transposon fully reverted the female sterility (data not shown). Analysis by quantitative RT-PCR using primers that

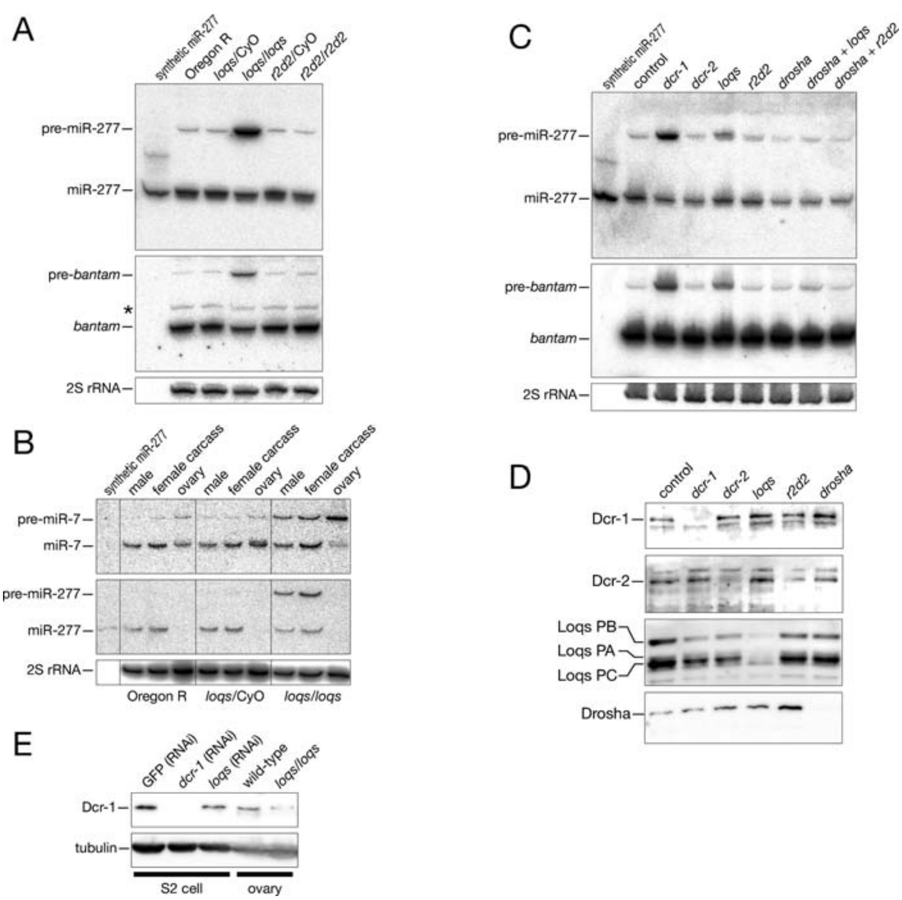

Figure 2. Loss of Loqs Function Increases the Steady-State Concentration of Pre-miRNA

(A) Northern analysis of total RNA from wild-type, $loqs^{f00791}$ heterozygotes and homozygotes, and *r2d2* heterozygotes and homozygotes for whole males, probed for miR-277 and *bantam*. The membrane was first hybridized with the miR-277 probe, stripped and probed for 2S rRNA as a loading control, then stripped again and probed for *bantam* miRNA. Asterisk: the 2S probe was not completely removed before the hybridization with the *bantam* probe, resulting in an additional band above the mature *bantam* RNA.

(B) Total RNA from whole males, female carcasses remaining after ovary dissection, and dissected ovaries was probed for miR-7. As a control for successful dissection, the blot was also probed for miR-277, which is not expressed in ovaries (KF and PDZ, unpublished results). 2S rRNA again served as a loading control.

(C) Depletion of *dcr-1* or *loqs* in S2 cells by RNAi leads to pre-miRNA accumulation. Total RNA was isolated after dsRNA-triggered RNAi of the indicated genes. The control sample was treated with dsRNA corresponding to the polylinker sequence of pLitmus28i.

(D) Depletion of Dcr-1, Dcr-2, Loqs, and Drosha was confirmed by Western blotting.

(E) Western blotting analysis demonstrates that Dcr-1 levels are not significantly reduced by depletion of Loqs by RNAi in S2 cells, but are lower in $loqs^{f00791}$ mutant ovaries.

DOI: 10.1371/journal.pbio.0030236.g002

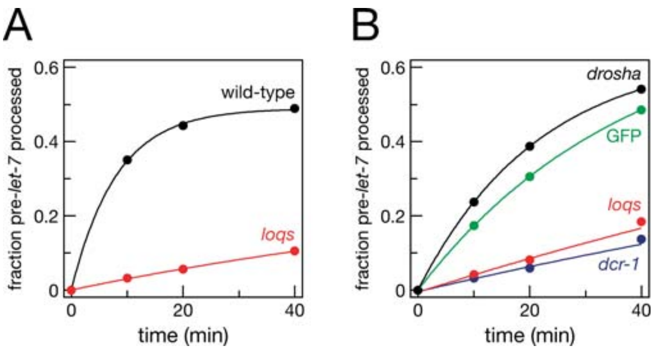

Figure 3. Loqs Is Required for Efficient pre-*let-7* Processing In Vitro

(A) *loqs*^{f00791} mutant ovary lysates processed pre-*let-7* into mature *let-7* miRNA ~19-fold more slowly than wild-type. The data were fit to a first-order exponential equation, and initial velocities calculated from the fitted curve.

(B) Analysis of pre-*let-7* processing in extracts from S2 cells. The cells were treated twice with dsRNA corresponding to the indicated genes.

DOI: 10.1371/journal.pbio.0030236.g003

amplify all three *loqs* mRNA splice variants (see Materials and Methods) showed that somatic female *loqs*^{f00791} tissues express approximately 5-fold (4.76 ± 0.24; $n = 3$) less *loqs* mRNA than wild-type, while *loqs*^{f00791} mutant ovaries express approximately 40-fold (42 ± 0.33; $n = 3$) less *loqs* mRNA than wild-type ovaries. Testes express approximately 3-fold (2.9 ± 0.5; $n = 3$) less *loqs* mRNA in the *loqs*^{f00791} mutant than in wild type. These data suggest that the mutant phenotype should be strongest in ovaries, consistent with the mutation causing female sterility as its most obvious defect.

In Vivo, Normal Pre-miRNA Processing Requires Loqs

To assess the function of *loqs* in miRNA biogenesis, we isolated total RNA from *loqs*^{f00791} males and determined the steady-state levels of mature and pre-miRNA for miR-277 and *bantam* (Figure 2A), which are both expressed in adult tissues. We detected a 100-fold increase in pre-miR-277 and a 12-fold increase in pre-*bantam* RNAs in homozygous mutant *loqs*^{f00791} males, but not in heterozygous *loqs*^{f00791} or heterozygous or homozygous *r2d2* mutant males. In contrast, the amount of mature miR-277 or *bantam* was only slightly reduced in the *loqs*^{f00791} homozygotes.

Since *loqs* mRNA expression is lowest in the ovaries of *loqs*^{f00791} mutant flies, we analyzed the levels of pre-miR-7 and mature miR-7, a miRNA that is expressed in whole males, manually dissected ovaries, and the female carcasses remaining after removing the ovaries (Figure 2B). While pre-miR-7 increased in all *loqs*^{f00791} homozygous mutant tissues, relative to wild-type or *loqs* heterozygotes, the disruption of miR-7

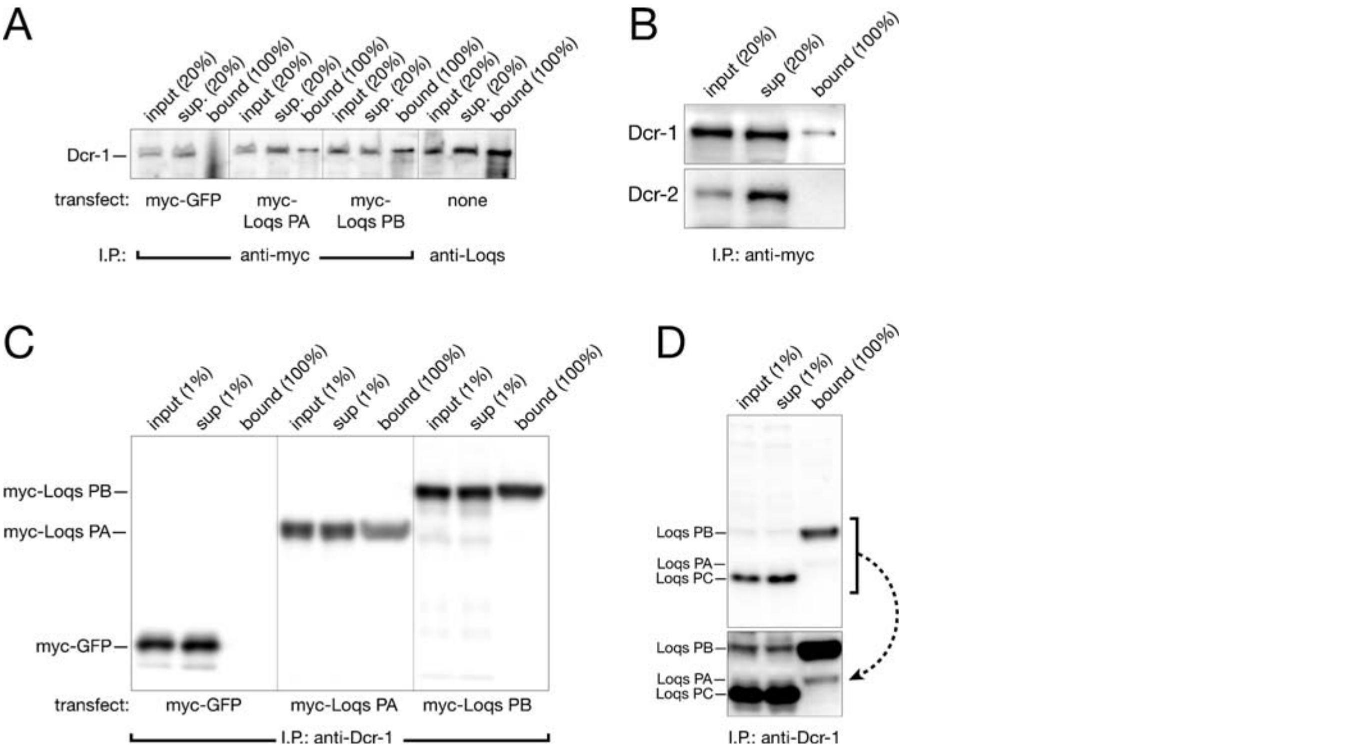

Figure 4. Loqs and Dcr-1 Are Present in a Common Protein Complex in S2-Cells

(A) Dcr-1 associates with myc-tagged Loqs PA or PB, and with endogenous Loqs protein. Immunoprecipitation with anti-myc or anti-Loqs antibody was performed using lysates from S2 cells transfected with the indicated expression plasmid. Dcr-1 was detected by Western blotting.

(B) myc-tagged Loqs PB stably associates with Dcr-1 but not Dcr-2. S2 cells were transfected with plasmid expressing myc-tagged Loqs PB, then lysed and immunoprecipitated with anti-myc antibody. The immunoprecipitates were analyzed by Western blotting using anti-Dcr-1 or anti-Dcr-2 antibodies.

(C) S2 cells were transfected with plasmid expressing myc-tagged GFP, Loqs PA, or Loqs PB, then extracted and immunoprecipitated with anti-Dcr-1 antibody. The immunoprecipitates were analyzed by Western blotting using anti-myc antibody.

(D) Anti-Dcr-1 antibody was used to immunoprecipitate Dcr-1 and associated proteins from S2 cell lysates, and the immunoprecipitates were analyzed by Western blotting using anti-Loqs antibody to detect endogenous Loqs protein. The major Loqs protein isoform recovered was Loqs PB. In a longer exposure (bottom panel), a band corresponding in size to Loqs PA is visible. The most abundant Loqs isoform the input sample, Loqs PC, which lacks the third dsRBD, did not immunoprecipitate with Dcr-1, suggesting that the third dsRBD is required for the association of Loqs with Dcr-1.

DOI: 10.1371/journal.pbio.0030236.g004

production in ovaries was striking: not only did pre-miR-7 accumulate, but also mature miR-7 was dramatically reduced. These data suggest that Loqs protein function is required for the maturation of miRNA and demonstrate a direct correlation between *loqs* mutant allele strength and disruption of miRNA processing.

Loqs Is Required for Pre-miRNA Processing in *Drosophila* S2 Cells

To confirm the function of *loqs* in pre-miRNA processing, we depleted cultured *Drosophila* S2 cells of *loqs* mRNA by RNAi (Figure 2C). Eight days after incubating S2 cells with dsRNA corresponding to the first 300 nucleotides of the *loqs* coding sequence, we determined the steady-state levels of pre-miRNA and mature miRNA for miR-277 and *bantam*. Relative to an unrelated dsRNA control, dsRNA corresponding to *dcr-1* caused a approximately 9-fold and approximately 23-fold increase in steady-state pre-miR-277 and *bantam* levels, respectively, and dsRNA corresponding to *loqs* caused a approximately 2-fold and approximately 6-fold increase in steady-state pre-miR-277 and *bantam* levels, respectively. In these experiments, RNAi of *dcr-1* more completely depleted Dcr-1 protein than RNAi of *loqs* reduced Loqs protein (Figure 2D). RNAi of *dcr-2, r2d2,* or *drosha* did not alter pre-miRNA levels for either miR-277 or *bantam,* nor did it alter Dcr-1 or Loqs levels. The Drosha/Pasha protein complex functions before pre-miRNA processing, converting primary miRNA (pri-miRNA) to pre-miRNA. Consistent with the idea that Loqs functions with Dcr-1 to convert pre-miRNA to mature miRNA, RNAi of *drosha* together with *loqs* alleviated the high pre-miRNA levels observed for RNAi of *loqs* alone, demonstrating that Loqs acts after Drosha.

Next, we examined processing of 20 nM exogenous pre-*let-7* into mature *let-7* in lysates from ovaries or S2 cells (Figure 3). Initial velocities were calculated for each reaction to permit comparison of processing rates (see Materials and Methods). Lysate from homozygous *loqs*^{f00791} mutant ovaries processed pre-*let-7* RNA to mature *let-7* approximately 19-fold more slowly than wild-type ovary lysate (Figure 3A). Moreover, lysate prepared from S2 cells soaked with a green fluoresecent protein (GFP) control dsRNA (GFP[RNAi]) or *drosha* dsRNA (*drosha*[RNAi]) accurately and efficiently converted exogenous pre-*let-7* RNA into mature *let-7*. In contrast, both *dcr-1*(RNAi) and *loqs*(RNAi) S2 cell lysates converted pre-miRNA to mature miRNA approximately 5- and approximately 4-fold, respectively, more slowly than the control lysate (Figure 3B). Thus, Loqs is required for production in vivo of normal levels of miR-7, miR-277, and *bantam,* and the efficient conversion of pre-*let-7* to mature *let-7* in vitro. Together, these four miRNAs include both miRNAs found on the 5′ and on the 3′ side of the pre-miRNA stem, suggesting a general role for Loqs in pre-miRNA processing.

Reduction of R2D2 protein by RNAi destabilizes Dcr-2; conversely, RNAi of Dcr-2 renders R2D2 unstable [21]. In contrast, RNAi of *loqs* in S2 cells reduced Dcr-1 protein levels by no more than 15% (Figure 2D and E), suggesting that Loqs functions together with Dcr-1 in pre-miRNA processing, rather than that Loqs is simply needed to stabilize Dcr-1 protein. However, *loqs*^{f00791} mutant ovaries, which lack detectable Loqs protein, contain 70% less Dcr-1 than wild-type (Figure 2E). A role for Loqs in both Dcr-1 function and in Dcr-1 stability suggests that the two proteins physically interact, like R2D2 and Dcr-2. Therefore, we tested if Dcr-1 and Loqs are components of a common complex.

A Dcr-1 Protein Complex Contains Loqs

We expressed in S2 cells myc-tagged versions for two protein isoforms of Loqs, Loqs PA and Loqs PB, and immunoprecipitated the tagged proteins with anti-myc monoclonal antibodies. We analyzed the immunoprecipitated protein by Western blotting using a polyclonal anti-Dcr-1 antibody. Figure 4A shows that Dcr-1 protein co-immunoprecipitated with myc-tagged Loqs. When myc-tagged GFP was expressed in place of myc-tagged Loqs, no Dcr-1 protein

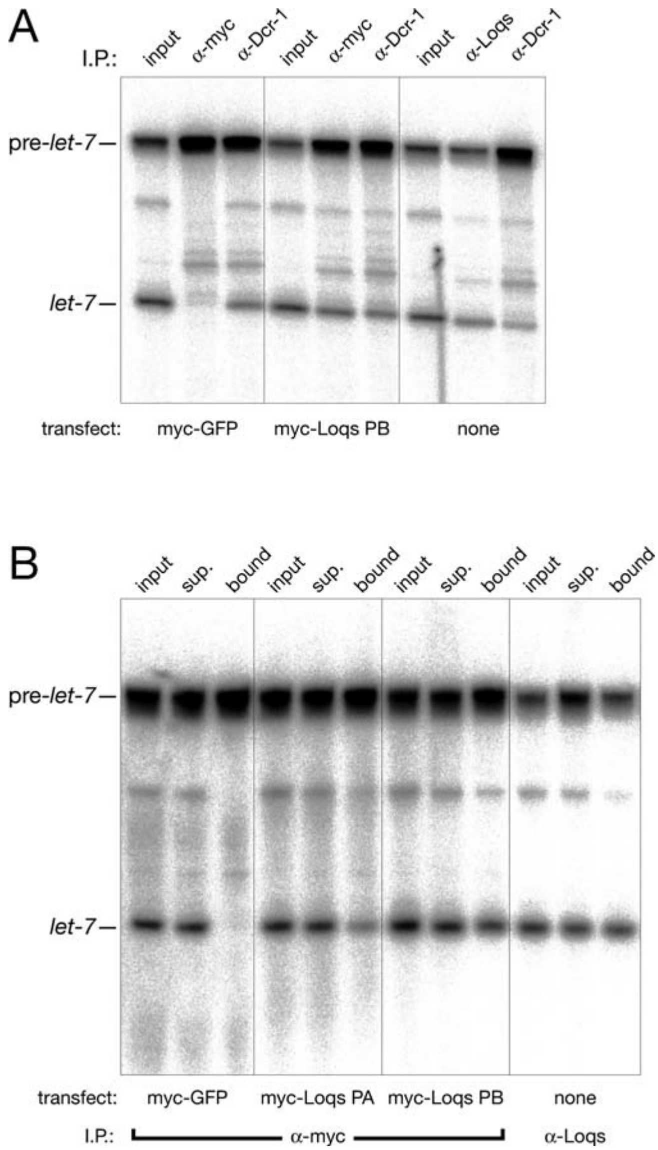

Figure 5. Loqs Is Associated with Pre-miRNA Processing Activity in S2 Cells

(A) Pre-miRNA processing activity co-immunoprecipitates with myc-tagged Loqs PB and with endogenous Dcr-1 or endogenous Loqs, but not with myc-tagged GFP.

(B) Pre-miRNA processing activity co-purifies by immunoprecipitation with both Loqs protein isoforms that interact with Dcr-1, Loqs PA, and Loqs PB. The extracts used in (A) and (B) were independently prepared.

DOI: 10.1371/journal.pbio.0030236.g005

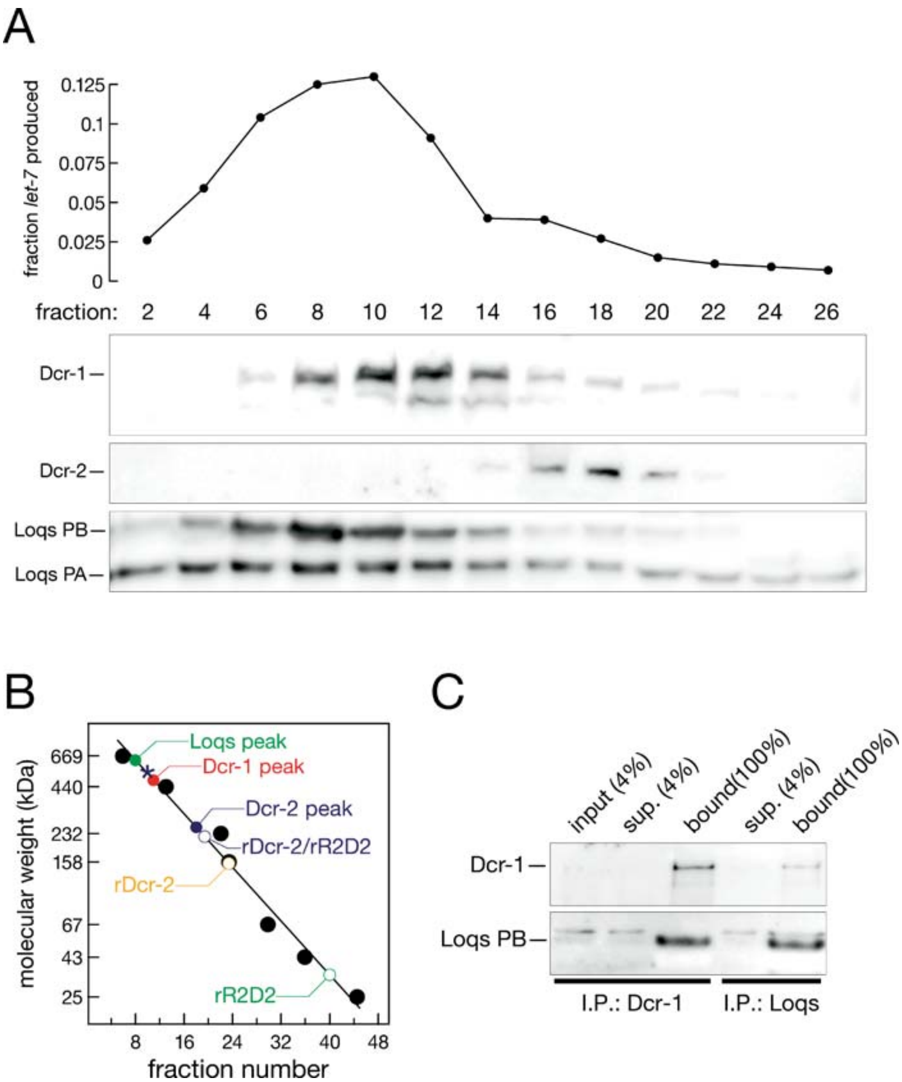

Figure 6. Analysis of Complexes Containing Pre-miRNA Processing Activity, Dcr-1, and Loqs

(A) S2 cell lysate was fractionated by gel filtration chromatography and analyzed for pre-*let-7* processing activity, and Dcr-1, Dcr-2, and Loqs proteins.
(B) The sizes of the distinct complexes containing Loqs (~630 kDa), Dcr-1 (~480 kDa), and Dcr-2 (~230 kDa) and the broad complex containing pre-miRNA processing activity (~525 kDa) were estimated using molecular weight standards (thyroglobulin, 669 kDa; ferritin, 440 kDa; catalase, 232 kDa; aldolase, 158 kDa; bovine serum albumin, 67 kDa; ovalbumin, 43 kDa; chymotrypsinogen A, 25 kDa) and recombinant Dcr-2 and R2D2 proteins (rDcr-2 and rR2D2). The blue asterisk denotes the peak of pre-*let-7* processing activity detected in (A).
(C) Fractions containing the Dcr-1 peak were pooled and immunoprecipitated with either anti-Dcr-1 or anti-Loqs antibodies. Western blotting with anti-Dcr-1 and anti-Loqs antibodies demonstrated that Dcr-1 and Loqs remained associated through gel filtration chromatography.
DOI: 10.1371/journal.pbio.0030236.g006

was recovered in the anti-myc immunoprecipitate. Similarly, an affinity purified, polyclonal antibody directed against the N-terminus of endogenous Loqs protein also co-immunoprecipitated Dcr-1 protein (Figure 4A). This interaction was resistant to treatment with RNase A (data not shown). We could not detect co-immunoprecipitation of Dcr-2 with myc-tagged Loqs PB under conditions where Dcr-1 was readily detected (Figure 4B), but we cannot exclude that Dcr-2 is a substoichiometric component of a complex that contains both Dcr-1 and Loqs (see below).

When immunoprecipitated with anti-Dcr-1 antibody, both myc-tagged Loqs protein isoforms—PA and PB—associated with Dcr-1 (Figure 4C). Moreover, the antibody against endogenous Loqs protein detected two bands corresponding

Figure 7. Silencing of a miRNA-Responsive YFP Reporter Requires *loqs* but Not *r2d2*

(A) A YFP transgene expressed from the Pax6-promoter showed strong fluorescence in the eye and weaker fluorescence in the antennae. Due to the underlying normal red eye pigment, the YFP fluorescence was observed in only those ommatidia that are aligned with the optical axis of the stereomicroscope. In heterozygous *loqs*^{f00791}/CyO flies bearing a miR-277-responsive, Pax6-promotor-driven, YFP transgene, YFP fluorescence was visible in the antennae but was repressed in the eye. In contrast, in homozygous mutant *loqs*^{f00791} flies, YFP fluorescence was readily detected in the eye. A strong mutation in *r2d2* did not comparably alter repression of the miR-277-regulated YFP reporter. The exposure time for the unregulated YFP reporter strain was one-fourth that used for the miR-277-responsive YFP strain. The exposure times were identical for the heterozygous and homozygous *loqs* and *r2d2* flies.
(B) Additional images of eyes from *loqs*^{f00791} heterozygous and homozygous flies bearing the miR-277-responsive YFP reporter transgene diagrammed in (A).

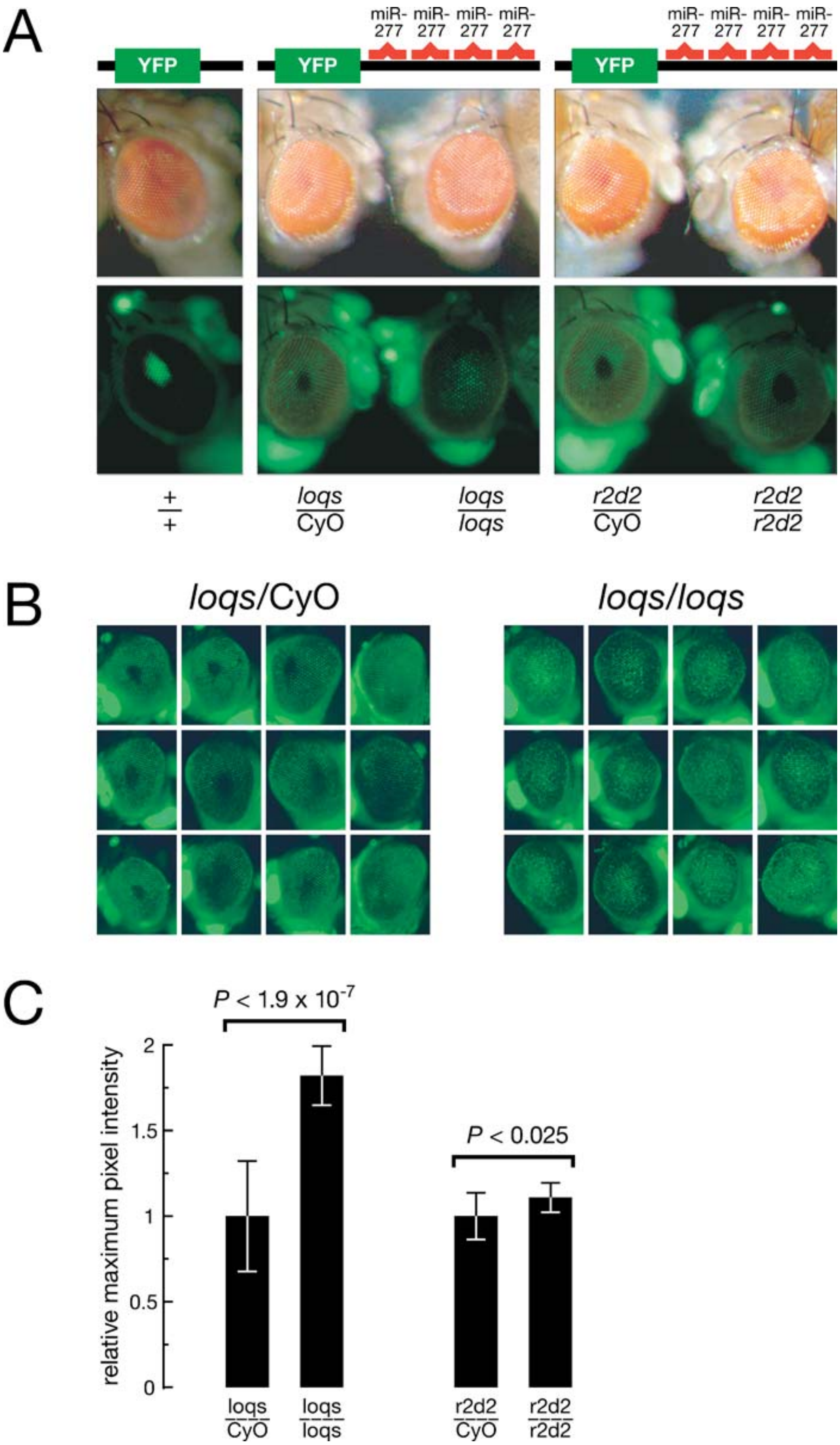

(C) Quantification of fluorescence of the miR-277-responsive YFP transgene in eyes heterozygous or homozygous for *loqs* or *r2d2*. The maximum pixel intensity was measured for each eye (excluding antennae and other tissues where miR-277 does not appear to function). The graph displays the average ($n = 13$) maximum pixel intensity ± standard deviation for each homozygous genotype, normalized to the average value for the corresponding heterozygotes. Statistical significance was estimated using a two-sample Student's *t*-test assuming unequal variance.
The images in (A) were acquired using a sensitive, GFP long-pass filter set that transmits yellow and red autofluorescence. Images in (B) and for quantitative analysis were acquired using a YFP-specific band-pass filter set that reduced the autofluorescence recorded.
DOI: 10.1371/journal.pbio.0030236.g007

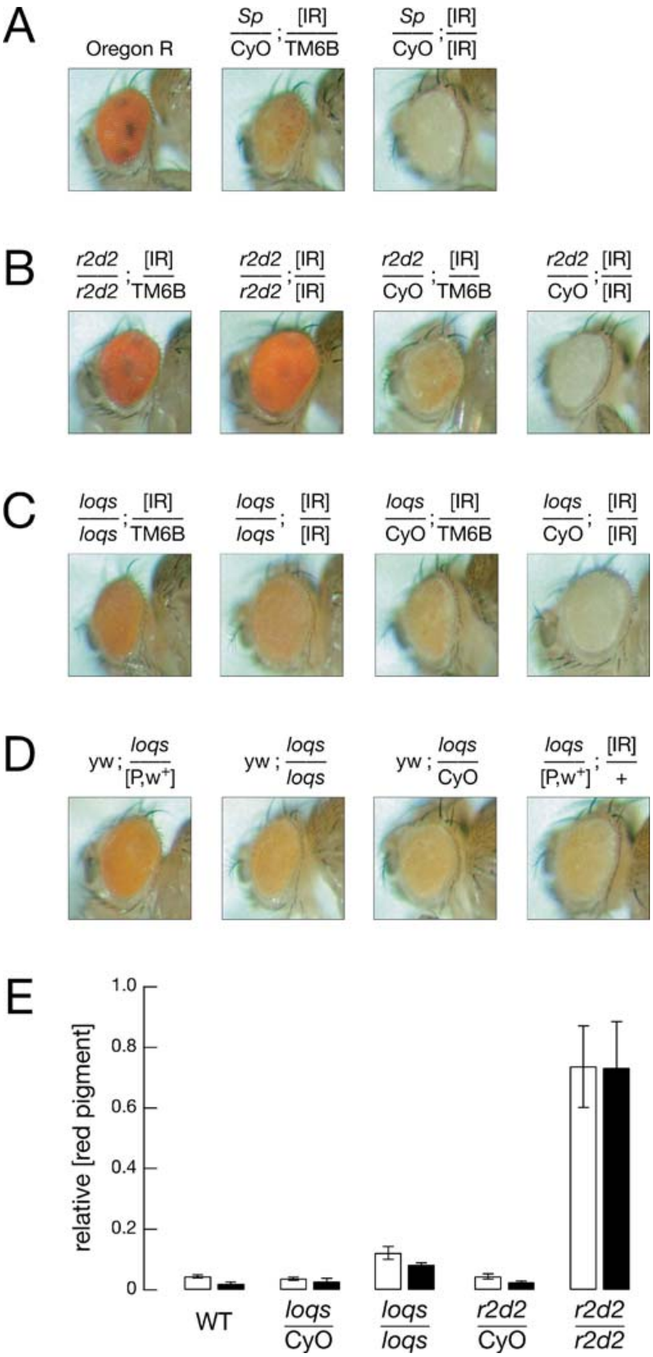

Figure 8. Silencing of *white* by an IR Partially Depends on *loqs*

(A) The red eye color of wild-type flies (left) changes to orange (center) and white (right) in response to one or two copies, respectively, of a *white* IR transgene, which silences the endogenous *white* gene.

(B) Homozygous mutant *r2d2* flies fail to silence *white,* even in the presence of two copies of the *white*-IR transgene; heterozygous *r2d2*/CyO flies repress *white* expression.

(C) In flies homozygous for $loqs^{f00791}$, silencing of *white* by the *white*-IR is less efficient; two copies of the *white*-IR do not produce completely white eyes, whereas they do in heterozygous $loqs^{f00791}$/CyO.

(D) The eye color change in $loqs^{f00791}$ flies is not caused by the increased $white^{+}$ gene dose resulting from the mini-*white* marker in the *piggyBac* transposon that causes the $loqs^{f00791}$ mutation. Flies *trans*-heterozygous for $loqs^{f00791}$ and a mini-*white*-marked P-element have more red eye pigment than $loqs^{f00791}$ homozygous flies, but show more efficient silencing by the *white*-IR than $loqs^{f00791}$ homozygous animals.

(E) The eye pigment of the indicated genotypes was extracted and quantified by green light (480 nm) absorbance, relative to wild-type flies bearing no *white*-IR transgenes. The graph shows the mean and standard deviation of five independent measurements per genotype.

DOI: 10.1371/journal.pbio.0030236.g008

in size to Loqs PA and Loqs PB in the proteins immunoprecipitated with the anti-Dcr-1 antibody (Figure 4D). Loqs PB comprises only approximately 22% of the total Loqs protein in S2 cells, but corresponded to approximately 95% of the Loqs associated with Dcr-1. Loqs PA, which is expressed at comparable levels in S2 cells, accounts for most of the remaining Loqs associated with Dcr-1. In contrast, the putative Loqs PC protein comprises the majority of S2 cell Loqs, but was not recovered in the Dcr-1 immunoprecipitate. Intriguingly, Loqs PA and PB contain a third dsRBD that Loqs PC lacks; perhaps this third dsRBD is required for the association of Loqs with Dcr-1.

The immunoprecipitated Dcr-1–Loqs complexes accurately converted pre-miRNA to mature miRNA (Figure 5). Pre-miRNA processing by the immunoprecipitates was efficient and accurate when we used the anti-Dcr-1 antibody (Figure 5A), and when we used anti-myc antibody and expressed myc-tagged Loqs, but not when we used the anti-myc antibody and expressed myc-tagged GFP (Figure 5A and 5B). Thus, Dcr-1 and Loqs co-associate in a complex capable of converting pre-miRNA into mature miRNA. Our data also demonstrate that an N-terminal tandem myc tag does not perturb Loqs function in pre-miRNA cleavage.

Next, we estimated the size of the pre-miRNA processing complex by gel filtration chromatography. Pre-miRNA processing activity chromatographed as a broad approximately 525-kDa peak that overlapped the peaks of both Dcr-1 and Loqs proteins (Figure 6A and 6B). Dcr-1 protein chromatographed as an approximately 480-kDa complex that overlapped the peak of Loqs PB, which chromatographed as an approximately 630-kDa complex. The Loqs PB isoform accounts for most of the Dcr-1-associated Loqs in S2 cells (see Figure 4D). The apparent size of the Dcr-1 complex suggests that it is either associated with proteins in addition to Loqs or that the complex has an elongated shape that increases its apparent molecular weight. Pre-miRNA processing activity, Loqs, and Dcr-1 were all well resolved from the approximately 230-kDa peak of Dcr-2 (theoretical mass = 197.7 kDa), which corresponds to the Dcr-2/R2D2 heterodimer (theoretical mass = 232.7 kDa). Although the peaks of Loqs and Dcr-1 do not co-migrate, Dcr-1 was stably associated with Loqs after gel filtration: Dcr-1 and Loqs reciprocally co-immunoprecipitated from the pooled peak Dcr-1 fractions (Figure 6C). Loqs was not detected in the Dcr-2 peak by this method (data not shown). Loqs PC, which did not associate with Dcr-1 in immunoprecipitation, chromatographed as a 58-kDa protein, suggesting that it is a free monomeric protein (data not shown).

A Loqs Mutation Reduces Silencing of a miRNA-Controlled Reporter Transgene In Vivo

The $loqs^{f00791}$ mutation caused pre-miRNAs to accumulate in the soma and the germ line and strongly reduced mature miR-7 levels in the female germ line, suggesting that Loqs function is required for miRNA-directed silencing in vivo. We introduced a miRNA-regulated yellow fluorescent protein (YFP) reporter into *loqs*^{f00791} homozygous mutant flies. This transgenic reporter expresses in the eye a YFP mRNA bearing four miR-277 binding sites in its 3′ UTR. The four miRNA-binding sites pair with all but the central three nucleotides of miR-277 and are, therefore, predicted to repress reporter mRNA translation rather than trigger mRNA cleavage (Figure 7A). YFP fluorescence was readily detected in the eye and antennae in control flies in which the 3′ UTR of the YFP transgene lacked the four miR-277 binding sites (Figure 7A). When the reporter contained the miR-277 binding sites, YFP expression was repressed in the eye but readily visible in the antennae, indicating that miR-277 is expressed in the eye (*loqs*/CyO, Figure 7A and B). This expression was verified independently by Northern blots of RNA isolated from eyes dissected away from other tissues of the head (data not shown). Silencing of the miR-277-responsive YFP reporter in the eye was reduced in *loqs*^{f00791} homozygous mutant flies (*loqs*/*loqs*, Figure 7A, B and C). As a control, we examined the effect of a strong *r2d2* mutation on YFP reporter expression (Figure 7A and C). We measured the maximum fluorescence intensity in each eye for all four genotypes. Figure 7C shows that there was a significant ($P < 1.9 \times 10^{-7}$) increase in YFP fluorescence in eyes homozygous for the weak hypomorphic allele *loqs*^{f00791}. This allele reduced miR-277 levels in the soma approximately 2-fold (see Figure 2B); fluorescence in the eye of homozygous mutant *loqs* flies was 1.8 ± 0.17 (average maximum intensity ± standard deviation; $n = 13$) times greater than in the eyes of their age-matched heterozygous siblings. In contrast, flies homozygous for a strong hypomorphic *r2d2* mutation show only a modest change in fluorescence (1.1 ± 0.09; $n = 13$; $P < 0.025$). The Dcr-2 partner protein R2D2 is required for RNAi triggered by exogenous dsRNA [21] or transgenes expressing long dsRNA hairpins (see below and Figure 8). We conclude that the reduced levels of Loqs protein in the *loqs*^{f00791} mutant lead to a statistically significant reduction in miRNA-directed silencing and that the Loqs paralog R2D2 plays little, if any, role in miRNA function.

Loqs Participates in Silencing Triggered by Long dsRNA In Vivo

dsRNA transcribed as an inverted repeat (IR) triggers silencing of corresponding mRNAs in flies [23,40]. For IR-silencing of the *white* gene, whose gene product is required to produce the red pigment that colors fly eyes, the extent of silencing is proportionate to the number of copies of the IR-*white* transgene [23,40] (Figure 8A), but is relatively insensitive to the number of copies of *white* present (TD and PDZ, unpublished). RNAi in *Drosophila* requires both Dcr-2, which transforms long dsRNA into siRNA, and R2D2, which collaborates with Dcr-2 to load siRNA into RISC. Thus, IR-silencing of *white* mRNA is lost in both *dcr-2* [23] and *r2d2* mutant flies (Figure 8B). We quantified the extent of *white* silencing by extracting the eye pigment in acidic ethanol and measuring its absorbance at 480 nm (Figures 8E and S1). Loss of R2D2 function in flies expressing one (or two) copies of the *white* IR transgene and two copies of the endogenous *white* locus restored red pigment levels to 74 ± 13 (or 73 ± 15 for two copies of IR-*white*) percent of wild-type flies lacking the *white*-IR. *loqs*^{f00791} mutant flies were also defective in IR-triggered *white* silencing, but to a much smaller extent (Figure 8C and 8E). The *loqs*^{f00791} mutation restored pigment levels in flies carrying one copy of the *white* IR-expressing transgene to $12 \pm 2\%$ of wild-type and to $8 \pm 0.6\%$ for flies carrying two copies of the *white*-IR ($n = 5$; Figures 8C and E). *loqs*^{f00791} heterozygotes were statistically indistinguishable from wild-type flies bearing one copy of IR-*white*, whose eye pigment concentration was 4 ± 0.5 (or 2 ± 0.6 for two copies of IR-*white*) percent of wild-type in the absence of the IR-*white* transgene.

Insertion of a mini-*white*-expressing piggyBac transposon causes the *loqs*^{f00791} allele. Thus, *loqs*^{f00791} heterozygotes have two copies of the endogenous *white* locus and one copy of mini-*white*; *loqs*^{f00791} homozygotes have two copies of endogenous *white* and two copies of mini-*white*. The presence of this additional copy of mini-*white* does not account for the darker red color of *white*-silenced *loqs*^{f00791} flies, because *loqs*^{f00791} heterozygotes bearing two copies of *white*, one copy of mini-*white* (in the piggyBac transposon inserted at *loqs*), and one copy of a P-element expressing mini-*white* are effectively silenced by IR-*white* (Figure 8D). In the absence of the IR-*white* transgene, the total amount of *white* expression in these flies is higher than in *loqs*^{f00791} homozygotes (Figure 8D). Thus, reduction of Loqs function accounts for the partial desilencing of *white* in this system. The modest loss of silencing in the *loqs*^{f00791} mutant flies may reflect the incomplete loss of Loqs protein in this allele. However, Carthew and co-workers previously reported that a *dcr-1* null mutation leads to a similar, partial loss of *white* IR-silencing [23]. The small eye phenotype of *dcr-1* null mutants unfortunately renders a quantitative comparison to *loqs*^{f00791} impossible. We propose that—as for pre-miRNA processing—Dcr-1 and Loqs act together to enhance silencing by siRNAs.

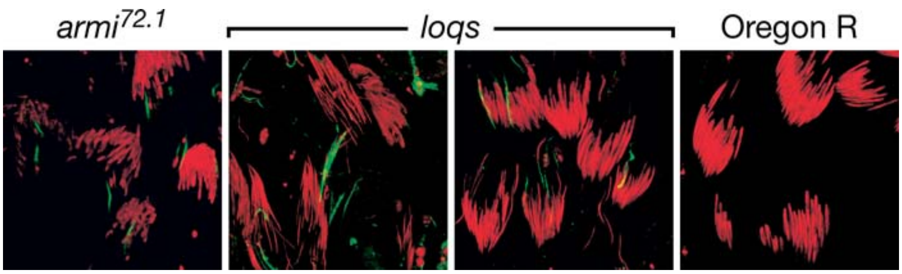

Figure 9. Silencing of *Stellate* by the dsRNA-Generator *Su(Ste)* Requires *loqs*

Testes were stained for DNA (red) and Stellate protein (green). Defects in RNA silencing often lead to accumulation of Stellate protein crystals in testes. For example, the testes from the strong allele *armi*$^{72.1}$, but not wild-type Oregon R testes, show Stellate protein staining. Testes from *loqs*^{f00791} males show strong accumulation of Stellate protein, consistent with their significantly impaired fertility.

DOI: 10.1371/journal.pbio.0030236.g009

Silencing of the Endogenous Stellate Locus Requires Loqs

loqs^{f00791} males are incompletely fertile. When Oregon R females were mated to *loqs*^{f00791} homozygous mutant males, only 17% of embryos hatched ($n = 479$); for *loqs*^{f00791} heterozygous males, 47% of embryos hatched ($n = 466$). Ninety percent of embryos hatched ($n = 753$) for wild-type Oregon R males. Genes required for RNA silencing often reduce male fertility, because the X-linked gene *Ste* is epigenetically silenced in testes by dsRNA derived from the bi-directionally transcribed *Suppressor of Stellate (Su(Ste))* locus [41]. *Ste* silencing is genetically similar, but not identical, to RNAi, in that like RNAi it requires the function of the gene *armitage (armi)* [24], but unlike RNAi does not require *r2d2* (VVV and PDZ, unpublished data). In the absence of *Ste* silencing, Stellate protein accumulates as protein crystals in the testes. *loqs*^{f00791} mutants contain Stellate crystals in their testes (Figure 9), much like *armi*$^{72.1}$ mutants, identifying a second role for *loqs* in silencing by endogenous RNA triggers, distinct from its function in miRNA biogenesis.

A Germ-Line Stem Cell Defect in *loqs*^{f00791} Mutant Females

The *loqs* gene has a critical function in oogenesis, as *loqs*^{f00791} females have small ovaries (Figure 10A) and are completely sterile. *Drosophila* ovaries comprise ovarioles that contain developmentally ordered egg chambers, which are produced continuously in the adult by germ-line stem cell division. As a result, mutations that block stem cell division or maintenance lead to ovarioles containing few egg chambers. *loqs*^{f00791} mutant females lay no eggs. Whereas wild-type females contain 7 ± 0.8 ($n = 15$) previtellogenic egg chambers per ovariole, *loqs*^{f00791} contain only 3 ± 0.8 ($n = 20$). Excision of the *piggybac* transposon in *loqs*^{f00791} restores fertility, demonstrating that these defects reflect loss of Loqs function. The mature oocytes in *loqs*^{f00791} ovarioles have normal dorsal appendages, indicating that dorsoventral patterning is normal. In contrast, mutations in *armi, spnE,* and *aub* disrupt both dorsoventral and anteroposterior patterning [42–44]. These mutations all disrupt RNAi and *Ste* silencing, but display no global defects in miRNA biogenesis or function, unlike *loqs* [24,41,45,46].

Oogenesis is initiated in the germarium, which contains the germ-line stem cells as well as the early germ-line cysts that will form egg chambers. In *loqs*^{f00791} mutant ovarioles, the germaria generally contain a limited number of cells that stain for Vasa, indicating that they are of germ-line origin (Figure 10B). No mitotic figures were observed, nor were separate cysts. Germ-line stem cells and their daughter cells, the cystoblasts, are characterized by the presence of a spherical structure, the spectrosome, that stains intensely with anti-Spectrin antibodies [47–49]. We stained wild-type and *loqs*^{f00791} germaria with anti-α-Spectrin antibodies (Figures 10C and S2). We could not detect spectrosomes in the *loqs* mutant germaria, suggesting that in these germaria, dissected from flies 3–4 d old, no stem cells remained. Stem cells must have originally been present, because *loqs* mutant ovaries produce some late-stage oocytes. Thus, most of the original stem cells may have died or differentiated into cystoblasts without renewing the stem cell pool. At present, we cannot distinguish between these alternatives. We conclude that *loqs*^{f00791} mutants, which are defective in three distinct types of RNA silencing, fail to maintain germ-line stem cells.

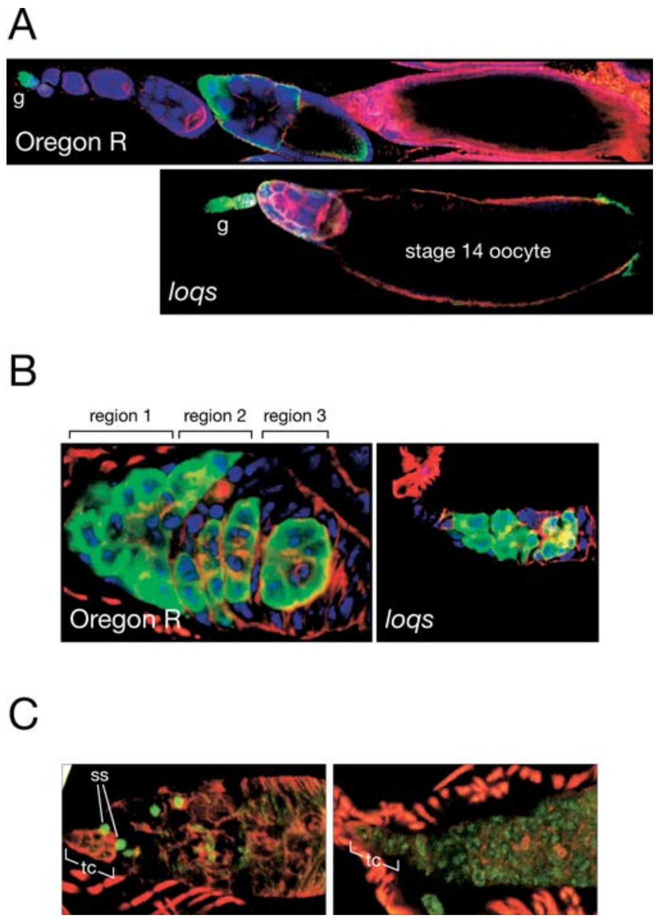

Figure 10. *loqs*^{f00791} Fail to Maintain Germ-Line Stem Cells

(A) Wild-type ovarioles contain a germarium and a developmentally ordered array of six to eight egg chambers, whereas *loqs*^{f00791} mutant ovarioles contain a smaller than normal germarium, two or three pre-vitellogenic egg chambers, and a late-stage egg chamber. Wild-type and *loqs* ovarioles are shown at the same magnification.

(B) In wild-type ovarioles, the germarium contains several newly formed germ-line cysts surrounded by somatic follicle cells. In contrast, *loqs*^{f00791} mutant germaria contain few germ-line cells, which are not organized into distinct cysts. The follicle cell layer is also significantly reduced in *loqs*^{f00791} germaria.

(C) Wild-type and *loqs* mutant germaria labeled for α-Spectrin (green) and filamentous Actin (red). In wild type, anti-α-Spectrin labels the spectrosome (ss), a structure characteristic of germ-line stem cells, which are normally found at the anterior of the germarium, apposed to the somatic terminal cells (tc). The cystoblasts, the daughters of the stem cells, also contain a spectrosome, but are located posterior to the stem cells. In *loqs* mutant ovaries, spectrosome-containing cells were not detected, indicating that normal germ-line stem cells are not present. These observations indicate that stem cells are not maintained.

In (A) and (B), ovaries were labeled for filamentous actin (red) using rhodamine phalloidin, DNA (blue) using TOTO3 (Molecular Probes), and the germ-line marker Vasa (green) using rabbit anti-Vasa antibody detected with fluorescein-conjugated anti-rabbit secondary antibody. In (B) and (C), wild-type and *loqs* germaria are shown at the same magnification.

DOI: 10.1371/journal.pbio.0030236.g010

Discussion

RNase III Endonucleases Act with dsRNA-Binding Partner Proteins in RNA Silencing

Collectively, Dcr-1 and Loqs, Drosha and Pasha, and Dcr-2 and R2D2 comprise six of the 12 dsRBD proteins predicted to be encoded by the *Drosophila* genome [50]. Thus, at least half of all dsRBD proteins in flies participate in RNA silencing. In

Caenorhabditis elegans, the R2D2-like dsRBD protein RDE-4 is required for RNA interference and interacts with DCR-1, the sole worm Dicer gene [51]. RDE-4 is equally similar to Loqs (E-value = 0.03) and R2D2 (E-value = 0.026; search restricted to *C. elegans* proteins). The Drosha/Pasha complex is also present in *C. elegans* [10] as well as cultured human cells [11–13]. Similarly, the *Arabidopsis thaliana* dsRBD protein HYL1 is required for the production of mature miRNAs, and *hyl1* mutant plants have a phenotype similar to that of *dicer-like 1 (dcl1)* [52,53]. Hiraguri and co-workers [54] recently demonstrated that HYL1 is a dsRNA-binding protein that binds DCL1 and that the HYL1 paralog DRB4 binds the Dicer protein DCL4. Pairing of RNase III endonucleases with dsRBD proteins is thus a recurring theme in RNA silencing.

A dsRBD Partner for Human Dicer?

The human genome encodes one Dicer protein, which is more closely related to *Drosophila* Dcr-1 than Dcr-2. Sequence analysis of human proteins for similarity to either *C. elegans* RDE-4 or *Drosophila* R2D2 does not identify a reasonable candidate for a dsRBD partner protein for human Dicer. In contrast, the human TRBP is highly similar to *Drosophila* Loqs (E-value = 5×10^{-36}). For comparison, the human proteins most similar to R2D2 or RDE-4 give E-values of 8×10^{-8} and 0.42, respectively, when the search is restricted to human proteins. Human TRBP was first identified [55] because it binds HIV *trans*-activator RNA (TAR), a stem-loop structure required for active HIV transcription [56–58]. Remarkably, the secondary structure of TAR resembles a miRNA precursor, and the recent discovery of Epstein-Barr virus-encoded miRNAs [59] has fueled speculation that TAR may be a viral pre-miRNA [60].

Deletion of PRBP, the mouse homolog of TRBP, yields viable mice that often die at the age of weaning. Surviving homozygous mutant males show defects in spermatogenesis attributed to abnormal sperm maturation rather than proliferation [61]. In contrast, Dicer knockout mice show very early embryonic lethality [62]. If mouse Dicer and PRBP collaborate to produce mature miRNA, the essential function of Dicer during mouse development must either be independent of miRNA function, or a redundant factor must replace PRBP during embryonic development but not spermatogenesis.

Loqs and Dcr-1 Protein Complexes

Together with *dcr-1,* the gene *loqs* is required in flies for normal pre-miRNA processing. Loqs and Dcr-1 reciprocally co-immunoprecipate. Pre-miRNA processing activity also co-immunoprecipitates with Dcr-1 and Loqs. However, in gel filtration chromatography, the two proteins overlap but do not precisely co-purify. Loqs and Dcr-1 may form a protein complex analogous to the Dcr-2/R2D2 and Drosha/Pasha complexes [10,21], but this complex may be transient, with Loqs also associating with other components of the RNA silencing machinery, perhaps even escorting the mature miRNA to Ago1, an approximately 110-kDa Argonaute protein associated with mature miRNAs in flies. In fact, the predominant Loqs-containing complex in S2 cell lysate is about 150 kDa larger than the peak of Dcr-1, so it could contain Dcr-1, Loqs, and Ago1. The data of Siomi and co-workers demonstrating that Ago1 associates with both Dcr-1 [28] and Loqs (Saito K, et al. DOI: 10.1371/journal.pbio.0030235) support such a view.

Cross-Talk between the Dcr-1 and Dcr-2 Pathways in *Drosophila*

In humans and *C. elegans,* a single Dicer gene is responsible for generating both siRNAs and miRNAs. *Drosophila* has apparently duplicated both its ancestral Dicer RNase III endonuclease and its dsRBD partner protein, dedicating Dcr-1/Loqs to miRNA processing and Dcr-2/R2D2 to RNAi. Nonetheless, these two pathways are not completely separate, because cells lacking *dcr-1* are not fully competent for IR-triggered silencing [23]. Dcr-1 is not required for siRNA production, yet embryo extracts lacking Dcr-1 fail to assemble RISC [23]. Dcr-1 has been proposed to be a component of "holo-RISC," an 80S complex containing many, but not all, components of the RNAi pathway in flies [63]. The $loqs^{f00791}$ mutation also reduced the efficiency of IR-triggered silencing in vivo. Therefore, we propose that Dcr-1 must partner with Loqs not only during the processing of pre-miRNA to mature miRNA, but also to ensure Dcr-1 function in the Dcr-2-dependent RNAi pathway.

Carthew and colleagues found no function for Dcr-2 in miRNA biogenesis [23]. Consistent with their results, we found little if any requirement for R2D2 in miRNA-directed silencing (see Figure 7C). Moreover, null or strong hypomorphic alleles of either *dcr-2* or *r2d2* show no overt phenotype, whereas the $dcr\text{-}1^{Q1147X}$ null mutation is embryonic lethal [23].

Stellate Silencing Requires Loqs

Endogenous silencing of the *Stellate* locus in testes is genetically distinct from miRNA-directed silencing, because it requires *armitage,* a gene that plays no general role in miRNA biogenesis or function [24]. *Stellate* silencing resembles RNAi in that *Stellate* expression is repressed by a dsRNA trigger transcribed from the *Su(Ste)* gene. *Su(Ste)* dsRNA produces siRNAs, called repeat-associated siRNAs, that are longer than the siRNAs produced in the RNAi pathway in *Drosophila* [41]. Even the weak allele described in this study, $loqs^{f00791}$, which reduces *loqs* mRNA levels only approximately 3-fold in testes, dramatically de-silences *Stellate.* Given the intimate association of Dcr-1 with Loqs, our data raise the possibility that Loqs acts to silence *Stellate* in collaboration with Dcr-1, which may generate the *Su(Ste)* repeat-associated siRNAs.

Germ-Line Stem Cells and miRNAs

The $loqs^{f00791}$ mutation is the first viable allele in *Drosophila* with a generalized defect in miRNA production. The allele may therefore be useful for future phenotypic analysis of miRNA-dependent pathways during the life cycle of *Drosophila.* The most obvious phenotype of $loqs^{f00791}$ is female sterility. $loqs^{f00791}$ homozygotes produce few egg chambers, indicating a defect in germ-line stem cell maintenance or division. The $loqs^{f00791}$ phenotype is similar to mutants in *piwi* [64], which encodes a member of the Argonaute protein family of core RISC components. In *piwi* mutant ovaries, germ-line stem cells fail to divide and instead differentiate directly into cystoblasts, depleting the germarium of germ-line stem cells. *loqs* mutants display a similar phenotype: we did not detect germ-line stem cells (i.e., spectrosome-containing cells) in $loqs^{f00791}$ homozygous germaria, suggesting that Loqs is required to maintain stem cells. Piwi is required in terminal filament cells, somatic cells surrounding the tip of the germarium, to send a signal that prevents germ-line stem cells from differentiating [64,65]. Piwi is also required in germ-line stem cells themselves to stimulate their proliferation [65]. Perhaps Piwi is at the core of an effector complex loaded with small RNA produced by Dcr-1 and Loqs. Intriguingly, *dcr-1* knockout mice die at embryonic day 7.5, apparently devoid of stem cells [62].

Materials and Methods

PiggyBac excision. To establish that insertion of the f00791 piggyBac transposon in the *loqs* gene caused the female sterility of *loqs*^{f00791} mutants, we excised the transposon by introducing into *loqs*^{f00791} heterozygotes a transgene expressing the piggyBac transposase from a Hermes element inserted on Chromosome 3 [66]. F1 male progeny of these flies were mated to *yw; Sp*/CyO virgins, and the resulting F2 progeny screened for loss of *white* expression (i.e., white eyes). Of 100 F2 progeny examined, one *white*$^{-}$ male was recovered. A line established from this fly was homozygous female fertile.

Real-time RT-PCR analysis. Two μg of total RNA was reverse transcribed using 5′-GCG AAT TCT TTT TTT TTT TTT TTT TTT TTT-3′ oligonucleotide as primer and Superscript II reverse transcriptase (Invitrogen, Carlsbad, California, United States). After extension, cDNA samples were diluted 3-fold with water. One μl of diluted cDNA was used for quantitative PCR using the Quantitect SyBr-green kit (Qiagen, Valencia, California, United States) in a DNA Engine Opticon 2 (MJ Research [Bio-Rad, Hercules, California, United States]). Oligonucleotide primers were 5′-ATG GAC CAG GAG AAT TTC CAC GGC-3′ and 5′-GGC CTC GTC GCT GGG CAA TAT TAC-3′ for *loqs* and 5′-AAG TTG CTG CTC TGG TTG TCG-3′ and 5′-GCC ACA CGC AGC TCA TTG TAG-3′ for *actin5C*. Amplification efficiencies were identical for both oligonucleotide pairs.

RNA isolation and detection by Northern blot. RNA was isolated from whole flies, dissected organs or S2 cells using Trizol (Invitrogen) according to the manufacturer's instructions. The RNA was quantified by absorbance at 260 nm, and 2–10 μg of total RNA was resolved by electrophoresis through a 20% denaturing acrylamide/urea gel (National Diagnostics, Atlanta, Georgia, United States). As a positive control for miR-277 hybridization, 10 fmol of phosphorylated miR-277 synthetic oligonucleotide (Dharmacon, Lafayette, Colorado, United States) was included on the gel. After electrophoresis, the gel was transferred to Hybond N+ (Amersham-Pharmacia, Little Chalfont, United Kingdom) in 0.5x TBE in a semi-dry transfer system (Transblot SD, Bio-Rad) at 20 V for 60 min. The RNA was UV cross-linked to the membrane (Stratalinker, Stratagene, La Jolla, California, United States) and pre-hybridized in 10 ml Church buffer [67] for 60 min at 37 °C.

RNA (Dharmacon) or DNA (IDT, Coralville, Iowa, United States) probes (25 pmol per reaction) were 5′-radiolabeled with polynucleotide kinase (New England Biolabs, Beverly, Massachusetts, United States) and γ-^{32}P-ATP (New England Nuclear, Boston, Massachusetts, United States) (330 μCi per reaction; specific activity 7,000 Ci/mmol). After labeling, unincorporated radioactivity was separated from the labeled probe using a Sephadex G-25 spin column (Roche, Basel, Switzerland). The labeled probe oligonucleotide was added to 10 ml of Church buffer and used for hybridization. For RNA probes, hybridization was carried out at 65 °C; DNA probes were hybridized at 37 °C. For both, hybridization was overnight followed by five 30-min washes with 2× SSC/0.1% (w/v) SDS. Membranes were exposed to phosphorimaging screens (Fuji, Tokyo, Japan). To strip probes, the membranes were boiled twice in 0.1% SDS for 1 min in a microwave oven. The following probes were used for detection: 5′-UCG UAC CAG AUA GUG CAU UUU CA-3′ for miR-277; 5′-CAG CTT TCA AAA TGA TCT CAC T-3′ for bantam; 5′-ACA ACA AAA UCA CUA GUC UUC CA-3′ for miR-7; 5′-TAC AAC CCT CAA CCA TAT GTA GTC CAA GCA-3′ for 2S rRNA.

Molecular cloning and generation of transgenic flies. Plasmids for the expression of myc-Loqs PA (pKF111) and myc-Loqs PB (pKF109) were created by PCR amplifying *loqs* mRNA with oligonucleotides 5′-AGC GGA TCC ATG GAA CAA AAA CTT ATT TCT GAA GAA GAC TTG GAA CAA AAA CTT ATT TCT GAA GAA GAC TTG GCC ATG GAC CAG GAG AAT TTC CAC GGC-3′ (appending two myc-tags to the N-terminus of Loqs) and 5′-TTA TGC GGC CGC CTA CTT CTT GGT CAT GAT CTT CAA GTA CTC-3′ from male and ovary cDNA, respectively. The reaction products were cloned into pUbi-Casper-SV40, which was created by inserting the SV-40 polyadenylation signal from pEGFP-N1 (Clontech, Palo Alto, California, United States) into pUbi-Casper2 (kind gift from Dr. Inge The). The vector for myc-tagged GFP expression (pKF63) was constructed similarly.

The vector for the expression of miR-277-responsive myc-YFP was constructed by first inserting the annealed oligonucleotides 5′-CAT GGA ACA AAA ACT TAT TTC TGA AGA AGA CTT GGG-3′ and 5′-CAT GCC CAA GTC TTC TTC AGA AAT AAG TTT TTG TTC-3′ into NcoI-cut pBSII-ITR1.1k-EYFP (a kind gift from Dr. Malcom Fraser) to add an N-terminal myc-tag. Then the vector was digested with NotI/XbaI and the annealed oligonucleotides 5′-GGC CTG TCG TAC CAG AGG ATG CAT TTA CAG TGT CGT ACC AGA GGA TGC ATT TAT GTC GTA CCA GAG GAT GCA TTT ACA GTG TCG TAC CAG AGG ATG CAT TTA-3′ and 5′-CTA GTA AAT GCA TCC TCT GGT ACG ACA CTG TAA ATG CAT CCT CTG GTA CGA CAT AAA TGC ATC CTC TGG TAC GAC ACT GTA AAT GCA TCC TCT GGT ACG ACA-3′ inserted, appending four miR-277 target sites to the 3′ UTR. Subsequently, the Pax6/EYFP/miR-277-target/SV-40-polyA cassette [68–70] was cloned into pP{Car20.1} [71] creating pKF77. All of the described constructs were sequence verified. Transgenic flies were obtained by injection of pKF77 with Δ2–3 helper plasmid into *ry*^{506} embryos using standard methods [72].

S2 cell culture and RNAi. *Drosophila* S2 cells were the kind gift of Dr. Neal Silverman. The cells were cultured in Schneider's *Drosophila* medium (Life Technologies, Carlsbad, California, United States) supplemented with 10% FBS, penicillin-streptomycin mix (Life Technologies), and 0.2% of conditioned Schneider's medium. Transfection of plasmids was performed using siLentFect (Bio-Rad).

Gene fragments for the preparation of dsRNA were cloned into a Litmus28i vector (NEB) that was modified into a T/A cloning vector [73]. The following oligonucleotide pairs were used to obtain gene fragments: 5′-TTG GGC GAC GTT TTC GAG TCG ATC-3′ and 5′-TTT GGC CGC CGT GCA CTT GGC AAT-3′ for *dcr-1*; 5′-CTG CCC ATT TGC TCG ACA TCC CTC C-3′ and 5′-TTA CAG AGG TCA AAT CCA AGC TTG-3′ for *dcr-2*; 5′-ATG GAC CAG GAG AAT TTC CAC GGC-3′ and 5′-GGC CTC GTC GCT GGG CAA TAT TAC-3′ for *loqs*; 5′-ATA CAA TCT CCA CCA ATT TGT AGG-3′ and 5′-CGT CAA ATT ATT TAA AAT ATT TGT TTC-3′ for *r2d2*; 5′-AGC AGC AGC AGT GAT AGC GAT GGC-3′ and 5′-TCG GTT ATT TTA TTT GTT GCT TTA ATG-3′ for *Drosha*; 5′-GAT CAC ATG GTC CTG CTG GAG TTC GTG-3′ and 5′-CAG GTT CAG GGG GAG GTG TG-3′ for GFP. Gene fragments were amplified from the plasmid templates with both flanking T7 RNA polymerase promoters using oligonucleotides 5′-CTA TGA CCA TGA TTA CGC CAA GC-3′ and 5′-CAC GAC GTT GTA AAA CGA CGG CCA-3′. RNA synthesis from the PCR products was performed as described [74], and the phenol-extracted RNA products were denatured for 5 min at 95 °C and then re-annealed for 30 min at 65 °C. The concentration of dsRNA was estimated by native agarose gel electrophoresis and comparison to a DNA standard. S2 cells were seeded at 10^6 cells/ml, and dsRNA was added directly to the growth medium at a final concentration of 10 μg/ml. After three days, additional dsRNA was added, and the cells were diluted 5-fold on the following day to permit further growth. Eight days after the initial dsRNA treatment, the cells were harvested by centrifugation, washed three times in phosphate-buffered saline, and re-suspended per ml of original culture in 15 μl of lysis buffer (30 mM HEPES-KOH [pH 7.4], 100 mM KOAc, 2 mM $Mg(OAc)_2$), supplemented with protease inhibitors (Complete, Roche). The cells were disrupted either with 50 strokes of a Dounce homogenizer using a "B" pestle or by freeze/thawing. The extract was separated from debris by centrifugation at 18,000 × g for 30 min and aliquots frozen at −80 °C.

In vitro pre-miRNA processing. Synthetic *Drosophila* pre-*let-7* bearing the characteristic end structure created by *Drosha* processing of pri-miRNA (5′-UGA GGU AGU AGG UUG UAU AGU AGU AAU UAC ACA UCA UAC UAU ACA AUG UGC UAG CUU UCU-3′) was 5′-^{32}P radiolabeled with PNK, gel purified, and re-folded by heating at 95 °C for 2 min, then incubating at 37 °C for 1 h. Pre-*let-7* (20 nM) was incubated in a standard RNAi reaction with 50% (v/v) S2 cell lysate for 30 min. The reaction was deproteinized with Proteinase K and Phenol [74], then resolved by electrophoresis in a 15% denaturing polyacrylamide gel. Pre-*let-7* and *let-7* were quantified by phosphorimagery (BAS-5000; Fuji). The fraction processed (y) and time (t) was analyzed using Igor Pro 4.09A (Wavemetrics, Portland, Oregon, United States) by fitting the data to $y = k_1 - k_1 e^{(-k_2 t)}$, where $k_1 k_2$ corresponds to the initial velocity.

Immunoprecipitation and immunoblotting. For immunoprecipitation, 100 μl of S2 cell extract were incubated with 2 μl affinity-purified antibody or 2 μl monoclonal anti-myc antibodies (clone 9E10, Sigma, St. Louis, Missouri, United States) for 30 min at 4 °C. Subsequently, protein A/G agarose (Calbiochem, San Diego, California, United States) or anti-rabbit IgG agarose (eBioscience, San Diego, California, United States) was added and the samples agitated at 4 °C for 90 min. For RNase treatment, RNase A was added to a final concentration of 50 μg/ml, and the samples incubated for 15 min at 4 °C prior to immunoprecipitation. Beads were washed four times with 1 ml of lysis buffer containing 1% (v/v) Triton X-100 (Sigma).

For Western blotting, the proteins were separated on 8% polyacrylamide/SDS gels and transferred to PVDF-membrane. All incubations and washes were in TBS containing 0.02% (v/v) Tween-20. For the rabbit primary antibodies, we used a secondary antibody that does not recognize the reduced form of rabbit IgG (Trueblot, eBioscience), permitting detection of Loqs, which migrates near the heavy antibody chain present in the immunoprecipitates.

To generate anti-Loqs antibody, two rabbits were immunized with the KLH-conjugated peptide MDQENFHGSSC. The specificity of the antibody was verified by Western blotting using extracts prepared from S2 cells transfected with the myc-Loqs PB expression vector, using untransfected S2 cell extract for comparison. Both rabbit antisera reacted with the over-expressed protein and against three small endogenous proteins. The antibody was affinity purified using the peptide antigen immobilized on agarose beads. Anti-Dcr-2 antibody was raised in chicken using the KLH-conjugated peptide CNKADKSKDRTYKTE. IgY was affinity-purified from egg yolk using peptide antigen immobilized on agarose beads. Anti-Drosha antibody was kindly provided by Greg Hannon [10].

Gel-filtration chromatography. 200 μl of S2 cell extract was separated by chromatography on a Superdex-200 HR 10/300 GL column (Amersham-Pharmacia) using a BioCad Sprint (PerSeptive Biosystems, Framingham, Massachusetts, United States) as described [75]. Protein from three-quarters of every other fraction was precipitated with 10% (v/v) trichloroacetic acid and 0.001% (w/v) deoxycholate and analyzed by Western blotting. The remainder of each fraction was analyzed for pre-miRNA processing activity.

Analysis of YFP reporter fluorescence and eye color using the white-IR transgene. Fluorescence and normal light images were taken with a Leica MZ-FLIII stereomicroscope equipped with a cooled color CCD-camera (Firecam, Leica, Wetzlar, Germany). The control animals expressing YFP without the miR-277 target sites contained a pBAC{3xP3-EYFP, p-Gal4Δ-K10} insertion on the X chromosome [66]. Maximal pixel intensity was determined using ImageGuage 4.2 (Fuji). The average intrinsic background fluorescence present in Oregon R eyes ($n = 4$) was subtracted from the value determined for each YFP-expressing eye. Eye pigment was measured as described [76]. The heads of 10 males (3–4 d post eclosion) of each genotype were manually dissected. For each genotype, five samples of two heads each were homogenized in 0.1 ml of 0.01 M HCl in ethanol. The homogenates were placed at 4 °C overnight, warmed to 50 °C for 5 min, clarified by centrifugation, and the optical density at 480 nm of the supernatant measured relative to the value for the Oregon R stock.

Analysis of stellate expression in testes and determination of hatch rates and immunofluorescence microscopy. Stellate expression and hatch rates were analyzed as described previously [24]. Immunofluorescence microscopy was as described previously [77]. Spectrosome and fusome were labeled with monoclonal antibody 1B1 (Developmental Studies Hybridoma Bank, Iowa City, Iowa, United States), as described by Lin and Spradling [78].

Supporting Information

Figure S1. A Concentration Series Generated by Dilution of the Eye Pigment Extract from Oregon R Flies

The concentration of each sample, relative to the undiluted sample, was plotted versus its absorbance at 480 nm. The data were fit to a line using Igor Pro 5.01.

Found at DOI: 10.1371/journal.pbio.0030236.sg001 (622 KB EPS).

Figure S2. Loqs Disrupts Germ-Line Stem Cell Maintenance

Wild type and *loqs* mutants were labeled for α-Spectrin and Actin. In the merged images, α-Spectrin is green; Actin is red. Two examples of wild-type and $loqs^{f00791}$ mutant germaria are shown. In wild type, anti-α-Spectrin labeled both the spectrosome, a spherical structure unique to the germ-line stem cells and their daughters, the cystoblasts, and the highly branched fusome found in the cystocytes. The stem cells are located at the anterior of the germarium. In germaria isolated from 3 to 4 day-old *loqs* mutant females, none of the cells showed a prominent spectrosome, although fusome was detected. Thus, stem cells were originally present but were not maintained. The germ-line cells that remain appear to be cystocytes. The muscle sheath surrounding the ovarioles stains intensely for Actin. α-Spectrin was labeled with a monoclonal antibody; filamentous Actin was labeled with rhodamine-phalloidin.
Scale bar in the upper right panel = 10 μm.

Found at DOI: 10.1371/journal.pbio.0030236.sg002 (4.8 MB EPS).

Accession Numbers

The Arabidopsis Information Resource (http://www.arabidopsis.org) accession numbers for the genes and gene products discussed in this paper are: DCL1 (AT1G01040) and Hyl1 (AT1G09700).

The Ensembl (http://www.ensembl.org/Homo_sapiens) accession numbers for the genes and gene products discussed in this paper are: *C. elegans rde4* (T20G5.11) and *dcr1* (K12H4.8), human DGCR8 (NSG00000128191), Ago2 (ENSG00000123908), Exportin5 (ENSG00000124571) and TRBP (ENSG00000139546), and mouse PRBP (ENSMUSG00000023051).

The FlyBase (http://flybase.bio.indiana.edu) accession numbers for the genes and gene products discussed in this paper are: *ago1* (CG6671, FBgn0026611), *ago2* (CG7439, FBgn0046812), *armi* (CG11513, FBgn0041164), *aub* (CG6137, FBgn0000146), *dcr-1* (CG4792, FBgn0039016), *dcr-2* (CG6493, FBgn0034246), *drosha* (G8730, FBgn0031051), *loqs* (CG6866, FBgn0032515), *pasha* (CG1800, FBgn0039861), *piwi* (CG6122, FBgn0004872), *r2d2* (CG7138, FBgn0031951), *spnE* (CG3158, FBgn0003483), *Stellate* (FBgn0003523), *Su(Ste)* (FBgn0003582), *vasa* (CG3506, FBgn0003970), and *white* (CG2759, FBgn0003996).

The Rfam (http://www.sanger.ac.uk/Software/Rfam/mirna/index.shtml) accession numbers for the genes and gene products discussed in this paper are: *bantam* (MI0000387), *let-7* (MI0000416), miR-277 (MI0000360), miR-7 (MI0000127), and TAR (RF00250).

Acknowledgments

We thank members of the Zamore lab for encouragement, helpful discussions, and comments on the manuscript, and Birgit Koppetsch for help with confocal microscopy. We thank Richard Carthew and Dean P. Smith for kindly sharing fly stocks and Greg Hannon (anti-Dcr-1, anti-Drosha), Maria Pia Bozzetti (anti-Stellate) and Paul Lasko (anti-Vasa) for antibodies, Malcom Fraser for EYFP plasmids, and Inge The and Vivian Su for S2 cell expression vectors. PDZ is a W.M. Keck Foundation Young Scholar in Medical Research. This work was supported in part by grants from the National Institutes of Health to PDZ (GM62862-01 and GM65236-01) and WET (HD049116), and to post-doctoral fellowships from the Human Frontier Science Program to KF and YT.

Competing interests. The authors have declared that no competing interests exist.

Author contributions. KF, YT, TD, VVV, WET, and PDZ conceived and designed the experiments. KF, YT, TD, VVV, DPB, CK, and WET performed the experiments. KF, YT, TD, VVV, DPB, CK, WET, and PDZ analyzed the data. KF, YT, TD, VVV, AMD, DPB, CK, WET, and PDZ contributed reagents/materials/analysis tools. KF, WET, YT, and PDZ wrote the paper. ■

References

1. Bartel DP (2004) MicroRNAs: Genomics, biogenesis, mechanism, and function. Cell 116: 281–297.
2. He L, Hannon GJ (2004) MicroRNAs: Small RNAs with a big role in gene regulation. Nat Rev Genet 5: 522–531.
3. Lee Y, Jeon K, Lee JT, Kim S, Kim VN (2002) MicroRNA maturation: Stepwise processing and subcellular localization. EMBO J 21: 4663–4670.
4. Bracht J, Hunter S, Eachus R, Weeks P, Pasquinelli A (2004) Trans-splicing and polyadenylation of let-7 microRNA primary transcripts. RNA 10: 1586–1594.
5. Cai X, Hagedorn C, Cullen B (2004) Human microRNAs are processed from capped, polyadenylated transcripts that can also function as mRNAs. RNA 10: 1957–1966.
6. Lee Y, Kim M, Han J, Yeom KH, Lee S, et al. (2004) MicroRNA genes are transcribed by RNA polymerase II. EMBO J 23: 4051–4060.
7. Parizotto E, Dunoyer P, Rahm N, Himber C, Voinnet O (2004) In vivo investigation of the transcription, processing, endonucleolytic activity, and functional relevance of the spatial distribution of a plant miRNA. Genes Dev 18: 2237–2242.

8. Baskerville S, Bartel DP (2005) Microarray profiling of microRNAs reveals frequent coexpression with neighboring miRNAs and host genes. RNA 11: 241–247.
9. Lee Y, Ahn C, Han J, Choi H, Kim J, et al. (2003) The nuclear RNase III Drosha initiates microRNA processing. Nature 425: 415–419.
10. Denli AM, Tops BB, Plasterk RH, Ketting RF, Hannon GJ (2004) Processing of primary microRNAs by the Microprocessor complex. Nature 432: 231–235.
11. Gregory RI, Yan KP, Amuthan G, Chendrimada T, Doratotaj B, et al. (2004) The Microprocessor complex mediates the genesis of microRNAs. Nature 432: 235–240.
12. Han J, Lee Y, Yeom KH, Kim YK, Jin H, et al. (2004) The Drosha-DGCR8 complex in primary microRNA processing. Genes Dev 18: 3016–3027.
13. Landthaler M, Yalcin A, Tuschl T (2004) The human DiGeorge syndrome critical region gene 8 and its *D. melanogaster* homolog are required for miRNA biogenesis. Curr Biol 14: 2162–2167.
14. Yi R, Qin Y, Macara IG, Cullen BR (2003) Exportin-5 mediates the nuclear export of pre-microRNAs and short hairpin RNAs. Genes Dev 17: 3011–3016.
15. Lund E, Guttinger S, Calado A, Dahlberg JE, Kutay U (2004) Nuclear export of microRNA precursors. Science 303: 95–98.
16. Zeng Y, Cullen BR (2004) Structural requirements for pre-microRNA binding and nuclear export by Exportin 5. Nucleic Acids Res 32: 4776–4785.
17. Grishok A, Pasquinelli AE, Conte D, Li N, Parrish S, et al. (2001) Genes and mechanisms related to RNA interference regulate expression of the small temporal RNAs that control *C. elegans* developmental timing. Cell 106: 23–34.
18. Hutvágner G, McLachlan J, Pasquinelli AE, Balint , Tuschl T, et al. (2001) A cellular function for the RNA-interference enzyme Dicer in the maturation of the let-7 small temporal RNA. Science 293: 834–838.
19. Ketting RF, Fischer SE, Bernstein E, Sijen T, Hannon GJ, et al. (2001) Dicer functions in RNA interference and in synthesis of small RNA involved in developmental timing in *C. elegans*. Genes Dev 15: 2654–2659.
20. Park W, Li J, Song R, Messing J, Chen X (2002) CARPEL FACTORY, a Dicer homolog, and HEN1, a novel protein, act in microRNA metabolism in *Arabidopsis thaliana*. Curr Biol 12: 1484–1495.
21. Liu Q, Rand TA, Kalidas S, Du F, Kim HE, et al. (2003) R2D2, a bridge between the initiation and effector steps of the *Drosophila* RNAi pathway. Science 301: 1921–1925.
22. Carmell MA, Hannon GJ (2004) RNase III enzymes and the initiation of gene silencing. Nat Struct Mol Biol 11: 214–218.
23. Lee YS, Nakahara K, Pham JW, Kim K, He Z, et al. (2004) Distinct roles for *Drosophila* Dicer-1 and Dicer-2 in the siRNA/miRNA silencing pathways. Cell 117: 69–81.
24. Tomari Y, Du T, Haley B, Schwarz DS, Bennett R, et al. (2004) RISC assembly defects in the *Drosophila* RNAi mutant *armitage*. Cell 116: 831–841.
25. Tomari Y, Matranga C, Haley B, Martinez N, Zamore PD (2004) A protein sensor for siRNA asymmetry. Science 306: 1377–1380.
26. Martinez J, Patkaniowska A, Urlaub H, Lührmann R, Tuschl T (2002) Single-stranded antisense siRNAs guide target RNA cleavage in RNAi. Cell 110: 563–574.
27. Hutvágner G, Zamore PD (2002) A microRNA in a multiple-turnover RNAi enzyme complex. Science 297: 2056–2060.
28. Schwarz DS, Hutvágner G, Haley B, Zamore PD (2002) Evidence that siRNAs function as guides, not primers, in the *Drosophila* and human RNAi pathways. Mol Cell 10: 537–548.
29. Okamura K, Ishizuka A, Siomi H, Siomi MC (2004) Distinct roles for Argonaute proteins in small RNA-directed RNA cleavage pathways. Genes Dev 18: 1655–1666.
30. Parker JS, Roe SM, Barford D (2004) Crystal structure of a PIWI protein suggests mechanisms for siRNA recognition and slicer activity. EMBO J 23: 4727–4737.
31. Song JJ, Smith SK, Hannon GJ, Joshua-Tor L (2004) Crystal structure of Argonaute and its implications for RISC slicer activity. Science 305: 1434–1437.
32. Ma JB, Yuan YR, Meister G, Pei Y, Tuschl T, et al. (2005) Structural basis for 5′-end-specific recognition of guide RNA by the A. fulgidus Piwi protein. Nature 434: 666–670.
33. Parker JS, Roe SM, Barford D (2005) Structural insights into mRNA recognition from a PIWI domain-siRNA guide complex. Nature 434: 663–666.
34. Liu J, Carmell MA, Rivas FV, Marsden CG, Thomson JM, et al. (2004) Argonaute2 is the catalytic engine of mammalian RNAi. Science 305: 1437–1441.
35. Meister G, Landthaler M, Patkaniowska A, Dorsett Y, Teng G, et al. (2004) Human Argonaute2 mediates RNA cleavage targeted by miRNAs and siRNAs. Mol Cell 15: 185–197.
36. Rand TA, Ginalski K, Grishin NV, Wang X (2004) Biochemical identification of Argonaute 2 as the sole protein required for RNA-induced silencing complex activity. Proc Natl Acad Sci U S A 101: 14385–14389.
37. Marchler-Bauer A, Bryant SH (2004) CD-Search: Protein domain annotations on the fly. Nucleic Acids Res 32: W327–331.
38. Drysdale RA, Crosby MA, Gelbart W, Campbell K, Emmert D, et al. (2005) FlyBase: Genes and gene models. Nucleic Acids Res 33 Database Issue: D390–395.
39. Thibault ST, Singer MA, Miyazaki WY, Milash B, Dompe NA, et al. (2004) A complementary transposon tool kit for *Drosophila melanogaster* using P and piggyBac. Nat Genet 36: 283–287.
40. Kennerdell JR, Carthew RW (2000) Heritable gene silencing in *Drosophila* using double-stranded RNA. Nat Biotechnol 18: 896–898.
41. Aravin AA, Naumova NM, Tulin AV, Vagin VV, Rozovsky YM, et al. (2001) Double-stranded RNA-mediated silencing of genomic tandem repeats and transposable elements in the *D. melanogaster* germline. Curr Biol 11: 1017–1027.
42. Schupbach T, Wieschaus E (1991) Female sterile mutations on the second chromosome of *Drosophila melanogaster*. II. Mutations blocking oogenesis or altering egg morphology. Genetics 129: 1119–1136.
43. Gonzalez-Reyes A, Elliott H, St Johnston D (1997) Oocyte determination and the origin of polarity in *Drosophila*: The role of the spindle genes. Development 124: 4927–4937.
44. Cook HA, Koppetsch BS, Wu J, Theurkauf WE (2004) The *Drosophila* SDE3 homolog armitage is required for oskar mRNA silencing and embryonic axis specification. Cell 116: 817–829.
45. Kennerdell JR, Yamaguchi S, Carthew RW (2002) RNAi is activated during *Drosophila* oocyte maturation in a manner dependent on aubergine and spindle-E. Genes Dev 16: 1884–1889.
46. Aravin AA, Klenov MS, Vagin VV, Bantignies F, Cavalli G, et al. (2004) Dissection of a natural RNA silencing process in the *Drosophila* melanogaster germ line. Mol Cell Biol 24: 6742–6750.
47. Lin H, Yue L, Spradling AC (1994) The *Drosophila* fusome, a germline-specific organelle, contains membrane skeletal proteins and functions in cyst formation. Development 120: 947–956.
48. Lin H, Spradling AC (1995) Fusome asymmetry and oocyte determination in *Drosophila*. Dev Genet 16: 6–12.
49. Deng W, Lin H (1997) Spectrosomes and fusomes anchor mitotic spindles during asymmetric germ cell divisions and facilitate the formation of a polarized microtubule array for oocyte specification in *Drosophila*. Dev Biol 189: 79–94.
50. Lasko P (2000) The *Drosophila melanogaster* genome: Translation factors and RNA binding proteins. J Cell Biol 150: F51–56.
51. Tabara H, Yigit E, Siomi H, Mello CC (2002) The dsRNA binding protein RDE-4 interacts with RDE-1, DCR-1, and a DexH-Box helicase to direct RNAi in *C. elegans*. Cell 109: 861–871.
52. Han MH, Goud S, Song L, Fedoroff N (2004) The *Arabidopsis* double-stranded RNA-binding protein HYL1 plays a role in microRNA-mediated gene regulation. Proc Natl Acad Sci U S A 101: 1093–1098.
53. Vazquez F, Gasciolli V, Crete P, Vaucheret H (2004) The nuclear dsRNA binding protein HYL1 is required for microRNA accumulation and plant development, but not posttranscriptional transgene silencing. Curr Biol 14: 346–351.
54. Hiraguri A, Itoh R, Kondo N, Nomura Y, Aizawa D, et al. (2005) Specific interactions between Dicer-like proteins and HYL1/DRBfamily dsRNA-binding proteins in *Arabidopsis thaliana*. Plant Mol Biol 57: 173–188.
55. Gatignol A, Buckler-White A, Berkhout B, Jeang KT (1991) Characterization of a human TAR RNA-binding protein that activates the HIV-1 LTR. Science 251: 1597–1600.
56. Berkhout B, Silverman RH, Jeang KT (1989) Tat *trans*-activates the human immunodeficiency virus through a nascent RNA target. Cell 59: 273–282.
57. Dingwall C, Ernberg I, Gait MJ, Green SM, Heaphy S, et al. (1990) HIV-1 tat protein stimulates transcription by binding to a U-rich bulge in the stem of the TAR RNA structure. EMBO J 9: 4145–4153.
58. Marciniak RA, Calnan BJ, Frankel AD, Sharp PA (1990) HIV-1 Tat protein *trans*-activates transcription in vitro. Cell 63: 791–802.
59. Pfeffer S, Zavolan M, Grasser FA, Chien M, Russo JJ, et al. (2004) Identification of virus-encoded microRNAs. Science 304: 734–736.
60. Bennasser Y, Le SY, Yeung ML, Jeang KT (2004) HIV-1 encoded candidate micro-RNAs and their cellular targets. Retrovirology 1: 43.
61. Zhong J, Peters AH, Lee K, Braun RE (1999) A double-stranded RNA binding protein required for activation of repressed messages in mammalian germ cells. Nat Genet 22: 171–174.
62. Bernstein E, Kim SY, Carmell MA, Murchison EP, Alcorn H, et al. (2003) Dicer is essential for mouse development. Nat Genet 35: 215–217.
63. Pham JW, Pellino JL, Lee YS, Carthew RW, Sontheimer EJ (2004) A Dicer-2-dependent 80s complex cleaves targeted mRNAs during RNAi in *Drosophila*. Cell 117: 83–94.
64. Cox DN, Chao A, Baker J, Chang L, Qiao D, et al. (1998) A novel class of evolutionarily conserved genes defined by piwi are essential for stem cell self-renewal. Genes Dev 12: 3715–3727.
65. Cox DN, Chao A, Lin H (2000) piwi encodes a nucleoplasmic factor whose activity modulates the number and division rate of germline stem cells. Development 127: 503–514.
66. Horn C, Offen N, Nystedt S, Hacker U, Wimmer EA (2003) piggyBac-based insertional mutagenesis and enhancer detection as a tool for functional insect genomics. Genetics 163: 647–661.
67. Church G, Gilbert W (1984) Genomic sequencing. Proc Natl Acad Sci U S A 81: 1991–1995.
68. Berghammer A, Klingler M, Wimmer E (1999) A universal marker for transgenic insects. Nature 402: 370–371.
69. Horn C, Jaunich B, Wimmer E (2000) Highly sensitive, fluorescent transformation marker for *Drosophila* transgenesis. Dev Genes Evol 210: 623–629.

70. Horn C, Wimmer E (2000) A versatile vector set for animal transgenesis. Dev Genes Evol 210: 630–637.
71. Simon JA, Sutton CA, Lobell RB, Glaser RL, Lis JT (1985) Determinants of heat shock-induced chromosome puffing. Cell 40: 805–817.
72. Rubin GM, Spradling AC (1982) Genetic transformation of *Drosophila* with transposable element vectors. Science 218: 348–353.
73. Kovalic D, Kwak JH, Weisblum B (1991) General method for direct cloning of DNA fragments generated by the polymerase chain reaction. Nucleic Acids Res 19: 4560.
74. Haley B, Tang G, Zamore PD (2003) In vitro analysis of RNA interference in *Drosophila melanogaster*. Methods 30: 330–336.
75. Nykänen A, Haley B, Zamore PD (2001) ATP requirements and small interfering RNA structure in the RNA interference pathway. Cell 107: 309–321.
76. Pal-Bhadra M, Leibovitch BA, Gandhi SG, Rao M, Bhadra U, et al. (2004) Heterochromatic silencing and HP1 localization in *Drosophila* are dependent on the RNAi machinery. Science 303: 669–672.
77. Theurkauf WE (1994) Immunofluorescence analysis of the cytoskeleton during oogenesis and early embryogenesis. Methods Cell Biol 44: 489–505.
78. Lin H, Spradling A (1997) A novel group of pumilio mutations affects the asymmetric division of germline stem cells in the *Drosophila* ovary. Development 124: 2463–2476.

microPrimer: the biogenesis and function of microRNA

Tingting Du and Phillip D. Zamore*

Department of Biochemistry and Molecular Pharmacology, University of Massachusetts Medical School, Worcester, MA 01605, USA

*Author for correspondence (e-mail: phillip.zamore@umassmed.edu)

Development 132, 4645-4652
Published by The Company of Biologists 2005
doi:10.1242/dev.02070

Summary

Discovered in nematodes in 1993, microRNAs (miRNAs) are non-coding RNAs that are related to small interfering RNAs (siRNAs), the small RNAs that guide RNA interference (RNAi). miRNAs sculpt gene expression profiles during plant and animal development. In fact, miRNAs may regulate as many as one-third of human genes. miRNAs are found only in plants and animals, and in the viruses that infect them. miRNAs function very much like siRNAs, but these two types of small RNAs can be distinguished by their distinct pathways for maturation and by the logic by which they regulate gene expression.

Development

microHistory

The first miRNA, *lin-4*, was identified in 1993 in a genetic screen for mutants that disrupt the timing of post-embryonic development in *Caenorhabditis elegans* (Lee et al., 1993). Cloning of the locus revealed that *lin-4* produces a 22-nucleotide non-coding RNA, rather than a protein-coding mRNA (Lee et al., 1993). *lin-4* represses the expression of *lin-14*, which encodes a nuclear protein (Lee et al., 1993; Wightman et al., 1993) whose concentration must be reduced for worms to progress from their first larval stage to the second (Rougvie, 2005). The negative regulation of *lin-14* by *lin-4* requires partial complementarity between *lin-4* and sites in the 3′-untranslated region (UTR) of *lin-14* mRNA (Ha et al., 1996; Olsen and Ambros, 1999). It was not until 2000 that a second miRNA, *let-7*, was discovered, again in worms (Reinhart et al., 2000). *let-7* functions in a manner similar to *lin-4*, repressing the expression of the *lin-41* and *hbl-1* mRNAs by binding to their 3′ UTRs (Reinhart et al., 2000; Slack et al., 2000; Lin et al., 2003; Vella et al., 2004). *let-7* is conserved throughout metazoans (Pasquinelli et al., 2000), and the discovery of *let-7* (Reinhart et al., 2000), together with the subsequent large-scale searches for additional miRNAs, established miRNAs as a new and large class of ribo-regulators (Lagos-Quintana et al., 2001; Lau et al., 2001; Lee and Ambros, 2001), and fueled speculation that tiny RNAs are a major feature of the gene regulatory networks of animals. Now more than 1600 miRNAs have been identified in plants, animals and viruses (Lai et al., 2003; Lim et al., 2003a; Lim et al., 2003b). The human genome alone may contain 800-1000 miRNAs, a large portion of which may be specific to primates (Bentwich et al., 2005; Berezikov et al., 2005; Xie et al., 2005).

microMaturation

miRNAs are transcribed by RNA polymerase II as primary miRNAs (pri-miRNAs), which range from hundreds to thousands of nucleotides in length (Cai et al., 2004; Lee et al., 2004; Parizotto et al., 2004). Most miRNAs are transcribed from regions of the genome that are distinct from previously annotated protein-coding sequences (Fig. 1). Some miRNA-encoding loci reside well apart from other miRNAs, suggesting that they form their own transcription units; others are clustered and share similar expression patterns, implying that they are transcribed as polycistronic transcripts (Lagos-Quintana et al., 2001; Lau et al., 2001; Lee et al., 2002; Reinhart et al., 2002). About half of the known mammalian miRNAs are within the introns of protein-coding genes, or within either the introns or exons of non-coding RNAs, rather than in their own unique transcription units (Rodriguez et al., 2004). Intronic miRNAs usually lie in the same orientation as, and are coordinately expressed with, the pre-mRNA in which they reside; that is, they share a single primary transcript (Rodriguez et al., 2004; Baskerville and Bartel, 2005). A very few miRNAs reside in the untranslated regions of protein-coding mRNAs; it is likely that these transcripts can make either the miRNA or the protein, but not both, from a single molecule of mRNA (Cullen, 2004).

Animal microMaturation

In animals, two processing steps yield mature miRNAs (Fig. 2A). Each step is catalyzed by a ribonuclease III (RNase III) endonuclease together with a double-stranded RNA-binding domain (dsRBD) protein partner. First, Drosha, a nuclear RNase III, cleaves the flanks of pri-miRNA to liberate an ~70-nucleotide stem loop, the precursor miRNA (pre-miRNA) (Lee et al., 2002; Lee et al., 2003; Denli et al., 2004; Gregory et al., 2004; Han et al., 2004; Landthaler et al., 2004). The efficient processing of pri-miRNA by Drosha requires: a large terminal loop (⩾10 nucleotides) in the hairpin; a stem region that is about one helical turn longer than the slightly more than two helical turns of the stem of the resulting pre-miRNA; and 5′ and 3′ single-stranded RNA extensions at the base of the future pre-miRNA (Lee et al., 2003; Zeng and Cullen, 2003; Zeng and Cullen, 2005; Zeng et al., 2005). Accurate and efficient pri-miRNA processing by Drosha requires a dsRBD protein, known as Pasha in *Drosophila*, Pash-1 *C. elegans* and DGCR8 in mammals (Denli et al., 2004; Gregory et al., 2004; Han et al., 2004; Landthaler et al., 2004). The resulting pre-miRNA have 5′ phosphate and 3′ hydroxy termini, and two- or three-nucleotide 3′ single-stranded overhanging ends, all of which are characteristics of RNase III cleavage of dsRNA. Thus, Drosha cleavage defines either the 5′ or the 3′ end of the mature miRNA. (The mature miRNA resides in the 5′ arm of some pre-miRNA and in the 3′ arm in others.) The pre-miRNA is then exported from nucleus to cytoplasm by Exportin 5/RanGTP, which specifically recognizes the characteristic end structure of pre-miRNAs (Yi et al., 2003; Bohnsack et al., 2004; Lund et al., 2004; Zeng and Cullen, 2004).

In the cytoplasm, a second RNase III, Dicer, together with its dsRBD protein partner, Loquacious (Loqs) in *Drosophila* or the *trans-activator RNA (tar)*-binding protein (TRBP) in humans, makes a pair of cuts that defines the other end of the mature miRNA, liberating an ~21-nucleotide RNA duplex (Bernstein et al., 2001; Grishok et al., 2001; Hutvagner et al., 2001; Ketting et al., 2001; Chendrimada et al., 2005; Forstemann et al., 2005; Jiang et al., 2005; Saito et al., 2005). This RNA duplex has essentially the same structure as a double-stranded siRNA, except that the mature miRNA is only partially paired to the miRNA* – the small RNA that resides on the side of the pre-miRNA stem opposite the miRNA – because the stems of pre-miRNAs are imperfectly double stranded. From the miRNA/miRNA* duplex, one strand, the miRNA, preferentially enters the protein complex that represses target gene expression, the RNA-induced silencing complex (RISC), whereas the other strand, the miRNA* strand, is degraded. The choice of strand relies on the local thermodynamic stability of the miRNA/miRNA* duplex – the strand whose 5′ end is less stably paired is loaded into the RISC (Khvorova et al., 2003; Schwarz et al., 2003). This thermodynamic difference arises, in part, because miRNAs tend to begin with uracil, and, in part, because miRNA/miRNA* duplexes contain mismatches and bulges that favor the miRNA strand being loaded into the RISC.

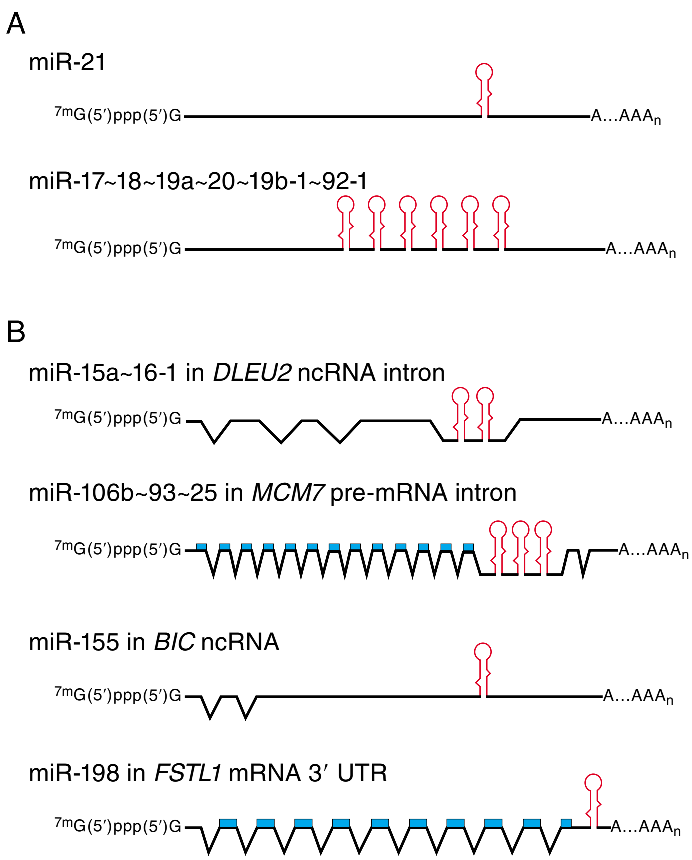

Fig. 1. The structure of human pri-miRNAs. (A) Two examples of miRNAs with their own transcription units, such as miR-21 and the polycistronic miR-17–92-1 cluster (Cai et al., 2004; He et al., 2005). (B) miRNAs that are transcribed with other genes. miR-15a~16-1 resides in the intron of a non-coding RNA (ncRNA) (Calin et al., 2004) and miR-106b~93~25 lies in the intron of a protein-coding RNA (Rodriguez et al., 2004). miR-155 is found in the exon of a ncRNA (Eis et al., 2005), whereas miR-198 is in the exon of a protein-coding mRNA (Cullen, 2004). DLEU2, deleted in lymphocytic leukemia 2; MCM7, minichromosome maintenance deficient 7; BIC, B-cell integration cluster; FSTL1, follistatin-like 1.

Plant microMaturation

miRNA maturation in plants differs from the pathway in animals because plants lack a Drosha homolog (Fig. 2B). Instead, the RNase III enzyme DICER-LIKE 1 (DCL1), which is homologous to animal Dicer, is required for miRNA maturation (Park et al., 2002; Reinhart et al., 2002; Papp et al., 2003; Xie et al., 2004). In plants, DCL1 is localized in the nucleus and can make both the first pair of cuts made by Drosha and the second pair of cuts made by animal Dicer. As for animal Dicer, a dsRNA-binding domain protein partner, HYL1, has been implicated in DCL1 function in plant miRNA maturation (Papp et al., 2003; Vazquez et al., 2004a). The resulting miRNA/miRNA* duplex is exported from the nucleus by HASTY (HST), the plant ortholog of Exportin 5, and completes its assembly into the RISC in the cytoplasm (Peragine et al., 2004; Park et al., 2005). Unlike animal miRNAs, which end with free 2′, 3′ hydroxyl groups, plant miRNAs have a methyl group on the ribose of the last nucleotide. The terminal methyl group is added by the *S*-adenosyl methionine (SAM)-dependent methyltranferase HEN1, and the modification of the miRNA by HEN1 either protects the miRNA from further modification or degradation, or may facilitate its assembly into the RISC (Boutet et al., 2003; Yu et al., 2005). In plants, RNA-dependent RNA polymerases may use small RNAs as primers to synthesize double-stranded RNA from aberrant single-stranded transcripts, raising the possibility that the terminal methoxy modification on miRNA serves to prevent miRNA from acting as primers.

The RISC directs gene silencing

The RISC carries out small RNA-directed gene silencing in both the miRNA and the RNAi pathways in plants and animals (Hammond et al., 2000; Hammond et al., 2001; Hutvagner and Zamore, 2002; Zeng et al., 2002; Doench et al., 2003). When the small RNA guide in the RISC pairs extensively to a target mRNA, the RISC functions as an endonuclease, cleaving the mRNA between the target nucleotides paired to bases 10 and 11 of the miRNA or siRNA. The core component of every RISC is a member of the Argonaute (Ago) protein family, whose members all contain a central PAZ domain (named after the family member proteins Piwi, Argonaute and Zwille) and a carboxy terminal PIWI domain. Structural studies show that the PIWI domain binds to small RNAs at their 5′ end, whereas the PAZ domain binds to the 3′ end of single-stranded RNAs (Song et al., 2003; Yan et al., 2003; Lingel et al., 2004; Parker et al., 2004; Ma et al., 2005; Parker et al., 2005).

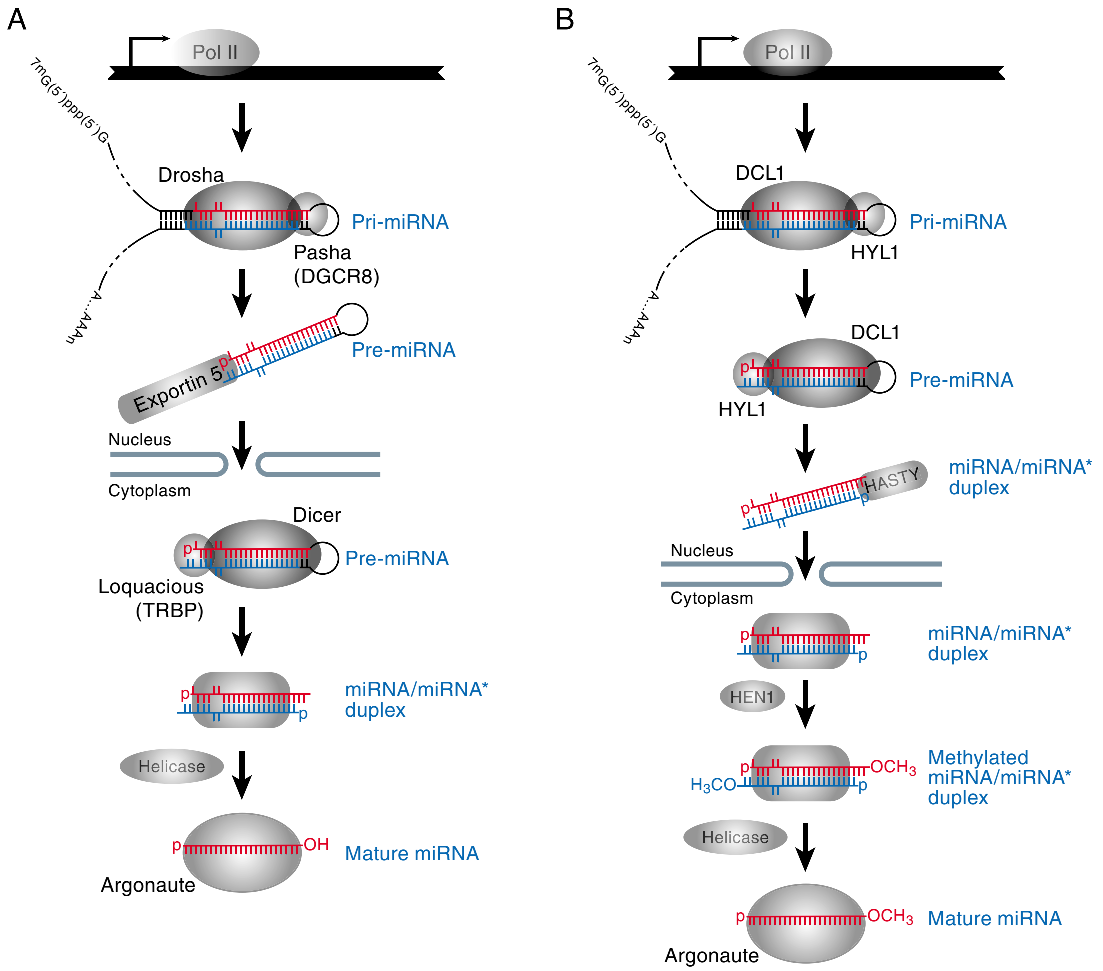

Fig. 2. The miRNA biogenesis pathway. (A) Animal and (B) plant miRNA biogenesis. Mature miRNAs are indicated in red, whereas the miRNA* strands are in blue.

Moreover, the three-dimensional structure of the PIWI domain closely resembles that of RNase H, the enzyme that cleaves the RNA strand of an RNA-DNA hybrid (Song et al., 2004; Nowotny et al., 2005), and both structural and biochemical studies have confirmed that Argonaute is the target-cleaving endonuclease of the RISC (Liu et al., 2004; Rand et al., 2004; Song et al., 2004; Bamberger and Baulcombe, 2005; Qi et al., 2005; Rivas et al., 2005). Notably, a subpopulation of Argonaute proteins do not retain all the amino acids that are crucial for RISC catalytic activity, and thus cannot cleave a target RNA even when the small RNA guide is sufficiently complimentary to the target (Liu et al., 2004; Meister et al., 2004b; Rivas et al., 2005). The RISC-associated proteins include the putative RNA-binding protein VIG (Vasa intronic gene), the Fragile-X related protein in *Drosophila*, the exonuclease Tudor-SN, and several putative helicases (Caudy et al., 2002; Hutvagner and Zamore, 2002; Ishizuka et al., 2002; Mourelatos et al., 2002; Caudy et al., 2003). The molecular function of these proteins in RNA silencing is not known.

microMechanism

miRNAs regulate their target genes via two main mechanisms: target mRNA cleavage and 'translational repression'.

In plants, most miRNAs have perfect or near perfect complementarity to their mRNA targets (Rhoades et al., 2002). Upon binding to their mRNA targets, the miRNA-containing RISCs function as endonucleases, cleaving the mRNA (Llave et al., 2002; Tang et al., 2003). Single miRNA-binding motifs are found both in the coding regions, such as the miR-166-targeting site in the *PHABULOSA* mRNA, and in the untranslated regions of miRNA-regulated plant mRNAs, such as the miR-156-targeting site in the *SPL4* mRNA, albeit mainly in coding sequences, perhaps because cleavage here most strongly inactivates translation of the mRNA into functional protein (Rhoades et al., 2002). At least eight animal miRNA, miR-127, miR-136, miR-196, miR-431, miR-433-3p, miR-433-5p, miR-434-3p and miR-434-5, and two viral miRNAs, miR-BART2 and SVmiRNA, also act to cleave their targets (Mansfield et al., 2004; Pfeffer et al., 2004; Yekta et al., 2004; Davis et al., 2005; Sullivan et al., 2005).

In contrast to plant miRNAs, the complementarity between animal miRNAs and their targets is usually restricted to the 5′ region (nucleotides 2-8 or 2-7) of the miRNA, i.e. to the 3′ region of the target site (Lewis et al., 2003; Lai, 2004; Brennecke et al., 2005; Lewis et al., 2005; Xie et al., 2005). This 5′ miRNA region has been called the 'seed region' to describe its disproportionate contribution to target-RNA binding. Because the seed region of a miRNA is so short, miRNA are predicted to regulate surprisingly large numbers of genes; the complete complement of human miRNAs may regulate as many as one-third of the human protein-coding genes (Lewis et al., 2005; Xie et al., 2005)! In the absence of extensive complementarity between the miRNA and the target, binding of the RISC blocks translation of the target mRNA into protein, rather than catalyzing its cleavage into two pieces (Olsen and Ambros, 1999). Recent results suggest that regulation by miRNAs can direct target mRNA degradation through a pathway that is distinct from small RNA-directed endonucleolytic cleavage (Bagga et al., 2005; Lim et al., 2005). In human cells, the core component of the RISCs, Argonaute proteins, together with mRNAs that are targeted for silencing by miRNAs are concentrated in cytoplasmic foci called Processing bodies (P-bodies) (Liu et al., 2005; Pillai et al., 2005; Sen and Blau, 2005). (P-bodies are also known as cytoplasmic bodies or GW-bodies.) miRNAs may initially block translational initiation, causing the miRNA-programmed RISC and the target mRNA to be re-localized to the P-body (Pillai et al., 2005). In *C. elegans*, a P-body protein, AIN-1, interacts with the miRNA-programmed RISC component ALG-1, an Argonaute protein, and is sufficient to localize ALG-1 to the P-body (Ding et al., 2005). Thus, P-body-mediated miRNA-directed regulation may be a general mechanism among animals.

microFunctions

miRNAs function in a broad range of biological processes in plants and animals (Kidner and Martienssen, 2005; Alvarez-Garcia and Miska, 2005). The first insight into their function came from phenotypic studies of mutations that disrupt core components of the miRNA pathway. *dicer* mutants show diverse developmental defects, including abnormal embryogenesis in *Arabidopsis*, delayed germ-line stem-cell (GSC) division in *Drosophila*, germ-line defects in *C. elegans*, abnormal embryonic morphogenesis in zebrafish and stem-cell differentiation defects in mice (Knight and Bass, 2001; Park et al., 2002; Bernstein et al., 2003; Wienholds et al., 2003; Giraldez et al., 2005; Hatfield et al., 2005). Similarly, the disruption of Argonaute function causes widespread developmental defects, such as defective stem-cell maintenance and failure to form axillary meristem in an *Arabidopsis* mutant for *PINHEAD/ZWILLE (PNH/ZLL)* or *ARGONAUTE 1 (AGO1)*, a stem-cell self-renewal defect in *Drosophila piwi* mutants, and defective early development in *C. elegans alg-1* and *alg-2* mutants (Bohmert et al., 1998; Cox et al., 1998; Moussian et al., 1998; Grishok et al., 2001). *Arabidopsis* plants mutant for *ZIPPY* (*ZIP*), an Argonaute gene, and *HASTY* (*HST*), which encodes the miRNA export receptor, exhibit a precocious vegetative phenotype and produce abnormal flowers (Peragine et al., 2004). Overall, these phenotypes suggest that at least a subset of miRNAs play important roles in early development.

Target prediction

The functional characterization of miRNAs relies largely on the identification of their regulatory targets. In plants, because miRNAs are almost perfectly complementary to their targets, target prediction is straightforward (Rhoades et al., 2002), and automated plant miRNA target prediction can now be performed online (Zhang, 2005). At least half of the predicted plant miRNA targets are transcription factors, although transcription factors represent only 6% of *Arabidopsis* protein-coding genes (Riechmann et al., 2000; Rhoades et al., 2002; Jones-Rhoades et al., 2004). Typically, many members of a family of related transcription factors are coordinately repressed by a single miRNA. These miRNA-regulated transcription factors control developmental patterning, cell proliferation, and environmental and hormonal responses (Kidner and Martienssen, 2005). *DCL1* and *AGO1* themselves are also miRNA targets, suggesting a negative-feedback mechanism in which miRNAs tune their own expression (Rhoades et al., 2002a; Xie et al., 2003; Vaucheret et al., 2004).

The bioinformatic prediction of animal miRNA targets is more complex because animal miRNAs display only modest complementarity to their targets. Different algorithms have been developed to predict animal miRNA targets, using at least some of the following criteria: (1) perfect or nearly perfect pairing of the 'seed region' at the 5′ end of the miRNAs and the 3′ UTR of the target mRNA; (2) putative miRNA-binding site conservation between closely related species; (3) multiple miRNA-binding sites in a single target; and (4) lack of a strong secondary structure at the miRNA-binding site on the target (Enright et al., 2003; Lewis et al., 2003; Stark et al., 2003; Kiriakidou et al., 2004; Rajewsky and Socci, 2004; Brennecke et al., 2005; Krek et al., 2005; Lewis et al., 2005; Zhao et al., 2005). The computational prediction of animal miRNA targets suggests that the logic of miRNA regulation differs between animals and plants (see Box 1). In animals, miRNA has been proposed to fine-tune the expression of hundreds of genes, but to dramatically downregulate the expression of a much smaller number of transcripts (Bartel, 2004); such dramatic downregulation of transcript levels appears to be widespread for plant miRNAs. Moreover, animal miRNAs, but perhaps not plant miRNAs, may act combinatorially, with several miRNAs binding a single transcript. Thus, one miRNA might be expressed early in development, reducing the steady-state level of protein synthesis from a targeted mRNA by just a bit, a tuning function. The subsequent expression of additional miRNAs targeting the same mRNA would lower its expression still further (Bartel, 2004). Cell culture experiments suggest that when multiple miRNAs bind the same target, they act cooperatively, reducing mRNA translation by more than the sum of their individual effects (Doench et al., 2003).

miRNA-target relationships can also be identified by beginning with a target mRNA and searching for one or more regulatory miRNAs. In one case, the earlier finding that GY-box, Brd-box and K-box motifs in the 3′ UTR of Notch mRNAs mediate their post-transcriptional repression helped to identify three families of *Drosophila* miRNAs that are direct regulators of Notch target genes (Lai and Posakony, 1997; Lai et al., 1998; Lai, 2002; Stark et al., 2003; Lai et al., 2005). Another example is the proposal that miR-16 in *Drosophila* plays a role in AU-rich element (ARE)-mediated mRNA degradation (Jing et al., 2005). Because depletion by RNAi of key RNA silencing proteins – Dcr-1, Ago-1 and Ago-2 – inhibited the rapid mRNA decay normally triggered by AREs, the authors broke with 'microOrthodoxy' and proposed that the ARE is a potential miRNA target site, perhaps binding miR-16 in a unconventional mode that does not require seed-sequence pairing.

Development

microProfiling

miRNA profiling has also been used to identify miRNAs with potentially important developmental roles. The rationale is that if a miRNA is highly expressed in a tissue or cell type or at a specific developmental stage, it may reasonably play a regulatory role in specifying tissue or cell identity, or in regulating developmental timing. miRNA expression can be profiled by the cloning and sequencing miRNAs from specific tissues or developmental states (a labor-intensive method that has the benefit of uncovering new miRNAs), or by microarray analysis (a more high-throughput method that can only reveal the expression of known miRNAs). For example, *miR-181*, which is highly expressed in mouse bone marrow B-lymphoid cells, but not in T-cells, was found to promote hematopoietic differentiation towards the B-cell lineage (Chen et al., 2004). *miR-375*, an evolutionarily conserved, pancreatic islet-specific miRNA identified by small RNA cloning from glucose-responsive murine pancreatic cell lines, suppresses glucose-induced insulin secretion by repressing *myotrophin* (*Mtpn*) expression (Poy et al., 2004). miRNA expression profiling has also identified a zebrafish miRNA that regulates brain morphogenesis, *miR-430*, whose expression peaks 4 hours after fertilization (when most fish miRNAs are first expressed) and decreases after 24 hours (Chen et al., 2005; Giraldez et al., 2005), and also *miR-1*, a mouse miRNA whose expression is confined to cardiac and skeletal muscle precursor cells, and which may control the balance between differentiation and proliferation during cardiogenesis by regulating the expression of *Hand2* mRNA (Wienholds et al., 2005; Zhao et al., 2005).

To date, hundreds of miRNAs have been identified in different organisms, which makes it possible to study their function individually by suppressing their expression in cells. However, genetic depletion, i.e. making miRNA mutants, is labor intensive. 2′-*O*-methyl antisense oligonucleotides complementary to endogenous miRNAs provide an alternative to genetic mutation. These antisense oligonucleotides transiently block miRNA function (Hutvagner et al., 2004; Meister et al., 2004a). Thus, injecting into worms a 2′-*O*-methyl oligonucleotide that binds *let-7* recapitulates the *let-7* mutant phenotype (Hutvagner et al., 2004). In early syncitial *Drosophila* embryos, where injection of oligonucleotides is straightforward, a panel of 2′-*O*-methyl oligonucleotides was used to reveal the embryonic loss-of-function phenotypes of 46 miRNAs (Leaman et al., 2005). This study suggests that miRNAs specifically regulate a broad range of developmental events. In another study, Lecellier et al. used antisense locked-nucleic acid (LNA) oligonucleotides, nucleic acid molecules that are modified to dramatically increase their binding affinities, to block miR-32 in cultured human cells, a miRNA proposed to mediate innate anti-viral defense (Lecellier et al., 2005). RNAi itself has also been used to block miRNA expression in cultured cells, but its broad utility is not yet established (Jing et al., 2005; Lee et al., 2005).

Human viruses also express their own miRNAs (Pfeffer et al., 2004; Cai et al., 2005; Pfeffer et al., 2005; Sullivan et al., 2005). Viral miRNAs are proposed to regulate both viral and host gene expression (Pfeffer et al., 2004; Cai et al., 2005), but only viral mRNA targets have been experimentally validated (Pfeffer et al., 2004). Recently, Simian Virus 40-encoded miRNAs have been identified. These viral miRNAs accumulate at late times in infection, and target early viral RNAs for cleavage and reduce viral susceptibility to cytotoxic T cells (Sullivan et al., 2005). Whether viral miRNAs always mediate the cleavage of viral mRNAs or whether they can also act more like animal miRNAs to 'tune' gene expression remains unknown.

Box 1. MicroRNAs and siRNAs: the logic of small RNAs

Small interfering RNAs (siRNAs) are a class of small RNA guides that are distinct from miRNAs (Tomari and Zamore, 2005). These two classes of RNA cannot be distinguished by either their chemical composition or their function. Both are produced by Dicer-mediated cleavage of longer, double-stranded RNA precursors. Consequently, both miRNAs and siRNAs are ~21 nucleotides in length, with 5′-phosphate and 3′-hydroxy termini. siRNAs and miRNAs are functionally interchangeable: both can direct target mRNA cleavage or translational repression, depending on the degree of complementarity between the small RNA and its target. Nonetheless, the two classes of small RNAs can be distinguished both by their biogenesis pathways and by the logic by which they regulate target genes, especially in animals. miRNAs are processed from small hairpin transcripts, called pre-miRNAs, which are embedded in much longer primary transcripts, the pri-miRNA. Each miRNA corresponds to ~21 nucleotides of one arm of the pre-miRNA stem. The resulting miRNA may regulate tens or hundreds of target RNAs, whose only common features are the short sequences that are complementary to as few as six or seven bases of the miRNA. siRNAs, by contrast, derive from endogenous or exogenous long double-stranded RNAs, typically comprising hundreds or thousands of base pairs. Such precursor double-stranded RNAs typically yield many siRNAs from both strands. The regulatory targets of siRNAs are usually highly homologous to the trigger double-stranded RNA itself, i.e. the trigger and target genes are paralogs. In some cases, such as with heterochromatic siRNAs, which initiate heterochromatin assembly, the trigger and target genes are one-and-the-same. A notable exception is trans-acting siRNAs (tasiRNAs) in plants, in which only a few of the many siRNAs generated from the long, double-stranded RNA trigger appear to correspond to regulated target RNAs (Allen et al., 2005; Peragine et al., 2004; Vazquez et al., 2004b).

microPrognostication

A dozen years after their discovery, miRNAs represent a large class of regulators of gene expression that control a broad range of physiological and developmental processes in plants and animals. An immediate challenge is to tabulate the functions of each and every miRNA. For this, improved computational and experimental methods for the identification of miRNA targets will be essential. These efforts will no doubt be informed by our expanding knowledge of the mechanism by which miRNAs recognize and regulate their targets. The regulation of miRNA expression and maturation remains largely unknown, but many laboratories have begun to map where miRNAs are expressed and what factors regulate their transcription. Perhaps the most important goal in understanding miRNAs will be to describe how miRNAs function as a network, for it is in studying the coordinate action of multiple miRNAs on a single mRNA target that we are likely to reach a deeper understanding of the logic of these small but powerful ribo-regulators.

References

Allen, E., Xie, Z., Gustafson, A. M. and Carrington, J. C. (2005). microRNA-directed phasing during trans-acting siRNA biogenesis in plants. *Cell* **121**, 207-221.

Alvarez-Garcia, I. and Miska, E. A. (2005). MicroRNA function: animal development and human disease. *Development* **132**, 4653-4662.

Bagga, S., Bracht, J., Hunter, S., Massirer, K., Holtz, J., Eachus, R. and Pasquinelli, A. E. (2005). Regulation by let-7 and lin-4 miRNAs results in target mRNA degradation. *Cell* **122**, 553-563.

Bartel, D. P. (2004). MicroRNAs: genomics, biogenesis, mechanism, and function. *Cell* **116**, 281-297.

Baskerville, S. and Bartel, D. P. (2005). Microarray profiling of microRNAs reveals frequent coexpression with neighboring miRNAs and host genes. *RNA* **11**, 241-247.

Baumberger, N. and Baulcombe, D. C. (2005). Arabidopsis ARGONAUTE1 is an RNA Slicer that selectively recruits microRNAs and short interfering RNAs. *Proc. Natl. Acad. Sci. USA* **102**, 11928-11933.

Bentwich, I., Avniel, A., Karov, Y., Aharonov, R., Gilad, S., Barad, O., Barzilai, A., Einat, P., Einav, U., Meiri, E. et al. (2005). Identification of hundreds of conserved and nonconserved human microRNAs. *Nat. Genet.* **37**, 766-770.

Berezikov, E., Guryev, V., van de Belt, J., Wienholds, E., Plasterk, R. H. and Cuppen, E. (2005). Phylogenetic shadowing and computational identification of human microRNA genes. *Cell* **120**, 21-24.

Bernstein, E., Caudy, A. A., Hammond, S. M. and Hannon, G. J. (2001). Role for a bidentate ribonuclease in the initiation step of RNA interference. *Nature* **409**, 363-366.

Bernstein, E., Kim, S. Y., Carmell, M. A., Murchison, E. P., Alcorn, H., Li, M. Z., Mills, A. A., Elledge, S. J., Anderson, K. V. and Hannon, G. J. (2003). Dicer is essential for mouse development. *Nat. Genet.* **35**, 215-217.

Bohmert, K., Camus, I., Bellini, C., Bouchez, D., Caboche, M. and Benning, C. (1998). AGO1 defines a novel locus of Arabidopsis controlling leaf development. *EMBO J.* **17**, 170-180.

Bohnsack, M. T., Czaplinski, K. and Gorlich, D. (2004). Exportin 5 is a RanGTP-dependent dsRNA-binding protein that mediates nuclear export of pre-miRNAs. *RNA* **10**, 185-191.

Boutet, S., Vazquez, F., Liu, J., Beclin, C., Fagard, M., Gratias, A., Morel, J. B., Crete, P., Chen, X. and Vaucheret, H. (2003). Arabidopsis HEN1: a genetic link between endogenous miRNA controlling development and siRNA controlling transgene silencing and virus resistance. *Curr. Biol.* **13**, 843-848.

Brennecke, J., Stark, A., Russell, R. B. and Cohen, S. M. (2005). Principles of microRNA-target recognition. *PLoS Biol.* **3**, E85.

Cai, X., Hagedorn, C. H. and Cullen, B. R. (2004). Human microRNAs are processed from capped, polyadenylated transcripts that can also function as mRNAs. *RNA* **10**, 1957-1966.

Cai, X., Lu, S., Zhang, Z., Gonzalez, C. M., Damania, B. and Cullen, B. R. (2005). Kaposi's sarcoma-associated herpesvirus expresses an array of viral microRNAs in latently infected cells. *Proc. Natl. Acad. Sci. USA* **102**, 5570-5575.

Calin, G. A., Sevignani, C., Dumitru, C. D., Hyslop, T., Noch, E., Yendamuri, S., Shimizu, M., Rattan, S., Bullrich, F., Negrini, M. et al. (2004). Human microRNA genes are frequently located at fragile sites and genomic regions involved in cancers. *Proc. Natl. Acad. Sci. USA* **101**, 2999-3004.

Caudy, A. A., Myers, M., Hannon, G. J. and Hammond, S. M. (2002). Fragile X-related protein and VIG associate with the RNA interference machinery. *Genes Dev.* **16**, 2491-2496.

Caudy, A. A., Ketting, R. F., Hammond, S. M., Denli, A. M., Bathoorn, A. M., Tops, B. B., Silva, J. M., Myers, M. M., Hannon, G. J. and Plasterk, R. H. (2003). A micrococcal nuclease homologue in RNAi effector complexes. *Nature* **425**, 411-414.

Chen, C. Z., Li, L., Lodish, H. F. and Bartel, D. P. (2004). MicroRNAs modulate hematopoietic lineage differentiation. *Science* **303**, 83-86.

Chen, P. Y., Manninga, H., Slanchev, K., Chien, M., Russo, J. J., Ju, J., Sheridan, R., John, B., Marks, D. S., Gaidatzis, D. et al. (2005). The developmental miRNA profiles of zebrafish as determined by small RNA cloning. *Genes Dev.* **19**, 1288-1293.

Chendrimada, T. P., Gregory, R. I., Kumaraswamy, E., Norman, J., Cooch, N., Nishikura, K. and Shiekhattar, R. (2005). TRBP recruits the Dicer complex to Ago2 for microRNA processing and gene silencing. *Nature* **436**. 740-744.

Cox, D. N., Chao, A., Baker, J., Chang, L., Qiao, D. and Lin, H. (1998). A novel class of evolutionarily conserved genes defined by piwi are essential for stem cell self-renewal. *Genes Dev.* **12**, 3715-3727.

Cullen, B. R. (2004). Transcription and processing of human microRNA precursors. *Mol. Cell* **16**, 861-865.

Davis, E., Caiment, F., Tordoir, X., Cavaille, J., Ferguson-Smith, A., Cockett, N., Georges, M. and Charlier, C. (2005). RNAi-mediated allelic trans-interaction at the imprinted Rtl1/Peg11 locus. *Curr. Biol.* **15**, 743-749.

Denli, A. M., Tops, B. B., Plasterk, R. H., Ketting, R. F. and Hannon, G. J. (2004). Processing of primary microRNAs by the Microprocessor complex. *Nature* **432**, 231-235.

Ding, L., Spencer, A., Morita, K. and Han, M. (2005). The developmental timing regulator AIN-1 interacts with miRISCs and may target the Argonaute protein ALG-1 to cytoplasmic P Bodies in C. elegans. *Mol. Cell* **19**, 437-447.

Doench, J. G., Petersen, C. P. and Sharp, P. A. (2003). siRNAs can function as miRNAs. *Genes Dev.* **17**, 438-442.

Eis, P. S., Tam, W., Sun, L., Chadburn, A., Li, Z., Gomez, M. F., Lund, E. and Dahlberg, J. E. (2005). Accumulation of miR-155 and BIC RNA in human B cell lymphomas. *Proc. Natl. Acad. Sci. USA* **102**, 3627-3632.

Enright, A. J., John, B., Gaul, U., Tuschl, T., Sander, C. and Marks, D. S. (2003). MicroRNA targets in Drosophila. *Genome Biol.* **5**, R1.

Forstemann, K., Tomari, Y., Du, T., Vagin, V. V., Denli, A. M., Bratu, D. P., Klattenhoff, C., Theurkauf, W. E. and Zamore, P. D. (2005). Normal microRNA maturation and germ-line stem cell maintenance requires Loquacious, a double-stranded RNA-binding domain protein. *PLoS Biol.* **3**, E236.

Giraldez, A. J., Cinalli, R. M., Glasner, M. E., Enright, A. J., Thomson, J. M., Baskerville, S., Hammond, S. M., Bartel, D. P. and Schier, A. F. (2005). MicroRNAs regulate brain morphogenesis in zebrafish. *Science* **308**, 833-838.

Gregory, R. I., Yan, K. P., Amuthan, G., Chendrimada, T., Doratotaj, B., Cooch, N. and Shiekhattar, R. (2004). The Microprocessor complex mediates the genesis of microRNAs. *Nature* **432**, 235-240.

Grishok, A., Pasquinelli, A. E., Conte, D., Li, N., Parrish, S., Ha, I., Baillie, D. L., Fire, A., Ruvkun, G. and Mello, C. C. (2001). Genes and mechanisms related to RNA interference regulate expression of the small temporal RNAs that control C. elegans developmental timing. *Cell* **106**, 23-34.

Ha, I., Wightman, B. and Ruvkun, G. (1996). A bulged lin-4/lin-14 RNA duplex is sufficient for Caenorhabditis elegans lin-14 temporal gradient formation. *Genes Dev.* **10**, 3041-3050.

Hammond, S. M., Bernstein, E., Beach, D. and Hannon, G. J. (2000). An RNA-directed nuclease mediates post-transcriptional gene silencing in Drosophila cells. *Nature* **404**, 293-296.

Hammond, S. M., Boettcher, S., Caudy, A. A., Kobayashi, R. and Hannon, G. J. (2001). Argonaute2, a link between genetic and biochemical analyses of RNAi. *Science* **293**, 1146-1150.

Han, J., Lee, Y., Yeom, K. H., Kim, Y. K., Jin, H. and Kim, V. N. (2004). The Drosha-DGCR8 complex in primary microRNA processing. *Genes Dev.* **18**, 3016-3027.

Hatfield, S. D., Shcherbata, H. R., Fischer, K. A., Nakahara, K., Carthew, R. W. and Ruohola-Baker, H. (2005). Stem cell division is regulated by the microRNA pathway. *Nature* **435**, 974-978.

He, L., Thomson, J. M., Hemann, M. T., Hernando-Monge, E., Mu, D., Goodson, S., Powers, S., Cordon-Cardo, C., Lowe, S. W., Hannon, G. J. et al. (2005). A microRNA polycistron as a potential human oncogene. *Nature* **435**, 828-833.

Hutvagner, G. and Zamore, P. D. (2002). A microRNA in a multiple-turnover RNAi enzyme complex. *Science* **297**, 2056-2060.

Hutvagner, G., McLachlan, J., Pasquinelli, A. E., Balint, E., Tuschl, T. and Zamore, P. D. (2001). A cellular function for the RNA-interference enzyme Dicer in the maturation of the let-7 small temporal RNA. *Science* **293**, 834-838.

Hutvagner, G., Simard, M. J., Mello, C. C. and Zamore, P. D. (2004). Sequence-specific inhibition of small RNA function. *PLoS Biol.* **2**, E98.

Ishizuka, A., Siomi, M. C. and Siomi, H. (2002). A Drosophila fragile X protein interacts with components of RNAi and ribosomal proteins. *Genes Dev.* **16**, 2497-2508.

Jiang, F., Ye, X., Liu, X., Fincher, L., McKearin, D. and Liu, Q. (2005). Dicer-1 and R3D1-L catalyze microRNA maturation in Drosophila. *Genes Dev.* **19**, 1674-1679.

Jing, Q., Huang, S., Guth, S., Zarubin, T., Motoyama, A., Chen, J., Di Padova, F., Lin, S. C., Gram, H. and Han, J. (2005). Involvement of microRNA in AU-rich element-mediated mRNA instability. *Cell* **120**, 623-634.

Jones-Rhoades, M. W. and Bartel, D. P. (2004). Computational identification of plant microRNAs and their targets, including a stress-induced miRNA. *Mol. Cell* **14**, 787-799.

Ketting, R. F., Fischer, S. E., Bernstein, E., Sijen, T., Hannon, G. J. and Plasterk, R. H. (2001). Dicer functions in RNA interference and in synthesis of small RNA involved in developmental timing in C. elegans. *Genes Dev.* **15**, 2654-2659.

Khvorova, A., Reynolds, A. and Jayasena, S. D. (2003). Functional siRNAs and miRNAs exhibit strand bias. *Cell* **115**, 209-216.

Kidner, C. A. and Martienssen, R. A. (2005). The developmental role of microRNA in plants. *Curr. Opin. Plant Biol.* **8**, 38-44.

Kiriakidou, M., Nelson, P. T., Kouranov, A., Fitziev, P., Bouyioukos, C., Mourelatos, Z. and Hatzigeorgiou, A. (2004). A combined computational-experimental approach predicts human microRNA targets. *Genes Dev.* **18**, 1165-1178.

Knight, S. W. and Bass, B. L. (2001). A role for the RNase III enzyme DCR-1 in RNA interference and germ line development in Caenorhabditis elegans. *Science* **293**, 2269-2271.

Krek, A., Grun, D., Poy, M. N., Wolf, R., Rosenberg, L., Epstein, E. J., MacMenamin, P., da Piedade, I., Gunsalus, K. C., Stoffel, M. et al. (2005). Combinatorial microRNA target predictions. *Nat. Genet.* **37**, 495-500.

Lagos-Quintana, M., Rauhut, R., Lendeckel, W. and Tuschl, T. (2001). Identification of novel genes coding for small expressed RNAs. *Science* **294**, 853-858.

Lai, E. C. (2002). Micro RNAs are complementary to 3′ UTR sequence motifs that mediate negative post-transcriptional regulation. *Nat. Genet.* **30**, 363-364.

Lai, E. C. (2004). Predicting and validating microRNA targets. *Genome Biol.* **5**, 115.

Lai, E. C. and Posakony, J. W. (1997). The Bearded box, a novel 3′ UTR sequence motif, mediates negative post-transcriptional regulation of Bearded and Enhancer of split Complex gene expression. *Development* **124**, 4847-4856.

Lai, E. C., Burks, C. and Posakony, J. W. (1998). The K box, a conserved 3′ UTR sequence motif, negatively regulates accumulation of enhancer of split complex transcripts. *Development* **125**, 4077-4088.

Lai, E. C., Tomancak, P., Williams, R. W. and Rubin, G. M. (2003). Computational identification of Drosophila microRNA genes. *Genome Biol.* **4**, R42.

Lai, E. C., Tam, B. and Rubin, G. M. (2005). Pervasive regulation of Drosophila Notch target genes by GY-box-, Brd-box-, and K-box-class microRNAs. *Genes Dev.* **19**, 1067-1080.

Landthaler, M., Yalcin, A. and Tuschl, T. (2004). The human DiGeorge syndrome critical region gene 8 and Its D. melanogaster homolog are required for miRNA biogenesis. *Curr. Biol.* **14**, 2162-2167.

Lau, N. C., Lim, L. P., Weinstein, E. G. and Bartel, D. P. (2001). An abundant class of tiny RNAs with probable regulatory roles in Caenorhabditis elegans. *Science* **294**, 858-862.

Leaman, D., Chen, P. Y., Fak, J., Yalcin, A., Pearce, M., Unnerstall, U., Marks, D. S., Sander, C., Tuschl, T. and Gaul, U. (2005). Antisense-mediated depletion reveals essential and specific functions of microRNAs in Drosophila development. *Cell* **121**, 1097-1108.

Lecellier, C. H., Dunoyer, P., Arar, K., Lehmann-Che, J., Eyquem, S., Himber, C., Saib, A. and Voinnet, O. (2005). A cellular microRNA mediates antiviral defense in human cells. *Science* **308**, 557-560.

Lee, R. C. and Ambros, V. (2001). An extensive class of small RNAs in Caenorhabditis elegans. *Science* **294**, 862-864.

Lee, R. C., Feinbaum, R. L. and Ambros, V. (1993). The C. elegans heterochronic gene lin-4 encodes small RNAs with antisense complementarity to lin-14. *Cell* **75**, 843-854.

Lee, Y., Jeon, K., Lee, J. T., Kim, S. and Kim, V. N. (2002). MicroRNA maturation: stepwise processing and subcellular localization. *EMBO J.* **21**, 4663-4670.

Lee, Y., Ahn, C., Han, J., Choi, H., Kim, J., Yim, J., Lee, J., Provost, P., Radmark, O., Kim, S. et al. (2003). The nuclear RNase III Drosha initiates microRNA processing. *Nature* **425**, 415-419.

Lee, Y., Kim, M., Han, J., Yeom, K. H., Lee, S., Baek, S. H. and Kim, V. N. (2004). MicroRNA genes are transcribed by RNA polymerase II. *EMBO J.* **23**, 4051-4060.

Lee, Y. S., Kim, H. K., Chung, S., Kim, K. S. and Dutta, A. (2005). Depletion of human micro-RNA miR-125b reveals that it is critical for the proliferation of differentiated cells but not for the down-regulation of putative targets during differentiation. *J. Biol. Chem.* **280**, 16635-16641.

Lewis, B. P., Shih, I. H., Jones-Rhoades, M. W., Bartel, D. P. and Burge, C. B. (2003). Prediction of mammalian microRNA targets. *Cell* **115**, 787-798.

Lewis, B. P., Burge, C. B. and Bartel, D. P. (2005). Conserved seed pairing, often flanked by adenosines, indicates that thousands of human genes are microRNA targets. *Cell* **120**, 15-20.

Lim, L. P., Glasner, M. E., Yekta, S., Burge, C. B. and Bartel, D. P. (2003a). Vertebrate microRNA genes. *Science* **299**, 1540.

Lim, L. P., Lau, N. C., Weinstein, E. G., Abdelhakim, A., Yekta, S., Rhoades, M. W., Burge, C. B. and Bartel, D. P. (2003b). The microRNAs of Caenorhabditis elegans. *Genes Dev.* **17**, 991-1008.

Lim, L. P., Lau, N. C., Garrett-Engele, P., Grimson, A., Schelter, J. M., Castle, J., Bartel, D. P., Linsley, P. S. and Johnson, J. M. (2005). Microarray analysis shows that some microRNAs downregulate large numbers of target mRNAs. *Nature* **433**, 769-773.

Lin, S. Y., Johnson, S. M., Abraham, M., Vella, M. C., Pasquinelli, A., Gamberi, C., Gottlieb, E. and Slack, F. J. (2003). The C. elegans hunchback homolog, hbl-1, controls temporal patterning and is a probable microRNA target. *Dev. Cell* **4**, 639-650.

Lingel, A., Simon, B., Izaurralde, E. and Sattler, M. (2004). Nucleic acid 3′-end recognition by the Argonaute2 PAZ domain. *Nat. Struct. Mol. Biol.* **11**, 576-577.

Liu, J., Carmell, M. A., Rivas, F. V., Marsden, C. G., Thomson, J. M., Song, J. J., Hammond, S. M., Joshua-Tor, L. and Hannon, G. J. (2004). Argonaute2 is the catalytic engine of mammalian RNAi. *Science* **305**, 1437-1441.

Liu, J., Valencia-Sanchez, M. A., Hannon, G. J. and Parker, R. (2005). MicroRNA-dependent localization of targeted mRNAs to mammalian P-bodies. *Nat. Cell Biol*. **7,** 719-723

Llave, C., Xie, Z., Kasschau, K. D. and Carrington, J. C. (2002). Cleavage of Scarecrow-like mRNA targets directed by a class of Arabidopsis miRNA. *Science* **297**, 2053-2056.

Lund, E., Guttinger, S., Calado, A., Dahlberg, J. E. and Kutay, U. (2004). Nuclear export of microRNA precursors. *Science* **303**, 95-98.

Ma, J. B., Yuan, Y. R., Meister, G., Pei, Y., Tuschl, T. and Patel, D. J. (2005). Structural basis for 5′-end-specific recognition of guide RNA by the A. fulgidus Piwi protein. *Nature* **434**, 666-670.

Mansfield, J. H., Harfe, B. D., Nissen, R., Obenauer, J., Srineel, J., Chaudhuri, A., Farzan-Kashani, R., Zuker, M., Pasquinelli, A. E., Ruvkun, G. et al. (2004). MicroRNA-responsive 'sensor' transgenes uncover Hox-like and other developmentally regulated patterns of vertebrate microRNA expression. *Nat. Genet.* **36**, 1079-1083.

Meister, G., Landthaler, M., Dorsett, Y. and Tuschl, T. (2004a). Sequence-specific inhibition of microRNA- and siRNA-induced RNA silencing. *RNA* **10**, 544-550.

Meister, G., Landthaler, M., Patkaniowska, A., Dorsett, Y., Teng, G. and Tuschl, T. (2004b). Human Argonaute2 mediates RNA cleavage targeted by miRNAs and siRNAs. *Mol. Cell* **15**, 185-197.

Mourelatos, Z., Dostie, J., Paushkin, S., Sharma, A., Charroux, B., Abel, L., Rappsilber, J., Mann, M. and Dreyfuss, G. (2002). miRNPs: a novel class of ribonucleoproteins containing numerous microRNAs. *Genes Dev.* **16**, 720-728.

Moussian, B., Schoof, H., Haecker, A., Jurgens, G. and Laux, T. (1998). Role of the ZWILLE gene in the regulation of central shoot meristem cell fate during Arabidopsis embryogenesis. *EMBO J.* **17**, 1799-1809.

Nowotny, M., Gaidamakov, S. A., Crouch, R. J. and Yang, W. (2005). Crystal structures of RNase H Bound to an RNA/DNA hybrid: substrate specificity and metal-dependent catalysis. *Cell* **121**, 1005-1016.

Olsen, P. H. and Ambros, V. (1999). The lin-4 regulatory RNA controls developmental timing in Caenorhabditis elegans by blocking LIN-14 protein synthesis after the initiation of translation. *Dev. Biol.* **216**, 671-680.

Papp, I., Mette, M. F., Aufsatz, W., Daxinger, L., Schauer, S. E., Ray, A., van der Winden, J., Matzke, M. and Matzke, A. J. (2003). Evidence for nuclear processing of plant micro RNA and short interfering RNA precursors. *Plant Physiol.* **132**, 1382-1390.

Parizotto, E. A., Dunoyer, P., Rahm, N., Himber, C. and Voinnet, O. (2004). In vivo investigation of the transcription, processing, endonucleolytic activity, and functional relevance of the spatial distribution of a plant miRNA. *Genes Dev.* **18**, 2237-2242.

Park, M. Y., Wu, G., Gonzalez-Sulser, A., Vaucheret, H. and Poethig, R. S. (2005). Nuclear processing and export of microRNAs in Arabidopsis. *Proc. Natl. Acad. Sci. USA* **102**, 3691-3696.

Park, W., Li, J., Song, R., Messing, J. and Chen, X. (2002). CARPEL FACTORY, a Dicer homolog, and HEN1, a novel protein, act in microRNA metabolism in *Arabidopsis thaliana*. *Curr. Biol.* **12**, 1484-1495.

Parker, J. S., Roe, S. M. and Barford, D. (2004). Crystal structure of a PIWI protein suggests mechanisms for siRNA recognition and slicer activity. *EMBO J.* **23**, 4727-4737.

Parker, J. S., Roe, S. M. and Barford, D. (2005). Structural insights into mRNA recognition from a PIWI domain-siRNA guide complex. *Nature* **434**, 663-666.

Pasquinelli, A. E., Reinhart, B. J., Slack, F., Martindale, M. Q., Kuroda, M. I., Maller, B., Hayward, D. C., Ball, E. E., Degnan, B., Muller, P. et al. (2000). Conservation of the sequence and temporal expression of let-7 heterochronic regulatory RNA. *Nature* **408**, 86-89.

Peragine, A., Yoshikawa, M., Wu, G., Albrecht, H. L. and Poethig, R. S. (2004). SGS3 and SGS2/SDE1/RDR6 are required for juvenile development and the production of trans-acting siRNAs in Arabidopsis. *Genes Dev.* **18**, 2368-2379.

Pfeffer, S., Zavolan, M., Grasser, F. A., Chien, M., Russo, J. J., Ju, J., John, B., Enright, A. J., Marks, D., Sander, C. et al. (2004). Identification of virus-encoded microRNAs. *Science* **304**, 734-736.

Pfeffer, S., Sewer, A., Lagos-Quintana, M., Sheridan, R., Sander, C., Grasser, F. A., van Dyk, L. F., Ho, C. K., Shuman, S., Chien, M. et al. (2005). Identification of microRNAs of the herpesvirus family. *Nat. Methods* **2**, 269-276.

Pillai, R. S., Bhattacharyya, S. N., Artus, C. G., Zoller, T., Cougot, N., Basyuk, E., Bertrand, E. and Filipowicz, W. (2005). Inhibition of translational initiation by let-7 microRNA in human cells. *Science* **309**, 1573-1576.

Poy, M. N., Eliasson, L., Krutzfeldt, J., Kuwajima, S., Ma, X., Macdonald, P. E., Pfeffer, S., Tuschl, T., Rajewsky, N., Rorsman, P. et al. (2004). A pancreatic islet-specific microRNA regulates insulin secretion. *Nature* **432**, 226-230.

Qi, Y., Denli, A. M. and Hannon, G. J. (2005). Biochemical Specialization within Arabidopsis RNA Silencing Pathways. *Mol. Cell* **19**, 421-428.

Rajewsky, N. and Socci, N. D. (2004). Computational identification of microRNA targets. *Dev. Biol.* **267**, 529-535.

Rand, T. A., Ginalski, K., Grishin, N. V. and Wang, X. (2004). Biochemical identification of Argonaute 2 as the sole protein required for RNA-induced silencing complex activity. *Proc. Natl. Acad. Sci. USA* **101**, 14385-14389.

Reinhart, B. J., Slack, F. J., Basson, M., Pasquinelli, A. E., Bettinger, J. C., Rougvie, A. E., Horvitz, H. R. and Ruvkun, G. (2000). The 21-nucleotide let-7 RNA regulates developmental timing in Caenorhabditis elegans. *Nature* **403**, 901-906.

Reinhart, B. J., Weinstein, E. G., Rhoades, M. W., Bartel, B. and Bartel, D. P. (2002). MicroRNAs in plants. *Genes Dev.* **16**, 1616-1626.

Rhoades, M. W., Reinhart, B. J., Lim, L. P., Burge, C. B., Bartel, B. and Bartel, D. P. (2002). Prediction of plant microRNA targets. *Cell* **110**, 513-520.

Riechmann, J. L., Heard, J., Martin, G., Reuber, L., Jiang, C., Keddie, J., Adam, L., Pineda, O., Ratcliffe, O. J., Samaha, R. R. et al. (2000). Arabidopsis transcription factors: genome-wide comparative analysis among eukaryotes. *Science* **290**, 2105-2110.

Rivas, F. V., Tolia, N. H., Song, J. J., Aragon, J. P., Liu, J., Hannon, G. J. and Joshua-Tor, L. (2005). Purified Argonaute2 and an siRNA form recombinant human RISC. *Nat. Struct. Mol. Biol.* **12**, 340-349.

Rodriguez, A., Griffiths-Jones, S., Ashurst, J. L. and Bradley, A. (2004). Identification of mammalian microRNA host genes and transcription units. *Genome Res.* **14**, 1902-1910.

Rougvie, A. D. (2005). Keeping time with microRNAs. *Development*, **132.** 3787-3798.

Saito, K., Ishizuka, A., Siomi, H. and Siomi, M. C. (2005). Processing of pre-microRNAs by the dicer-1-loquacious complex in Drosophila cells. *PLoS Biol.* **3**, E235.

Schwarz, D. S., Hutvagner, G., Du, T., Xu, Z., Aronin, N. and Zamore, P. D. (2003). Asymmetry in the assembly of the RNAi enzyme complex. *Cell* **115**, 199-208.

Sen, G. L. and Blau, H. M. (2005). Argonaute 2/RISC resides in sites of mammalian mRNA decay known as cytoplasmic bodies. *Nat. Cell. Biol.* **7**, 633-636.

Slack, F. J., Basson, M., Liu, Z., Ambros, V., Horvitz, H. R. and Ruvkun, G. (2000). The lin-41 RBCC gene acts in the C. elegans heterochronic pathway between the let-7 regulatory RNA and the LIN-29 transcription factor. *Mol. Cell* **5**, 659-669.

Song, J. J., Liu, J., Tolia, N. H., Schneiderman, J., Smith, S. K., Martienssen, R. A., Hannon, G. J. and Joshua-Tor, L. (2003). The crystal structure of the Argonaute2 PAZ domain reveals an RNA binding motif in RNAi effector complexes. *Nat. Struct. Biol.* **10**, 1026-1032.

Song, J. J., Smith, S. K., Hannon, G. J. and Joshua-Tor, L. (2004). Crystal structure of Argonaute and its implications for RISC slicer activity. *Science* **305**, 1434-1437.

Stark, A., Brennecke, J., Russell, R. B. and Cohen, S. M. (2003). Identification of Drosophila MicroRNA targets. *PLoS Biol.* **1**, E60.

Sullivan, C. S., Grundhoff, A. T., Tevethia, S., Pipas, J. M. and Ganem, D. (2005). SV40-encoded microRNAs regulate viral gene expression and reduce susceptibility to cytotoxic T cells. *Nature* **435**, 682-686.

Tang, G., Reinhart, B. J., Bartel, D. P. and Zamore, P. D. (2003). A biochemical framework for RNA silencing in plants. *Genes Dev.* **17**, 49-63.

Tomari, Y. and Zamore, P. D. (2005). Perspective: machines for RNAi. *Genes Dev.* **19**, 517-529.

Vaucheret, H., Vazquez, F., Crete, P. and Bartel, D. P. (2004). The action of ARGONAUTE1 in the miRNA pathway and its regulation by the miRNA pathway are crucial for plant development. *Genes Dev.* **18**, 1187-1197.

Vazquez, F., Gasciolli, V., Crete, P. and Vaucheret, H. (2004a). The nuclear dsRNA binding protein HYL1 is required for microRNA accumulation and plant development, but not posttranscriptional transgene silencing. *Curr. Biol.* **14**, 346-351.

Vazquez, F., Vaucheret, H., Rajagopalan, R., Lepers, C., Gasciolli, V., Mallory, A. C., Hilbert, J. L., Bartel, D. P. and Crete, P. (2004b). Endogenous trans-acting siRNAs regulate the accumulation of Arabidopsis mRNAs. *Mol. Cell* **16**, 69-79.

Vella, M. C., Choi, E. Y., Lin, S. Y., Reinert, K. and Slack, F. J. (2004). The C. elegans microRNA let-7 binds to imperfect let-7 complementary sites from the lin-41 3′UTR. *Genes Dev.* **18**, 132-137.

Wienholds, E., Koudijs, M. J., van Eeden, F. J., Cuppen, E. and Plasterk, R. H. (2003). The microRNA-producing enzyme Dicer1 is essential for zebrafish development. *Nat. Genet.* **35**, 217-218.

Wienholds, E., Kloosterman, W. P., Miska, E., Alvarez-Saavedra, E., Berezikov, E., de Bruijn, E., Horvitz, R. H., Kauppinen, S. and Plasterk, R. H. (2005). MicroRNA expression in zebrafish embryonic development. *Science* **309**, 310-311.

Wightman, B., Ha, I. and Ruvkun, G. (1993). Posttranscriptional regulation of the heterochronic gene lin-14 by lin-4 mediates temporal pattern formation in C. elegans. *Cell* **75**, 855-862.

Xie, X., Lu, J., Kulbokas, E. J., Golub, T. R., Mootha, V., Lindblad-Toh, K., Lander, E. S. and Kellis, M. (2005). Systematic discovery of regulatory motifs in human promoters and 3′ UTRs by comparison of several mammals. *Nature* **434**, 338-345.

Xie, Z., Kasschau, K. D. and Carrington, J. C. (2003). Negative feedback regulation of Dicer-Like1 in Arabidopsis by microRNA-guided mRNA degradation. *Curr. Biol.* **13**, 784-789.

Xie, Z., Johansen, L. K., Gustafson, A. M., Kasschau, K. D., Lellis, A. D., Zilberman, D., Jacobsen, S. E. and Carrington, J. C. (2004). Genetic and functional diversification of small RNA pathways in plants. *PLoS Biol.* **2**, E104.

Yan, K. S., Yan, S., Farooq, A., Han, A., Zeng, L. and Zhou, M. M. (2003). Structure and conserved RNA binding of the PAZ domain. *Nature* **426**, 468-474.

Yekta, S., Shih, I. H. and Bartel, D. P. (2004). MicroRNA-directed cleavage of HOXB8 mRNA. *Science* **304**, 594-596.

Yi, R., Qin, Y., Macara, I. G. and Cullen, B. R. (2003). Exportin-5 mediates the nuclear export of pre-microRNAs and short hairpin RNAs. *Genes Dev.* **17**, 3011-3016.

Yu, B., Yang, Z., Li, J., Minakhina, S., Yang, M., Padgett, R. W., Steward, R. and Chen, X. (2005). Methylation as a crucial step in plant microRNA biogenesis. *Science* **307**, 932-935.

Zeng, Y. and Cullen, B. R. (2003). Sequence requirements for micro RNA processing and function in human cells. *RNA* **9**, 112-123.

Zeng, Y. and Cullen, B. R. (2004). Structural requirements for pre-microRNA binding and nuclear export by Exportin 5. *Nucleic Acids Res.* **32**, 4776-4785.

Zeng, Y. and Cullen, B. R. (2005). Efficient processing of primary microRNA hairpins by Drosha requires flanking non-structured RNA sequences. *J. Biol. Chem.* **280,** 27595-27603.

Zeng, Y., Wagner, E. J. and Cullen, B. R. (2002). Both natural and designed micro RNAs can inhibit the expression of cognate mRNAs when expressed in human cells. *Mol. Cell* **9**, 1327-1333.

Zeng, Y., Yi, R. and Cullen, B. R. (2005). Recognition and cleavage of primary microRNA precursors by the nuclear processing enzyme Drosha. *EMBO J.* **24**, 138-148.

Zhang, Y. (2005). miRU: an automated plant miRNA target prediction server. *Nucleic Acids Res.* **33**, W701-W704.

Zhao, Y., Samal, E. and Srivastava, D. (2005). Serum response factor regulates a muscle-specific microRNA that targets Hand2 during cardiogenesis. *Nature* **436**, 214-220.

Cell

Sorting of *Drosophila* Small Silencing RNAs

Yukihide Tomari,[1,2,*] Tingting Du,[1] and Phillip D. Zamore[1,*]
[1] Department of Biochemistry and Molecular Pharmacology, University of Massachusetts Medical School, Worcester, MA 01605, USA
[2] Institute of Molecular and Cellular Biosciences, The University of Tokyo, Bunkyo-ku, Tokyo, 113-0032, and PRESTO, Japan Science and Technology Agency, Kawaguchi-shi, Saitama, 332-0012, Japan
*Correspondence: tomari@iam.u-tokyo.ac.jp (Y.T.), phillip.zamore@umassmed.edu (P.D.Z.)
DOI 10.1016/j.cell.2007.05.057

SUMMARY

In *Drosophila*, small interfering RNAs (siRNAs), which direct RNA interference through the Argonaute protein Ago2, are produced by a biogenesis pathway distinct from microRNAs (miRNAs), which regulate endogenous mRNA expression as guides for Ago1. Here, we report that siRNAs and miRNAs are sorted into Ago1 and Ago2 by pathways independent from the processes that produce these two classes of small RNAs. Such small-RNA sorting reflects the structure of the double-stranded assembly intermediates—the miRNA/miRNA* and siRNA duplexes—from which Argonaute proteins are loaded. We find that the Dcr-2/R2D2 heterodimer acts as a gatekeeper for the assembly of Ago2 complexes, promoting the incorporation of siRNAs and disfavoring miRNAs as loading substrates for *Drosophila* Ago2. A separate mechanism acts in parallel to favor miRNA/miRNA* duplexes and exclude siRNAs from assembly into Ago1 complexes. Thus, in flies small-RNA duplexes are actively sorted into Argonaute-containing complexes according to their intrinsic structures.

INTRODUCTION

Small interfering RNAs (siRNAs) and microRNAs (miRNAs) play an unexpectedly large role in regulating plant and animal gene expression (Kloosterman and Plasterk, 2006). Twenty-one to twenty-three nucleotides long, these two classes of small silencing RNAs repress the expression of specific genes through mechanistically similar RNA silencing pathways (Baulcombe, 2004; Du and Zamore, 2005; Kim, 2005; Sontheimer, 2005; Tomari and Zamore, 2005). siRNAs are produced by the endonucleolytic cleavage of long, double-stranded RNA (dsRNA) by members of the Dicer family of dsRNA-specific endonucleases (Bernstein et al., 2001). When extensively complementary to their mRNA targets, siRNAs direct cleavage of the phosphodiester bond between the target nucleotides paired to siRNA bases 10 and 11 (Elbashir et al., 2001a; Elbashir et al., 2001b). All known plant miRNAs and at least eight mammalian miRNAs similarly guide cleavage of the mRNAs they regulate (reviewed in Du and Zamore, 2005). In contrast, most animal miRNAs lack sufficient complementarity to guide endonucleolytic cleavage of their regulatory targets. Instead, they promote sequence-specific repression of mRNA translation or accelerate mRNA decay, perhaps by recruiting components of more general mRNA turnover pathways (Valencia-Sanchez et al., 2006).

miRNAs reside in discrete genes and are produced by the sequential processing of long transcripts—pri-miRNAs—by the RNase III enzyme Drosha into pre-miRNAs and of pre-miRNAs by Dicer into miRNA-containing RNA duplexes (Cullen, 2004; Kim, 2005). More than 4000 miRNAs have been reported (Griffiths-Jones et al., 2006), many of which are evolutionally conserved, whereas others are restricted to primates or even to humans (Bentwich et al., 2005; Berezikov et al., 2005, 2006). miRNA are proposed to regulate diverse cellular functions, including developmental timing, cell proliferation, cell death, and fat metabolism. They may also act to make biological regulatory circuits more robust (Stark et al., 2005). miRNA-regulated genes typically contain in their 3′ untranslated regions (UTRs) several partially complementary binding sites for one or more miRNAs (Lewis et al., 2003, 2005; Krek et al., 2005).

Members of the Argonaute (Ago) family of small-RNA-binding proteins lie at the core of all known RNA silencing effector complexes, collectively called RNA-induced silencing complexes (RISCs). RISC variants are distinguished by their Argonaute protein. In *Drosophila*, miRNAs partition between Ago1- and Ago2-RISC (Förstemann et al., 2007 [this issue of *Cell*]), whereas siRNAs associate almost exclusively with Ago2-RISC (Hammond et al., 2001; Okamura et al., 2004). Ago1- and Ago2-RISC are functionally distinct, silencing different types of target RNAs by different mechanisms (Förstemann et al., 2007).

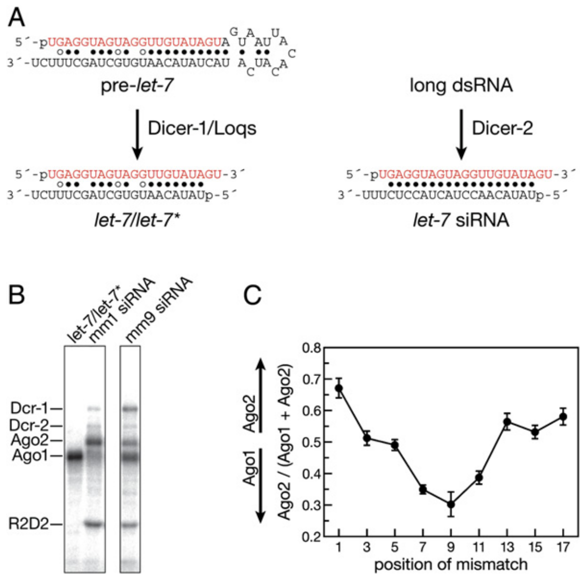

Figure 1. RNA Duplex Structure Determines the Partitioning of a Small RNA between *Drosophila* Ago1 and Ago2

(A) A schematic of the distinct small-RNA duplexes produced by Dcr-1 processing of pre-miRNAs and Dcr-2 processing of long dsRNA.

(B) UV crosslinking at 254 nm of exemplary small-RNA duplexes.

(C) A central mismatch directs the duplex into Ago1 instead of Ago2. The fraction of each duplex crosslinked to Ago2 relative to the sum of RNA crosslinked to Ago1 and to Ago2 is presented as the average ± standard deviation for three independent trials.

Both siRNAs and miRNAs are proposed to be loaded into Argonaute protein-containing RISCs from double-stranded intermediates generated by Dicer: siRNA duplexes and miRNA/miRNA* duplexes (Figure 1A). In flies, loading of double-stranded siRNAs into Ago2-RISC is facilitated by the RISC-loading complex (RLC) (Liu et al., 2003, 2006; Pham et al., 2004; Tomari et al., 2004a, 2004b; Pham and Sontheimer, 2005; Kim et al., 2006). The RLC comprises several proteins, including Dicer-2 and its dsRNA-binding partner protein, R2D2. Which strand of the siRNA duplex is assembled into Ago2-RISC is thought to be determined by the orientation of the Dicer-2/R2D2 heterodimer on the siRNA duplex (Tomari et al., 2004a). The strand loaded, the guide strand, typically has a 5′ end less tightly base paired in the duplex than the passenger strand, which is destroyed during the loading process (Khvorova et al., 2003; Schwarz et al., 2003). Passenger-strand destruction and RISC maturation are initiated for Ago2-RISC assembly by guide-strand-directed endonucleolytic cleavage of the passenger strand by Ago2, as if the passenger strand were an mRNA target (Matranga et al., 2005; Rand et al., 2005; Kim et al., 2006; Leuschner et al., 2006). One strand—the miRNA strand—of a miRNA/miRNA* duplex is similarly selectively loaded into Ago1-containing RISC, but the proteins facilitating Ago1 loading remain to be identified (Okamura et al., 2004). Both siRNA and miRNA/miRNA* duplexes contain a ~19 base pair double-stranded core flanked by ~2 nt single-stranded 3′ overhanging ends (Figure 1A). However, the guide and passenger strands of an siRNA duplex are complementary throughout its ~19 bp central domain, whereas the miRNA and miRNA* strands invariably contain G:U wobble pairs, mismatches, and internal loops in this region.

In flies, distinct Dicer complexes produce siRNAs and miRNAs (Lee et al., 2004). miRNAs are cleaved from pre-miRNA by Dicer-1 (Dcr-1), acting with its dsRNA-binding protein partner, Loquacious (Loqs) (Förstemann et al., 2005; Jing et al., 2005; Saito et al., 2005). siRNAs are produced from long dsRNA by Dicer-2 (Dcr-2), which partners with the dsRNA-binding protein R2D2 (Liu et al., 2003). Thus, the different origins of miRNAs and siRNAs might direct them to distinct Argonaute proteins, with Dcr-1/Loqs recruiting Ago1 to miRNAs and Dcr-2/R2D2 directing siRNAs to Ago2. Alternatively, the specific structural differences between a miRNA/miRNA* duplex and an siRNA duplex (Figure 1A) might promote their sorting into Ago1- and Ago2-containing RISC, respectively. Here, we report that the Dcr-2/R2D2 heterodimer acts as a gatekeeper for the assembly of Ago2-RISC, promoting the incorporation of siRNAs and disfavoring the use of miRNAs as loading substrates for *Drosophila* Ago2. An independent mechanism acts in parallel to favor assembly of miRNA/miRNA* duplexes into Ago1-RISC and to exclude siRNAs from incorporation into Ago1. These two pathways compete for loading small-RNA duplexes with structures intermediate between that of an siRNA and a typical miRNA/miRNA* duplex, and such small RNAs partition between Ago1 and Ago2. Thus, small-RNA duplexes are actively sorted into Argonaute-containing complexes according to their intrinsic structures, rather than as a consequence of their distinct biogenesis pathways.

RESULTS

A Central Mismatch Favors Small-RNA Loading into Ago1

The structure of a small-RNA duplex could determine into which Argonaute paralog it is loaded. To test this hypothesis, we synthesized ten small-RNA duplexes: an authentic *let-7/let-7** duplex; a functionally asymmetric *let-7* siRNA, in which the guide and passenger strands were fully paired except at guide position 1 (mm1 siRNA duplex); and eight *let-7* siRNA duplex derivatives incorporating one additional mismatch between the guide and passenger strands, at guide position 3, 5, 7, 9, 11, 13, 15, or 17 (mm3–mm17 siRNAs) (Figure S1). Each small-RNA duplex, which contained a 5′ ^{32}P-radiolabel on the *let-7* (guide) strand and a nonradioactive 5′ phosphate on the miRNA* or passenger strand, was incubated in *Drosophila* embryo lysate, then photocrosslinked with 254 nm UV light and analyzed by SDS-PAGE to identify small-RNA-bound proteins. The identity of crosslinked

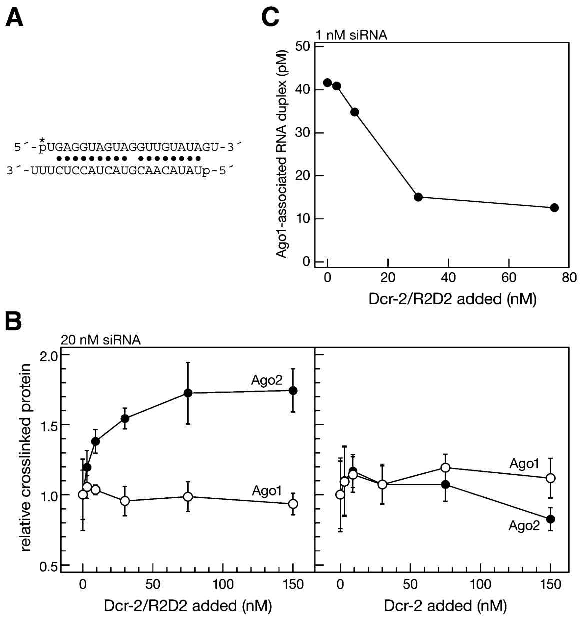

Figure 2. The Dcr-2/R2D2 Heterodimer, as a Component of the Ago2-Loading Machinery, Promotes Assembly of Ago2-RISC and Competes with Assembly of Ago1-RISC

(A) Sequence of the small-RNA duplex (mm11) used in (B) and (C).

(B) Dcr-2/R2D2, but not Dcr-2 alone, directs the association of a small-RNA duplex with Ago2. Twenty nanomoles per liter of mm11 duplex, whose *let-7* strand partitions between Ago1 and Ago2, was incubated with wild-type lysate supplemented with increasing amounts of Dcr-2/R2D2 or Dcr-2 alone. Ago1- and Ago2-association were measured by 254 nm UV crosslinking. The data (average ± standard deviation for three trials) were normalized to the crosslinking observed in the absence of supplemental recombinant Dcr-2/R2D2 or Dcr-2 alone.

(C) One nanomoles per liter of mm11 duplex was incubated with wild-type lysate supplemented with increasing concentrations of Dcr-2/R2D2, the Ago1-associated siRNA recovered by immunoprecipitation with anti-Ago1 monoclonal antibody and quantified by scintillation counting.

proteins was assigned by their immunoprecipitation with specific antibodies and their loss in lysate prepared from mutant ovaries or embryos.

The authentic *let-7*/*let-7** duplex crosslinked only to Ago1, whereas the *let-7* mm1 siRNA duplex crosslinked predominantly to Ago2 (Figure 1B). Introducing a position 9 mismatch into the siRNA (mm9) shifted the balance in favor of Ago1, while retaining significant Ago2 association. Quantitative analysis of the ratio of Ago1 to Ago2 crosslinking for the entire series of mismatched *let-7* siRNA derivatives revealed that central mismatches direct small-RNA duplexes into Ago1 rather than Ago2 (Figure 1C).

A Role for the Dcr-2/R2D2 Heterodimer in Small-RNA Partitioning

How does a central mismatch influence Argonaute loading? Such a disruption to siRNA structure might disfavor its association with the RLC (reducing Ago2 loading), favor its association with the Ago1-loading machinery, or both.

To test the idea that central mismatches reduce the association of a small-RNA duplex with the RLC, we incubated a *let-7* siRNA bearing a mismatch at position 11 (mm11) (Figure 2A) with embryo lysate supplemented with purified recombinant Dcr-2/R2D2 heterodimer or Dcr-2 alone. In the absence of supplemental recombinant protein, the mm11 duplex partitioned between Ago1 (~60%) and Ago2 (~40%). Increasing the concentration of the Dcr-2/R2D2 heterodimer, the core constituent of the RLC, increased the amount of duplex crosslinked to Ago2 (Figure 2B). In contrast, increasing the concentration of Dcr-2 alone did not enhance crosslinking of the duplex to Ago2, consistent with earlier observations that R2D2 is required to recruit Dcr-2 to siRNA for RISC loading (Liu et al., 2003, 2006). Moreover, in the absence of R2D2, Dcr-2 reduced Ago2 crosslinking to siRNA (Figure 2B), suggesting that Dcr-2 forms a complex with siRNA that cannot load Ago2 (see below and Figure S2). Together, the data in Figures 1C and 2B suggest that a central mismatch weakens the binding of the Dcr-2/R2D2 heterodimer to a small-RNA duplex, disfavoring its assembly into Ago2-RISC; increasing the concentration of the Dcr-2/R2D2 heterodimer increases loading of the small RNA into Ago2 by overcoming its reduced affinity for the RLC.

Competition between Ago1 and Ago2 Pathways

Although increasing Dcr-2/R2D2 concentration promoted loading of the mm11 duplex into Ago2, the crosslinking assay cannot determine whether the Ago2- and Ago1-loading pathways compete for loading of an siRNA, because the majority of the 20 nM RNA duplex remained unassociated with the Ago2-loading machinery (Schwarz et al., 2003; Haley and Zamore, 2004). This free RNA creates a reservoir of duplex that can, in principle, be loaded into Ago1. Unfortunately, reducing the concentration of small RNA in the crosslinking assay caused the RNA-crosslinked proteins to become undetectable.

To test if the Ago2- and Ago1-loading pathways compete for loading small-RNA duplexes, we used a lower concentration of small RNA and a more sensitive assay—immunoprecipitation—to measure the association of a small RNA with Ago1. (The assay cannot currently measure small-RNA association with Ago2, because no suitable anti-Ago2 antibody exists.) We incubated 1 nM 5′ ^{32}P-radiolabeled mm11 duplex in embryo lysate with increasing concentrations of Dcr-2/R2D2, immunoprecipitated Ago1 using a monoclonal anti-Ago1 antibody, and measured the concentration of Ago1-associated small-RNA duplex by scintillation counting. Increasing the concentration of Dcr-2/R2D2 decreased the amount of siRNA associated with Ago1 (Figures 2A and 2C), indicating that Ago1 loading competes with Dcr-2/R2D2-mediated loading of Ago2.

Measuring the Association of Small RNAs with the Dcr-2/R2D2 Heterodimer

To test directly the idea that the affinity of the Dcr-2/R2D2 heterodimer for a small-RNA duplex determines

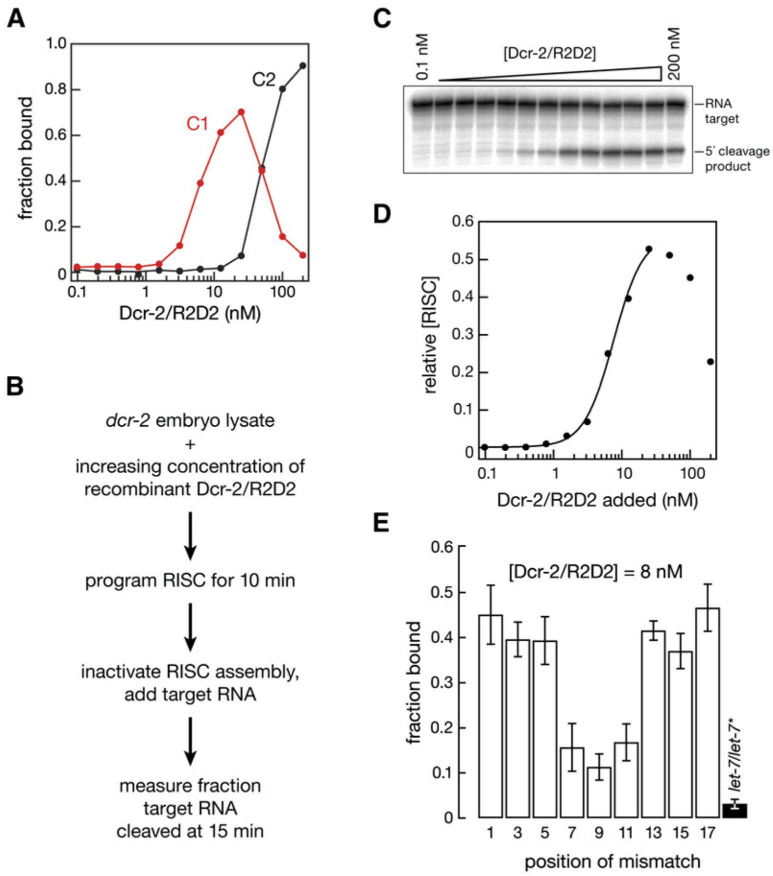

Figure 3. RISC Activity Coincides with the Formation of Dcr-2/R2D2:siRNA Ternary Complex C1, and a Central Mismatch in a Small-RNA Duplex Impairs the Complex Formation

(A) Quantification of concentration dependence of the two complexes formed when purified, recombinant Dcr-2/R2D2 heterodimer was incubated with siRNA. The native gel used for this analysis appears in Figure S3A.

(B) Experimental strategy for (C) and (D).

(C) Target cleavage activity was measured for RISC assembled in *dcr-2* mutant lysate—which lacks both Dcr-2 and R2D2—rescued with increasing amounts of recombinant Dcr-2/R2D2 heterodimer.

(D) Quantification of (C). The peak of the target cleavage activity corresponds to the peak of complex C1 formation in (A). The y axis reports the relative concentration of RISC, calculated from a standard curve relating relative RISC concentration to the fraction of target cleaved (Figure S4D).

(E) Each of the ten *let-7* small-RNA duplexes was 5′ ^{32}P-radiolabled and incubated with 8 nM Dcr-2/R2D2. Then, the fraction of RNA present as complex C1 was measured. No C2 was formed at this concentration of the heterodimer. Bars report the average ± standard deviation for three trials.

the extent of its loading into Ago2-RISC, we used a gel-mobility shift assay to measure the affinity of recombinant Dcr-2/R2D2 heterodimer for the series of ten *let-7* small-RNA duplexes. Purified recombinant Dcr-2/R2D2 and 5′ ^{32}P-radiolabeled small RNAs bearing a nonradioactive 5′ phosphate on the passenger or miRNA* strand were incubated for 30 min, then free siRNA resolved from protein:siRNA complexes by native gel electrophoresis in the presence of Mg^{2+}. Figure S3A shows a representative assay for the *let-7* mm1 siRNA duplex. With increasing concentration of Dcr-2/R2D2, we detected two distinct complexes: complex 1 (C1) peaked at ~20 nM Dcr-2/R2D2, whereas complex 2 (C2) appeared at higher concentrations of Dcr-2/R2D2, apparently replacing C1 (Figures S3A and 3A).

To determine if each complex contained Dcr-2, R2D2, or both, we repeated the assay using a *let-7* siRNA bearing a 5-iodo uracil at guide-strand position 20; 5-iodo U at this position allows the siRNA to be site-specifically photocrosslinked to Dcr-2 or R2D2 upon irradiation with 302 nm light (Tomari et al., 2004a). The *let-7* siRNA was incubated with 20 nM (for C1) or 100 nM Dcr-2/R2D2 (for C2) and photocrosslinked; the complexes were resolved by native gel electrophoresis, and then C1 and C2 were excised from the gel, and the crosslinked proteins in each complex were separated by SDS-PAGE (Figure S3B). Both C1 and C2 contained Dcr-2 and R2D2 crosslinked to siRNA (Figure S3C). Thus, both C1 and C2 reflect binding of the Dcr-2/R2D2 heterodimer to siRNA.

Which complex then corresponds to the active form of siRNA-bound Dcr-2/R2D2 heterodimer competent to load Ago2? We added increasing concentration of recombinant Dcr-2/R2D2 heterodimer to lysate prepared from *dcr-2*^{L811fsX} (Pham et al., 2004) mutant embryos, which lack both Dcr-2 and R2D2 (T.D. and P.D.Z., unpublished data). At each concentration of heterodimer, we measured the relative amount of Ago2-RISC activity assembled by determining the extent of cleavage after 15 min incubation with target RNA (Figures 3B–3D) when the reaction was linear (Figure S4). The Dcr-2/R2D2 concentration producing half-maximal target cleavage in this assay coincided with the apparent dissociation constant (K_{app}) for C1 production, indicating that C1 is the active complex for RISC loading (compare Figures 3A and 3D). Interestingly, at high concentrations of Dcr-2/R2D2 heterodimer, which favor the production of C2 (Figure 3A), target cleavage was inhibited (Figure 3D), reinforcing the view that complex C1 is the active, Ago2-loading form of siRNA-bound heterodimer and suggesting that C2 corresponds to a higher order, inactive aggregate of Dcr-2/R2D2 heterodimers.

Table 1. The Measured and Relative Affinities (± standard deviation) of the Dcr-2/R2D2 Heterodimer for Three Different Small-RNA Duplexes and of Dcr-2 Alone for siRNA

Dcr-2/R2D2 Heterodimer			
Small RNA	K_{app} (nM)	$K_{relative}$	Trials
let-7 mm1 siRNA duplex	7.8 ± 1.2	1.0 ± 0.2	3
mm9 duplex	16.3 ± 3.1	2.1 ± 0.3	3
let-7/*let-7** duplex	37.5 ± 4.6	4.8 ± 0.6	3
Dcr-2 Alone			
Small RNA	K_{app} (nM)	$K_{relative}$	Trials
let-7 mm1 siRNA duplex	94.6 ± 6.4	12.1 ± 0.8	4

The Affinity of the Dcr-2/R2D2 Heterodimer for a Small RNA Determines Its Loading into Ago2-RISC

Next, we examined the affinity of the Dcr-2/R2D2 heterodimer for various small-RNA duplexes. We measured the K_{app} of the heterodimer for formation of complex C1, the species active for Ago2-loading. Figure S5 (A and B) shows representative binding curves for the mm1 siRNA duplex, mm9 duplex and *let-7*/*let-7** duplex, and Table 1 summarizes the K_{app} for each determined in three independent trials. The Dcr-2/R2D2 heterodimer bound the mm9 duplex about half as tightly as it bound the *let-7* mm1 siRNA duplex, whereas the heterodimer bound the *let-7*/*let-7** duplex about 5-fold less tightly than it bound the corresponding siRNA. Although previous studies concluded that Dcr-2 does not detectably bind siRNA in the absence of R2D2 (Liu et al., 2006), we found that purified recombinant Dcr-2 alone readily bound the mm1 siRNA duplex, with a K_{app} of 94.6 ± 6.4 nM (average of four trials ± standard deviation; Figure S2). Thus, the apparent lack of Dcr-2 binding to siRNA reported previously likely reflects the ~12-fold lower affinity for siRNA of Dcr-2 alone compared to the intact heterodimer.

For the Dcr-2/R2D2 heterodimer, the order of relative affinities of Dcr-2/R2D2 for the three small-RNA duplexes correlated well with their extent of incorporation into Ago1- and Ago2-RISC: the greater the strength of binding of the heterodimer for a small RNA, the greater its association with Ago2 and the more reduced its association with Ago1. To further test this idea, we determined the fraction of small-RNA duplex bound to 8 nM Dcr-2/R2D2 heterodimer for all ten *let-7* small-RNA duplexes (Figure 3E). The amount of small RNA associated with Dcr-2/R2D2 in this assay correlated well with the amount of the small RNA assembled into Ago2 relative to Ago1 (Figures 1B and 1C).

Small-RNA Association with Ago1 Does Not Ensure the Production of Functional Ago1-RISC

Clearly, the affinity of the Dcr-2/R2D2 heterodimer for a small-RNA duplex is an important determinant of the extent to which the small RNA is loaded into Ago2. Our

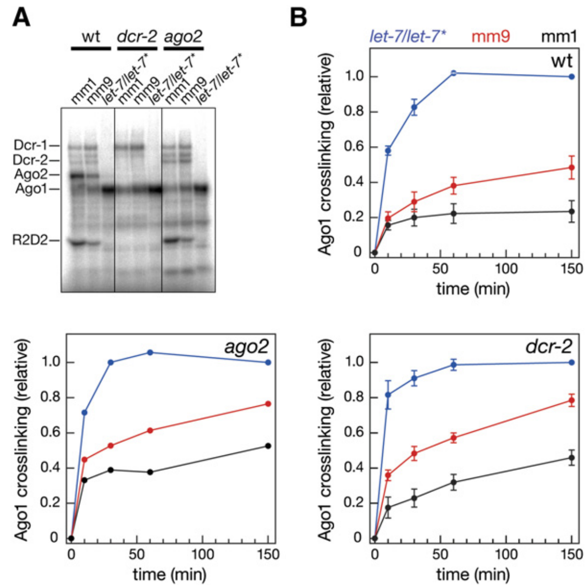

Figure 4. The Ago1-Loading Pathway Selects Small RNAs with Central Mismatches, Even in the Absence of the Competing Ago2 Pathway

(A) Three exemplary small-RNA duplexes were incubated with wild-type, *dcr-2*, or *ago2* embryo lysate and then photocrosslinked with shortwave UV to identify small-RNA-bound proteins.

(B) Kinetic analysis of small-RNA association with Ago1, monitored by UV photocrosslinking. The *let-7*/*let-7** duplex associated with Ago1 more rapidly than the mm9 duplex, which was more rapidly bound by Ago1 than the mm1 siRNA duplex. In the absence of the Ago2-loading machinery or Ago2 itself, association of the small-RNA duplexes with Ago1 was accelerated, consistent with the idea that the Ago1 and Ago2 pathways compete for loading with small-RNA duplexes. Each data point represents the average ± standard deviation for three trials.

data also suggest that Ago1 and Ago2 compete for loading with a small-RNA duplex (Figure 2C). In theory, small RNAs whose structure disfavors their loading into Ago2 pathway, might enter the Ago1-loading pathway simply by default. To test this idea, we examined the loading of the mm1 siRNA duplex, mm9 duplex, and *let-7*/*let-7** duplex into Ago1 in lysate prepared from $dcr\text{-}2^{L811fsX}$ and from $ago2^{414}$ mutant embryos. In the $dcr\text{-}2^{L811fsX}$ and $ago2^{414}$ lysates, where Ago2 is not loaded, the relative amount of each small-RNA duplex loaded into Ago1, measured by photocrosslinking, remained essentially unchanged from that observed in wild-type lysate (Figure 4A). Even in the absence of Ago2-loading machinery or Ago2 itself, Ago1 was preferentially loaded with the *let-7*/*let-7** duplex, largely rejected the mm1 siRNA duplex, and accepted some of the mm9 duplex. Thus, both the Ago1- and the Ago2-loading pathways are selective, with each favoring a small-RNA structure disfavored by the other.

While the extent of Ago1 loading was essentially the same in the wild-type and mutant lysates, the rate at which the three small-RNA duplexes associated with Ago1 was

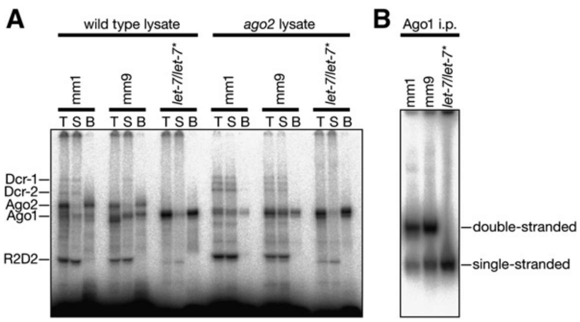

Figure 5. *let-7*/*let-7 Duplex, But Not the mm1 siRNA Duplex Nor the mm9 Duplex, Efficiently Assembled Mature Ago1-RISC**

(A) The three exemplary small-RNA duplexes were incubated with wild-type or *ago2* embryo lysate for 1 hr, UV photocrosslinked, and then mature RISC, which contains single-stranded *let-7* RNA, separated from pre-RISC, which contains double-stranded RNA, using an immobilized 2′-*O*-methyl *let-7* ASO. T, total; S, supernatant (double stranded); B, bound (single stranded). The Ago1-associated *let-7* mm1 siRNA duplex and the mm9 duplex remained largely double stranded, suggesting that mature Ago1-RISC was not efficiently formed from the Ago1 pre-RISC assembled with these duplexes. Most of the Ago1-associated *let-7* loaded from the *let-7*/*let-7** duplex was present as single-stranded *let-7* bound to Ago1. That is, the conversion of *let-7*/*let-7** Ago1-pre-RISC to *let-7* Ago1-RISC was very efficient. In contrast, the mm1 siRNA duplex and mm9 duplex efficiently loaded single-stranded *let-7* into Ago2; these small-RNA duplexes were efficiently converted from Ago2 pre-RISC to mature Ago2-RISC.

(B) Each small-RNA duplex was incubated with wild-type embryo lysate, the Ago1-associated RNA recovered by immunoprecipitation, and then the small RNA isolated and single-stranded RNA separated from dsRNA by native gel electrophoresis. As in (A), the *let-7* mm1 siRNA duplex and mm9 duplexes produced mainly Ago1-associated double-stranded RNA, whereas the *let-7*/*let-7** duplex yielded almost entirely Ago1-bound single-stranded *let-7*.

accelerated in both the *ago2*^{414} and *dcr-2*^{L811fsX} lysates (Figure 4B). This effect was most pronounced for the *let-7*/*let-7** duplex, which was loaded twice as fast in the *dcr-2*^{L811fsX} mutant lysate, which lacks the Ago2-loading machinery. The finding that, in the absence of the Ago2-loading machinery, Ago1 is more rapidly loaded with its authentic substrate, the *let-7*/*let-7** duplex, suggests that miRNA/miRNA* duplexes bind the Dcr-2/R2D2 heterodimer transiently, even when they ultimately make little or no Ago2-RISC.

Conversely, a small-RNA duplex favored to produce Ago2-RISC associated with Ago1 in both the absence and presence of Ago2 (Figures 4A and 4B). But does this Ago1-associated small RNA correspond to mature RISC, which contains only the miRNA or guide strand of the original duplex, or pre-RISC, a RISC-assembly intermediate in which the double-stranded miRNA/miRNA* or siRNA is bound to Argonaute (Matranga et al., 2005; Rand et al., 2005; Kim et al., 2006; Leuschner et al., 2006)? We determined if the *let-7* strand was bound to Ago1 or Ago2 as single-stranded or double-stranded RNA. For the mm1, the mm9 and the *let-7*/*let-7** duplexes, each 5′-^{32}P-radiolabeled small-RNA duplex was incubated with wild-type or *ago2*^{414} mutant lysate to assemble RISC and photocrosslinked to identify siRNA-associated proteins, and then single-stranded RNA-crosslinked proteins captured using an immobilized 2′-*O*-methyl antisense oligo (ASO) complementary to *let-7* (Figure 5A); in this assay, proteins crosslinked to double-stranded siRNA or miRNA/miRNA* remain in the supernatant. (Dcr-1, Dcr-2, and R2D2 were never recovered with the immobilized ASO, consistent with previous observations that they bind only double-stranded small RNAs [Tomari et al., 2004a)]. As expected, the majority of the crosslinked Ago2 was recovered with the immobilized ASO for the *let-7* mm1 siRNA duplex, whereas most of the crosslinked Ago1 was recovered with the immobilized ASO for the *let-7*/*let-7** duplex. We conclude that the *let-7* mm1 siRNA duplex efficiently assembled mature Ago2-RISC, whereas the *let-7*/*let-7** duplex efficiently assembled mature Ago1-RISC. The mm9 duplex also efficiently assembled mature Ago2-RISC.

Much of the Ago1-associated *let-7* loaded from the mm1 siRNA duplex or the mm9 duplex, however, remained double stranded, suggesting that the Ago1-loading machinery or Ago1 itself cannot efficiently dissociate the passenger strand from a highly base paired duplex (Figure 5A). In contrast, little double-stranded, Ago2-associated *let-7* was observed for the mm1 siRNA duplex or mm9 duplex in the wild-type lysate, likely reflecting the rapid cleavage of the passenger strand by Ago2. This is consistent with our findings that Ago1 is not an efficient endonuclease (Förstemann et al., 2007).

We note that in the absence of Ago2, some *let-7*-programmed Ago1-RISC was formed from the mm1 siRNA duplex. The low efficiency of incorporation of the *let-7* siRNA guide strand into mature Ago1-RISC, together with the reduced endonuclease activity of Ago1 compared to Ago2, likely explains the small amount of siRNA-directed target cleavage observed in vitro in lysate prepared from *ago2*^{414} (Okamura et al., 2004) and *r2d2*^{1} mutant embryos (Liu et al., 2006).

Immunoprecipitation experiments confirmed these photocrosslinking and ASO-binding studies (Figure 5B). RISC was assembled with 5′ ^{32}P-radiolabeled mm1 siRNA duplex, the mm9 duplex, or the *let-7*/*let-7** duplex and immunoprecipitated with anti-Ago1 monoclonal antibody; immunoprecipitated proteins were removed by digestion with protease at room temperature, and then the ^{32}P-radiolabeled small RNAs were resolved by native gel electrophoresis to assess if they were single or double stranded. For both the mm1 siRNA duplex and the mm9 duplex, most of the Ago1-associated *let-7* was double stranded. In contrast, essentially all of the Ago1-associated *let-7* loaded from the *let-7*/*let-7** duplex was single stranded, indicating it had been successfully assembled into functional Ago1-RISC. Our data suggest that the conversion of pre-Ago1-RISC to mature Ago1-RISC requires additional structural features that help separate the two siRNA strands, such as mismatches in the siRNA seed

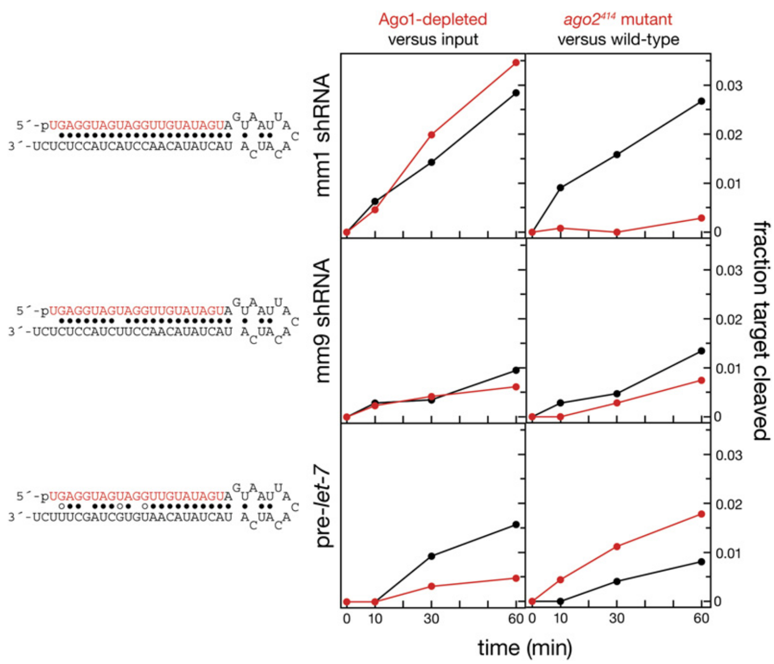

Figure 6. The Double-Stranded Structure of Small-RNA Duplexes Generated by Dicing Longer Precursors Determines How They Are Partitioned between Ago1- and Ago2-RISC

Two short hairpin RNAs and pre-*let-7* were incubated in embryo lysate for 1 hr to generate *let-7* by dicing and program RISC; then RISC activity in cleaving a *let-7*-complementary target RNA (0.5 nM) was measured. At left, Ago1 was immunodepleted before adding the target RNA. The red data points therefore report Ago2-RISC activity. At right, the precursors were incubated in *ago2*^{414} mutant lysate, so the red data points represent only Ago1-RISC activity. For the Ago1 experiments, the precursor concentration was 20 nM; for the *ago2*^{414} experiments, it was 100 nM.

region. Such features might act in a pathway similar to the "bypass" mechanism that facilitates the conversion of pre-RISC to mature RISC for Ago2 when passenger-strand cleavage is blocked (Matranga et al., 2005). In fact, when miRNA* cleavage by human Ago2 is blocked, seed mismatches between the miRNA and its miRNA* accelerate separation of the two strands (Matranga et al., 2005). We note that *Drosophila* Ago1 is more closely related to human Ago2 than to the conspecific Ago2 protein.

Even When Small RNAs Are Diced from Longer Precursors, Their Duplex Structure Determines Small-RNA Sorting

In cells, small-RNA duplexes are produced from longer precursors by dicing. How faithfully do our studies of small-RNA sorting, which bypass this step, reflect the cellular pathway? To answer this question, we programmed *Drosophila* embryo lysate with three different Dicer substrates: (1) a short-hairpin RNA designed to generate an asymmetric *let-7* siRNA after dicing (mm1 shRNA); (2) the same shRNA, but also containing a mismatch at *let-7* position 9 (mm9 shRNA); and (3) authentic pre-*let-7* RNA. (As reported previously [Hutvágner and Zamore, 2002], less active RISC was produced in vitro from hairpin substrates than when siRNAs are used directly.)

We first incubated each precursor with embryo lysate to generate *let-7*-programmed RISC, and then we added a target RNA containing a site complementary to *let-7* and monitored target cleavage (Figure 6). Of the three precursor RNAs, mm1 shRNA produced the most active RISC. To determine the degree to which the target cleavage observed for each precursor RNA reflected Ago1-RISC programmed with *let-7*, we immunodepleted Ago1 after the RISC assembly step but before adding target RNA. Our immunodepletion strategy removed more than 98% of the Ago1 protein (Figure S6). Depletion of Ago1 reproducibly enhanced to a small extent the rate of target cleavage for mm1 shRNA, but had little effect on mm9 shRNA. In contrast, most of the RISC activity produced by pre-*let-7* was removed when Ago1 was immunodepleted. These results are consistent with mm1 shRNA loading Ago2 and pre-*let-7* loading Ago1.

To determine the degree to which the target cleavage observed for each precursor RNA reflected Ago2-RISC programmed with *let-7* (Figure 6), we compared the amount of *let-7*-directed target cleaving activity generated from each precursor in wild-type lysate to that generated in *ago2*^{414} lysate, which lacks Ago2 protein. Little or no RISC activity was detected for mm1 shRNA in the *ago2*^{414} mutant lysate. In contrast, for pre-*let-7* more RISC activity was detected for the *ago2*^{414} mutant than for the wild-type lysate, presumably because the loss of competition with the Ago2 pathway resulted in more Ago1-RISC. As for the Ago1 immunodepletion experiment, mm9 shRNA produced less active RISC than the other two substrates. This RISC activity was reduced in the *ago2*^{414} mutant lysate, consistent with our finding (Figure 5) that most of the Ago1-RISC produced by an mm9 siRNA was inactive because the siRNA remained double stranded. We conclude that dicing has little or no influence on the subsequent partitioning of a small-RNA duplex between Ago1- and Ago2-RISC.

DISCUSSION

Here we show that in *Drosophila* the structure of a small-RNA duplex determines its partitioning between Ago1- and Ago2-RISC. Our data suggest a simple model for

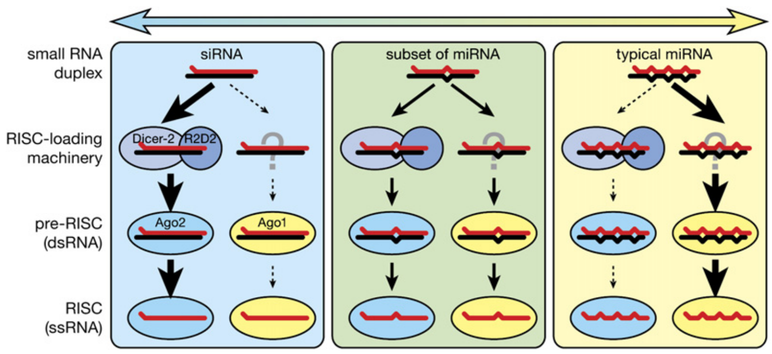

Figure 7. A Model for Small Silencing RNA Sorting in *Drosophila*

Dcr-2/R2D2 bind well to highly paired small-RNA duplexes but poorly to duplexes bearing central mismatches; such duplexes are therefore disfavored for loading into Ago2. Ago1 favors small RNAs with central mismatches, but no Ago1-loading proteins have yet been identified. Ago1- and Ago2-loading compete each other, increasing the selectivity of small-RNA sorting. The partitioning of a small-RNA duplex between the Ago1 and Ago2 pathways reflects its structure. A typical miRNA/miRNA* duplex, such as *let-7* or *bantam*, loads mainly Ago1, whereas a standard siRNA duplex loads mostly Ago2. Some miRNA/miRNA* duplexes containing extensively paired central regions, such as miR-277/miR-277* (see Förstemann et al., 2007), partition between Ago1 and Ago2. Sorting of small-RNA duplexes into Ago1 and Ago2 produces pre-RISC, in which the duplex is bound to the Argonaute protein. Subsequently, mature RISC, which contains only the siRNA guide or miRNA strand of the original duplex, is formed. The separation of the miRNA and miRNA* or the siRNA guide and passenger strands also reflects the structure of the small-RNA duplex. For Ago1, we hypothesize that mismatches between the miRNA and the miRNA* or siRNA guide and passenger strands in the seed sequence are required for the efficient conversion of pre-RISC to mature RISC. For Ago2, such seed sequence mismatches are not needed because Ago2 can efficiently cleave the passenger or miRNA* strand, liberating the guide or miRNA from the duplex.

this partitioning (Figure 7), with a central unpaired region serving as both an antideterminant for the Ago2-loading pathway and a preferred binding substrate for the Ago1 pathway. Supporting this view, miRNAs that contain central mismatches, such as *let-7* and *bantam*, assemble primarily into Ago1-RISC (Okamura et al., 2004). The accompanying manuscript (Förstemann et al., 2007) shows that miR-277, whose central region is base paired, partitions between Ago1 and Ago2 in vivo.

Both the Ago2- and Ago1-loading pathways are selective. For Ago2, the affinity of the Dcr-2/R2D2 heterodimer for a small-RNA duplex provides the primary source of small-RNA selectivity. In the absence of either the Ago2-loading machinery or Ago2 itself, Ago1 is nonetheless preferentially loaded with a miRNA/miRNA* duplex; an siRNA duplex still loads poorly into Ago1. Thus, the Ago1-loading pathway is also inherently selective and not a default pathway that assembles small RNAs rejected by the Ago 2 pathway. We do not yet know if this selectivity is a direct property of Ago1, of an Ago1-loading machinery that remains to be identified, or both.

Previous bioinformatic analyses noted that a central region of thermodynamic instability was a common feature of miRNA/miRNA* duplexes (Khvorova et al., 2003; Han et al., 2006). Our data ascribe a function in flies to this common miRNA/miRNA* structural feature: directing the miRNA into Ago1 and away from Ago2. Mammalian miRNA/miRNA* duplexes also typically contain a central unpaired region, but it is not yet known if they are preferentially loaded into one of the four mammalian Ago-subclade Argonaute proteins.

What is the biological significance in flies of sorting miRNAs into Ago1 and siRNAs into Ago2? One idea, supported by the accompanying manuscript (Förstemann et al., 2007), is that Ago1 and Ago2 are functionally distinct, with only Ago2 silencing targets that possess extensive complementarity to the small-RNA guide and only Ago1 directing repression of targets that contain multiple but only partially complementary miRNA-binding sites. Sorting small RNAs between Ago1 and Ago2 may also prevent miRNAs from saturating the Ago2 machinery, which might compromise Ago2-mediated antiviral defense (Galiana-Arnoux et al., 2006; Obbard et al., 2006; Wang et al., 2006; Zambon et al., 2006). Conversely, excluding from Ago1 siRNAs produced in response to viral infection may minimize competition between such antiviral siRNAs and endogenous miRNAs, protecting flies from misregulation of gene expression during a viral infection. Restricting a robust RNAi—i.e., target cleavage—response to siRNAs loaded into Ago2 may also minimize undesirable, miRNA-like regulation of cellular genes by virally derived siRNAs. Thus, small-RNA sorting ensures that miRNAs are largely restricted to Ago1, whose relaxed requirement for complementarity between a miRNA and a regulated mRNA target allows each miRNA to control many different mRNAs, and that siRNAs are restricted to Ago2, whose silencing activity requires more extensive complementarity between the target and the siRNA guide.

Nonetheless, a final question remains unanswered: why do some iconoclastic miRNA/miRNA* duplexes contain features that favor their loading into Ago2?

EXPERIMENTAL PROCEDURES

General Methods

Preparation of 0–2 hr embryo lysate, lysis buffer, and 2x PK buffer; in vitro assembly of RISC, inactivation of RISC assembly by NEM treatment; in vitro RNAi reactions; purification of recombinant Dcr-2/R2D2 purification; and UV photocrosslinking of proteins to 5-iodo-uracil-containing siRNAs were performed as described previously (Nykanen et al., 2001; Haley et al., 2003; Tomari et al., 2004a). In vitro RNAi target cleavage was performed with 20 nM siRNA and 10 nM ^{32}P-cap radiolabeled target RNA for Figure 3C and S4 and 0.5 nM target in Figure 6.

254 nm UV Photocrosslinking

20 nM 5′-^{32}P-labeled small-RNA duplex was incubated with lysate in a standard RNAi reaction (Haley et al., 2003) and then irradiated with 254 nM UV light for 5 min using a Stratalinker (Stratagene) with the sample ∼3 cm below the UV bulbs. The photocrosslinked proteins were then resolved by 4%–20% gradient SDS-polyacrylamide gel electrophoresis (Criterion precast gels; BioRad). 2′-*O*-methyl ASO were used to isolate proteins photocrosslinked to single-stranded *let-7* as described previously (Tomari et al., 2004a).

Ago1 Coimmunoprecipitation of Small RNAs

1 nM 5′-^{32}P-radiolabeled *let-7* mm11 duplex (Figure 2C) or 20 nM 5′-^{32}P-radiolabeled mm1, mm9, and *let-7*/*let-7** duplexes (Figure 5B) were incubated for 1 hr with wild-type embryo lysate. The reactions were then incubated with anti-Ago1 mouse monoclonal antibody (Okamura et al., 2004) tethered to Dynabeads protein G paramagnetic beads (Invitrogen) for 1 hr. The beads were washed by lysis buffer three times and the radioactivity of the bound RNA was measured by scintillation counting (Figure 2C) or the beads were deproteinized with 2 mg/ml (f.c.) proteinase K in 2x PK buffer at room temperature for 30 min, the supernatant precipitated with 2.5 volumes of absolute ethanol, and the precipitate resolved by electrophoresis in a 20% native polyacrylamide gel (19:1) containing 1x TBE and 3 mM $MgCl_2$ (Figure 5B). Control experiments demonstrated that the *let-7*/*let-7** duplex remains double stranded under these gel conditions.

Anti-Ago1 antibody beads were prepared by incubating 5 μl of tissue culture supernatant from the anti-Ago1 antibody-producing cells for every 5 μl protein G beads for 1 hr on ice and then washing the beads three times. Five microliters of these beads bearing the Ago1 antibody were used per 10–20 μl reaction.

Native Gel Analysis of Dcr-2/R2D2:RNA and Dcr-2:RNA Complexes

Approximately 100 pM 5′-^{32}P-labeled small-RNA duplexes were incubated for 30 min with recombinant Dcr-2/R2D2 heterodimer or Dcr-2 alone in lysis buffer containing 5 mM DTT, 0.1 mg/ml BSA, 3% (w/v) ficoll-400, and 5% (v/v) glycerol and then resolved by electrophoresis on a 5.25% native polyacrylamide gel (37.5:1) containing 0.5x TBE and 1.5 mM $MgCl_2$. RNA and complexes were detected by phosphorimagery, quantified using an FLA-5000 image analyzer and ImageGuage 4.22 software (Fujifilm), and fit to the Hill equation with IGOR Pro 5 software (WaveMetrics).

Ago1 Immunodepletion

For immunodepletion, 120 μl Dynabeads Protein G paramagnetic bead suspension (Invitrogen) was incubated overnight with 120 μl anti-Ago1 mouse monoclonal antibody (1B8) (Okamura et al., 2004) at 4°C with gentle agitation. Next, the magnetic beads were washed three times with lysis buffer and then split among three tubes. Each precursor RNA was incubated in 100 μl standard RNAi reaction at room temperature for 1 hr. Subsequently, 60 μl of the reaction was added to the anti-Ago1 magnetic beads, and the mixture was agitated gently at 4°C overnight. The supernatant was removed, and the beads were washed three times with lysis buffer. The input, supernatant, and beads (the immunoprecipitate) were subsequently analyzed by western blotting to confirm Ago1 depletion, by native gel analysis to measure the amount of Ago1-associated single-stranded *let-7*, and by a target cleavage assay to measure RISC activity.

Supplemental Data

Supplemental Data include six figures and can be found with this article online at http://www.cell.com/cgi/content/full/130/2/299/DC1/.

ACKNOWLEDGMENTS

We thank Mikiko and Haruhiko Siomi for anti-Ago1 antibody and *ago2*^{414} flies, Richard Carthew for *dcr-2*^{L811fsX} flies, Qinghua Liu for Dcr-2- and R2D2-expressing baculoviruses, Alicia Boucher for assistance with fly husbandry, Gwen Farley for technical assistance, and members of the Zamore lab for advice, suggestions, and critical comments on the text. P.D.Z. is a W.M. Keck Foundation Young Scholar in Medical Research. This work was supported in part by grants from the National Institutes of Health to P.D.Z. (GM62862 and GM65236) and a postdoctoral fellowship from the Human Frontier Science Program to Y.T.

Received: January 18, 2007
Revised: April 20, 2007
Accepted: May 23, 2007
Published: July 26, 2007

REFERENCES

Baulcombe, D. (2004). RNA silencing in plants. Nature *431*, 356–363.

Bentwich, I., Avniel, A., Karov, Y., Aharonov, R., Gilad, S., Barad, O., Barzilai, A., Einat, P., Einav, U., Meiri, E., et al. (2005). Identification of hundreds of conserved and nonconserved human microRNAs. Nat. Genet. *37*, 766–770.

Bernstein, E., Caudy, A.A., Hammond, S.M., and Hannon, G.J. (2001). Role for a bidentate ribonuclease in the initiation step of RNA interference. Nature *409*, 363–366.

Berezikov, E., Guryev, V., van de Belt, J., Wienholds, E., Plasterk, R.H., and Cuppen, E. (2005). Phylogenetic shadowing and computational identification of human microRNA genes. Cell *120*, 21–24.

Berezikov, E., Thuemmler, F., van Laake, L.W., Kondova, I., Bontrop, R., Cuppen, E., and Plasterk, R.H. (2006). Diversity of microRNAs in human and chimpanzee brain. Nat. Genet. *38*, 1375–1377.

Cullen, B.R. (2004). Transcription and processing of human microRNA precursors. Mol. Cell *16*, 861–865.

Du, T., and Zamore, P.D. (2005). microPrimer: the biogenesis and function of microRNA. Development *132*, 4645–4652.

Elbashir, S.M., Lendeckel, W., and Tuschl, T. (2001a). RNA interference is mediated by 21- and 22-nucleotide RNAs. Genes Dev. *15*, 188–200.

Elbashir, S.M., Martinez, J., Patkaniowska, A., Lendeckel, W., and Tuschl, T. (2001b). Functional anatomy of siRNAs for mediating efficient RNAi in *Drosophila* melanogaster embryo lysate. EMBO J. *20*, 6877–6888.

Förstemann, K., Tomari, Y., Du, T., Vagin, V.V., Denli, A.M., Bratu, D.P., Klattenhoff, C., Theurkauf, W.E., and Zamore, P.D. (2005). Normal microRNA maturation and germ-line stem cell maintenance requires Loquacious, a double-stranded RNA-binding domain protein. PLoS Biol. *3*, e236.

Förstemann, K., Horwich, M.D., Wee, L.M., Tomari, Y., and Zamore, P.D. (2007). *Drosophila* microRNAs are sorted into functionally distinct Argonaute protein complexes after their production by Dicer-1. Cell *130*, this issue, 287–297.

Galiana-Arnoux, D., Dostert, C., Schneemann, A., Hoffmann, J.A., and Imler, J.L. (2006). Essential function in vivo for Dicer-2 in host defense against RNA viruses in *Drosophila*. Nat. Immunol. *7*, 590–597.

Griffiths-Jones, S., Grocock, R.J., van Dongen, S., Bateman, A., and Enright, A.J. (2006). miRBase: microRNA sequences, targets and gene nomenclature. Nucleic Acids Res. *34*, D140–D144.

Haley, B., and Zamore, P.D. (2004). Kinetic analysis of the RNAi enzyme complex. Nat. Struct. Mol. Biol. *11*, 599–606.

Haley, B., Tang, G., and Zamore, P.D. (2003). In vitro analysis of RNA interference in *Drosophila* melanogaster. Methods *30*, 330–336.

Hammond, S.M., Boettcher, S., Caudy, A.A., Kobayashi, R., and Hannon, G.J. (2001). Argonaute2, a link between genetic and biochemical analyses of RNAi. Science *293*, 1146–1150.

Han, J., Lee, Y., Yeom, K.H., Nam, J.W., Heo, I., Rhee, J.K., Sohn, S.Y., Cho, Y., Zhang, B.T., and Kim, V.N. (2006). Molecular basis for the recognition of primary microRNAs by the Drosha-DGCR8 complex. Cell *125*, 887–901.

Hutvágner, G., and Zamore, P.D. (2002). A microRNA in a Multiple-Turnover RNAi Enzyme Complex. Science *297*, 2056–2060.

Jing, Q., Huang, S., Guth, S., Zarubin, T., Motoyama, A., Chen, J., Di Padova, F., Lin, S.C., Gram, H., and Han, J. (2005). Involvement of microRNA in AU-rich element-mediated mRNA instability. Cell *120*, 623–634.

Khvorova, A., Reynolds, A., and Jayasena, S.D. (2003). Functional siRNAs and miRNAs exhibit strand bias. Cell *115*, 209–216.

Kim, V.N. (2005). MicroRNA biogenesis: coordinated cropping and dicing. Nat. Rev. Mol. Cell Biol. *6*, 376–385.

Kim, K., Lee, Y.S., and Carthew, R.W. (2006). Conversion of pre-RISC to holo-RISC by Ago2 during assembly of RNAi complexes. RNA *13*, 22–29.

Kloosterman, W.P., and Plasterk, R.H. (2006). The diverse functions of microRNAs in animal development and disease. Dev. Cell *11*, 441–450.

Krek, A., Grun, D., Poy, M.N., Wolf, R., Rosenberg, L., Epstein, E.J., MacMenamin, P., da Piedade, I., Gunsalus, K.C., Stoffel, M., and Rajewsky, N. (2005). Combinatorial microRNA target predictions. Nat. Genet. *37*, 495–500.

Lee, Y.S., Nakahara, K., Pham, J.W., Kim, K., He, Z., Sontheimer, E.J., and Carthew, R.W. (2004). Distinct roles for *Drosophila* Dicer-1 and Dicer-2 in the siRNA/miRNA silencing pathways. Cell *117*, 69–81.

Leuschner, P.J., Ameres, S.L., Kueng, S., and Martinez, J. (2006). Cleavage of the siRNA passenger strand during RISC assembly in human cells. EMBO Rep. *7*, 314–320.

Lewis, B.P., Shih, I.H., Jones-Rhoades, M.W., Bartel, D.P., and Burge, C.B. (2003). Prediction of mammalian microRNA targets. Cell *115*, 787–798.

Lewis, B.P., Burge, C.B., and Bartel, D.P. (2005). Conserved seed pairing, often flanked by adenosines, indicates that thousands of human genes are microRNA targets. Cell *120*, 15–20.

Liu, Q., Rand, T.A., Kalidas, S., Du, F., Kim, H.E., Smith, D.P., and Wang, X. (2003). R2D2, a Bridge Between the Initiation and Effector Steps of the *Drosophila* RNAi Pathway. Science *301*, 1921–1925.

Liu, X., Jiang, F., Kalidas, S., Smith, D., and Liu, Q. (2006). Dicer-2 and R2D2 coordinately bind siRNA to promote assembly of the siRISC complexes. RNA *12*, 1514–1520.

Matranga, C., Tomari, Y., Shin, C., Bartel, D.P., and Zamore, P.D. (2005). Passenger-strand cleavage facilitates assembly of siRNA into Ago2-containing RNAi enzyme complexes. Cell *123*, 607–620.

Nykanen, A., Haley, B., and Zamore, P.D. (2001). ATP requirements and small interfering RNA structure in the RNA interference pathway. Cell *107*, 309–321.

Obbard, D.J., Jiggins, F.M., Halligan, D.L., and Little, T.J. (2006). Natural selection drives extremely rapid evolution in antiviral RNAi genes. Curr. Biol. *16*, 580–585.

Okamura, K., Ishizuka, A., Siomi, H., and Siomi, M.C. (2004). Distinct roles for Argonaute proteins in small RNA-directed RNA cleavage pathways. Genes Dev. *18*, 1655–1666.

Pham, J.W., and Sontheimer, E.J. (2005). Molecular requirements for RNA-induced silencing complex assembly in the Drosophila RNA interference pathway. J. Biol. Chem. *280*, 39278–39283.

Pham, J.W., Pellino, J.L., Lee, Y.S., Carthew, R.W., and Sontheimer, E.J. (2004). A Dicer-2-dependent 80s complex cleaves targeted mRNAs during RNAi in *Drosophila*. Cell *117*, 83–94.

Rand, T.A., Petersen, S., Du, F., and Wang, X. (2005). Argonaute2 cleaves the anti-guide strand of siRNA during RISC activation. Cell *123*, 621–629.

Saito, K., Ishizuka, A., Siomi, H., and Siomi, M.C. (2005). Processing of pre-microRNAs by the Dicer-1-Loquacious complex in *Drosophila* cells. PLoS Biol. *3*, e235.

Schwarz, D.S., Hutvágner, G., Du, T., Xu, Z., Aronin, N., and Zamore, P.D. (2003). Asymmetry in the assembly of the RNAi enzyme complex. Cell *115*, 199–208.

Sontheimer, E.J. (2005). Assembly and function of RNA silencing complexes. Nat. Rev. Mol. Cell Biol. *6*, 127–138.

Stark, A., Brennecke, J., Bushati, N., Russell, R.B., and Cohen, S.M. (2005). Animal microRNAs confer robustness to gene expression and have a significant impact on 3′UTR evolution. Cell *123*, 1133–1146.

Tomari, Y., Matranga, C., Haley, B., Martinez, N., and Zamore, P.D. (2004a). A protein sensor for siRNA asymmetry. Science *306*, 1377–1380.

Tomari, Y., Du, T., Haley, B., Schwarz, D.S., Bennett, R., Cook, H.A., Koppetsch, B.S., Theurkauf, W.E., and Zamore, P.D. (2004b). RISC assembly defects in the *Drosophila* RNAi mutant armitage. Cell *116*, 831–841.

Tomari, Y., and Zamore, P.D. (2005). Perspective: machines for RNAi. Genes Dev. *19*, 517–529.

Valencia-Sanchez, M.A., Liu, J., Hannon, G.J., and Parker, R. (2006). Control of translation and mRNA degradation by miRNAs and siRNAs. Genes Dev. *20*, 515–524.

Wang, X.H., Aliyari, R., Li, W.X., Li, H.W., Kim, K., Carthew, R., Atkinson, P., and Ding, S.W. (2006). RNA interference directs innate immunity against viruses in adult *Drosophila*. Science *312*, 452–454.

Zambon, R.A., Vakharia, V.N., and Wu, L.P. (2006). RNAi is an antiviral immune response against a dsRNA virus in *Drosophila* melanogaster. Cell. Microbiol. *8*, 880–889.

Cell Research (2007) 17:661-663.

www.nature.com/cr

Beginning to understand microRNA function

Tingting Du[1], Phillip D Zamore[1]

[1]*University of Massachusetts Medical School, 364 Plantation Street, Worcester, MA 01605-2324.*
phillip.zamore@umassmed.edu

Cell Research (2007) **17**:661-663. doi: ; published online 13 Aug 2007

MicroRNAs (miRNAs) are ~22 nt small RNAs expressed by plants, animals, viruses and at least one unicellular organism, the green alga, *Chlamydomonas reinhardtii* [1]. Most miRNAs are transcribed as primary miRNAs (pri-miRNAs) by RNA polymerase II, although a few are transcribed by RNA polymerase III. In animals, pri-miRNAs are converted to mature miRNAs by two successive endonucleolytic cleavages [2]. The pri-miRNA is first cut in the nucleus by Drosha, a ribonuclease III (RNase III) enzyme, acting with its double-stranded RNA-binding domain (dsRBD) protein partner, called DGCR8 in vertebrates and Pasha in invertebrates, into an ~70 nt stem loop, the precursor miRNA (pre-miRNA). After its export to cytoplasm by Exportin 5, the pre-miRNA is cut into mature miRNA by a second RNase III enzyme, Dicer, which partners in mammals with one of two dsRBD proteins—TRBP (HIV-1 *tar* RNA-binding protein) or PACT, or in *Drosophila melanogaster* with the dsRBD protein Loquacious (Loqs). The mature miRNA is then loaded into an effector complex, the RNA-induced silencing complex (RISC), whose core component is always a member of the Argonaute (Ago) family of RNA-guided RNA regulatory proteins [3]. Recently, an alternative processing pathway was identified for a distinct sub-group of miRNAs in *Drosophila* and *C. elegans* [4, 5]. These miRNAs exploit the pre-mRNA splicing machinery to generate a pre-miRNA directly, bypassing the processing of a pri-miRNA by Drosha. For these miRNAs, the pre-miRNA is at once the precursor of a mature miRNA and a compact, fully functional intron, hence the name, 'mirtrons'.

In animals, miRNAs typically bind to the 3′ untranslated region (UTR) of their target mRNAs through sequences that are only partially complementary. The 5′ region of the miRNA (roughly nucleotides 2–8) contributes disproportionately to target-RNA binding [3]. This 'seed region' is the primary determinant of binding specificity, making miRNAs surprisingly promiscuous: many miRNAs regulate hundreds of different mRNAs. A common consequence of such seed-mediated miRNA binding is a decrease in the amount of the protein encoded by the target mRNA. However, the precise molecular mechanism of miRNA-mediated translational repression remains controversial. In fact, distinct mechanisms of repression have been proposed by different laboratories for different miRNA-target pairs and even for the same miRNA studied with remarkably similar experiments.

Early studies in *C. elegans* suggested that miRNAs blocked protein synthesis after the initiation of translation, because the abundance of repressed mRNA in polyribosomes appeared to be unaltered by miRNA binding [6]. Studies in cultured mammalian cells provided additional support for this model, as a significant fraction of miRNA-target mRNA remains associated with polyribosomes, despite a large decrease in protein accumulation from these mRNAs [7]. Moreover, the polysomes with which miRNAs associate appear to be translationally active, suggesting that the observed translational inhibition reflects either ribosomes departing the mRNA during protein synthesis or targeted destruction of nascent polypeptide chains as they emerge from the polypeptide exit tunnel [8, 9]. Yet, other studies in flies and mammals are at odds with these findings, suggesting that miRNAs do, in fact, block mRNA translation at the initiation step [10]. In these experiments, miRNA-directed inhibition requires the 7-methyl guanosine cap, implying a role for miRNA in blocking recognition of the cap by the translation initiation factor eIF4E.

Controversy also dogs the link between miRNA-directed mRNA repression and target mRNA degradation. Some studies report that mRNA levels are unchanged upon miRNA targeting, but others observe destruction of the mRNA upon miRNA binding, perhaps as a consequence of deadenylation and subsequent decapping by standard mRNA decay enzymes. Argonaute proteins, miRNAs, and their mRNA targets, all accumulate in cytoplasmic "Processing bodies" (P-bodies) that function to store and to degrade translationally silenced mRNA [11]. Though there are lines of evidence suggesting a direct role for P-bodies in miRNA-mediated silencing, other data suggest that the movement of miRNA-repressed mRNAs to P-bodies is a consequence, not a cause, of miRNA-directed translational repression [11]. For at least a subgroup of miRNAs, miRNA-mediated translational repression is reversible, with the mRNA shuttling between P-bodies and actively translating polysomes, and the P-body serving as a temporary refuge for miRNA-repressed, translationally quiescent mRNAs [12].

Despite the diversity of modes proposed for miRNA-directed translational inhibition, little is known about the molecular basis of any. Thus, new work by Kiriakidou *et al.* [14], Chendrimada *et al.* [15], and Thermann *et al.* [17] provides long overdue insight into how miRNAs decrease the rate of translational initiation. Remarkably, for the miRNA field, all three studies point to a single explanation for miRNAs' reducing the rate of translational initiation, i.e., the association of ribosomes with the 5′ end of mRNAs.

First, some necessary background. Argonaute proteins lie at the core of all effector complexes containing small RNAs, including miRNAs, small interfering RNAs (siRNAs) and PIWI-interacting RNAs (piRNAs). Argonaute proteins contain a central PAZ domain (named after the family member proteins, Piwi, Argonaute and Zwille), which binds to the 3′ end of single-stranded RNAs, and a carboxy terminal PIWI domain, which binds to the 5′ phosphate of small RNAs [13]. In the June 15th issue of *Cell*, Kiriakidou and colleagues identify within human Argonaute2 (Ago2) protein a sequence similar to eukaryotic initiation factor 4E (eIF4E) [14]. This motif is present only in the subset of Argonaute proteins implicated in miRNA-mediated translational repression, suggesting a special role for this domain in the miRNA pathway. Kiriakidou *et al*. go on to show that Ago2 binds to a cap-analog resin through the eIF4E-like domain, and that the interaction requires two evolutionarily conservative phenylalanine residues within the domain. Moreover, the cap-binding domain is required for miRNA-directed translational repression at the initiation step, but not when Ago2 regulates mRNA expression by cleaving its mRNA targets, as it does when it mediates siRNA-directed RNA interference (RNAi). The authors propose a straightforward model in which Ago2, bound to the mRNA target by a miRNA, competes with eIF4E for the mRNA cap, reducing the translation of the mRNA target into protein.

Chendrimada and colleagues used a different experimental approach to identify a role for a different translation factor, the protein eIF6, in miRNA-directed translational repression [15]. eIF6 has long been known to bind to free 60S ribosome subunits, preventing their joining the 40S subunit to generate translationally competent 80S ribosome particles [16]. Chendrimada *et al*. purified proteins associated with TRBP, the mammalian homolog of Loquacious, the *Drosophila* partner of Dicer-1. In mammals, TRBP is thought to participate in both miRNA production and the assembly of miRNAs into Ago2-containing complexes. Among the proteins that co-purified with TRBP were, as expected from earlier work, Dicer and Ago2, but also unexpectedly, protein components of the 60S ribosomal subunit and eIF6. Strengthening the case that eIF6 participates in miRNA-mediated mRNA repression, depletion of eIF6 from human cells counteracted miRNA-directed translational repression of a reporter mRNA, and depletion of eIF6 by RNAi in *C. elegans* decreased the endogenous silencing of mRNAs by miRNAs.

Chendrimada and co-workers propose that miRNAs block translation by recruiting eIF6 to their mRNA targets. eIF6 would then antagonize the joining of the two ribosomal subunits on the miRNA-regulated mRNA. Like Kiriakidou *et al.* [14], Chendrimada *et al.* [15] implicate the initiation step of translation as the miRNA regulated step, but unlike the Kiriakidou study, they do not detect a direct role for Argonaute proteins in antagonizing translational initiation. Conceivable, both the model of Kiriakidou *et al.*, which postulates that Argonaute2 binds the cap, blocking eIF4E binding, and that of Chendrimada *et al.*, which envisions Argonaute2 as simply increasing the local concentration of eIF6 on the target mRNA, may be true, with the combined action of these two, and perhaps other, translational initiation antagonists explaining miRNA-directed repression.

Contemporaneously, Thermann and colleagues used lysate from *Drosophila* embryos to recapitulate some aspects of miRNA-directed translational repression for a reporter mRNA bearing in its 3′ UTR six copies of an authentic miR-2 binding site [17]. (It is worth noting that the *Drosophila* mRNA, *reaper*, from which this miR-2-binding site derives, contains only a single copy of the site, not six.) The authors observed a reduction in 80S ribosome assembly on the reporter mRNA, suggesting inhibition at the translation initiation step. Surprisingly, some larger messenger ribonucleoprotein particles (mRNPs) formed on the reporter mRNA upon miRNA binding, even when polysome formation was blocked. The authors refer to these particles as 'pseudo-polysomes'. because they formed even when 60S joining was inhibited, and their formation was insensitive to the polysome disrupting agent puromycin. In theory, these large particles might contain one or both of the ribosomal subunits, but not fully assembled 80S ribosomes. These data clearly prompt a reevaluation of the polysomes described in early work to be associated with miRNA-regulated mRNAs. The *in vitro* experiments in flies also support the view that multiple steps in translational initiation, including cap-binding and subunit joining, are regulated by miRNAs: a 7-methyl guanosine cap was required for miRNA-induced silencing *in vitro*, but the enigmatic 'pseudo-polysomes' still formed when the authentic cap was replaced with a translationally incompetent ApppG cap analog.

While the experiments from these three laboratories add considerable support to the idea that miRNAs repress translational initiation, they do not exclude the possibility that the mechanisms of miRNA-directed mRNA regulation differ among organisms, among miRNAs, or even at different developmental stages. Alternatively, the location of miRNA-binding sites within an mRNA or the position of mismatches and bulges within the miRNA-binding sites may influence the mechanism by which productive translation is repressed. Clearly, much remains to be explained before the molecular basis of miRNA-directed translational repression is clear.

References

1 Molnar A, Schwach F, Studholme DJ, Thuenemann EC, Baulcombe DC. miRNAs control gene expression in the single-cell alga Chlamydomonas reinhardtii. Nature 2007; **447**:1126-1129.
2 Kim VN. MicroRNA biogenesis: coordinated cropping and dicing. Nat Rev Mol Cell Biol 2005; **6**:376-385.
3 Zamore PD, Haley B. Ribo-gnome: the big world of small RNAs. Science 2005; **309**:1519-1524.
4 Ruby JG, Jan CH, Bartel DP. Intronic microRNA precursors that bypass Drosha processing. Nature 2007; **448**:83-86.
5 Okamura K, Hagen JW, Duan H, Tyler DM, Lai EC. The Mirtron Pathway Generates microRNA-Class Regulatory RNAs in Drosophila. Cell 2007; doi:10.1016/j.cell.2007.06.028.
6 Olsen PH, Ambros V. The lin-4 regulatory RNA controls developmental timing in Caenorhabditis elegans by blocking LIN-14 protein synthesis after the initiation of translation. Dev Biol 1999; **216**:671-680.
7 Petersen CP, Bordeleau ME, Pelletier J, Sharp PA. Short RNAs Repress Translation after Initiation in Mammalian Cells. Mol Cell 2006; **21**:533-542.
8 Maroney PA, Yu Y, Fisher J, Nilsen TW. Evidence that microRNAs are associated with translating messenger RNAs in human cells. Nat Struct Mol Biol 2006; **13**:1102-1107.
9 Nottrott S, Simard MJ, Richter JD. Human let-7a miRNA blocks protein production on actively translating polyribosomes. Nat Struct Mol Biol 2006; **13**:1108-1114.
10 Pillai RS, Bhattacharyya SN, Artus CG, *et al*. Inhibition of translational initiation by Let-7 MicroRNA in human cells. Science 2005; **309**:1573-1576.
11 Eulalio A, Behm-Ansmant I, Izaurralde E. P bodies: at the crossroads of post-transcriptional pathways. Nat Rev Mol Cell Biol 2007; **8**:9-22.
12 Bhattacharyya SN, Habermacher R, Martine U, Closs EI, Filipowicz W. Relief of microRNA-mediated translational repression in human cells subjected to stress. Cell 2006; **125**:1111-1124.
13 Song JJ, Smith SK, Hannon GJ, Joshua-Tor L. Crystal structure of Argonaute and its implications for RISC slicer activity. Science 2004; **305**:1434-1437.
14 Kiriakidou M, Tan GS, Lamprinaki S, De Planell-Saguer M, Nelson PT, Mourelatos Z. An mRNA m(7)G Cap Binding-like Motif within Human Ago2 Represses Translation. Cell 2007; **129**:1141-1151.
15 Chendrimada TP, Finn KJ, Ji X, *et al*. MicroRNA silencing through RISC recruitment of eIF6. Nature 2007; **447**:823-828.
16 Ceci M, Gaviraghi C, Gorrini C, *et al*. Release of eIF6 (p27BBP) from the 60S subunit allows 80S ribosome assembly. Nature 2003; **426**:579-584.
17 Thermann R, Hentze MW. Drosophila miR2 induces pseudo-polysomes and inhibits translation initiation. Nature 2007; **447**:875-878.